ARISTOTLE UNIVERSITY OF THESSALONIKI
FACULTY OF SCIENCES
SCHOOL OF GEOLOGY

GEORGIA KOSTAKI
MSc Geologist

LATE JURASSIC-EARLY CRETACEOUS SHALLOW WATER
SEDIMENTS ON THE TOP OF THE TETHYAN OPHIOLITES OF THE
HELLENIDES (NORTHERN GREECE)

DISSERTATION THESIS

THESSALONIKI
2023

ΑΡΙΣΤΟΤΕΛΕΙΟ ΠΑΝΕΠΙΣΤΗΜΙΟ ΘΕΣΣΑΛΟΝΙΚΗΣ
ΣΧΟΛΗ ΘΕΤΙΚΩΝ ΕΠΙΣΤΗΜΩΝ
ΤΜΗΜΑ ΓΕΩΛΟΓΙΑΣ

ΓΕΩΡΓΙΑ ΚΩΣΤΑΚΗ
MSc Γεωλόγος

ΑΝΩ ΙΟΥΡΑΣΙΚΑ-ΚΑΤΩ ΚΡΗΤΙΔΙΚΑ ΙΖΗΜΑΤΑ ΡΗΧΗΣ ΘΑΛΑΣΣΑΣ
ΠΟΥ ΒΡΙΣΚΟΝΤΑΙ ΠΑΝΩ ΣΤΟΥΣ ΟΦΙΟΛΙΘΟΥΣ ΤΗΣ ΤΗΘΥΟΣ
ΕΝΤΟΣ ΤΩΝ ΕΛΛΗΝΙΔΩΝ (ΒΟΡΕΙΑ ΕΛΛΑΔΑ)

ΔΙΔΑΚΤΟΡΙΚΗ ΔΙΑΤΡΙΒΗ

ΘΕΣΣΑΛΟΝΙΚΗ
2023

GEORGIA KOSTAKI
MSc Geologist

LATE JURASSIC-EARLY CRETACEOUS SHALLOW WATER SEDIMENTS ON THE TOP OF THE TETHYAN OPHIOLITES OF THE HELLENIDES (NORTHERN GREECE)

It was carried out at the Department of Structural, Historical and Applied Geology of the School of Geology A.U.TH.
It was submitted at the School of Geology A.U.TH. in October 2023

Date of Dissertation Defense: 13/12/2023

Annex Number of the Scientific Annals of School of Geology N°: 243

Advisory Committee

Emer. Professor Adamantios Kilias, Principal Advisor
Professor Hans-Jürgen Gawlick, Member of the Advisory Committee
Professor Nikolaos Kantiranis, Member of the Advisory Committee

Examination Committee

Emer. Professor, Adamantios Kilias
Professor, Hans-Jürgen Gawlick
Professor, Nikolaos Kantiranis
Professor, Markos Tranos
Professor, George Siridis
Assoc. Professor, Alexandros Chatzipetros
Assis. Professor, Aggelos Maravelis

Citation:
Kostaki G., 2023. – Late Jurassic-Early Cretaceous shallow water sediments on the top of the Tethyan Ophiolites of the Hellenides (Northern Greece). Ph.D. Thesis, School of Geology, Aristotle University of Thessaloniki, Annex Number of Scientific Annals of the School of Geology No 243, 200 pp.
Κωστάκη Γ., 2023. – Ανω Ιουρασικά - Κάτω Κρητιδικά ιζήματα ρηχής θάλασσας που βρίσκονται πάνω στους οφιόλιθους της Τηθύος εντός των Ελληνίδων (Βόρεια Ελλάδα). Διδακτορική Διατριβή, Τμήμα Γεωλογίας Α.Π.Θ., Αριθμός Παραρτήματος Επιστημονικής Επετηρίδας Τμ. Γεωλογίας No 243, 200 σελ.

Declaration of authorship

„I declare in lieu of oath that this thesis is entirely my own work except where otherwise indicated. The presence of quoted or paraphrased material has been clearly signaled and all sources have been referred. The thesis has not been submitted for a degree at any other institution. The following thesis has been partially published in the Journal of Geological Society and the relevant sections should be referenced as follows: Kostaki, G., Gawlick, H.-J., Missoni, S., Kilias, A. & Katrivanos, E., 2023. New stratigraphic and paleontological data from carbonates related to the Vourinos-Pindos ophiolite emplacement: Implications for the provenance of the ophiolites (Hellenides). Journal of Geological Society, DOI:10.1144/jgs2023-127.

This article is part of the Ophiolites, mélanges and blueschist collection available at: https://www.lyellcollection.org/topic/collections/ophiolites-melanges-and-blueschists"

Acknowledgments

I am greatly honored, and I feel fortunate to have the respectable Professor Adamantios Kilias as my supervisor and mentor. I am most grateful for his continuous support, his patience, and his motivation throughout the time of our research. The completion of this dissertation could not have been possible without his valuable guidance and enlightening expertise. His willingness to give his time so generously to accompany me during field work as well as provide me with the tools that I needed to complete this work has been very much appreciated. Above all, I express my gratitude to him for inspiring me with confidence and enthusiasm for science and geology.

Likewise, it was a great opportunity and privilege to have as my supervisor Professor Hans-Jürgen Gawlick, to whom I would like to express my deepest appreciation for his kind help during field work, his valuable comments and advice during research time, as well as the long discussions we held on this work and other interesting subjects of geology. I extend my sincere gratitude to Professor Hans-Jürgen Gawlick for generously providing the invaluable data on conodonts, which played a crucial role in the completion of this thesis. I am also indebted to him for giving me the great chance to go to Leoben and work on this project.

Equally, I am sincerely grateful to the third member of the thesis adviser committee, Professor Nikolaos Kantiranis, for his expert advice and valuable pointers, as wells as his contribution to the preparation of this dissertation.

TABLE OF CONTENTS

CHAPTER 1. Introduction and Thesis Objectives

The present doctoral dissertation was carried out in the frame of the Postgraduate Program Studies in the School of Geology, Department of Structural, Historical, and Applied Geology, in the specialization of Structural Geology and Stratigraphy, and attempts to enable a better understanding of the tectonic development and geodynamic history of the Hellenides.

In the frame of the present thesis, new biostratigraphic and sedimentological research accompanied by structural analysis took place on sedimentary successions and mélanges located in northern Greece, on the top and below of the Jurassic obducted Neo-Tethyan ophiolites. These sedimentary successions and mélanges are associated with the Jurassic ophiolite obduction on the Pelagonian margin(s), in the Hellenides. This study was conducted in order to provide insights into questions regarding:

- the derivation of the Neo-Tethyan ophiolites,
- the direction and timing of the emplacement of the Neo-Tethyan ophiolites on the Pelagonian margin(s),
- the geodynamic evolution of the Neo-Tethys Ocean,
- and whether or not a distinct Pindos Ocean or deep-water Pindos Basin existed.

In the Hellenides, several geodynamic models are proposed about the origin of the ophiolites. These ophiolites in northern Greece are composed of Vardar-Axios ophiolites at the eastern side of the Pelagonian Zone and Vourinos-Pindos ophiolites at the western Pelagonian side (Figure 1.1).
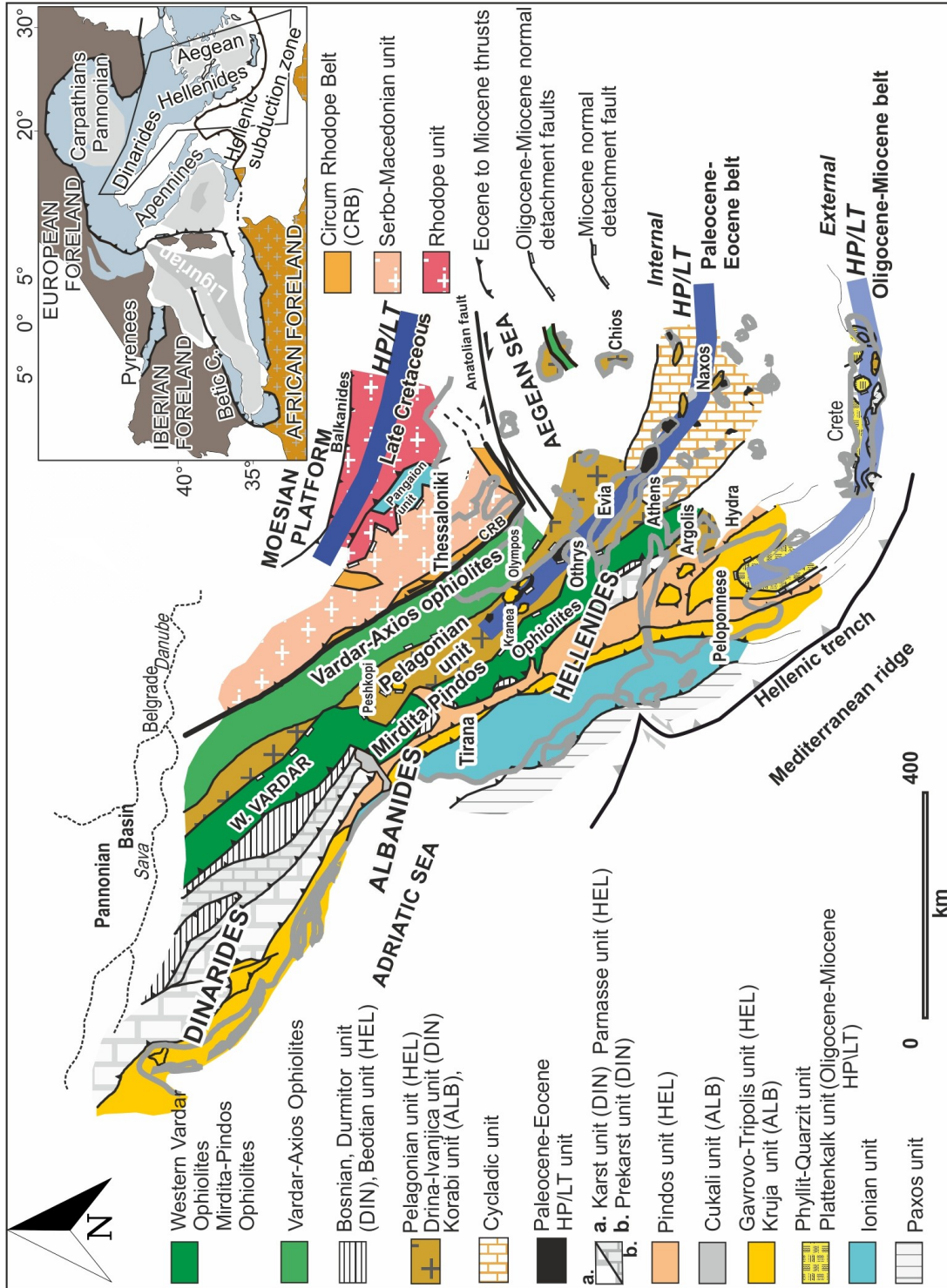
Figure 1.1 The main tectono-stratigraphic units of the Dinarides and the Hellenides. Insert: The Mediterranean region as part of a polyphase orogenic belt in south Europe (Kostaki et al. 2023: modified after Kilias 2021).

Some paleogeographic reconstructions propose that these ophiolites were rooted in two autonomous Mesozoic oceanic basins on each side of the Pelagonia, which in this model is regarded as an independent continental micro-plate (e.g., Mountrakis 1986, Jones et al. 1991, Robertson et al. 1991, 1996, Robertson and Shallo 2000, Stampfli and Borel 2002, Brown and Robertson 2004, Sharp and Robertson 2006, Rassios and Moores 2006, Stampfli and Kozur 2006, Karamata 2006, Dilek et al. 2008, Rassios and Dilek 2009, Robertson 2012, Saccani et al. 2015, 2017). According to those authors, the Pindos-Vourinos ophiolites originated from an ocean (Pindos Ocean) that was situated east of Ionian/Gavrovo Zone and the western part of the so-called Pelagonian continental micro-plate, while Vardar-Axios ophiolites originated from an ocean that was situated among the eastern Pelagonian and the Serbo-Macedonian continental margins.

A different geodynamic model proposes that both ophiolite belts are the remnants of an ophiolite nappe stack originating from one Mesozoic oceanic realm, which was situated at the eastern part of the Pelagonia (Zimmerman 1969, 1972, Bernoulli and Laubscher 1972, Aubouin 1973, Mercier et al. 1975, Dercourt et al. 1986, Bortolotti et al. 1996, 2012, Gawlick et al. 2008, 2016a, 2016b, 2017a, 2020, Schlagintweit et al. 2008, Schmid et al. 2008, 2020, Kilias et al. 2010, Missoni and Gawlick 2011, Katrivanos et al. 2013, Ferrière et al. 2015, 2016, Kilias 2021). In this concept, the Pelagonia during the Middle Triassic to the Middle Jurassic is regarded as the eastern passive continental margin of the Adriatic plate facing eastward the main wide Neo-Tethys Ocean, without any disruption from a distinct Pindos Ocean.

The sedimentary successions and mélanges studied in this dissertation thesis provide an opportunity to diminish the still controversial opinions regarding the origin of the ophiolites cropping out in the Hellenic realm. Structural analysis, microfacies analysis, conodont age dating, and radiolarian age dating were conducted on resediments and sedimentary successions exposed both above and below the Vourinos ophiolites, within and above the Avdella and Koziakas mélanges (associated with Pindos and Koziakas ophiolites, respectively), as well as on top of the Vardar-Axios ophiolites.

In particular, the resediments within and above the Middle to Late Jurassic Avdella and Koziakas mélanges, as well as the Early Cretaceous sedimentary successions above

the Vourinos and Vardar-Axios ophiolites, contain important information about the evolution, direction, and age of the ophiolite emplacement on top of the Pelagonian continental margin and give a significant chance to explore the Middle Jurassic to Early Cretaceous paleogeography and geodynamic evolution of the Hellenides.

The comprehensive analysis of components within these studied sedimentary formations helped in assessing the intensity and timing of erosion processes (Flügel 2004) that took place on the accreted Pelagonian continent after the ophiolite emplacement. It also contributed to determining the time of redeposition of the erosional products within foreland basins formed ahead of the advancing ophiolite nappe stack and upon the obducted ophiolites.

Furthermore, conodont age dating and biostratigraphic analysis, conducted for the first time on Triassic open-marine limestone blocks found in the Middle to Late Jurassic Avdella and Koziakas mélanges, offer evidence concerning their paleogeographic provenance, providing additional perspectives on the origin of the associated ophiolites.

Equally significant are the biostratigraphic results obtained from sedimentary successions that tectonically underlie the Vourinos ophiolites, dominated by Middle Triassic recrystallized carbonate rocks representing a part of the remaining segment of the overridden Pelagonian marginal formations.

All the results that emerged from this research are in alignment with the thesis objectives, focusing on understanding the origin and tectonic history of the ophiolites and extending to an improved comprehension of the configuration of the overridden former passive continental margin.

Moreover, the implications of these results lead to the recognition of common tectono-stratigraphic trends in the Hellenides, consistent with the Triassic to Jurassic sedimentary evolution as previously reconstructed in the Albanides and the Inner Dinarides. This sedimentation pattern, indicative of the geodynamic setting of the Neo-Tethys realm, is also valid in the Eastern and Southern Alps, as well as the Western Carpathians.

1.1 Thesis content and structure

This dissertation thesis consists of eight chapters and a brief synopsis, which is also translated into Greek, and relevant references. The thesis begins with an introduction to the Tethyan oceanic system, whose evolution had a major impact to the formation of the eastern Mediterranean mountain chains, including the Eastern and Southern Alps, the Western Carpathians, the Apennines, the Dinarides, the Albanides, the Hellenides, and units in the Pannonian realm (e.g., Pelso, Tisza). Following this, this chapter provides a summary of the Triassic to Jurassic sedimentary evolution related to the geodynamic setting of the Neo-Tethys realm, as reconstructed for the Inner Dinarides and Albanides (Gawlick et al. 2008, Sudar et al. 2013, Gawlick et al. 2017b, Gawlick and Missoni 2019). This sedimentation pattern is also valid for the Eastern and Southern Alps and the Western Carpathians and will assist in recognizing common tectono-stratigraphic trends in the Hellenides. In the same chapter, a geological overview of the main tectono-stratigraphic domains and key geological features comprising the Hellenic orogenic belt follows. Additionally, a concise overview is provided of popular paleogeographical reconstructions put forth by various research teams and authors in recent decades concerning the derivation of the two ophiolite belts occurring in the Hellenides. The chapter concludes with an examination of the definition and importance of the mélanges.

The third chapter provides a brief description of the microfacies concept, Facies Zones, Standard Microfacies Types, and carbonate classification systems, which have been shown to be the most useful for the purpose of this dissertation thesis.

The next chapter (fourth) aims to present the geological setting of the study area, which is composed of the Vourinos, Pindos and Koziakas ophiolites, as well as the associated mélanges and the overstep sequences. In this chapter, it was crucial to describe, based on preexisting research, the development and arrangement of the Pelagonian Zone, which represents the overridden former passive continental margin.

In the fifth chapter, the data obtained from microfacies analysis conducted on resediments and sedimentary successions, along with the findings from conodont and radiolarian age dating, are presented.

In the sixth chapter, the structures of the primary deformational events that have affected the studied region are described, while the seventh chapter delves into discussion of the biostratigraphic and structural data, together with relevant known research. Subsequently, all the available evidence is combined towards an evolutionary scenario regarding the ophiolite obduction over the Pelagonian passive continental margin, converting it into a lower plate during the Middle Jurassic. Moreover, the discussion extends to the events that took place subsequent to the ophiolite obduction.

In the final chapter, considering the resulted paleogeographic reconstruction, which enabled a better understanding of the Middle Jurassic to Early Cretaceous geotectonic evolution of the Hellenides, a conclusion about the provenance of the ophiolite belts present in the Hellenides was deduced.

CHAPTER 2. Geological Overview

2.1 Tethyan oceanic realm

The highest mountain ranges on Earth in their current form were shaped by the convergence and continental collision between segments of the Gondwana plate and the Eurasia plate, resulting in the Alpine-Himalayan orogenic chain (Mountrakis 2010) (Figure 2.1).

The Alpine-Himalayan orogenic system alternatively is referred to as the Alpine orogenic belt. This orogenic belt consists of a series of mountain ranges that extend from the Mediterranean region through Anatolia and the Caucasus, continuing into the mountains of Iran, the Transhimalayas, the Himalayas, and the Indochinese Peninsula, finally extending into the Java and Sumatra region (Figure 2.2).

In Europe, two main mountain range are distinguished from west to east:

a) The northern range comprises the Pyrenees, Northern Alps, Carpathians, Balkanides and Pontic Mountains.

b) The southern range includes the Appennine Mountains, Atlas Mountains, Southern Alps, Dinarides, Hellenides, and Taurus Mountains, which then extend into Asia.

The evolution of this orogeny is intimately tied to the formation, evolution and eventual closure of the Tethys Ocean, which had a profound impact on the geological history and the development of Earth's continents (Mountrakis 2010).
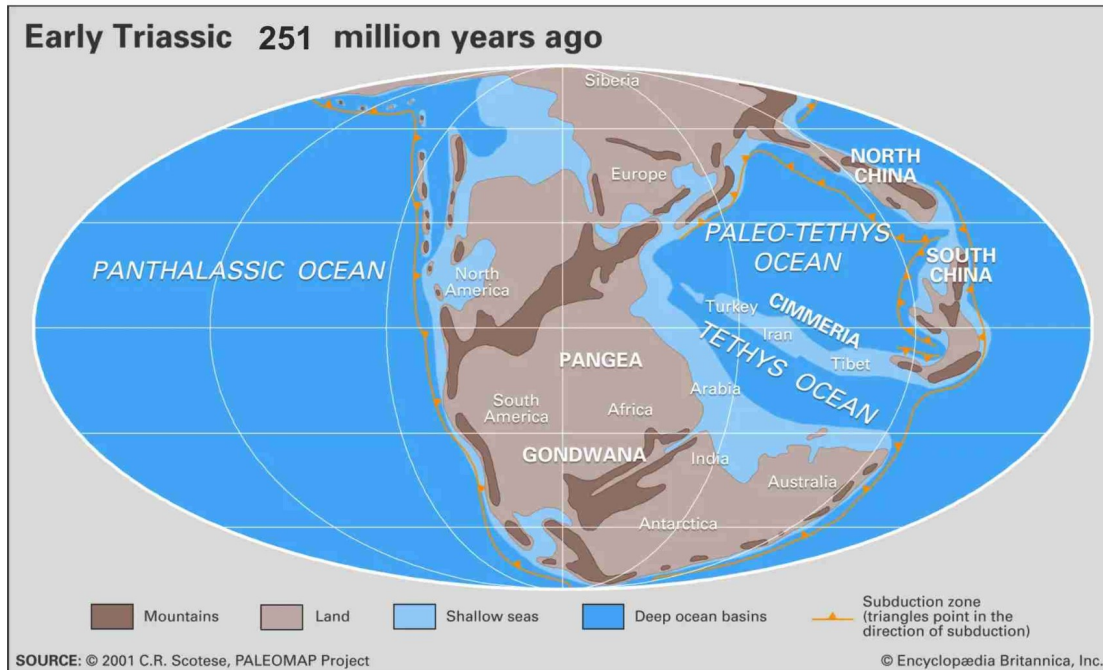
Figure 2.1 Paleogeographical reconstruction of the super-continent Pangaea illustrating the position of Tethyan ocean realms, separated by the Cimmerian continent comprising multiple plates. Laurasia encompassed North America and the northern portion of Eurasian, situated above the Alpine-Himalayan mountain ranges. On the other hand, Gondwana included South America, Africa, India, Australia, and the southern regions of Eurasian located below the Alpine-Himalayan chain. https://www.britannica.com/place/Tethys-Sea (04/07/2023).

The Tethys Ocean, as described Suess (1888, 1901), was an oceanic system that existed from the Triassic to Cenozoic era and extended from eastern Asia all the way to the southern/southeastern Europe.

Notably, according to Gawlick and Missoni (2019), the oceanic system separating the Eastern and Southern Alps, the Western Carpathians, the Apennines, the Dinarides, the Albanides, and the Hellenides from the rest of Europe is not considered part of the Tethyan oceanic realm from the Jurassic period onward. Instead, this oceanic system is an extension of the Central Atlantic Ocean to the east and is referred to as the Alpine Atlantic, encompassing the Ligurian-Piemont-Penninic-Vah Ocean (Figure 2.3) (Missoni and Gawlick 2011).

Figure 2.2 Illustration of the main orogenic belts formed after the collision of the Laurasia plate and segments of the Gondwana plate (Marko et al. 2020).

In a broader perspective, the Tethys Ocean (sensu stricto) existed previous to the break up of the super-continent Pangaea and was situated along the southeastern margin of Laurasia and the northeastern margin of Gondwana (Figure 2.1). As Pangaea gradually fragmented, with blocks rifting from Gondwana and drifting towards the Eurasia plate, the Tethys Ocean located between them was gradually consumed (Frisch et al. 2011). This process marked the gradual closure, resulting in the eventual disappearance of the Tethys Ocean in the Paleogene.

The complex tectonic setting involving multiple blocks between Gondwana and the Eurasian plate during the subduction of the Tethys Ocean adds complexity to the sequence of events in the Mesozoic era. The Şengör's model (1984, 1985) aims to clarify the confusion by presenting a paleogeographical reconstruction that describes the existence of two distinct oceanic regions (Gawlick and Missoni 2019). The Paleo-Tethys Ocean, which existed from the late Palaeozoic to early Cretaceous, occupied the northern region of the Tethyan realm, while the Neo-Tethys Ocean, from the Triassic to the Neogene, located southern of Paleo-Tethys ocean. According to this model, the Cimmerian continent acted as a separator between these two oceans, comprising multiple plates (Figures 2.1 and 2.4).
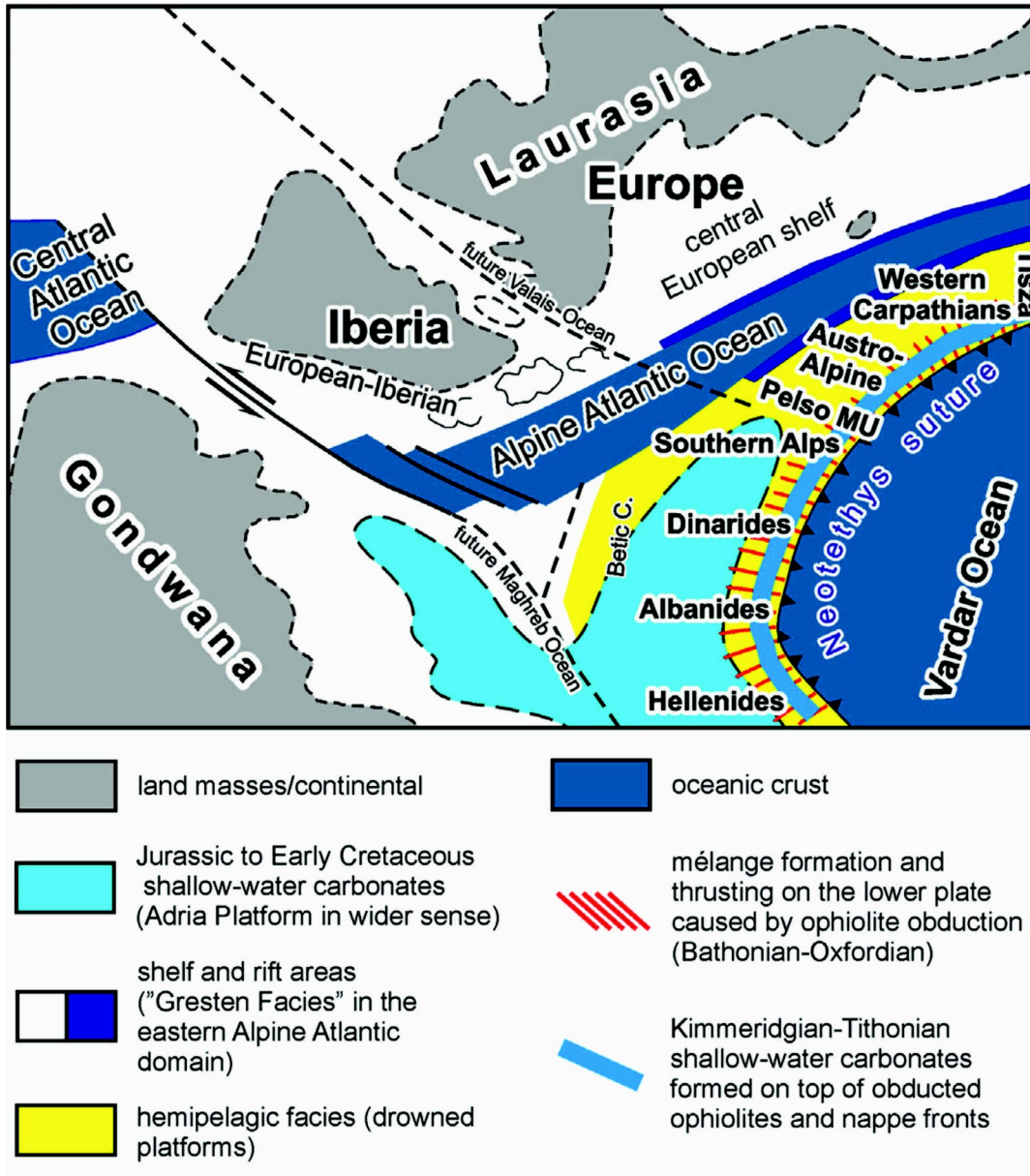
Figure 2.3 Paleogeographic reconstruction of the Western Tethyan realm and other oceanic systems during the Late Jurassic, illustrating the Neotethyan Belt striking from the Carpathians to the Hellenides and the Piemont/Ligurian Ocean (Alpine Atlantic) to the west (Missoni and Gawlick 2011).

The closure of the Paleo-Tethys Ocean in the northern part of the Cimmerian continent(s), and the subsequent collision, resulted in the formation of the Cimmerian Orogeny. Simultaneously, the closure of the Neo-Tethys Ocean led to the development of the Alpine Orogeny.
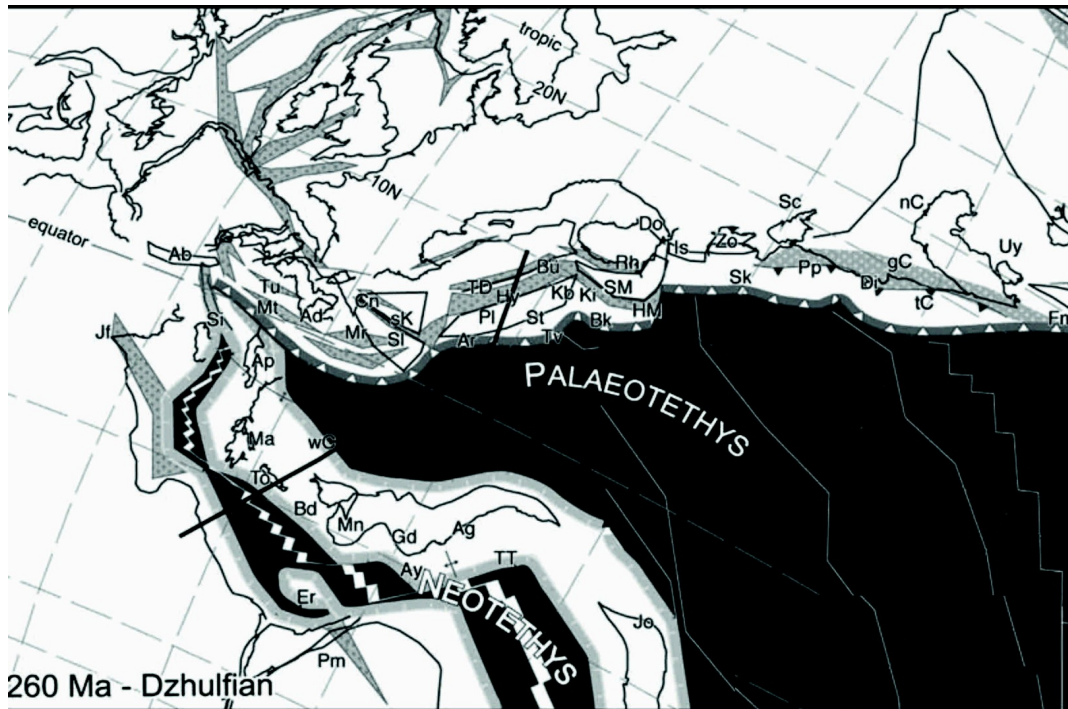
Figure 2.4 Western Tethys paleogeographical reconstruction for the Late Permian, illustrating the position of the Paleo-Tethys Ocean and the Neo-Tethys Ocean after Stampfli and Kozur (2006).

However, in the case of the eastern Mediterranean orogenic belt, which represents the western portion of the Tethys Ocean, the geological history is complicated compared to the Himalayas and other regions in Asia. The tectonic processes since Jurassic period have played a significant role in shaping the eastern Mediterranean region, which was affected by younger polyphase tectonics, including rotation and strike-slip motion.

The geotectonic evolution of this orogenic belt reflects a complete Wilson Cycle (Gawlick and Missoni 2019). It initiates with initial continental rifting and the separation of continents in the latest Permian, followed by the widening of the rift and the formation of a mid-ocean ridge with oceanic spreading during Middle Triassic (Pelsonian/Illyrian) (Bortolotti et al. 2004b, Gawlick and Missoni 2019). A passive margin evolves from the Middle Triassic to early Middle Jurassic along the eastern edge of the Adriatic plate (Gawlick and Missoni 2019). A geodynamic shift occurs, transitioning from extensional to compressional tectonics, in the Middle Jurassic, leading to the partial closure of the western part of the ocean (e.g., Gawlick et al. 2008,

2016, Kilias et al. 2010). The oceanic plate starts to subduct eastward beneath the other, resulting in the consumption of the oceanic crust into the Earth's mantle and the formation of an ensimatic island-arc (e.g., Zachariades 2007, Michail et al. 2016, Dilek et al. 2008, Saccani et al. 2015, 2017). Intra-oceanic subduction also triggers the development of a supra-subduction oceanic lithosphere in the back arc basin (e.g., Zachariades 2007).

During the Middle to Late Jurassic, ophiolite obduction over the former passive Adriatic margin and the propagation of nappe stack occurred from the distal shelf areas to the proximal areas, resulting in crustal thickening (e.g., Gawlick and Missoni 2015, Gawlick et al. 2016a, 2016b, 2017a, compare to Schmid et al. 2008, 2020, Karamata 2006, Robertson 2012, Bortolotti et al. 2012). Subsequently, in the Late Jurassic to Early Cretaceous, the orogen experience uplift, while the eastern part of the ocean remain open until the Paleogene (Gawlick et al. 2019). Ongoing convergence eventually lead to the collision of the tectonic plates involved, giving rise to the orogenic belt.

This geological history, described above, characterize the Eastern Alps, the Western Carpathians, the Dinarides, the Albanides, and the Hellenides, which are recognized as part of the Neotethyan Belt, a continuous NNE-SSW trending belt facing the north-western margin of the Neo-Tethys Ocean, existed from the Triassic until the Early Cretaceous (Figure 2.3) (Missoni and Gawlick 2011).

Although, the exact tectonic processes that transpired between the Eurasian plate and Adriatic plate during the Mesozoic era remain uncertain. The main disagreement concerns the number of micro-continents involved in forming the region as well as the number of oceans developed during that time (Figures 2.4 and 2.5) (e.g., see Channell and Kozur 1997, Karamata 2006, Schmid et al. 2008, Chiari et al. 2011, Robertson 2012). Moreover, the term Neo-Tethys is also used to describe a branch of oceanic realms situated southeast of the Alpine Atlantic and the Western Alps (Schmid et al. 2008 and references within).
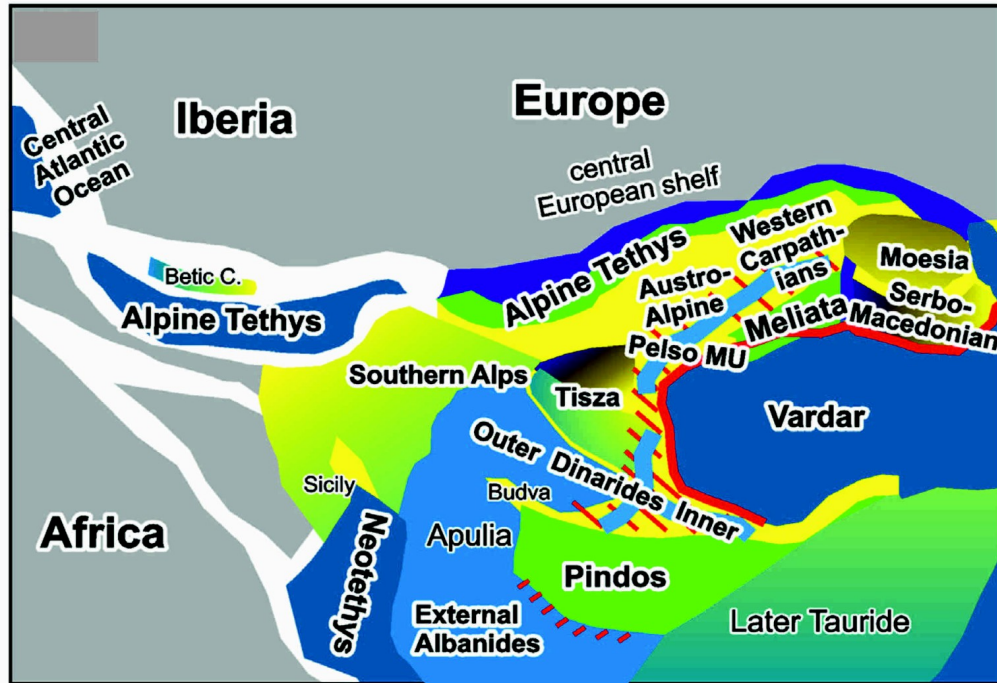
Figure 2.5 Western Tethys multi-ocean reconstruction for the Middle-Late Jurassic adapted from Stampfli and Kozur (2006) (Gawlick and Missoni 2019).

2.2 Evolution of the passive continental margin of the Western Neo-Tethys realm

The Triassic-Jurassic sedimentation pattern, as follows, has been reconstructed by Gawlick et al. (2008), (2017b), Sudar et al. (2013), Gawlick and Missoni (2019), and references therein, for the Inner Dinarides and the Albanides, which is also representative for the Eastern and Southern Alps, the Western Carpathians, and the Hellenides (Figure 2.6). This brief but compact description of sedimentary evolution is related to the geodynamic setting of the Neo-Tethys realm and is essential in order to comprehend the geology of the Hellenides.

Following the crustal extension in the western Tethys realm, the latest Permian period is marked by a rift stage, during which grabens formed. Subsequently, coarse-grained siliciclastic and evaporite sediments were deposited within these grabens.
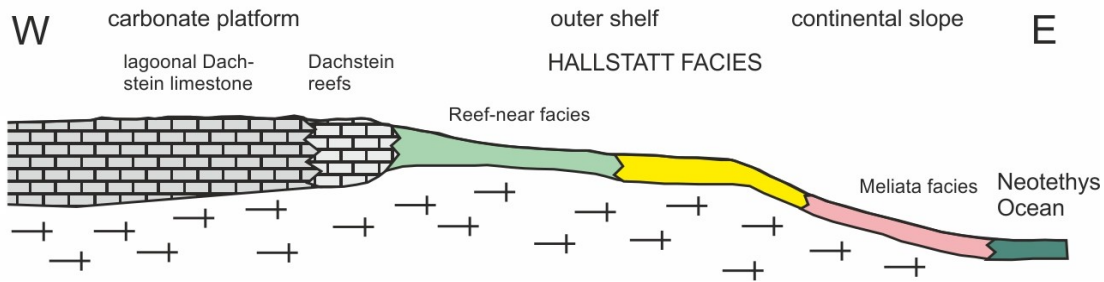
Figure 2.6 Middle to Late Triassic paleogeographic arrangement of the passive continental margin facing the Western Neo-Tethys realm (adapted from Gawlick et al.2016).

During the early Early Triassic, the deposition of the siliciclastic sediments persisted, which was succeeded by the initiation of carbonate production in the late Early Triassic.

Throughout the Early-Middle Triassic, there was a notable rise in carbonate production, resulting in the formation of shallow-water carbonate ramps (Steinalm Carbonate Ramp). From the Middle Anisian onward, a transition occurred from a restricted setting to an open-marine environment, reflecting a considerable drowning event that took place during that period. This transition is indicated by the red nodular limestone of the Bulog Formation, which is well-known in the Dinarides and Hellenides (e.g., Wendt 1973, Sudar et al. 2013).

The drowning event was accompanied by the development of a horst and graben morphology, that are signifying the final stages of the gradual break up Neo-Tethys Ocean (Sudar et al. 2013). During that period, the eastern passive margin of the Adriatic plate, which faced the Neo-Tethys Ocean to the east, started to shape (for a different view see Karamata 2006, Robertson 2012).

The Late Anisian was marked by extensive volcanic activity, probably linked to the ongoing process of oceanic break up, which had a negative impact on carbonate production (Gawlick et al. 2012). Throughout the Late Anisian to Late Ladinian, there was a continuous deposition of deep-water sediments. Consequently, the volcaniclastic rocks are intercalated with successions of radiolarites and siliceous limestones.

In the Late Ladinian carbonate production recovered as the Wetterstein Carbonate Platform commenced, which persisted until the Early Carnian. The initial phase of the platform development, is characterized by deposition in the central shelf of the passive

margin. The sea level change in earliest Early Carnian created favourable conditions for the growth and expansion of the carbonate platform towards the proximal regions of the passive margin (Missoni et al. 2012).

In the Middle Carnian, siliciclastic deposition, connected with a widely developed event (Schlager and Schöllnberger 1974), negatively impacted carbonate production, ultimately terminating the development of the Wetterstein Carbonate Platform.

During the Late Carnian, a significant increase in carbonate production occurred, leading to the deposition of shallow-water carbonates throughout the Norian and Rhaetian (Dachstein Carbonate Platform).

This late Middle Triassic sedimentary evolution, with the development of Wetterstein Carbonate Platform and the Dachstein Carbonate Platform, characterizes the shallow-water deposition in the proximal to central shelf area of the passive margin whereas towards the outer shelf region and continental slope, deep-water deposition occurred (Figure 2.6). Specifically during the Middle Triassic, in the reef-near facies of the outer shelf, bedded grey hemipelagic limestones with chert nodules were deposited (Figure 2.6) (Gawlick and Missoni 2019). Subsequently, in the Late Triassic, these grey limestones became intercalated with shallow-water turbidites derived from the central shelf area of the platform.

The outer shelf region underwent the deposition of the Hallstatt Facies, starting from the Middle Anisian, which are defined by condensed colorful open-marine limestones (Figure 2.6) (Krystyn 1980, 2008). At the same time, the continental slope region was distinguished by the Meliata Facies, consisting of Middle Triassic radiolarites and Late Triassic bedded grey limestone with chert nodules (Figure 2.6) (Gawlick and Missoni 2019).

During the Earliest Jurassic, sedimentation was affected by the see-level drop, resulting in the deposition of grey limestones with chert nodules in the deeper areas, whereas the Dachstein Carbonate Platform emerged.

After the sedimentation stabilized in the Hettangian, the Ammonitico Rosso Facies were deposited. Throughout the late Early to Middle Jurassic, sedimentation was mainly pelagic (Bernoulli and Jenkyns 1974), with the exception of the deposition of early Middle Jurassic red nodular limestones and red marly limestones.

During the Middle Jurassic, there was a reduction in carbonate production, which was replaced by the deposition of radiolarites (Baumgartner 1985, Baumgartner et al. 1995). Concurrently, the Alpine Atlantic began to open, and the Neo-Tethys realm was influenced by intra-oceanic subduction (Karamata 2006, Schmid et al. 2008, Gawlick and Missoni 2019). Subsequently, from the Middle Jurassic onward the passive continental margin transitioned into an active continental margin, representing the lower plate.

2.3 Hellenic orogenic belt

2.3.1 Internal and External Hellenides

The collision of tectonic blocks that rifted from the Gondwana continent to collide with Eurasia plate caused the emergence of an arc-shaped orogenic belt that encompasses the Dinarides and the Hellenides and expands into the Taurides (Kilias 2021). Contractional tectonics were initiated by the closure of a single or several Mesozoic Tethyan oceanic basins, which led to a very complex tectonic structure and multiple metamorphosed Hellenic realm (Kilias 2021). However, there is no agreement concerning the evolution of the Mesozoic tectonic processes that impacted in order to form the present situation, which characterizes the Hellenic orogenic belt. The main arguments revolve around the where and how many Mesozoic oceanic basins existed along the European and Adriatic continental plates.

The long-established classification of the Hellenides includes the Internal Hellenides and the External Hellenides, which are further divided into tectono-stratigraphic zones whose names are still widely used (Figure 2.7) (Brunn 1956, Aubouin 1959). During the Eocene to Oligocene, the Internal Hellenides were thrust westward towards the External Hellenides (Godfriaux 1968, Kilias 2021, and references therein).

Their differentiation is mainly based on the fact that the External Hellenides are generally characterized by continuous sedimentation from the Triassic to the Miocene and the absence of ophiolites. Additionally, they sustained only the Tertiary orogenic

processes, lacking the multiple deformational events that the Internal Hellenides underwent during the Mesozoic era (Kilias 2021). Another factor would be that the Internal Hellenides experienced considerable magmatic activity during the Mesozoic-Tertiary and Paleozoic eras.

2.3.1.1 External Hellenides

The External Hellenides comprise the areas that are located in western Greece, including the Ionian Islands, Epirus, the western part of the Central Greece Region, the biggest part of the Peloponnese, Crete, Karpathos, and Rhodos (Figure 2.7). These regions are included within the following main tectono-stratigraphic zones, which were progressively emplaced from east to west through intensive compressional tectonic processes.

The External Hellenides, as described by Kilias (2021) and references therein, haven't experienced consequential metamorphic events. They primarily consist of Mesozoic to Cenozoic pelagic and shallow-water carbonates, along with deep-water sediments and Paleocene to Miocene orogenic deposits.

Paxos Zone is characterized by Late Triassic evaporite deposition, followed by continuous carbonate sedimentation from the Late Triassic to the Oligocene-Miocene. While sedimentation primarily occurred in shallow-water environments, some deep-water facies are also encountered (Aubouin 1956, Kilias 2021, Zoumpouli et al. 2010, Papanikolaou 2013). The main difference from other External Hellenides is the absence of orogenic deposits.

Similarly to the Paxos Zone, the Ionian Zone experienced continuous Triassic to Early Jurassic shallow-water carbonate sedimentation on evaporites considered to be of Early Triassic or Permian-Triassic age (Brunn 1956, Aubouin 1959). The characteristic Pantokrator Formation was deposited during that time (Late Triassic-Early Jurassic).
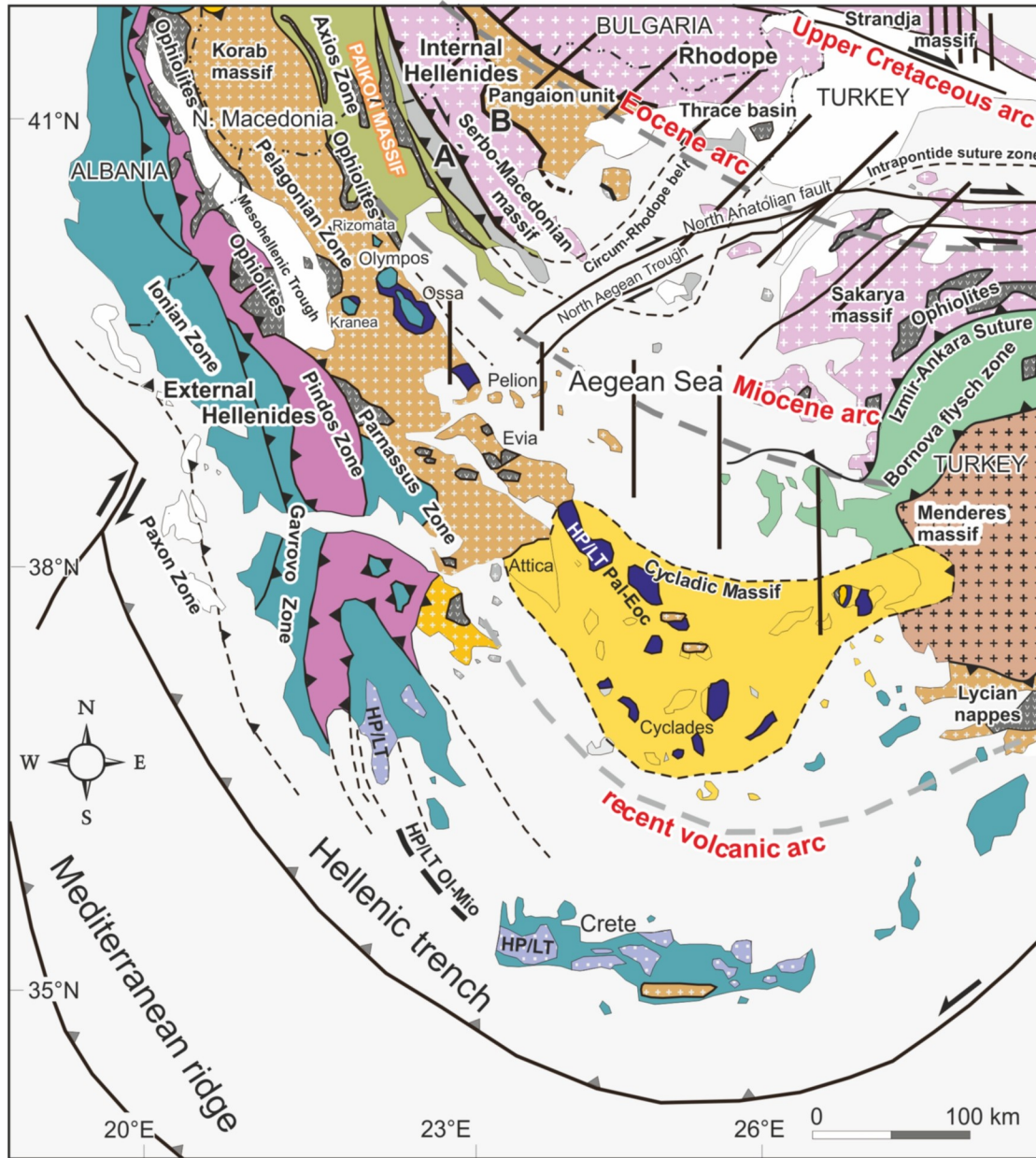
Figure 2.7 Geological map of the Internal and the External Hellenides, including the main tectono-stratigraphic zones of the Hellenides (modified after Kilias 2021).

However, from the Early Jurassic to the Eocene, the sedimentation shifted towards pelagic environments, leading to the deposition of radiolarites and pelagic limestones, such as the characteristic Ammonitico Rosso Facies and Vigla limestones (Kilias 2021, Mountrakis 2010, and references therein). Finally, sedimentation ended with the deposition of Oligocene-Miocene orogenic sediments. Noteworthy, even though the

sedimentation of the Ionian Zone is generally considered continuous, there are observations of unconformities in the Late Jurassic to Early Cretaceous (Mountrakis 2010, and references therein).

Furthermore, the Gavrovo Zone is situated between the Ionian Zone and the Pindos Zone and is also exposed as a tectonic window in several localities within the Hellenic orogenic belt (Godfriaux 1968, Godfriaux and Ricou 1991, Kilias 1995, Kilias et al. 2002). It is built up primarily by shallow-water carbonates, which were deposited continuously on a Paleozoic basement throughout the Triassic to Eocene, passing into Late Eocene-Early Oligocene orogenic deposits (Brunn 1956, Aubouin 1959, Mountrakis 2010).

The Paxos Zone, the Ionian Zone, and the Gavrovo Zone are acknowledged as portions of the Adriatic Plate. This plate was a block that rifted from Gondwana and subsequently drifted northward, eventually colliding with Eurasia. During this process, a carbonate platform evolved on the Adriatic continental plate, receiving continuous carbonate sedimentation from the Triassic to the Tertiary (Mountrakis 2010).

Meanwhile, the Pindos Zone is traditionally considered a tectono-stratigraphic zone part of the External Hellenides (Brunn 1956, Aubouin 1959). The Triassic to Middle Jurassic sedimentary evolution of the Pindos Zone is characterized by deep-water sediments, including radiolarian cherts and siliceous carbonates, along with a volcano-sedimentary sequence and various colored open-marine limestones. Above these Triassic to Middle Jurassic rocks, Late Jurassic sediments occur, including brecciated limestones, calc-sandstones, and limestones containing calpionella. This is followed by an Early Cretaceous formation known as the "Premier Flysch" of Pindos (Manakos 1983). Subsequently, during the Middle-Late Cretaceous, the Pindos Zone exhibited the deposition of pelagic limestones, succeeded by Paleocene-Eocene orogenic sediments (Brunn 1956, Aubouin 1959). The paleogeographic position of the Pindos Zone is very crucial and will further analyzed in a different chapter.

The Parnassus Zone, situated between the Pindos Zone and the Sub-Pelagonian Zone in central Greece, is also regarded as part of the External Hellenides. Its dominant rock formations include Middle Triassic dolomites, Late Triassic to Early Jurassic limestones, Middle Jurassic shallow-water oolitic limestones, Late Jurassic to Eocene

carbonates, and Eocene-Oligocene orogenic deposits (Mountrakis 2010, Kilias 2021). One of the notable features of the Parnassus Zone is the presence of bauxite deposits formed by laterization of ophiolites. Bauxite deposition took place in three distinct events (a late Middle Jurassic event, a Late Jurassic event, and a late Middle Cretaceous event), resulting in the formation of three separate bauxite horizons (Mountrakis 2010, Carras 1995, Nirta et al. 2018, and references therein).

In addition to the main tectono-stratigraphic zones mentioned earlier, the Plattenkalk and Phyllite-Quartzite units, are also distinguished, which are exhumed in the southern Peloponnese and Creta Island (Kilias et al. 1994, Fassoulas et al. 1994, Jolivet et al. 1994, Skourtsos and Lekkas 2010, Seybold et al. 2019, Kilias 2021). The Plattenkalk unit is composed of Triassic to Eocene pelagic carbonates with chert nodules or intercalated with cherts, comparable to the carbonates of the Ionian Zone (Bonneau 1984, Mountrakis 2010, Kilias 2021). Overlying tectonically the Plattenkalk unit is the Phyllite-Quartzite unit, considered to be of Permian-Triassic age (Kilias et al. 1994, Mountrakis 2010). It consists of phyllites, quartzites, and metamorphosed sediments, as well as a few intercalated volcanics.

2.3.1.2 Internal Hellenides

Further in eastern Greece, the Internal Hellenides are located, extending from Central and Western Macedonia, Thessaly, the eastern part of the Central Greece Region, Euboea, the Aegean Islands, and a part of the Peloponnese (Argolida) to Eastern Macedonia and Thrace (Mountrakis 2010). They are subdivided into several tectono-stratigraphic domains according to their paleogeographic and lithological characteristics, from west to east (Figure 2.7) (Brunn 1956, Aubouin 1959, Godfriaux 1968, Mercier 1968, Jacobshagen et al. 1978, Jacobshagen 1986, Mountrakis 1986, Kilias 1991, Papanikolaou 2009, Kilias et al. 2016, Kilias 2021): Sub-Pelagonian Zone, Pelagonian Zone (also known as Pelagonia), Axios Zone, and Circum-Rhodope Belt, as well as the Hellenic hinterland that is composed of the Serbo-Macedonian and Rhodope massifs.

The most characteristic rocks in the Internal Hellenides are mainly Paleozoic and older metamorphic rocks of various types, Mesozoic carbonates, ophiolites, sedimentary deposits, and igneous rocks (Mountrakis 2010, Kilias et al. 2010, Kilias 2021). The geotectonic evolution of the Internal Hellenides was strongly influenced by Middle Jurassic intra-oceanic subduction and the subsequent obduction of the Neo-Tethyan ophiolites onto of the Pelagonian marginal formations (e.g., Bernoulli and Laubscher 1972, Mercier et al. 1975, Zimmerman and Ross 1976, Robertson et al. 1996, Rassios and Moores 2006, Karamata 2006, Gawlick et al. 2008, Schmid et al. 2008, Kilias et al. 2010).

The Pelagonian Zone is characterized by its older rocks, primarily consisting of Paleozoic or older metamorphic rocks, such as gneisses, amphibolites, and schists, which have been intruded by Carboniferous granitoids (Mountrakis 1986, Koroneos et al. 1993, Kilias et al. 2010, Kilias 2021). Overlying these basement-type rocks is a Permian-Triassic volcano-sedimentary sequence, followed by Early Triassic to Middle Jurassic metamorphosed carbonates (Scherreicks 2000, Scherreicks et al., 2009, Mountrakis 1986). Throughout its geological history, the Pelagonian Zone has been subject to several metamorphic and deformational events (Kilias and Mountrakis 1987, Kilias et al. 2010, Kilias 2021).

The Early Triassic to Middle Jurassic carbonates are tectonically overlain by ophiolites, which are presently distinguished along two main ophiolite belts. These belts extend through the Albanides and the Dinarides, forming the Mirdita-Pindos and the Vardar-Axios ophiolite belts, along the western and eastern parts of the Pelagonian Zone and its northward continuation (Korabi Units), respectively. Beneath the ophiolites, well-preserved Middle-Late Jurassic ophiolitic mélanges are exposed in several localities.

Late Jurassic-Early Cretaceous sedimentary carbonate successions unconformably overlay the obducted ophiolites in several places, followed by late Early Cretaceous shallow-water carbonates passing upwards into Late Cretaceous-Paleocene orogenic sediments (Mercier 1968, Carras et al. 2004, Photiades et al. 2007). The presence of these ophiolites, including their mélanges and Late Jurassic carbonate sediments related to their emplacement, is the main interest of this work.

The Sub-Pelagonian Zone (Aubouin 1959) is characterized by Mesozoic deep-water sedimentary rocks and ophiolites, situated tectonically along the western segment of the Pelagonian Zone. The dominant rocks comprising the Sub-Pelagonian Zone are Early Triassic to Late Jurassic carbonates, open-marine limestones, and deep-water siliceous sediments (Kilias 2021).

On the other hand, the eastern segment of the Pelagonian Zone is overthrust by the Axios Zone, which includes the Vardar-Axios ophiolites (Bebien et al. 1986). Mercier (1968) subdivided the Axios Zone from west to east into Almopia, Paikon, and Peonia subzones. The Almopia subzone is composed of Paleozoic metamorphic rocks such as gneiss and schists, Mesozoic deep-water sediments, and ophiolites (Kauffmann et al. 1976). To the east, the Almopia subzone is thrust over by Paikon subzone.

The Paikon subzone is characterized by Triassic recrystallized carbonates intercalated with schists and phyllites, succeeded by a Middle-Late Jurassic volcano-sedimentary sequence. This is followed by a Late Jurassic to Early Cretaceous carbonate succession and ophiolites (Mercier 1968, Mavrides et al. 1982, Brown and Robertson 2004, Katrivanos et al. 2013). Katrivanos et al. (2013) suggested that the metamorphic rocks of the Paikon subzone possibly originated from the Pelagonian Zone and are exposed as multiple tectonic window below the obducted ophiolites and their overlying successions.

The Peonia subzone is mainly composed of Triassic-Jurassic recrystallized carbonates, other metamorphic and igneous rocks, as well as deep-water sediments and ophiolites, including their mélanges (Mercier 1968, Meinhold et al. 2009, Kilias 2021). Moreover, an early Late Jurassic (Oxfordian) granitic body (Fanos granite) intruded the ophiolites before their emplacement over the eastern Pelagonian margin (Michail et al. 2016).

The geochemical and petrological analysis conducted by Zachariadis (2007) provided that the formation of Vardar-Axios ophiolites took place during 170-155 Ma within a supra-subduction oceanic lithosphere (SSZ), which developed behind an eastward intra-oceanic subduction setting (e.g., Stampfli 2000, Zachariadis et al. 2006).

Several model regarding the derivation of the Vardar-Axios ophiolites propose that these ophiolites originated from a Mesozoic autonomous ocean situated among the

eastern margin of the Pelagonian continent and the broader Serbo-Macedonian and Rhodope massifs (e.g., Roddick et al. 1979, Smith and Spray 1984, Channell and Kozur 1997, Brown and Robertson 2004, Stampfli and Kozur 2006, Robertson et al. 2012).

Some authors and research groups (Robertson et al. 1996, Brown and Robertson 2003, 2004, Papanikolaou 2009, 2013, Saccani et al. 2008) consider that the Peonia subzone represents an oceanic basin that evolved as a back arc basin, forming supra-subduction (SSZ) ophiolites due to the subduction of the Almopia oceanic basin behind the Paikon volcanic arc (compare Ricou et al. 1998, Vergely and Mercier 2000).

According to current popular reconstructions, the Vardar-Axios ophiolites were formed in the Neo-Tethys oceanic floor and were emplaced in westward direction over the eastern Pelagonian continental margin (Schmid et al. 2008, 2020, Gawlick et al. 2008, 2016a, 2016b, 2017a, 2020, Kilias et al. 2010, Missoni and Gawlick 2011, Bortolotti et al. 2012, Katrivanos et al. 2013, Kostaki et al. 2013, 2014, Ferrière et al. 2015, 2016, Michail et al. 2016, Gawlick and Missoni 2019, Kilias 2021). Following the emplacement of the ophiolites in the Middle to early Late Jurassic, the western section of the Neo-Tethys Ocean underwent closure, while the eastern section is believed to have persisted as a significantly reduced SSZ Vardar-Axios Ocean, with portions of the oceanic floor lasting through the latest Cretaceous (Gawlick et al. 2008, 2016a, 2016b, 2017a, 2020, Kilias et al. 2010, Kilias 2021).

On the contrary, a different view about the Vardar-Axios ophiolites proposes that their emplacement over the Pelagonian margin took place in an eastward direction, deriving from the Pindos Ocean (e.g., Sharp and Robertson 2006).

The tectonic interface between the Axios Zone and the Hellenic hinterland, i.e., the Serbo-Macedonian and Rhodope massifs, is known as the Circum-Rhodope Belt (Kauffmann et al. 1976, Kilias et al. 1999, Tranos et al. 1999, Meinhold et al. 2009, Meinhold and Kostopoulos 2012). The most dominant rocks included in the Circum-Rhodope Belt are Triassic shallow-water and hemipelagic carbonates, an Early-Middle Jurassic turbiditic succession (Melissochori Formation: Kockel and Mollat 1977), deep-water sediments, and magmatic rocks including granites and mafic rocks, as well as a Late Paleozoic volcano-sedimentary sequence (Kauffmann et al. 1976).

The Hellenic hinterland exhibits a complicated tectonic structure characterized by imbricated nappes composed of several metamorphosed units (Kilias 2021). The Serbo-Macedonian and Rhodope massifs (Kockel et al. 1971, Kockel and Mollat 1977, Kilias et al. 1999, Kilias 2021, and references therein) comprise various types of Paleozoic and older metamorphic rocks, including intercalations of schists, gneisses, orthogneisses, and marble, as well as Mesozoic and Cenozoic granitoids intrutions (Dimitrijevic 1974, 1997). Additionally, there is a considerable presence of migmatites, amphibolites, mafic, and ultramafic rocks (Kilias 2021, and references therein).

Finally, another noteworthy feature of the Hellenic orogenic belt is the presence of two Paleogene sedimentary basins:

a) The Mesohellenic Trough formed during the Middle Eocene to Late Miocene, with its sediments deposited on Late Cretaceous limestones, covering a portion of the Pindos-Vourinos ophiolites (Vamvaka et al. 2006, Vamvaka et al. 2010, Kilias et al. 2013, 2015) and

b) the Thrace Basin formed during the Middle-Late Eocene to Oligocene on the metamorphic rocks of the Rhodope massif (Kilias and Mountrakis 1998, Kilias et al. 2013, Kilias et al. 2015).

Both basins are dominated by strike-slip motions that took place during the Oligocene to Miocene, which are related with the oblique plate convergence of the Adriatic plate and the Internal Hellenides (Vamvaka et al. 2006, Vamvaka et al. 2010, Kilias et al. 2013, Kilias et al. 2015).

2.4 Geodynamic models about the origin of the ophiolite belts

The ophiolites exposed along the Hellenides represent the remnants of the Mesozoic oceanic lithosphere and constitute a critical characteristic that assisted in acknowledging the geotectonic and geodynamic processes that formed the entire Hellenic orogenic belt (Figures 1.1 and 2.7) (e.g., Moores 1969, Bortolotti et al. 1969, Zimmerman 1969, 1972, Dercourt 1970, Bernoulli and Laubscher 1972, Dewey et al. 1973, Smith and Spray 1984, Channell and Kozur 1997). Despite the fact that they have undergone decades of research, their derivation remain a subject of controversy to this day (e.g., Mercier et al. 1975, Mountrakis 1986, Robertson and Shallo 2000, Stampfli and Borel 2002, Brown and Robertson 2004, Gawlick et al. 2008, 2020, Schmid et al. 2008, 2020, Kilias et al. 2010, Gawlick and Missoni 2019, Robertson 2012, Kilias 2021).

These ophiolites currently extend across the Albanides and the Dinarides, shaping the Mirdita-Pindos and Vardar-Axios ophiolite belts in the western and eastern segments of the Pelagonian Zone, including its northward continuation (Korabi Units), respectively (Figure 2.8). The most discussed geodynamic models addressing the paleogeographic provenance of the ophiolites within the Hellenic orogenic belt lack consensus regarding the paleogeographic location of the oceanic basin(s), as well as the direction and timing of emplacement of the ophiolites over the Pelagonian margin or margins. At this point, a brief summary of various reconstruction models, derived from published scientific perspectives regarding the origin of the ophiolite belts, is presented. This summary is adapted from Robertson (2012) (Figures 2.9 and 2.10).

- The first model suggests that all the ophiolites exposed in the two ophiolite belts originated from a single oceanic basin, potentially either the Pindos Ocean or the Vardar-Axios Ocean (Figure 2.9: a). This ocean experienced eastward subduction, leading to accretion of the formerly passive continental margin and detachment of a portion of the subducting plate, followed by subsequent ophiolite obduction on the Adriatic continental margin (e.g., Kober 1914, Bortolotti et al. 1996, 2004b).
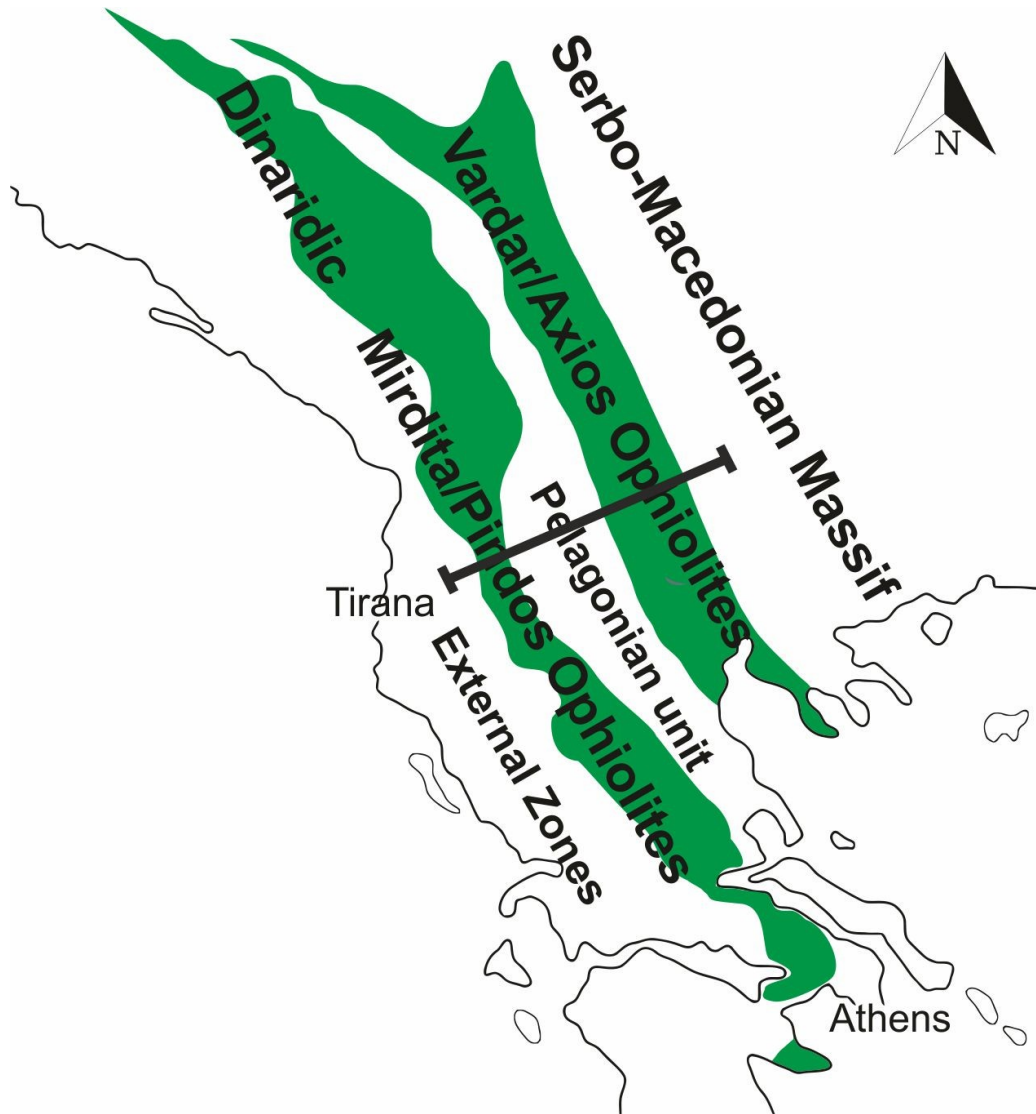
Figure 2.8 Mirdita-Pindos and Vardar-Axios ophiolite belts exhibiting across the Hellenic orogenic belt (adapted from Gawlick et al. 2017a).

- The second reconstruction model considers that all the ophiolites represent remnants of a single ophiolite nappe originating from the Neo-Tethys Ocean (or Vardar-Axios Ocean) situated to the east of the Pelagonian region, which was the eastern passive continental margin of the Adriatic plate (Figure 2.9: b). The Neo-Tethys Ocean underwent a gradual closure, commencing with intra-oceanic subduction, westward nappe stacking, and ophiolite obduction over the eastern Pelagonian continental margin in the Middle Jurassic. The easternmost part of

this ocean, however, remained open until the Late Cretaceous (Kilias et al. 2001, 2010, Gawlick et al. 2008, 2016a, 2016b, 2017a, 2020, Schlagintweit et al. 2008, Missoni and Gawlick 2011).

- The third one similarly supports the idea that all the ophiolites originated from an oceanic basin situated at the eastern Pelagonian margin, where they were obducted westward in Late Jurassic (Figure 2.9: c). In contrast to the second reconstruction model, this model acknowledges the existence of a deep-water basin (Pindos Basin) between the Pelagonian and Adriatic plates (e.g., Aubouin 1973, Bernoulli and Laubscher 1972, Dercourt et al. 1986, Schmid et al. 2008, Ferrière et al. 2015, 2016).

- The fourth model proposes that Vardar-Axios ophiolites were obducted westward onto the eastern Pelagonian margin during the Late Jurassic. Concurrently, to the west of the Pelagonian continental micro-plate, the Pindos Ocean existed until its subduction, which caused eastward ophiolite obduction on the western Pelagonian margin during the Cenozoic (Figure 2.9: d) (e.g., Stampfli and Kozur 2006, Stampfli and Borel 2002, Papanikolaou 2009).

- According to the fifth reconstruction model, all the ophiolites originated from the Pindos Ocean, situated between the Adriatic and Pelagonian continents, and were subsequently emplaced eastward over the western Pelagonian margin (Figure 2.9: e) (e.g., Robertson et al. 1991, Jones et al. 1992, Robertson and Shallo 2000, Karamata 2006, Rassios and Moores 2006, Dilek et al. 2007, Rassios and Dilek 2009).

- The sixth model regards that the Pindos ophiolites originated from the Pindos oceanic basin, situated between the Adriatic and Pelagonian continents. These ophiolites were subsequently emplaced eastward on the western Pelagonian margin during the Late Jurassic (Figure 2.10: f). In contrast, the Vardar-Axios ophiolites are believed to have originated from an ocean located at the east of the Pelagonian continent and were obducted westward over its margin (e.g., Mountrakis 1986).

Figure 2.9 Geodynamic models proposed about the origin of the ophiolites exposed in the Hellenic orogenic belt (Kostaki et al. 2023: adopted from Robertson 2012 and Gawlick et al. 2017b).

- The seventh model suggests that the Pindos ophiolites evolved during the Late Jurassic in an oceanic basin situated between the Adriatic and Pelagonian continents, affected by transpression (Figure 2.10: g). Subsequent to the eastward thrusting of a part of the oceanic crust over the western Pelagonian margin, a metamorphic sole was formed. Inverted faults that developed in the western part of the ocean caused westward ophiolite obduction over the former Adriatic passive margin (e.g., Shallo 1991).

- According to the eighth model, the evolution of a pull apart basin between the Adriatic and Pelagonian continents led to the development of oceanic crust. The closure of this oceanic basin resulted in bidirectional ophiolite emplacement onto the involved margins (Figure 2.10: h) (Shallo and Dilek 2003).

- The ninth reconstruction model considers that all the ophiolites derive from a single oceanic basin and were subsequently emplaced over the Pelagonian continental margin. Following the initial ophiolites emplacement, a large strike-slip fault dislocated them, creating two distinct ophiolite belts (Figure 2.10: i) (Smith and Spray 1984).

- The final model concerning ophiolite formation, as proposed Robertson (2012), commences with the Late Triassic opening of the Pindos Ocean, situated between the Adriatic and Pelagonian continents. The preferred scenario of Robertson (2012) suggests northeastward-directed ophiolite emplacement over the Pelagonian continent during the Late Jurassic, following late Middle Jurassic west-dipping subduction (Figure 2.10: j). The remaining part of this ocean underwent subduction until its ultimate closure, which took place in Late Cretaceous-Eocene times.

Regarding the proposed reconstruction models suggesting a Late Triassic or even Jurassic opening of the Pindos Ocean, it is crucial to emphasize that they are no longer supported after recent research findings in mélanges, which has revealed Middle Triassic oceanic remnants (e.g., Ozsvart et al. 2012, Gawlick et al. 2016a, 2016b).
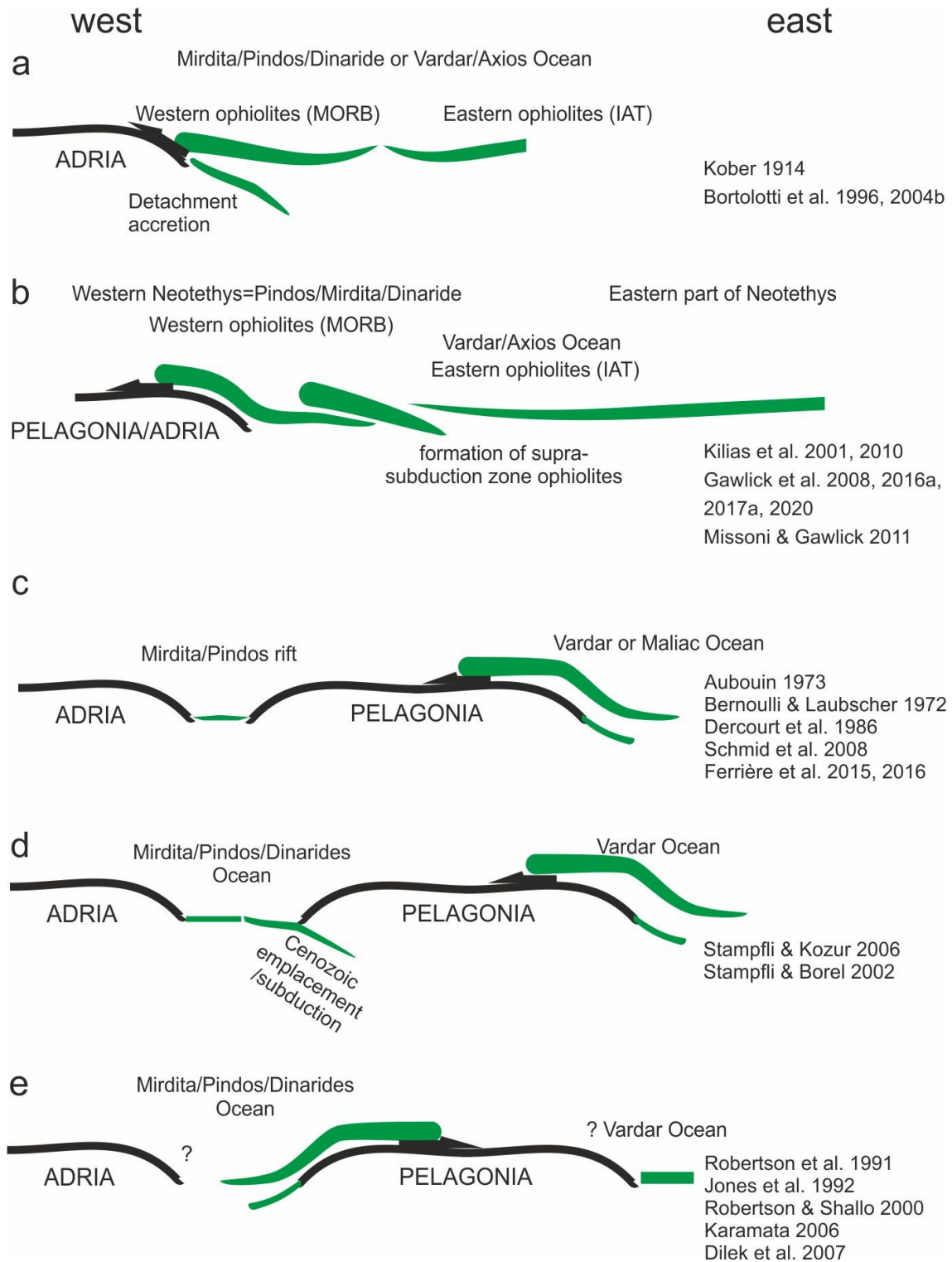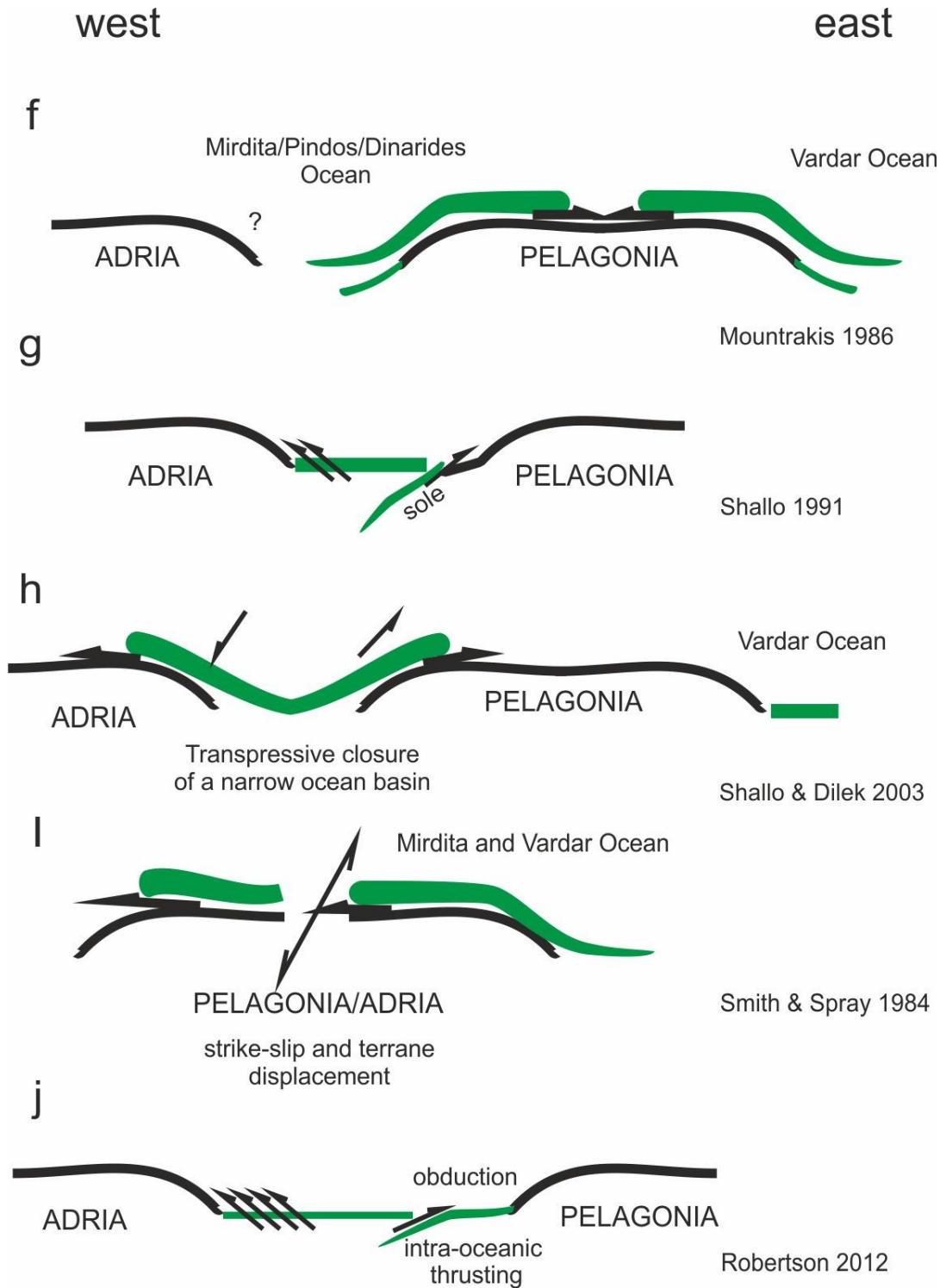
Figure 2.10 Geodynamic models proposed about the origin of the ophiolites exposed in the Hellenic orogenic belt (Kostaki et al. 2023: adopted from Robertson 2012 and Gawlick et al. 2017b).

2.5 Definition and importance of the mélanges

An important factor in advancing the ongoing debate on the derivation of the ophiolites is the examination of ophiolitic mélanges and the presence of exotic blocks within them. Consequently, this study explores ophiolitic mélanges associated with the Pindos and Koziakas ophiolites, specifically focusing on the incorporation of exotic carbonate blocks.

Greenly (1919) invented the term "mélange" based on his research of a rock formation on Anglesey. He described this formation using the following, "The majority of Gwna rocks were a chaotic assemblage of limestones, radiolarites, turbidites, and basalts, which may occur associated with peridotites, gabbros and blue-schists. They are widespread among active continental margins and mountain, kilometers in size and surrounded by a plastic rock matrix." Since then, mélanges have been recognized as chaotic formation consisting of a variety of rocks spanning different ages and associated with orogenic processes. Hence, the examination of mélanges within orogenic belts offers crucial insights (Festa et al. 2010, 2019).

Mélanges can be developed by different processes and mechanisms, and they endure multiple deformation events that disrupt and rework their primary structures (Festa et al. 2019). According to the definition provided by Festa et al. (2019), they are debrided as mappable bodies of mixed exotic rocks in an intensively deformed or fragmented matrix. The mélanges can be distinguished into tectonic mélanges (Hsü 1968), sedimentary mélanges (Festa et al. 2010, 2016, 2019 and references therein), and diapiric mélanges (Silver and Beutner 1980) based on the nature of the processes involved in their formation (Figure 2.11).

A specific type of mélanges can form during the process of ophiolite obduction, where trench-like deep-water basins develop in the lower plate position ahead of the advancing nappe stack formed in front of the obducting ophiolites. These trench-like deep-water basins receive synorogenic sediments, and as they integrate into the nappe stack, the sediments undergo shearing (Gawlick and Missoni 2019). This process ultimately results in the formation of the characteristic features observed in sedimentary mélanges.
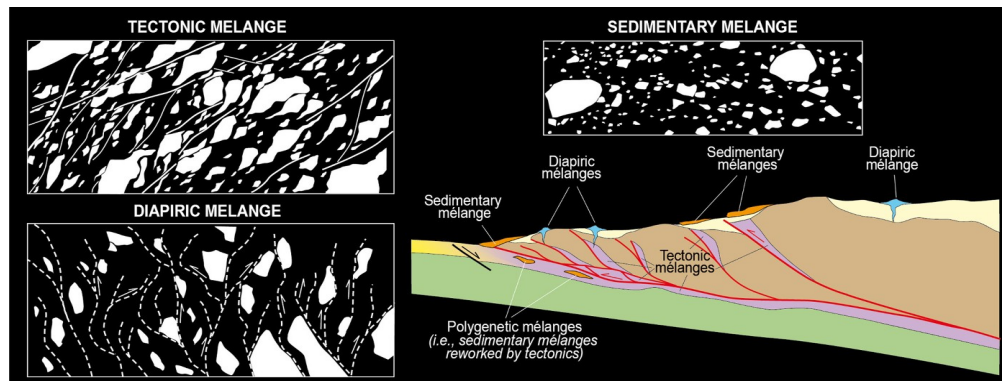
Figure 2.11 Types of mélanges resulted by different processes and mechanisms (Graphical abstract: Festa et al. 2019).

The nappe stack, along with the trench-like deep-water basins, experiences thrusting into the foreland during the ophiolite emplacement (Gawlick et al. 2008, 2016a, 2016b). Consequently, the internal deformation of the sediments within these basins is more intense closer to the obducting ophiolites, gradually diminishing in the distal parts of the propagating nappe stack (Gawlick and Missoni 2019).

Furthermore, as part of the obduction processes, an ophiolitic mélange takes shape at the lower part of the progressing ophiolites (see also Bortolotti et al. 2012, Schmid et al. 2008, 2020, Gawlick and Missoni 2019).

The mélanges formed through the described process include diverse kind of exotic blocks and Mass Transport Deposits within a fine-grained matrix. Generally, various mechanisms have been proposed regarding the manner in which exotic blocks becomes integrated into the mélanges (Şengör 2003, Camerlenghi and Pini 2009, Mutti et al. 2009).

a) Some researchers consider this a tectonic process created either ahead or at the lower parts of the nappes through procedures like tectonic reworking or imbrication (Häfner 1924, Burkhard 1988). Alternatively, it is viewed that these blocks are mechanically abraded and cut off from the lower plate (Schmid et al. 2008).

b) According to a different mechanism, exotic blocks may derive from the advancing nappe and then become incorporated into the nappe stack, resulting in mélanges characterized by tectonically deformed olistostromes and slide blocks (Trümpy 2006).

c) Additionally, they can constitute reworked elements initially developed ahead the advancing nappes (Beck 1912, Weidmann et al. 1984), subsequently overthrust by nappes (Gawlick and Missoni 2019).

Regardless of the varied proposed processes and the mechanisms responsible for the integration of diverse exotic blocks within these type of mélanges, the examination of these blocks plays a crucial role in tracing the route of the upper plate and subsequently reconstructing the geodynamic evolution of an area.

Before the convergence and the following ophiolite emplacement, the lower plate exhibited the typical arrangement of a passive continental margin adjacent to an oceanic realm, from which the ophiolites originated (Frisch and Gawlick 2003). During the obduction processes, the arrangement and structure of the passive continental margin are disrupted. However, careful analysis of the integrated exotic blocks within mélanges can provide detailed insights regarding the route of the ophiolites and therefore can serve as a tool to understand the original arrangement of the passive continental margin.

CHAPTER 3. Methodology

In the first part of this chapter, are briefly described the methods and the means that were used during this research. In the second part, an introduction to the microfacies concept, the Facies Zones, and the Standard Microfacies Types, as well as a short description of the most frequent systems used for carbonate classification, are provided.

The different contrasting aspects about the origin and the direction(s) of the ophiolite obduction created the necessity to make field observations and collect biostratigraphic information from sedimentary successions.

In the studied areas, a detailed examination of the lithology, sedimentary features, and tectonic structures was conducted. Tectonic structures were observed to determine their geometry and kinematics. Fieldwork guidance relied on 1:50.000 scale maps provided by the Institute of Geology and Mineral Exploration (IGME), Greece, including Knidi (Mavridis and Kelepertzis 1993), Kalabaka (Savouat and Lalechou 1972), Mirofillon (Kanakos 1983), and Mouzakion (Karfakis 1984).

Eventually, all the macroscopic observations during fieldwork led to the determination of suitable sampling positions for microfacies and biostratigraphic analysis (Figure 3.1).

Microfacies analysis were conducted to identify microfossils and paleontological characteristics, aiming to determine the paleogeographical environment and the age of the original deposition of the different components and blocks within the studied successions (Flügel 2004).
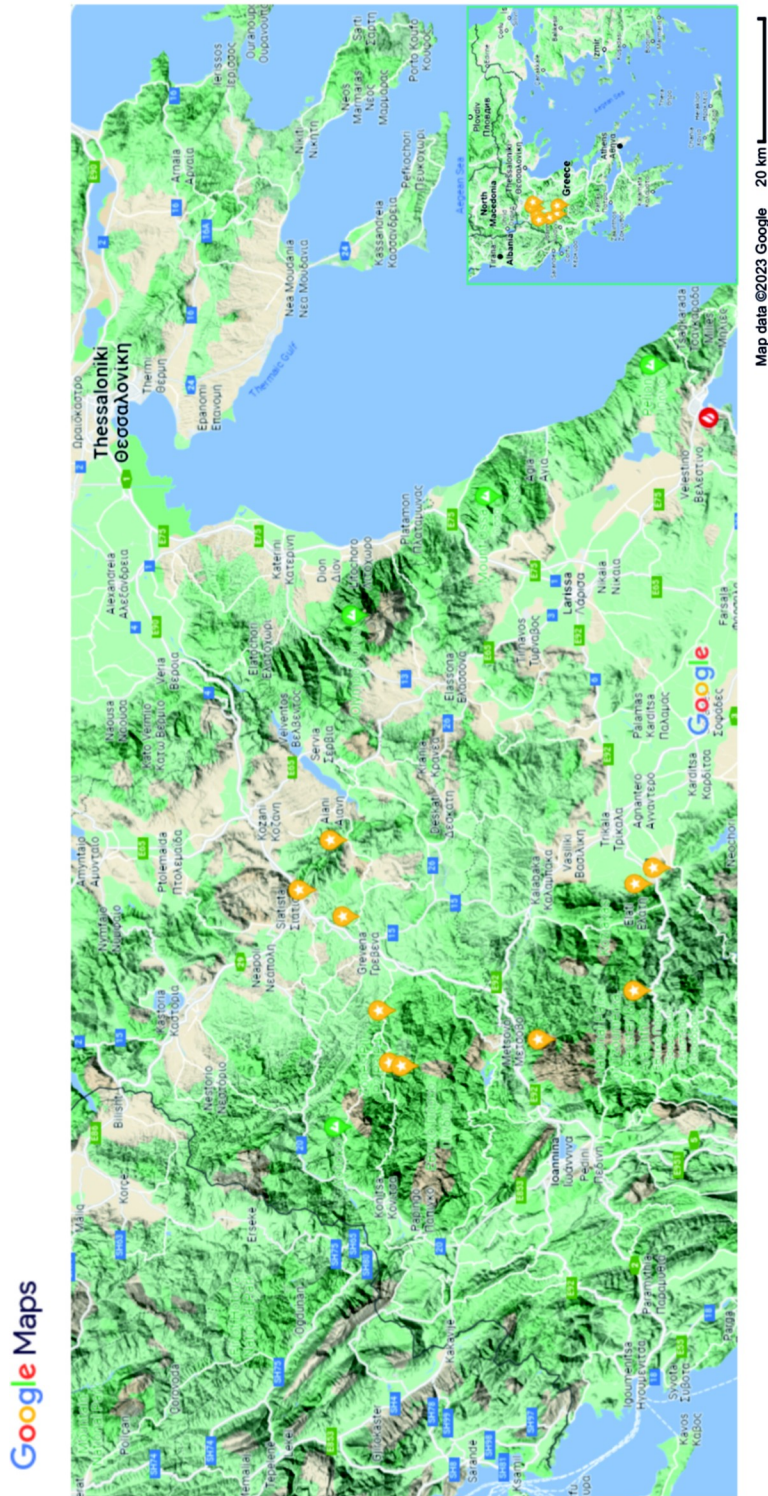
Figure 3.1 Geomorphological map of the northwestern Greece with highlighted yellow dots indicating sampling positions for microfacies analysis, conodont age dating, and radiolarian age dating (Google earth 11/11/2023).

Moreover, the analysis of components serves as a valuable method for understanding an eroded hinterland, offering detailed insights into the original paleogeographic setting and the timing of events (Blatt 1967, Zuffa 1980, 1985, Lewis 1984).

The collected samples originate from sedimentary rocks exposed in distinct outcrops, including the Vourinos massif in the vicinity of Poros, Chromio, and Palaiokastro villages, and within the Pindos mountain range near Perivoli, Ziakas, and Avdella villages (Figure 3.1). Additionally, samples were collected from outcrops in the eastern Koziakas mountain range, located near Agios Vissarion and Kori villages (Figure 3.1). Further information were provided from the examination of a sedimentary succession situated on top of Vardar-Axios ophiolites near Neochorouda village.

The collected samples were transported to the laboratory facilities of the Department of Mineralogy, Petrology, and Economic Geology at the Aristotle University of Thessaloniki. In this laboratory, forty-nine (49) thin sections were prepared, each having dimensions of (5) cm x (5) cm (Figures 3.2: a, b). Currently, both the rock samples and thin sections are stored at the Aristotle University of Thessaloniki, School of Geology, Department of Structural, Historical, and Applied Geology.

Ultimately, a thorough microscopic examination of all the thin sections was carried out to acquire the microfacies information from the rock samples (Figure 3.2: c). The relevant and more representative photographic material is provided in the following chapters.

Figure 3.2 Thin section preparation and microscopic study of the thin sections.

3.1 Microfacies analysis concept

The analysis of carbonate rocks ideally requires a combination of field observations, sampling, and laboratory work. Due to the fact that carbonate rocks in many cases consist of accumulations of formerly living organisms, their study provides valuable information about the paleoenvironmental conditions that occurred during their deposition (Flügel 2004).

One of the most essential tools for studying carbonate rocks is the use of microfacies, which Flügel (2004) defines as "the total of all sedimentological and paleontological data that can be described and classified from thin sections, peels, polished slabs, or rock samples". Provided that carbonate rocks exhibit distinct characteristics and fossil patterns, microfacies analysis assists in identifying the depositional settings and the hydrodynamic conditions.

In 1975, Wilson distinguished nine Standard Facies Zones (FZ) (Figure 3.3) that correspond to different parts of a rimmed carbonate platform based on sedimentological and biological aspects (Flügel 2004). Each Standard Facies Zone (FZ) represents an idealized sequence characterized by different facies, lithology, color, grain type, depositional texture, and fossil assemblages. However, generally in natural settings, fewer than nine Facies Zones are typically observed on a rimmed carbonate platform and commonly don't follow the layout as demonstrated by the Standard Facies model (Figure 3.3). Additionally, caution must be taken because this model does not consider the carbonate platforms as dynamic systems affected by climatic conditions and sea-level fluctuations, and it is not suitable for non-tropical carbonates and ramp deposits (Flügel 2004).

Microfacies of carbonate rocks with identical criteria have been categorized into 24 Standard Microfacies Types (SMF), according to Flügel (2004). These criteria include prevailing grain types, matrix types, depositional fabric, biota, and depositional texture types. The Standard Microfacies Types correspond to specific depositional settings within each facies belt, ranging from the deep-sea basin (SMF Type 1) to the subaerial exposed areas (SMF Type 24), as illustrated in Figure 3.3 (Flügel 2004).
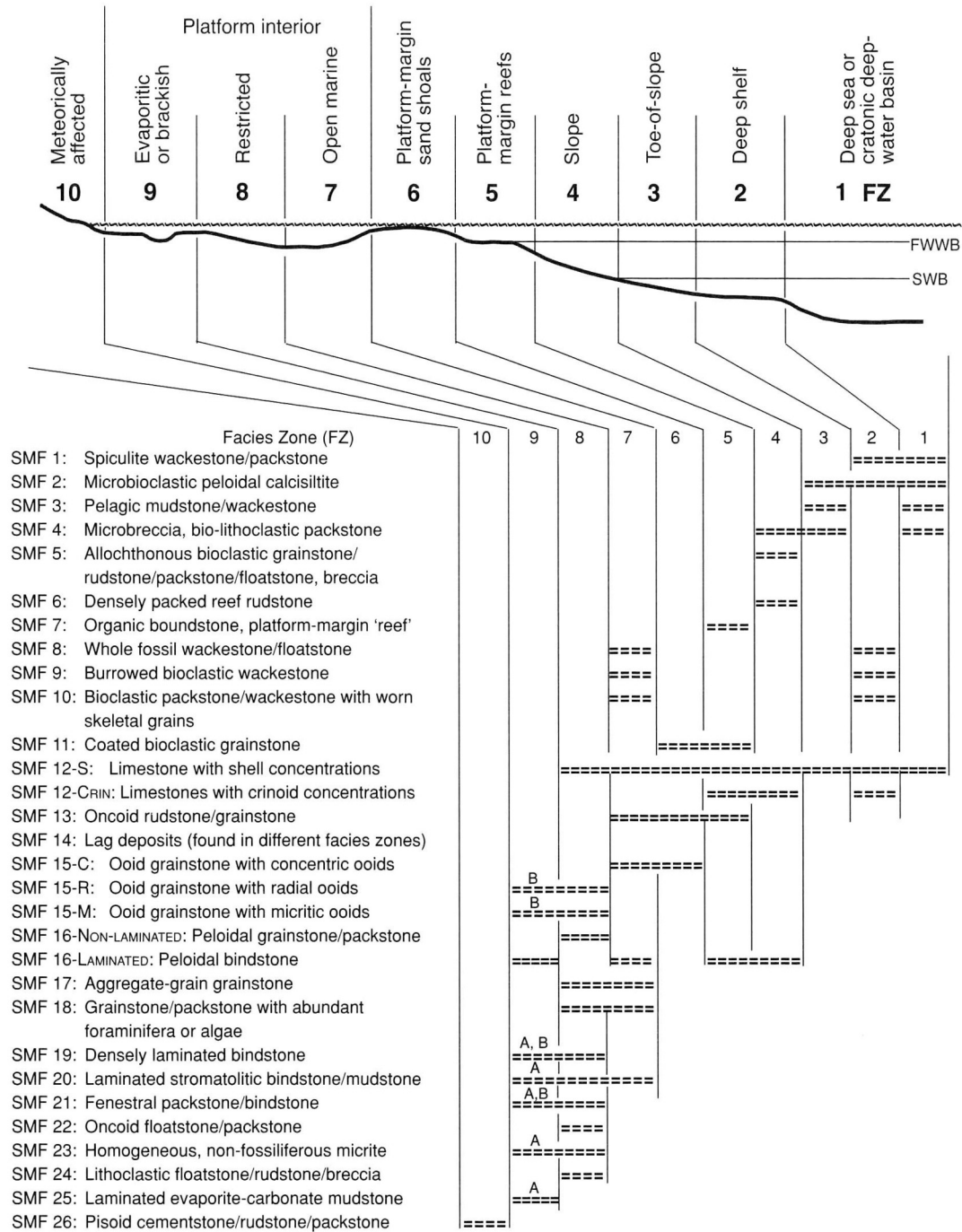
Figure 3.3 Distribution of SMF Types in the Standard Facies Zones of the generalized model for a rimmed carbonate platform after the Wilson model (Flügel 2004).

3.2. Carbonate classification

Carbonate classifications serve an essential and practical purpose during field work as well as in the laboratory for the study of thin sections. Folk (1959, 1962) and Dunham (1962) established the most widely acceptable classification systems, which are also used in this thesis. These systems are based on the depositional texture of the fossiliferous carbonate rocks.

Folk's concept is founded on the understanding that the textures of the carbonate rocks, as well as the siliciclastic rocks, are influenced by the hydrodynamic conditions that occur during deposition (Flügel 2004). The classification of Folk (1959) (Figure 3.4) is practically suitable for thin section studies and is based on the proportions of allochems (carbonate grains), micrite (microcrystalline calcite) matrix, and sparite cement (sparry calcite) that are contained in each specimen.

The Dunham classification system focuses on the depositional fabric and distinguishes two major groups of carbonate rocks (Figure 3.5), according to Flügel (2004):

a) Autochthonous carbonates, which consist of original components bound together at the time of deposition (boundstones). This group was further subdivided into bafflestone, bindstone, and framestone by Embry and Klovan in 1971.

b) Allochthonous carbonates, which consist of original components that were not organically bound. Depending on the proportion of mud to grains, they are further subdivided into mud-supported (mudstone and wackestone) or grain-supported (packstone and grainstone). Mudstone contains less than 10 percent grain, while wackestone contains more than 10 percent. Additionally, grainstone, in contrast to packstone, is characterized by the absence of mud.
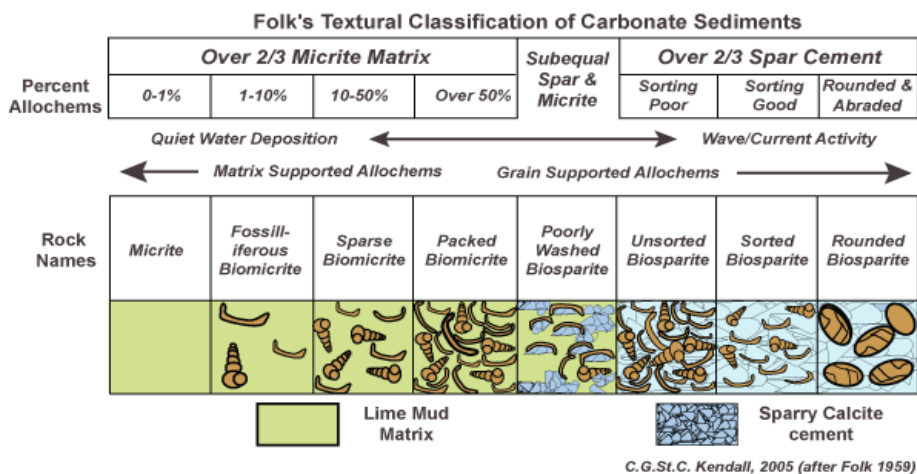
Figure 3.4 Textural classification of carbonate sediments by Folk (1959, 1962). http://www.sepmstrata.org/page.aspx?pageid=89 (26/10/2022).
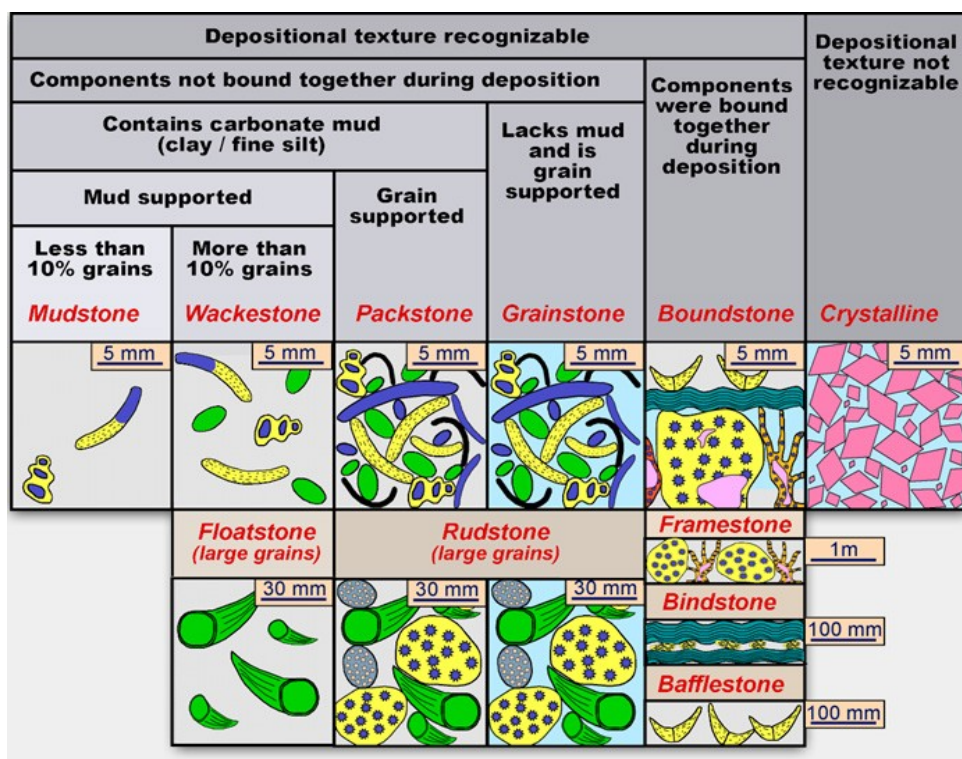
Figure 3.5 Fossiliferous carbonate classification after Dunham (1962) with modifications by Embry and Klovan 1971. https://www.beg.utexas.edu/lmod/_IOL-CM01/cm01-step03.htm (26/10/2022).

CHAPTER 4. Geotectonic Setting and Field Observations

4.1 Pindos and Vourinos ophiolites

The current position of the Pindos and Vourinos ophiolites provokes controversies about their original paleogeographic derivation (Figure 4.1; location 1 and 2) (Brunn 1956, Aubouin 1959, Moores 1969, Bortolotti et al. 1969, Zimmermann 1969, 1972, Dercourt 1970, Bernoulli and Laubscher 1972, Dewey et al. 1973). The Pindos and Vourinos ophiolites likely form a cohesive ophiolite mass, spanning approximately thirty (30) km westward from the Vourinos massif to the northern Pindos mountain range (Makris 1977, Saccani and Photiades 2004, Rassios and Moores 2006, Rassios and Dilek 2009). Their possible continuation is covered by the Upper Eocene to Lower-Middle Miocene deposits of the Mesohellenic Trough (Figure 4.1).

As discussed in an earlier chapter about the origin of these ophiolites, there is a contradiction regarding whether they are segments of the oceanic floor from an autonomous Pindos Ocean (Mountrakis 1986, Jones et al. 1991, Robertson et al. 1991, 1996, Robertson and Shallo 2000, Stampfli and Borel 2002, Brown and Robertson 2004, Stampfli and Kozur 2006, Sharp and Robertson 2006, Rassios and Moores 2006, Karamata 2006, Dilek et al. 2008, Rassios and Dilek 2009, Robertson 2012, Saccani et al. 2015, 2017) or they originate from the Neo-Tethys oceanic realm, located east of the Pelagonia (Zimmerman 1969, 1972, Bernoulli and Laubscher 1972, Aubouin 1973, Mercier et al. 1975, Dercourt et al. 1986, Bortolotti et al. 1996, 2012, Gawlick et al. 2008, 2016a, 2016b, 2017a, 2020, Schlagintweit et al. 2008, Schmid et al. 2008, 2020,
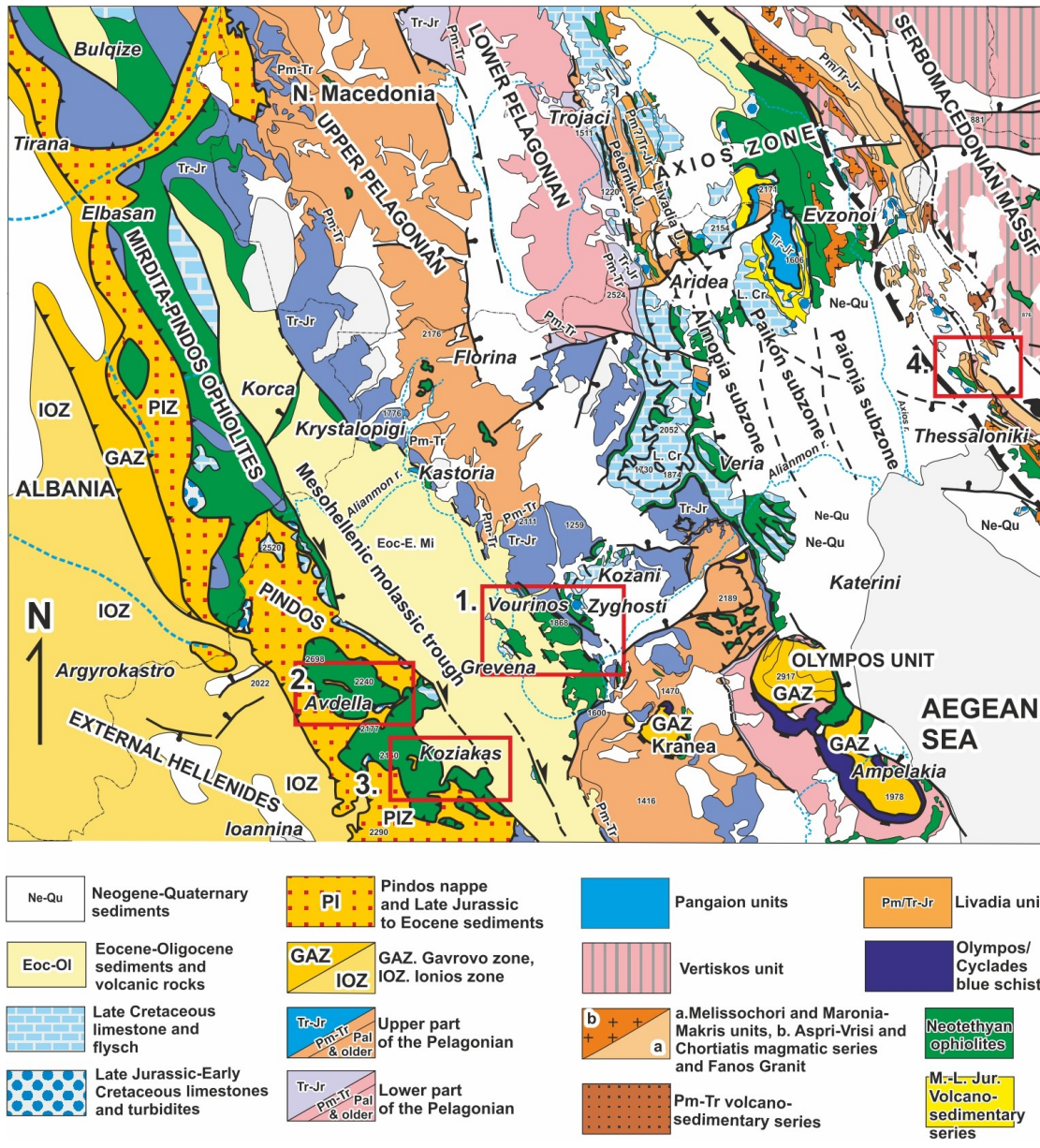
Figure 4.1 Geological map of the northwestern Greece modified after Kilias (2021). The studied areas are indicated.

Kilias et al. 2010, Missoni and Gawlick 2011, Katrivanos et al. 2013, Ferriére et al. 2015, 2016, Kilias 2021).

As described by Moores (1969), the Vourinos ophiolites exhibit the representative petrological features of a well-preserved ophiolite sequence. This sequence comprises, from bottom to top, an ultramafic complex primarily composed of harzburgites, succeeded by a gabbroic complex, followed by a sheeted dykes complex, and finally, a

mafic volcanic sequence often containing pillow basalts (Bortolotti et al. 2004b). The volcanic sequence is characterized by island arc tholeiites (IAT) and boninitic intrusive dykes representing a mature stage of a subduction setting (Capedri et al. 1980, Beccalura et al. 1984, Saccani and Photiades 2004, Saccani et al. 2004).

On the other hand, Pindos ophiolites feature a fragmented sequence comprising serpentinized harzburgites, ultramafic and mafic cumulates, mafic intrusives, a sheeted dykes complex, and mafic volcanic rocks (Saccani and Photiades 2004). The Pindos ophiolites exhibit geochemical characteristics with supra-subduction zone type (SSZ) and mid-ocean ridge basalt type (MORB) affinities (Capedri et al. 1980, Saccani and Photiades 2004). In contrast, the Vourinos ophiolites are characterized by a SSZ geochemical setting (Beccaluva et al. 1984). The initiation of intra-oceanic subduction within a mid-ocean ridge basalt type (MORB) lithosphere is supported by analyses of the metamorphic sole (Figure 4.2), with its formation dated to approximately 171 ±4 Ma (Late Bajocian) (Roddick et al. 1979, Spray and Roddick 1980, Spray et al. 1984, Dimo-Lahitte et al. 2001, Saccani et al.2004). Interestingly, the available ages obtained from the radiolarite sedimentary cover (Chiari et al. 2003: latest Bajocian-Early Bathonian) suggest that the SSZ ophiolites formed after the formation of the metamorphic sole.

Figure 4.2 Metamorphic sole formation beneath the Pindos ophiolites observable in the vicinity of Perivoli village ($39^0 95´62´´$N, $21^0 10´00´´$E).

Furthermore, beneath the obducted Vourinos and Pindos ophiolites, ophiolitic mélanges are exposed, displaying typical characteristic of a tectono-sedimentary formation (e.g., Avdella mélange) (Figures 4.3). These mélanges share common features, including their content and the age of their formation, with others found below ophiolite exposures in different regions in the Hellenides (Jones and Robertson 1991, 1994, Danelian and Robertson 2001, Bortolotti et al. 2004b, Ghikas et al. 2009, Ozsvart et al. 2012, Nirta et al. 2010, Ghon et al. 2018). Another distinctive feature of the Vourinos ophiolites are the economic chromite deposits that are hosted in the dunite bodies (Filippidis et al. 2000, Tzamos et al. 2017).
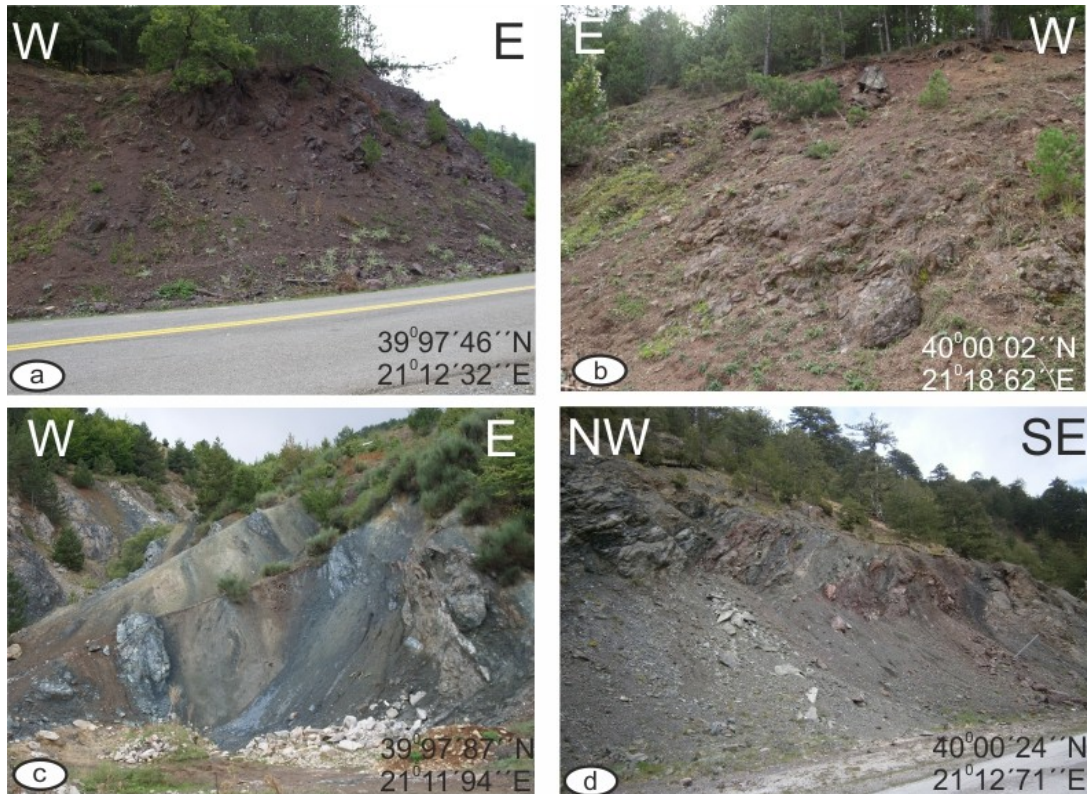
Figure 4.3 Field situation at different exposures of the Pindos ophiolites and the Avdella mélange in the northern Pindos mountain range: **a**, **b**) Pindos ophiolite outcrops visible along the local roads between Spileo and Perivoli villages. **c**) Block-in-matrix structure of the Avdella ophiolitic mélange observable close to Perivoli village. **d**) A mixture of exotic blocks integrated within the Avdella mélange exposed near Avdella village.

4.1.1 Avdella mélange

The widely recognized in the literature Avdella mélange (Jones and Robertson 1994), dated as Middle-Late Jurassic, is exposed beneath the obducted Pindos ophiolites (Figure 4.1; location 2). It is alternatively referred to as the Perivoli Complex (Kemp and Mccaig 1984). In specific locations, sedimentary carbonate successions, either from the Early Cretaceous or Late Cretaceous, overlie either the mélange directly or the ophiolites (Figure 4.4). The Avdella mélange was thrust over Paleocene-Eocene orogenic sediments through subsequent tectonic processes (Figure 4.5).

The mélange appears to have an intense internal deformation, characterized by folding (Kilias 2021). It demonstrates a block-in-matrix structure comprising a mixture of exotic blocks and slides of varying dimensions, ranging from centimeters to hundreds of meters (Figures 4.3 and 4.6). In particular, within the mélange, Triassic ophiolites accompanied by the relevant sedimentary radiolarite layer, siliciclastic volcano-sedimentary rocks, shallow-water carbonates sediments and Triassic carbonates, can be encountered (Figures 4.3 and 4.7). These blocks are integrated into an argillaceous-radiolaritic matrix of Jurassic origin (Kostaki et al. 2023).

The mélange comprises a wide array of ophiolite rocks, encompassing gabbros, serpentinites, and pillow-lava. Geochemically, they exhibit characteristics associated with a within-plate (WPB), to transitional enriched mid-ocean ridge (E-MORB) and normal mid-ocean ridge (N-MORB) types of geotectonic environment (Jones and Robertson 1991, 1994).

Concerning the age of the formation of the ophiolites, radiolarian biostratigraphic data linked to pillow basalts documented in the Avdella mélange by Ozsvart et al. (2012), suggests a Middle Triassic (upper Anisian) as the earliest. This demonstrates that oceanic spreading had initiated during that period, and the greater portion of this Triassic oceanic crust may have been consumed in the course of the intra-oceanic subduction, resulting in a poor preservation, mainly in certain places and in mélanges (Bortolotti et al. 2004b).
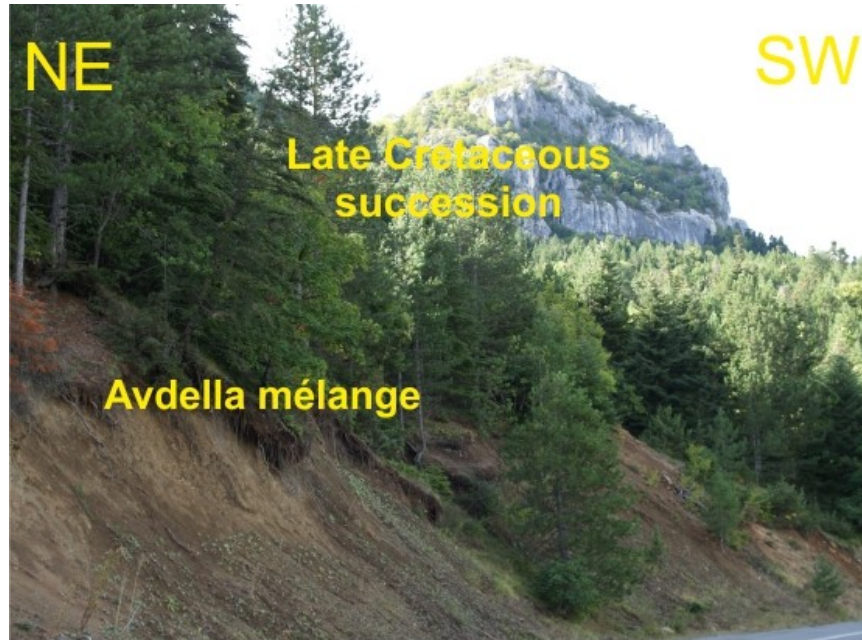
Figure 4.4 Exposure of the Avdella mélange and an overlying Late Cretaceous sedimentary carbonate succession observed near Ziakas village ($40^0 02´53´´$N, $21^0 25´25´´$E) (Kostaki et al. 2023).
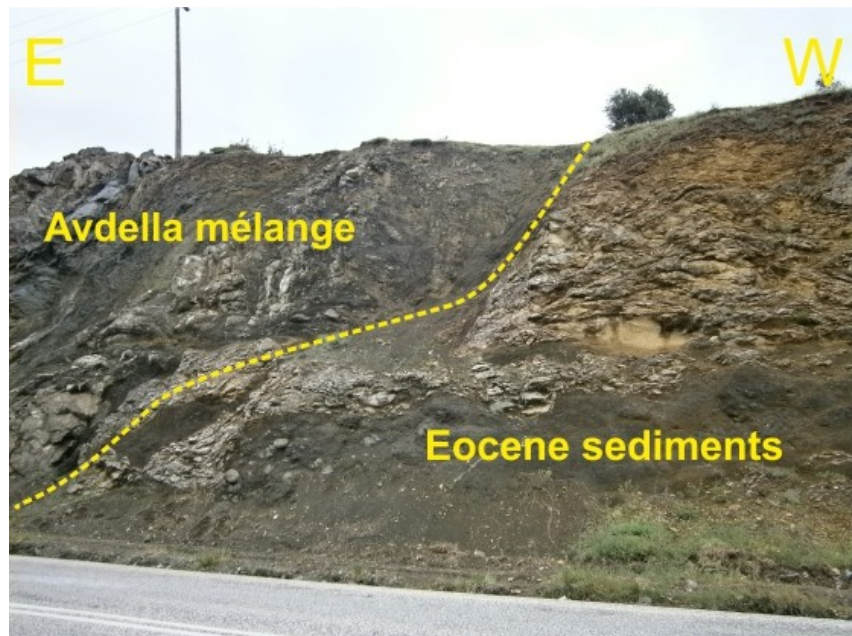
Figure 4.5 Outcrop near Perivoli village that exposes the Avdella mélange thrusting towards the west over Paleocene-Eocene orogenic sediments ($39^0 96´94´´$N, $21^0 12´58´´$E) (Kostaki et al. 2023).

Figure 4.6 Panoramic view of the Avdella mélange in the vicinity of Perivoli village (39^{0}97´87´´N, 21^{0}11´94´´E).

The youngest sediments reported within the mélange consist of Late Jurassic redeposited shallow-water limestones, containing the algae *Cladocoropsis*, and redeposited oolitic carbonates with debris enclosing algae and foraminifera of the Middle-Late Jurassic age (Jones and Robertson 1991, 1994).

Furthermore, the melange's Middle-Late Jurassic sediments indicate a deep-water environment, featuring turbiditic sequences that include ophiolite-derived material and red-brown ribbon radiolarites intercalated with red shales (Jones and Robertson 1991, 1994).

A comprehensive analysis of the integrated exotic carbonate blocks within the Avdella mélange was lacking. Previous studies by Migiros and Tselepidis (1990) reported the ammonoid dating of a hemipelagic limestone block, indicating an upper Scythian to lower Anisian age. Additionally, Ozsvart et al. (2012) conducted conodont dating on a red limestone block, revealing a Middle Anisian age. Therefore, in this study, it was essential to conduct a detailed analysis of exotic carbonate blocks exhibiting a variety of colors and sizes, resting in the matrix of the mélange, interpreted here as open-marine Triassic Hallstatt Limestone blocks (Figure 4.7).

Figure 4.7 Hallstatt Limestone blocks and green basalts within the Avdella mélange in the vicinity of Avdella village ($40^0 00'24''$N, $21^0 12'71''$E) (Kostaki et al. 2023).

4.2 Koziakas ophiolites

The Pindos ophiolites belt in the Hellenides extends further southeast, reappearing in the Koziakas mountain range (Figure 4.1; location 3). In this region, they are known as the Koziakas ophiolites. To the east, the Koziakas ophiolites are covered by the sediments of the Mesohellenic Trough (Karfakis 1984).

The Koziakas ophiolites exhibit identical petrological and geochemical characteristics to the Pindos ophiolites, suggesting that they were forged in the same supra-subduction geotectonic setting (Pomonis et al. 2002, 2005, Bortolotti et al. 2004b). Radiometric dating and geochemical analysis of their metamorphic sole reveal a Middle Jurassic age ($174\pm$ 3Ma and $161\pm$ 1 Ma) for the initiation of intra-oceanic subduction within a MORB-type lithosphere with IAT influence (Pomonis et al. 2002).

The complete ophiolite sequence has not been preserved, and the lower part of the sequence consists of mantle tectonites, such as spinel-harzburgites and plagioclase-harzburgites, intruded by a complex of gabbroic, plagiogranite, and doleritic dykes (Caperdi et al. 1985, Pomonis et al. 2005, Bortolotti et al. 2004a). The gabbroic dykes

and the doleritic dykes demonstrate N-MORB and E-MORB geochemical affinities, respectively, while the plagiogranite dykes display volcanic arc-type (VAG) geochemical imprint (Pomonis et al. 2005).

The upper part of the ophiolite sequence comprises massive dolerites and basalts, frequently displaying pillow-lava structures and intercalated with Mn-rich radiolarites (Caperdi et al. 1985, Pomonis et al. 2002, 2005). This volcanic sequence exhibits N-MORB, E-MORB, WPB, and boninitic geochemical imprints (Pomonis et al. 2005, 2007).

4.2.1 Koziakas mélange

An identical tectono-sedimentary sequence to the Avdella mélange is tectonically situated below the western section of the Koziakas ophiolites (Figure 4.1; location 3) (e.g., Jones and Robertson 1991, 1994, Bortolotti et al. 2004b, Saccani and Photiades 2005, Robertson 2012, Chiari et al. 2012, Ghon et al. 2018).

The Koziakas mélange comprises blocks and slides integrated into an argillaceous-radiolaritic matrix of Jurassic origin. These blocks primarily include Triassic carbonates, radiolarites, and ophiolites along with their relevant sedimentary radiolarite layer (Figure 4.8) (Bortolotti et al. 2004b, Pomonis et al. 2005, Chiari et al. 2012). Similarly to the situation in the Avdella mélange, there is a noticeable appearance of open-marine Hallstatt Limestone blocks and slides (Figures 4.8).

In detail, the predominant ophiolite blocks consist mainly of serpentinites, peridotites, gabbros, dolerites, pillow-lavas, and fragments of metamorphic sole (Pomonis et al. 2005). Geochemically, they exhibit differentiation; therefore, three groups have been identified by Saccani et al. (2003), i.e., a) transitional to alkaline basalts, trachyandesites, trachytes, b) MORB, and c) boninitic basaltic andesites and andesites.

Chiari et al. (2012), following geochemical analysis and dating of radiolarites covering the basalts, distinguished a tectonic unit in the upper portion of the mélange predominantly comprising Triassic basalts (Fourka Unit). These basalts show WPB-OIB

(within-plate and oceanic interplate basalts) and E-MORB geochemical imprints, while the ages obtained from the associated radiolarites range from the Latest Anisian to the Middle Norian.

Additionally, they dated a section composed of bedded radiolarites as Middle Carnian to early Late Carnian, which they include in the Fourka Unit. From the underlying mélange, the radiolarian assemblages are dated as latest Bajocian to Early Callovian, and the radiolarites associated with WPB-OIB as Early-Middle Bathonian (Chiari et al. 2012).

Moreover, blocks of trachyandesites interrelated with radiolarites and open-marine limestones that include fragments of the bivalve *Halobia* (Aubouin 1959) have been reported in the mélange, as well as nodular carbonates (Bernoulli and Jenkys 1974, Pomonis et al. 2005).

Clarifying the situation, the Koziakas mélange can be divided into a lower part dominated by Triassic Hallstatt Limestone blocks, radiolarites, and ophiolite blocks (Figures 4.8). This part is covered by Middle to Late Jurassic radiolaritic turbidites intercalated with oolitic limestones, and at higher levels, these radiolaritic turbidites are intercalated with Earliest Cretaceous shallow-water carbonate-clastic resediments (Ghon et al. 2018). Meanwhile, the upper and most eastern part exhibits the characteristics of a pure ophiolitic mélange.

The Koziakas mélange is tectonically positioned to the west over a Cretaceous succession known as the Thymiama succession, corresponding to the Boeotian Flysch (Bortolotti et al. 2004b, Karfakis 1984, Savouat and Lalechou 1972). In certain areas of the southern region of Koziakas, field observations reveal that the mélange overthrusts the Triassic Pindos successions directly. Moving further to the west, the entire tectono-stratigraphic sequence is thrust onto Eocene to Oligocene orogenic sediments (Neofotistos et al. 2010, Karfakis 1984, Savouat and Lalechou 1972).
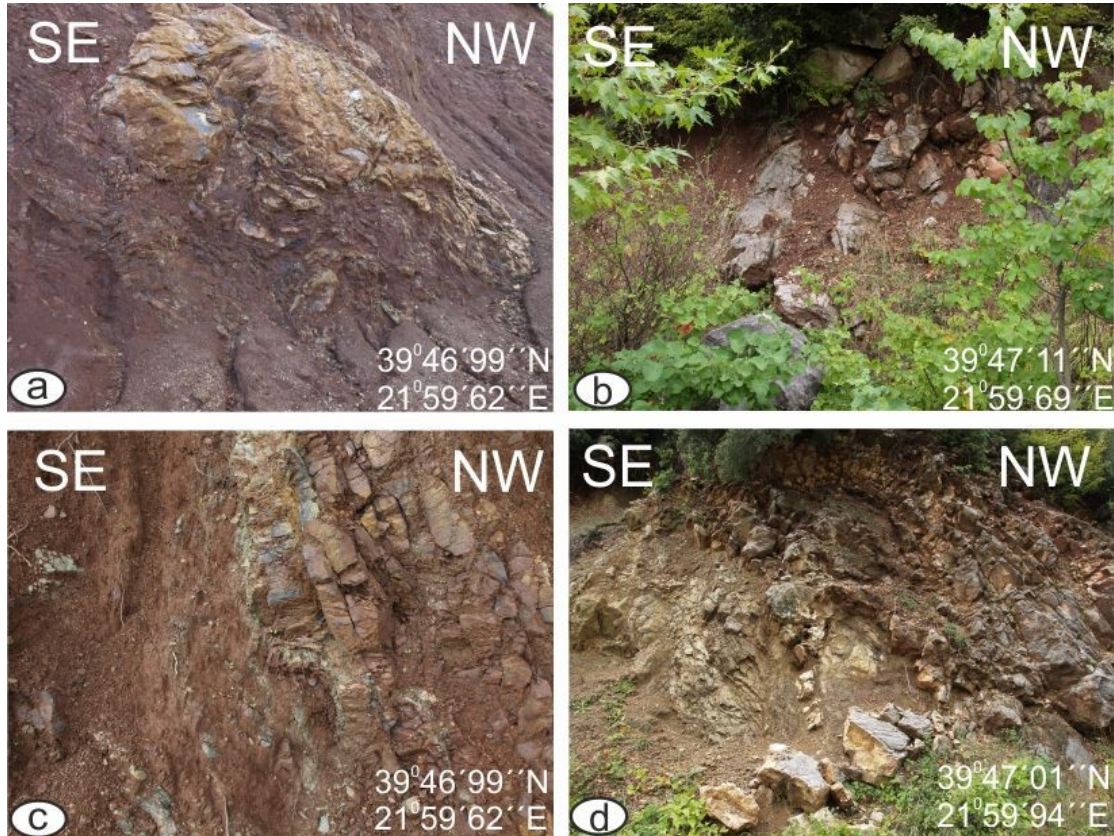
Figure 4.8 Field situation at different exposures of the Koziakas mélange in the eastern Koziakas mountain range, along the local road connecting Agios Vissarionas village and Monastery Dousiko: **a**) Carbonate block integrated within an argillaceous-radiolaritic matrix. **b**) Triassic open-marine limestone block in an argillaceous-radiolaritic matrix. **c**) Exposure of manganesiferous red cherts. **d**) Ophiolite blocks included in the Koziakas mélange.

4.3 Overstep sequences

Two overstep sequences associated with the obducted ophiolites can be identified, both featuring shallow-water carbonate sediments, which were initially deposited on top of the ophiolites at distinct times.

a) The first overstep sequence is represented by Late Jurassic shallow-water microfacies, primarily preserved as redeposited components within younger resediments.

b) The second sequence, considerably younger, was deposited during the late Early Cretaceous.

4.3.1 Late Jurassic overstep sequence

Late Jurassic shallow-water microfacies found in the Zyghosti area overlying Vourinos ophiolites and their middle Bathonian relevant sedimentary radiolarite layer, have been documented by Carras et al. (2004) (Figure 4.1; location 1). Common microfacies include bioclastic, intraclastic, and oolitic packstone, as well as oncoidal wackestone and packstone, boundstone, and rudstone.

Some of the most characteristic fossils documented by Carras et al. (2004) are corals, bivalves, echinoderms, gastropods, and the algae *Thaumatoporella*, *Salpingoporella pygmaea* (Guembel), *Salpingoporella annulata* Carozzi, *Bacinella irregularis* Radoicic and Pfenderinidae, and *Clypeina jurassica* Favre. Additionally, the foraminifera *Mohlerina basiliensis* (Mohler), *Labyrinthina mirabilis* Weynschenk, *Protopeneroplis striata* Weynschenk, and *Kurnubia palastiniensis* Henson are encountered. The microencruster *Crescentiella morronensis* (Crescenti) and the hydrozoan *Cladocoropsis mirabilis* Felix are also included.

Carras et al. (2004) interpret these microfacies as representing a carbonate platform succession, referred to as the Zyghosti Platform, which developed during the Middle to Late Jurassic. This platform is characterized by the alternation between high-energy oolitic and reefal facies with low-energy lagoonal facies.

Distinctive geological features such as neptunian dykes, karst unconformity surfaces, and lateritic deposits have been observed. These features serve as evidence of the emersion and partial erosion events that affected both the shallow-water carbonates and the underlying ophiolites during the Late Jurassic to Early Cretaceous (Carras et al. 2004, see also Bortolotti et al. 2004a, Fazzuoli and Carras 2007).

4.3.2 Late Early Cretaceous overstep sequence

The late Early Cretaceous carbonate sequence comprises shallow-water limestones that extensively overlay the Vourinos ophiolites, which have been significantly affected by laterization processes observable across an extended region (Figures 4.1; location 1 and 4.9) (Carras et al. 2004, Photiades et al. 2007, Pomoni-Papaioannou and Photiades 2007).

The sedimentary sequence is primarily characterized by conglomerates at its lower section, comprising reefal limestone components from the Late Jurassic (Figure 4.10). In certain areas, conglomerates are composed of components originating from the Triassic to Early Jurassic Pelagonian carbonate platform cover and its underlying crystalline basement rocks (Photiades et al. 2007).

Figure 4.9 a, **b**) Late Early Cretaceous limestones with orbitolinic foraminifera overlying directly the lateritized Vourinos ophiolites. **c**, **d**) Late Early cretaceous limestones exhibiting distinctive lateritic weathering ($40^0 22´07´´N$, $21^0 71´87´´E$).
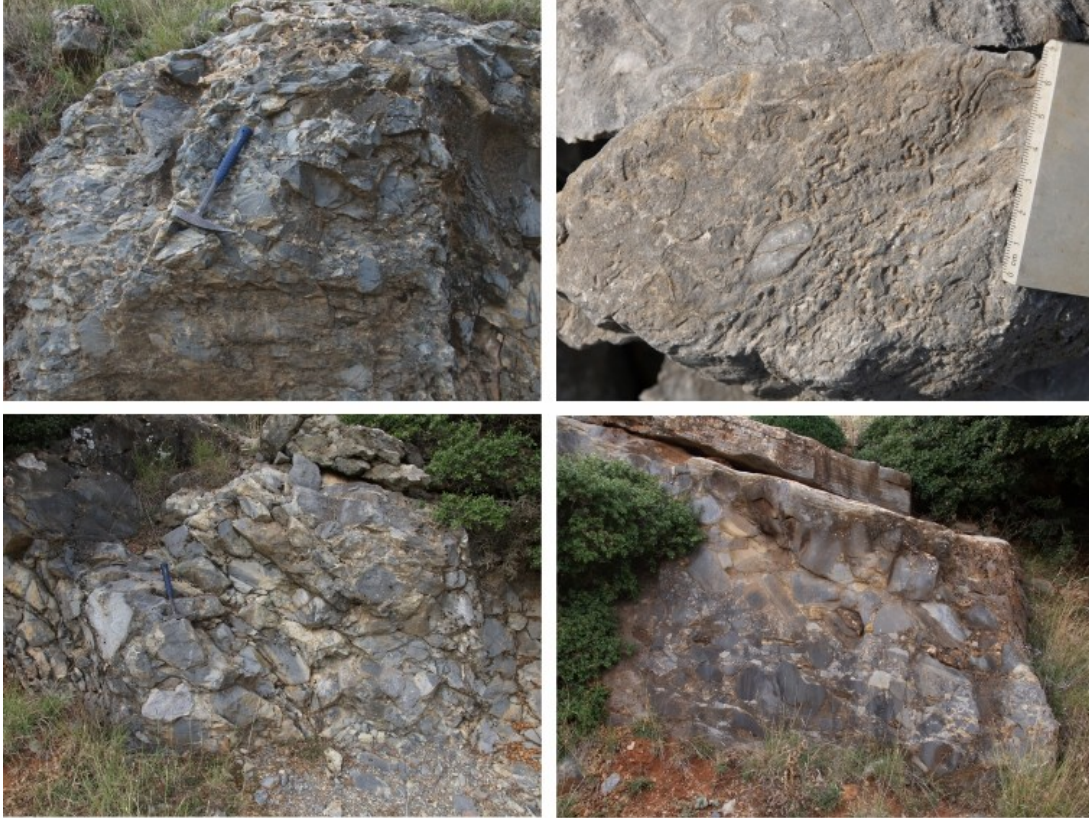
Figure 4.10 Late Early Cretaceous transgressive carbonate sediments, including conglomerates, breccias, and reefal limestones ($40^0 21´06´´N$, $21^0 73´13´´E$).

Photiades et al. (2007) documented that this section is succeeded by shallow-water sediments containing *Salpingoporella urladanasi* Conrad, Peybernes and Radoicic, which is assigned to the Barremian-Albian age. These are followed by limestones containing orbitolinid foraminifera.

From the Cenomanian onward, a transition to an open-marine environment is documented by the deposition of marine carbonate turbidites, which reflects a drowning event during that period. These turbidites were subsequently followed by Late Maastrichtian orogenic sediments (Carras et al. 2004, Bortolotti et al. 2004a, Photiades et al. 2007, Fazzuoli and Carras 2007).

4.4 Triassic to Jurassic stratigraphic synthesis of the Pelagonian Zone

Beneath the obducted ophiolites and their mélanges lie recrystallized and metamorphosed carbonate rocks, which constitute a portion of the remaining segment of the Pelagonian marginal formations that were overridden by the ophiolites and affected by the subsequent processes (Figures 4.1; location 1 and 4.11).

As mentioned earlier in sub-chapter (2.5) the obduction processes can disrupt the arrangement and structure of the passive continental margin. Rocks originating from the marginal formations can be discovered as exotic blocks integrated within mélanges, as observed in the Avdella and Koziakas mélanges. Therefore, understanding the origin of these exotic blocks is fundamental for uncovering the original arrangement of the passive continental margin and can provide detailed insights regarding the route of the ophiolites.

However, unrevealing the trajectory of ophiolites upon the Pelagonian margin or margins, requires a deeper understanding of the arrangement of the Pelagonian marginal formations before the obduction of the ophiolites. Thus, this sub-chapter offers a synthesis of the Triassic to Jurassic stratigraphy of the Pelagonian Zone, derived from various geological exposures documented in previous studies.

The latest Permian period is marked by a rift stage and the subsequent deposition of a volcano-sedimentary sequence. This kind of deposition started above a Paleozoic or older crystalline basement (Mountrakis et al. 1983, Mountrakis 1986, Koroneos et al. 1993, Kilias et al. 2010, Kilias 2021).

During the earliest Early Triassic, the deposition of the volcano-sedimentary sequence persisted, followed by shallow-water carbonate sedimentation. Exposures of Early Triassic shallow-water limestones can be found in various locations, such as in Othrys and in Hydra (see Angiolini et al. 1992, Ferrière et al. 2016).

The transition from a shallow-water to an open-marine environment during Late Anisian is crucial, as evidenced by the presence of red nodular limestones described in Hydra (Wendt 1973). These limestones, known as the Bulog Formation in the Dinarides, signify the continental break up of the Neo-Tethys Ocean (Dimitrijevic and Dimitrijevic 1991, Sudar et al. 2013). Associated with this event is believed to be the initial
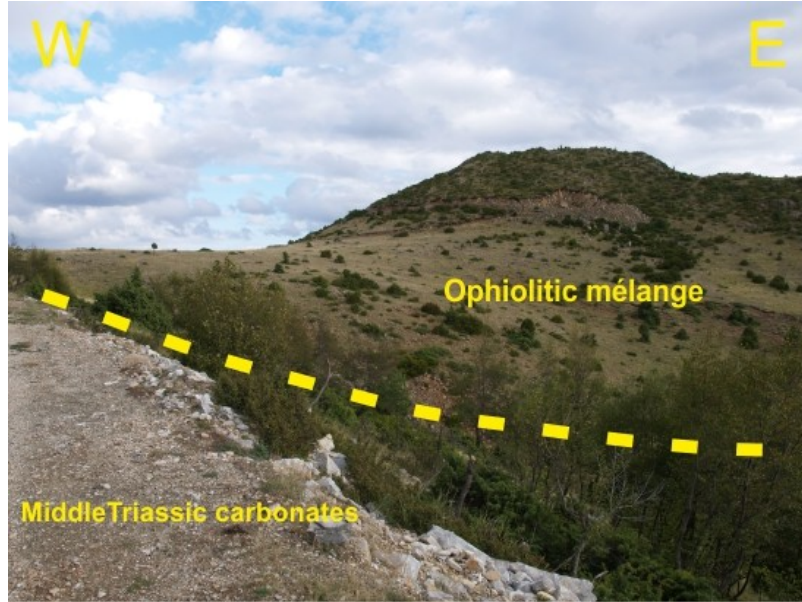
Figure 4.11 The Vourinos ophiolitic mélange that tectonically overlies Middle to early Late Triassic recrystallized and metamorphosed carbonates ($40^0 17'63''$ N, $21^0 68'00''$E).

deposition of Middle Anisian red limestones, dated with conodonts by Ozsvart et al. (2012), which was found as a block within the Avdella mélange.

The Late Anisian is marked by extensive volcanic activity and deposition of volcaniclastic rocks and hemipelagic sediments, potentially associated with the ongoing process of the continental break up (Figure 4.12) (Ferrière et al. 2016 and references therein).

After the rifting period, from the late Middle Triassic until the Early Jurassic, a passive margin developed, featuring characteristic facies arrangement that transitioned from a shallow-water carbonate platform to a hemipelagic shelf, typical of a central to outer shelf depositional setting (Figure 4.12).

The central Pelagonian shelf domain is well-documented and characterized by dark-grey, massive to well-bedded dolomites, along with dark-grey to brownish-grey, well-bedded limestones, which are known as the Pantokrator facies-formation (Late Triasssic-Early Jurassic) (Scherreicks 2000, Scherreicks et al. 2009). These facies are documented in multiple exposures, such as the Peloponnese (Argolis Peninsula; Baumgartner 1985, Angiolini et al. 1992), Hydra (Kube et al. 1998), and Evia (Scherreiks 2000, Scherreiks et al. 2009).

69

| | west | | | east | |
(ages)	central shelf	open shelf with shallow-water infuence	outer shelf	distal outer shelf	**Neotethys Ocean**
Middle Jurassic	Bositra limestones nodular siliceous limestone	radiolarites			
Early Jurassic	*Lithiotis* lime-stone / Ammonitico Rosso-facies	cherty limestones Drowning	red violet shales with fine-grained calcarenites		
Rhaetian	shallow-water Pantokrator facies-formation			Hallstatt Limestone Facies	
Norian		calcarenites calcirudites / cherty micritic limestones calciturbidites	cherty limestones		
Carnian	shallow-water limestones	cherty limestones	red radiolarites		
Ladinian					
Anisian — Illyrian		pelagic cherty limestones volcano-sedimentary rocks red nodular limestones			
Anisian — Pelsonian		Drowning			Not Existing
Anisian — Early		shallow-water limestones			
Early Triassic		siliciclastic			

Figure 4.12 Triassic to Jurassic stratigraphic synthesis of the Pelagonian Zone and the eastern Pelagonian margin, derived from various geological exposures (Based on: Wendt 1973, Vrielynck 1978, Mountrakis et al. 1983, Baumgartner 1985, Angiolini et al. 1992, Baumgartner et al. 1995, Kube et al. 1998, Scherreiks 2000, Scherreiks et al. 2009, Missoni and Gawlick 2011, Ferrière et al. 2016) (Kostaki et al. 2023).

Distinct facies are present between the central and the outer shelf regions, referred to as the reef-near facies, marked by the deposition of open-marine carbonates influenced by shallow-water material (Figure 4.12). These facies are exposed in Othrys, featuring calcarenites and calcirudites as documented by Ferrière et al. (2016). Moreover, transitional facies, even closer to the outer shelf region, occur in Othrys, consisting of cherty limestones with Carnian radiolarites and Norian cherty limestones.

Additional, reef-near facies occur in the Argolis Peninsula and Hydra, characterized by Middle Triassic-Early Jurassic cherty limestones, known as Adhami Limestones. These limestones include turbidites with shallow-water material deriving from the

Pantokrator facies-formation (Baumgartner 1985, for a different view see Clift and Robertson 1990).

The Triassic sedimentation history outlined so far aligns with the reconstructed sedimentation pattern (see sub-chapter 2.2) documented by other research groups, indicative for the Inner Dinarides, the Albanides, the Eastern and Southern Alps, as well as the Western Carpathians (e.g., Gawlick et al. 2008, 2017b, Sudar et al. 2013, Gawlick and Missoni 2019). Following this, the deep-water facies deposited in outer shelf region, during the Middle Anisian to Rhaetian, along the western Neo-Tethys realm are represented by the Hallstatt Facies, while the continental slope facies by the Meliata Facies (Figure 4.12) (e.g., Schlager 1969, Krystyn 1980, 1983, 2008, Mandl 1984, Lein 1987, Gawlick and Bohm 2000, Missoni and Gawlick 2011, Gawlick and Missoni 2015, Gawlick et al. 2012, 2017a, 2018).

The Meliata Facies have been totally consumed or eroded away and can only be reconstructed from blocks preserved within Jurassic mélanges along the Alpine-Carpathian-Dinaridic collisional belt (Gawlick and Missoni 2019). On the other hand, the Hallstatt Facies occur in multiple exposures across the Hellenides, such as in Othrys, Athens, Hydra, Argolis Peninsula, Crete, Naxos, and Chios (e.g., Sakellariou 1938, Mitzopoulos and Renz 1938, Bender 1962, 1970, Bender and Kockel 1963, Creutzburg et al. 1966, Romermann 1968, Wendt 1973, Dürr 1975, Kauffmann 1976, Angiolini et al. 1992, Pomoni and Tselepidis 2013).

The original paleogeographic position of the Hallstatt Limestones in the Hellenides is controversial discussed. They are situated within the Sub-Pelagonian Zone, which many authors consider as the western passive continental margin of the Pelagonian micro-plate adjacent to the so-called Pindos Ocean to the west (Mountrakis 1986, 2010, Robertson 2012, Robertson et al. 1996, Ferrière 1974, Clift and Robertson 1990, Tselepidis 2007, Pomoni and Tselepidis 2013).

Nonetheless, in the Argolis Peninsula, the Hallstatt Limestones are regarded as olistoliths in Middle-Late Jurassic radiolarian cherts, as proposed by Krystyn and Mariolakos (1975). These formations, including other marginal formations (e.g., Adhami Limestone) and the ophiolites, are believed to have originated from an oceanic realm situated to the east of the Pelagonian region, therefore are interpreted as far-

traveled nappes (e.g., Vrielynck 1978, Baumgartner 1985, Ferrière et al. 2016). Moreover, Hallstatt Limestones are preserved in western Pindos mountain range (Kostaki et al. 2023), a topic that will be examined more closely in an upcoming chapter.

In the central Pelagonian shelf domain, during the Early Jurassic, there was a shift towards deeper facies, leading to the deposition of the Ammonitico Rosso-facies (Figure 4.12) (Bernoulli and Jenkyns 1974, Baumgartner 1985). Furthermore, during the Pliensbachian, *Lithiotis* limestones were deposited, succeeded in the early Middle Jurassic by filament (Bositra) limestones and nodular siliceous limestones (Vlahovic et al. 2005, Scherreicks et al. 2009).

In the early-middle Bajocian, deposition of radiolarites began in the outer shelf region and gradually extended into the central shelf (Figure 4.12) (Baumgartner et al. 1995).

CHAPTER 5. Results - Biostratigraphic Data

This chapter presents the results of the microfacies analyses conducted on carbonates collected from various resediments and sedimentary successions, along with conodont and radiolarian age dating data. It is subdivided into six main sub-chapters.

Sub-chapter (5.1) presents the biostratigraphic results obtained from the analysis of Palaiokastro and Chromio successions. These successions represent the remaining segment of the Triassic Pelagonian marginal formations below Vourinos ophiolites (Figure 4.1; location 1).

Sub-chapter (5.2) provides the results obtained from conodont age dating of Triassic exotic blocks found within the Middle-Late Jurassic Avdella mélange, which is associated with the emplacement of Pindos ophiolites (Figure 4.1; location 2). In the same sub-chapter, a reconstruction of a dismembered Hallstatt succession from blocks within the Avdella mélange is presented. This reconstruction also led to a comparison with a similar Middle Triassic-Early Jurassic succession preserved in western Pindos mountain range.

Sub-chapter (5.3) offers the results obtained from microfacies analysis conducted on Late Jurassic shallow-water resedimented carbonates found within the Middle-Late Jurassic Avdella mélange (Figure 4.1; location 2).

Sub-chapter (5.4) presents the microfacies of an Earliest Cretaceous shallow-water succession on top of the Vardar-Axios ophiolites (Figure 4.1; location 4).

Sub-chapter (5.5) provides the results from conodont age dating on Triassic open-marine carbonate exotic blocks within Koziakas mélange (Figure 4.1; location 3).

Additionally, it presents the microfacies of oolitic limestones and carbonate-clastic resediments, as well as radiolarian data deriving from radiolarite-rich turbidites.

Sub-chapter (5.6) offers the results obtained from microfacies analysis conducted on a late Early Cretaceous transgressive carbonate succession, referred to as the Poros succession, which overlies the Vourinos ophiolites (Figure 4.1; location 1).

5.1 Pelagonian marginal formations below Vourinos ophiolites

Thick carbonate rocks, which have undergone recrystallization and metamorphism, are situated beneath the Vourinos ophiolites or their mélanges (Figures 5.1, 5.2, and 5.3) (Mavridis and Kelepertzis 1993). Field observations were made, and samples were collected from these carbonate rocks for conodont age dating. The studied successions are located in proximity to the villages of Palaiokastro and Chromio, illustrated in Figure (5.1) at position (1) and (2).

5.1.1 Palaiokastro Succession

In the lower section of the Palaiokastro Succession (Figure 5.1), there are grey metamorphosed and recrystallized shallow-water limestones that exhibit visible fissures (Figures 5.4 and 5.5). Overlying red limestones are present, which are equivalent to the Bulog Formation identified in other regions within the Hellenides (Hydra; Wendt 1973) and the Dinarides (Sudar et al. 2013). Therefore, the underlying grey metamorphosed recrystallized shallow-water limestones could correspond to the Steinalm Carbonate Formation, which represents the initiation of carbonate production during the late Early Triassic to Anisian. The development of fissures in these shallow-water limestones signify an extensional setting preceding the continental break up of the Neo-Tethys Ocean (Sudar et al. 2013). Subsequently, from the Middle Anisian onward, there was a transition in the depositional conditions from shallow-water to an open-marine environment. This transition led to the deposition of Late Anisian hemipelagic
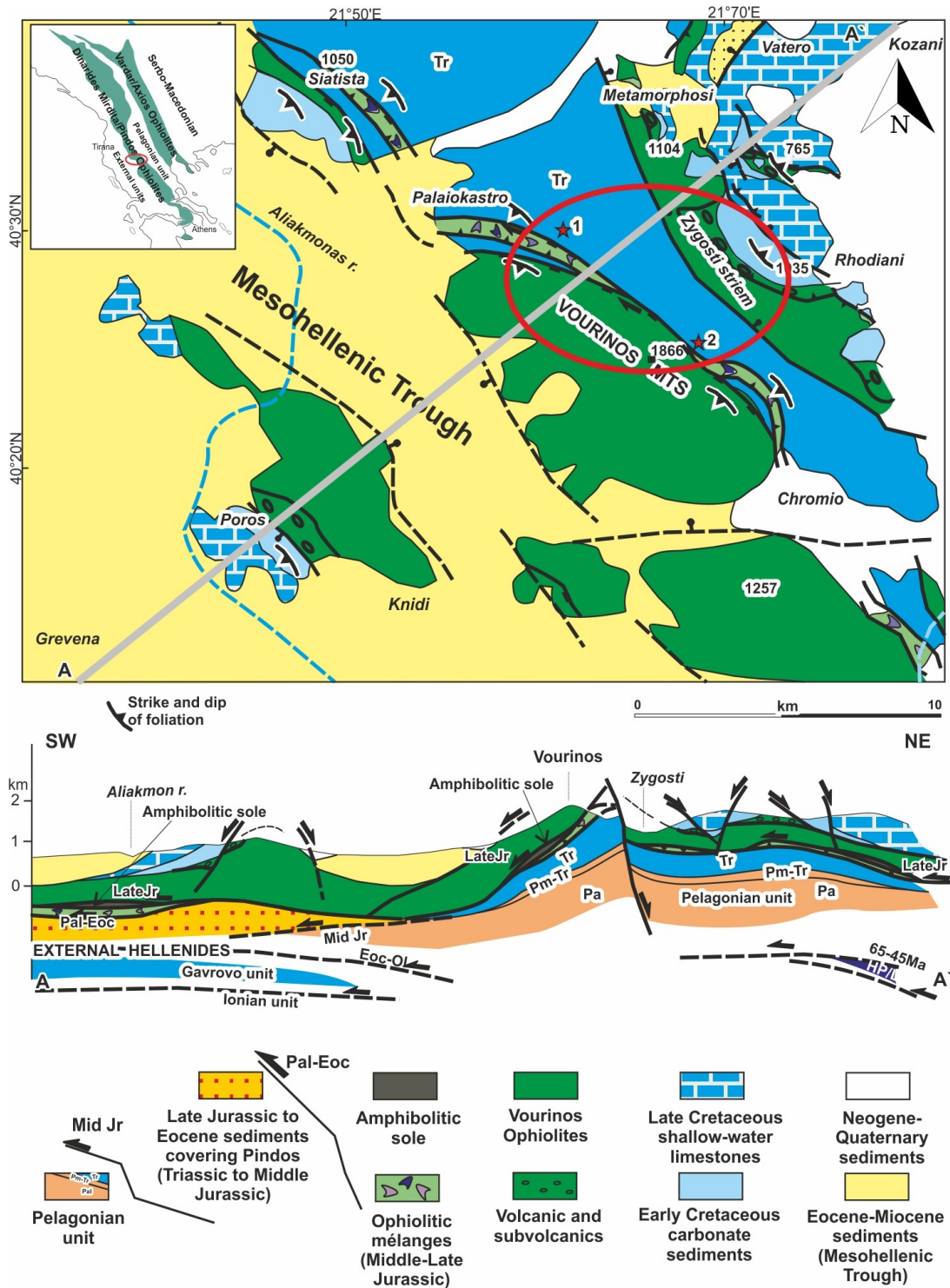
Figure 5.1 Simplified geological map and cross-sectional representation of the Vourinos ophiolites tectonically positioned above the Pelagonian marginal formations (Kostaki et al. 2023, based on Kilias 2021). The red markers indicate the studied areas: (**1**) Palaiokastro Succession and (**2**) Chromio Succession.
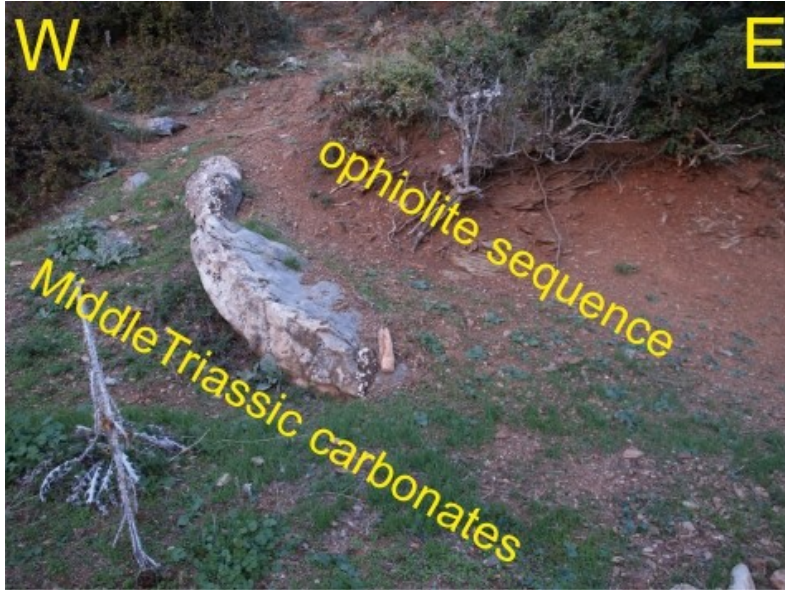
Figure 5.2 Early Late Triassic highly sheared and metamorphosed carbonates situated beneath the Vourinos ophiolitic mélange (Palaiokastro Succession) ($40^0 19'73''$N, $21^0 64'10''$E).

Figure 5.3 Middle Triassic to early Late Triassic carbonates tectonically underlying the Vourinos ophiolitic mélange (Chromio Succesion) ($40^0 17'63''$N, $21^0 68'00''$E).

carbonates, recognized as the Bulog Formation, characterized by abundant ammonoids and conodonts.

Figure 5.4 Highly sheared and recrystallized shallow-water carbonates (Palaiokastro Succession) ($40^0 19' 73'' N$, $21^0 64' 10'' E$).

Higher up in the stratigraphic section (Figure 5.5), there are volcaniclastic rocks that can be attributed to the volcanic phase documented during the Late Anisian (Late Illyrian) (Gawlick et al. 2012). This phase is associated with the final stages of the break up of the Neo-Tethys Ocean, which subsequently had a negative impact on carbonate production (Gawlick et al. 2012, Ferrière et al. 2016, and references therein). Consequently, above these volcaniclastic rocks, the section continues with reddish and grey radiolarites. The section culminates with bedded grey silicified limestones that contain shallow-water turbidites (Figures 5.2 and 5.5). These limestones are dated as Middle Triassic to Early Carnian based on the presence of the conodont taxon *Gladigondolella*-ME.

5.1.2 Chromio Succession

The Chromio section is equivalent with the upper section of the Palaiokastro Succession (Figure 5.1). Within this section, there are grey silicified limestones that contain shallow-water turbidites, overlying reddish and grey radiolarites (Figures 5.5 and 5.6).

The occurrence of these limestones conforms with the growth and the expansion of the Wetterstein Carbonate Platform during the Late Ladinian, which lasted until the Early Carnian.
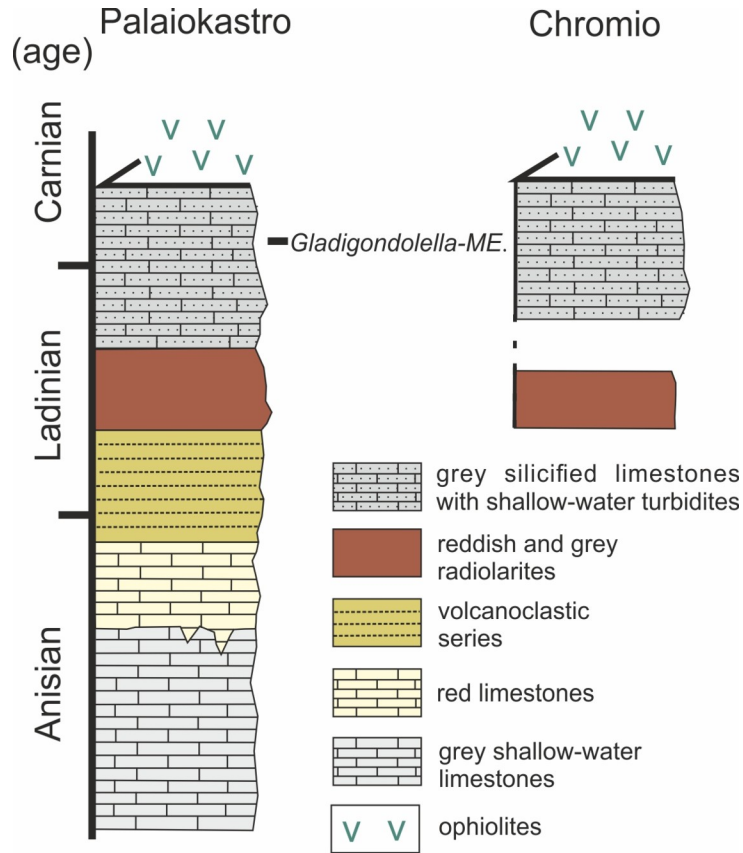
Figure 5.5 Palaiokastro and Chromio stratigraphic sections. The successions are primarily composed of Middle Triassic to early Late Triassic metamorphosed and recrystallized rocks, exposed below the Vourinos ophiolites (Kostaki et al. 2023).

Figure 5.6 Silicified limestones that contain shallow-water turbidites (Chromio Succession) ($40^0 17' 63'' N$, $21^0 68' 00'' E$).

5.2 Integrated exotic blocks within the Avdella mélange

Different exotic blocks, displaying a range of colors and sizes, are found within the Jurassic matrix of the Avdella mélange. Consequently, a comprehensive analysis of these blocks was conducted for the first time, using microfacies analysis and conodont age dating methods. Several samples were collected from blocks located in various outcrops along the local roads connecting the Perivoli and Avdella villages, as well as Ziakas and Perivoli villages, as illustrated in Figure (5.7).

5.2.1 Carbonate exotic blocks in the Avdella mélange

The sample GR (26) was collected from an outcrop in the vicinity of Avdella village, as illustrated in Figure (5.7) at position (1). This particular sample was collected from a red nodular limestone block (Figures 5.8), and its microfacies was determined to be radiolarian-filament wackestone (following Dunham's classification) or biomicrite (following Folk's classification). Conodont age dating was conducted based on the identification of the taxa *Gladigondolella*-ME and *Neocavitella* sp., which indicate an Early Carnian age.

Samples GR (34), GR (37), GR (189), and GR (193) were collected from an outcrop situated along the local roads connecting the Perivoli and Ziakas villages, as illustrated in Figure (5.7) at position (2). The sample GR (34) was collected from a red nodular limestone block (Figures 5.9). Conodont age dating was conducted based on the identification of the taxon *Epigondolella* sp., which assigns a Middle Norian age.

The sample GR (37) was collected from a polymictic olistostrome (Figure 5.10), and its microfacies analysis revealed it to be a reddish-grey radiolarian-filament wackestone (following Dunham's classification) or biomicrite (following Folk's classification). Conodont age dating was conducted based on the identification of the taxon *Norigondolella* cf. *Navicula*, which suggests an Early Norian age.

The sample GR (189) was collected from a red nodular limestone very siliceous block. Conodont age dating was not possible due to poor preservation of the conodonts.
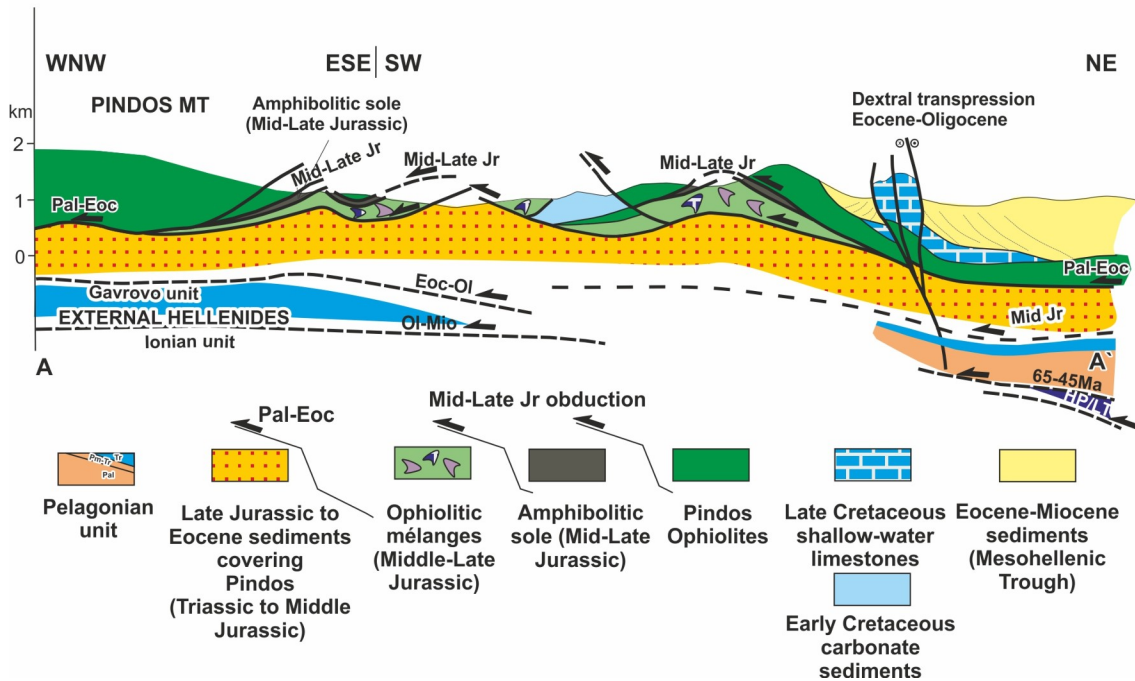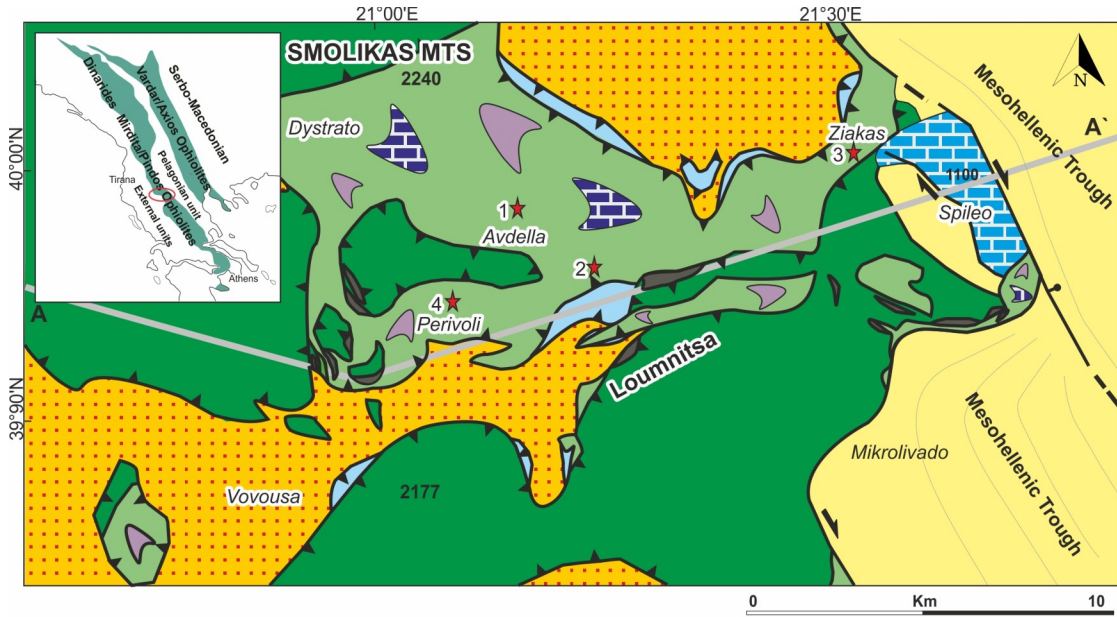
Figure 5.7 Simplified geological map and cross-sectional representation of the Pindos ophiolites tectonically positioned above the Middle to Late Jurassic Avdella mélange (Kostaki et al 2023, based on Kilias 2021). The red markers indicate the sampling positions.

80

The sample GR (193) was collected from a block of grey siliceous limestone containing red chert nodules (Figure 5.11). Conodont age dating was carried out by identifying the taxa *Norigondolella* cf. *navicula* and *Epigondolella rigoi,* which indicate an Early Norian age.
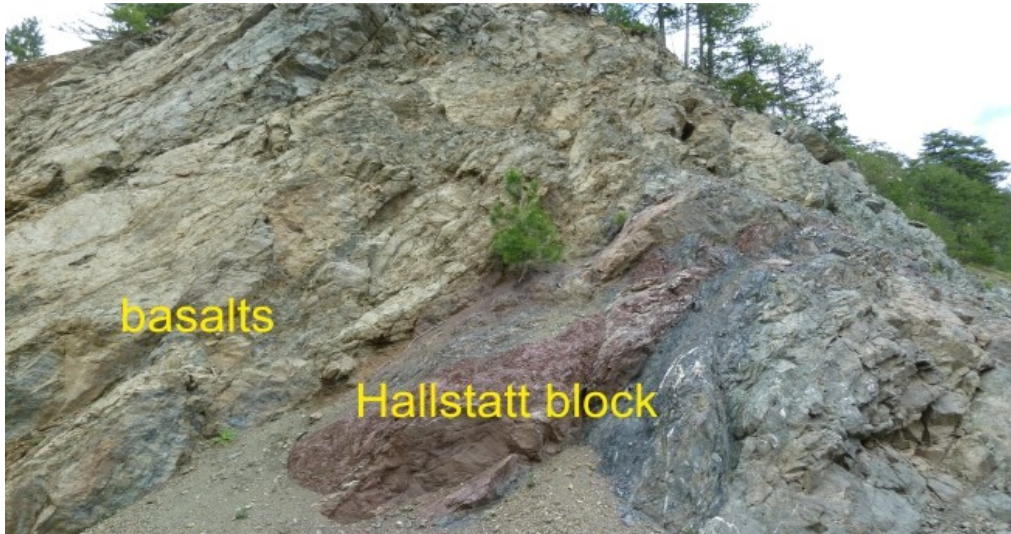
Figure 5.8 Sampling position GR (26): Red nodular limestone block integrated within the Avdella mélange (Kostaki et al. 2023) ($40^0 00' 24''$N, $21^0 12' 71''$E).

Figure 5.9 Sampling position GR (34): Red nodular limestone block integrated within the Avdella mélange (Kostaki et al. 2023) ($39^0 99´32´´N$, $21^0 17´84´´E$).
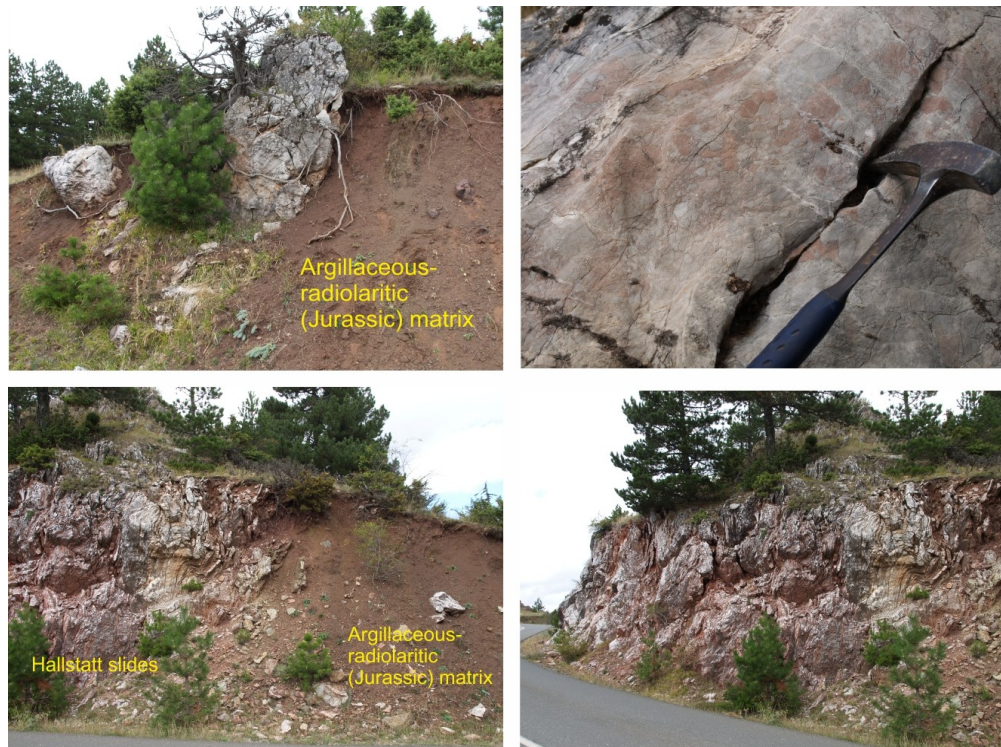
Figure 5.10 Sampling position GR (37): Polymictic olistrostrome within the argillaceous-radiolaritic matrix of the Avdella mélange (Kostaki et al. 2023) ($39^0 99´32´´N$, $21^0 17´84´´E$).
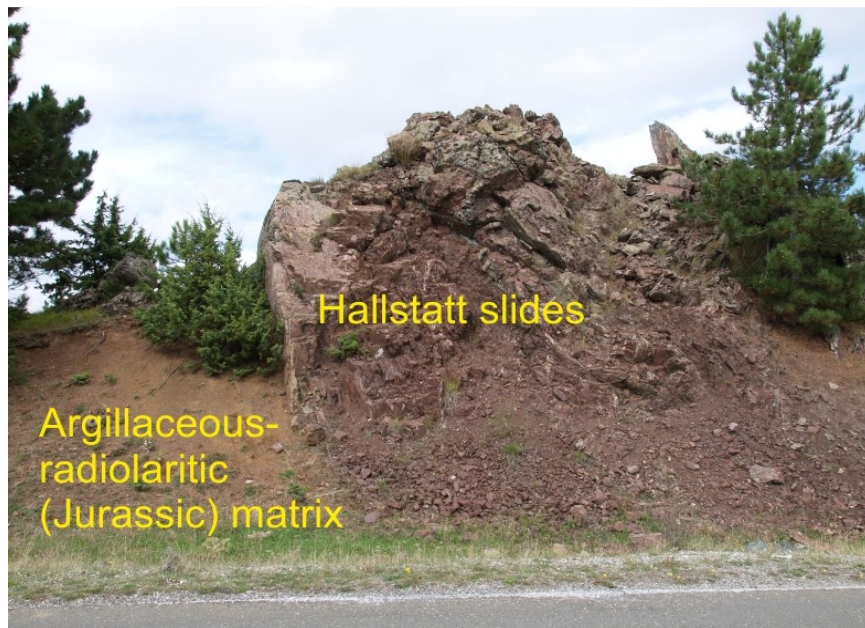
Figure 5.11 Sampling position GR (193): Block of grey siliceous limestone containing red chert nodules within the argillaceous-radiolaritic matrix of the Avdella mélange (Kostaki et al. 2023) ($39^0 99'32''$N, $21^0 17'84''$E).

5.2.2 Ziakas block

The Ziakas outcrop/section, as shown in Figure (5.7), is located at sampling position (3) in the vicinity of Ziakas area and constitutes a block within the Avdella mélange. The section starts with red radiolarites that exhibit folding with a main sense of shear top-to-the-SW (Figures 5.12). Upsection, there are continued alternations of siliceous claystones, radiolarites, and limestones (Figure 5.13). Progressing upwards, there are bedded grey siliceous limestones and slump deposits that exhibit distinctive synsedimentary folds (Figure 5.13).

Higher up in the section, occur bedded grey siliceous limestones, and their age is determined to be Late Ladinian-Early Carnian based on the identification of the conodont taxon *Gladigondolella* cf. *Malayensis*. (Figure 5.14). In the upper part of the section, green clayey radiolarites dominate, accompanied by alternations of clayey

Figure 5.12 Red radiolates displaying folds that indicate a main sense of shear top-to-the-SW (Ziakas outcrop/section; Avdella mélange) (Kostaki et al. 2023) (40^{0}02´53´´N, 21^{0}25´25´´E).

radiolarite, siliceous claystone, and limestone. Conodont age dating conducted on samples collected from these limestone beds, indicates a Julian age, as determined by the identification of the taxon *Gladigondolella*-ME (Figure 5.14).
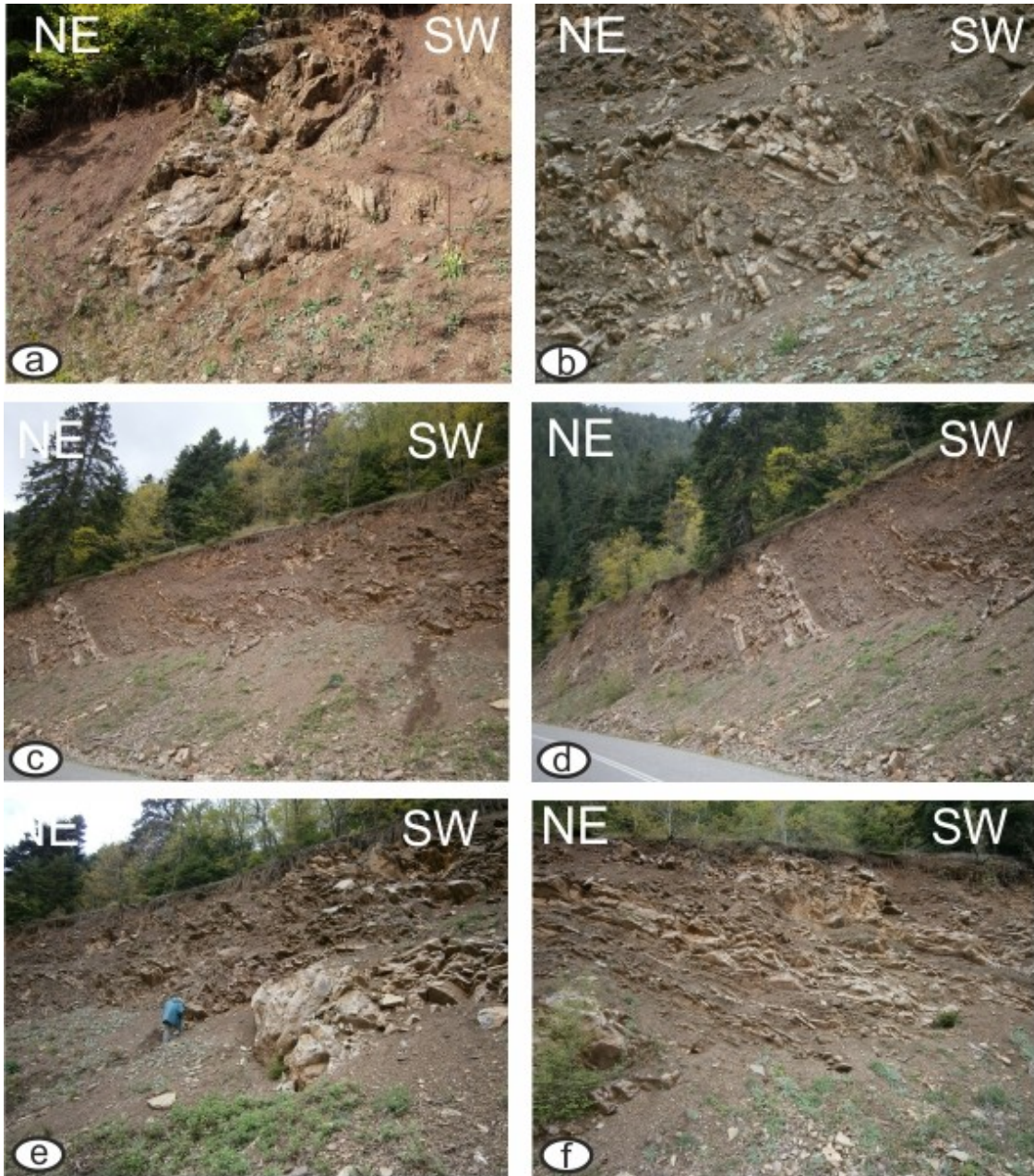
Figure 5.13 Field situation at Ziakas outcrop/section (Avdella mélange) ($40^0 02'53''$N, $21^0 25'25''$E): **a**) Red siliceous claystones and amalgamated limestones. **b**) Characteristic synsedimentary folds. **c**) Slump deposits. **d**) Alternations of siliceous claystones, radiolarites, and limestones. **e**) Red siliceous claystones and amalgamated limestones. **f**) Alternations of clayey radiolarite, siliceous claystone, and limestone.
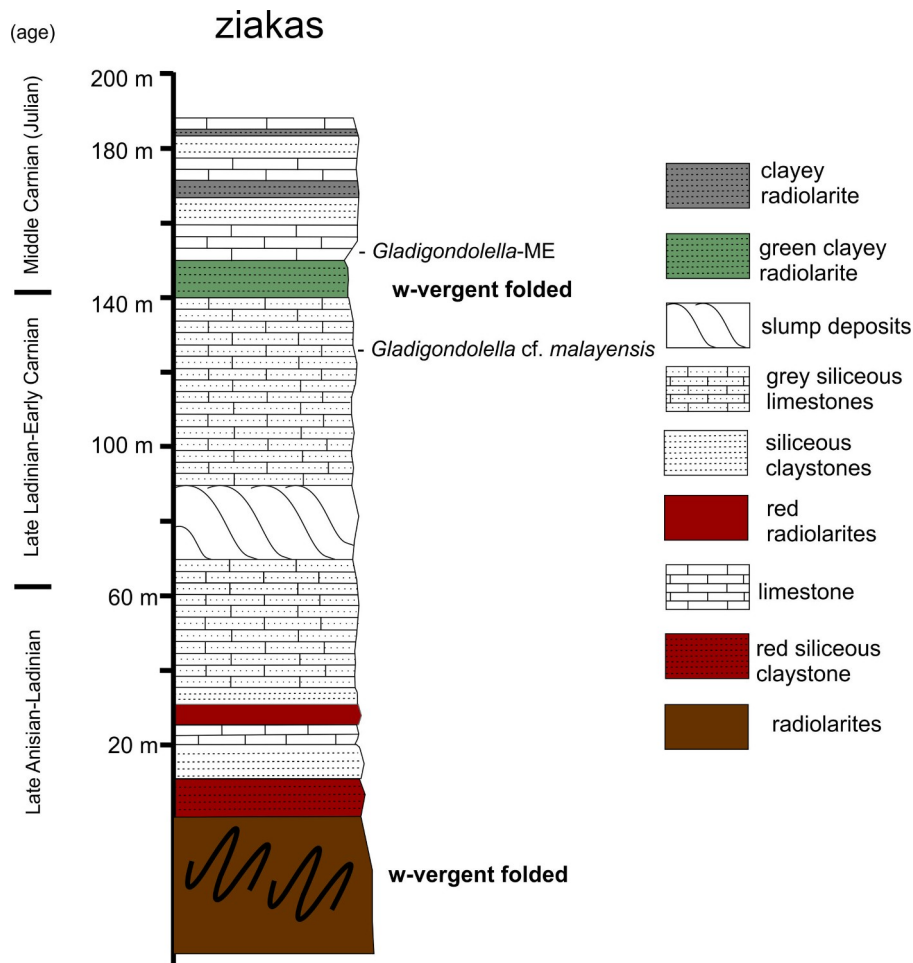
Figure 5.14 Ziakas block stratigraphic section (Kostaki et al. 2023).

5.2.3. Reconstruction of a dismembered Hallstatt succession from blocks in the Avdella mélange

New data obtained from microfacies analysis and conodont age dating of the exotic blocks found within the Jurassic matrix of the Avdella mélange provided valuable biostratigraphic information. By combing these findings, it is possibly to reconstruct a Middle-Late Triassic open-marine shelf that mirrors a Hallstatt Limestone succession (Figure 5.15) (Kostaki et al. 2023).

The Hallstatt Limestone succession is characterized by a certain lithology, microfacies, and stratigraphy. This succession displayed shared trends during its

sedimentary evolution from the Middle Anisian to Rhaetian, which was succeeded by Early Jurassic deep-water sediments (Sudar et al. 2010, Missoni and Gawlick 2011, Gawlick and Missoni 2015, Gawlick et al. 2017a, 2018, Gawlick and Missoni 2019, and references within).

The deposition of the Hallstatt Facies took place in the outer shelf region along the western Neo-Tethys realm, starting with the deposition of the red radiolarites during the Ladinian (Gawlick et al. 2017a, 2018). These red radiolarites were subsequently succeeded by grey siliceous limestones. The presence of red radiolarites in the Ziakas block, along with the bedded grey siliceous limestones determined to be Late Ladinian-Early Carnian, corresponds to the characteristics of the Hallstatt Facies.

A depositional gap is evident in the Middle to Upper Carnian, likely associated with the siliciclastic deposition that had a negative impact on carbonate sedimentation following the drowning of the Wetterstein Carbonate Platform (Missoni et al. 2012).

During the Late Carnian, the Hallstatt Facies is characterized by the deposition of thin-bedded red or grey-reddish limestones containing chert, which are succeeded by thick-bedded to massive limestones in the Early Norian (Gawlick et al. 2017a, 2018). This sedimentary evolution described corresponds to the identification of reddish-grey limestones and grey siliceous limestones with red chert nodules found as exotic blocks within the Avdella mélange, which have been dated as Early Norian.

The Hallstatt Facies continues during the Middle Norian with the deposition of thin-bedded red-grey nodular limestones (Gawlick et al. 2017a, 2018). These limestones can also be identified as red nodular limestone blocks within the Avdella mélange, which have been dated as Middle Norian.

During the Late Norian-Early Rhaetian, the Hallstatt Facies is distinguished by the deposition of irregular-bedded grey limestones, which frequently exhibit bioturbation (Gawlick et al. 2017a, 2018). In the Early Jurassic, the Hallstatt Limestone succession is succeeded by the deposition of grey bioturbated spicula-rich limestone, which is then followed by the deposition of siliceous sediments (Gawlick et al. 2017a, 2018). Finally, in Middle Jurassic, the outer shelf region exhibits the deposition of reddish-greenish radiolarites (Gawlick et al. 2017a, 2018).
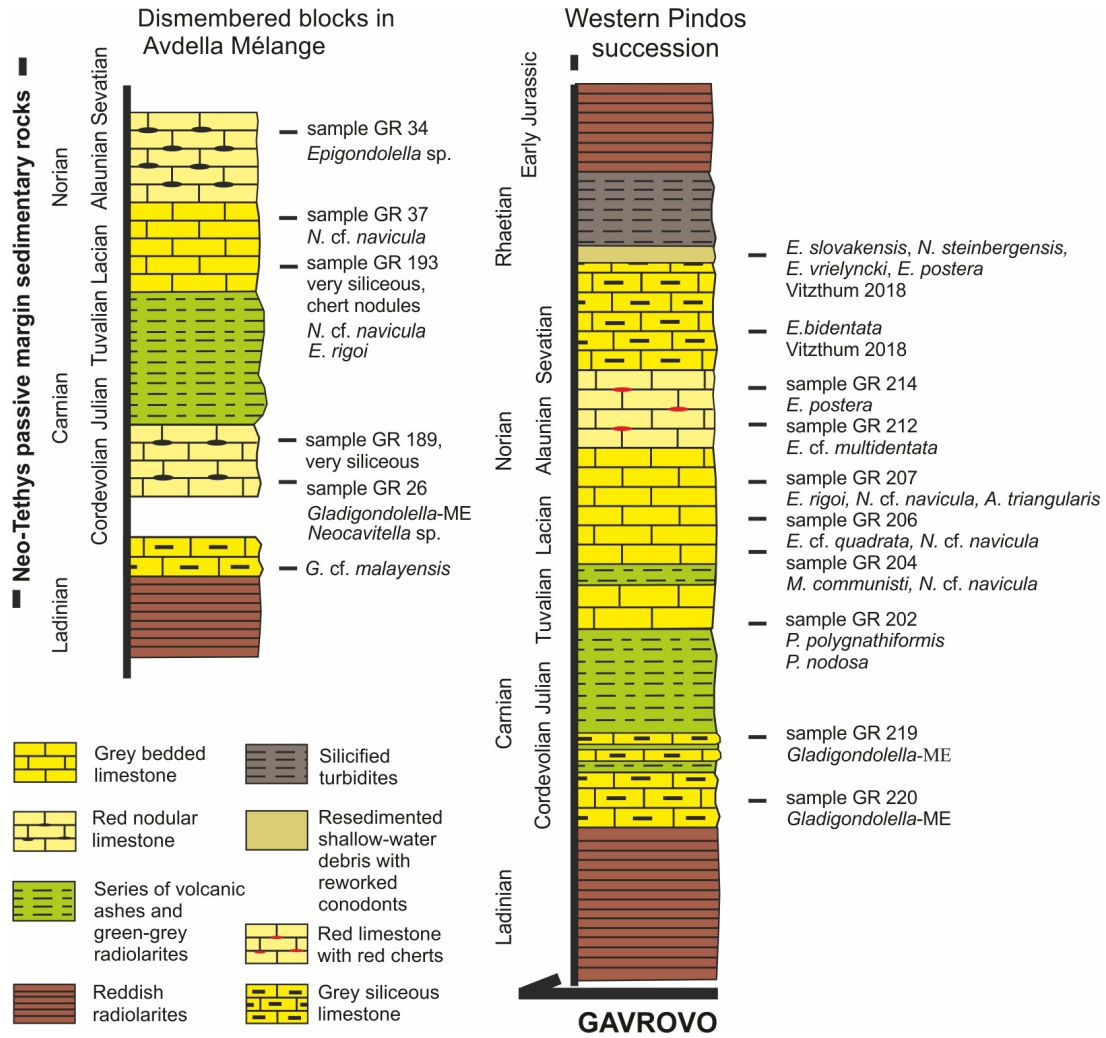
Figure 5.14 Reconstruction of a dismembered Hallstatt succession from reworked blocks in the Middle-Late Jurassic Avdella mélange and comparison between the western Pindos succession (Kostaki et al. 2023).

5.2.4 Comparison of the reconstructed Hallstatt succession from reworded blocks in the Avdella mélange with the western Pindos succession

The examination of reworked exotic blocks within the Avdella mélange provided the basis for reconstructing a dismembered Hallstatt succession (Figure 5.14). Extensive fieldwork was conducted in the broader adjacent region to determine its paleogeographic provenance, leading to the identification of a complete Middle

Triassic-Early Jurassic succession in the western Pindos mountain range, situated to the west of the Pelagonian Zone as part of Pindos Zone (Aubouin 1959). Consequently, further biostratigraphic investigation, using microfacies analysis and conodont age dating methods, was conducted on the Triassic rocks of the western Pindos succession (Figure 5.14). This investigation led to the establishment of their paleogeographical relationship with the dismembered Hallstatt succession, as they notably share identical stratigraphic characteristics (Kostaki et al. 2023). The distinctive feature of the western Pindos succession is the presence of colorful open-marine limestones and other deep-water sediments (Figure 5.15).

Specifically, following the biostratigraphic analysis, the resulted section begins with Early Carnian grey siliceous limestones that overlay Late Ladinian reddish radiolarites (Figures 5.14 and 5.16). The section progresses with grey siliceous limestones with alternations of a series of volcanic ashes and green-grey radiolarites. Moving up the section, this series becomes more dominant, succeeded by grey bedded limestones that are identified as Late Carnian-Early Norian (Figures 5.14 and 5.15). As the sections continues upwards, red limestones with red cherts follow, which are identified as Middle Norian (Figures 5.14 and 5.16)

Figure 5.15 Late Triassic grey bedded limestones, which are followed by red limestones with red cherts in the western Pindos succession ($39^0 28' 94'' N$, $21^0 43' 35'' E$).
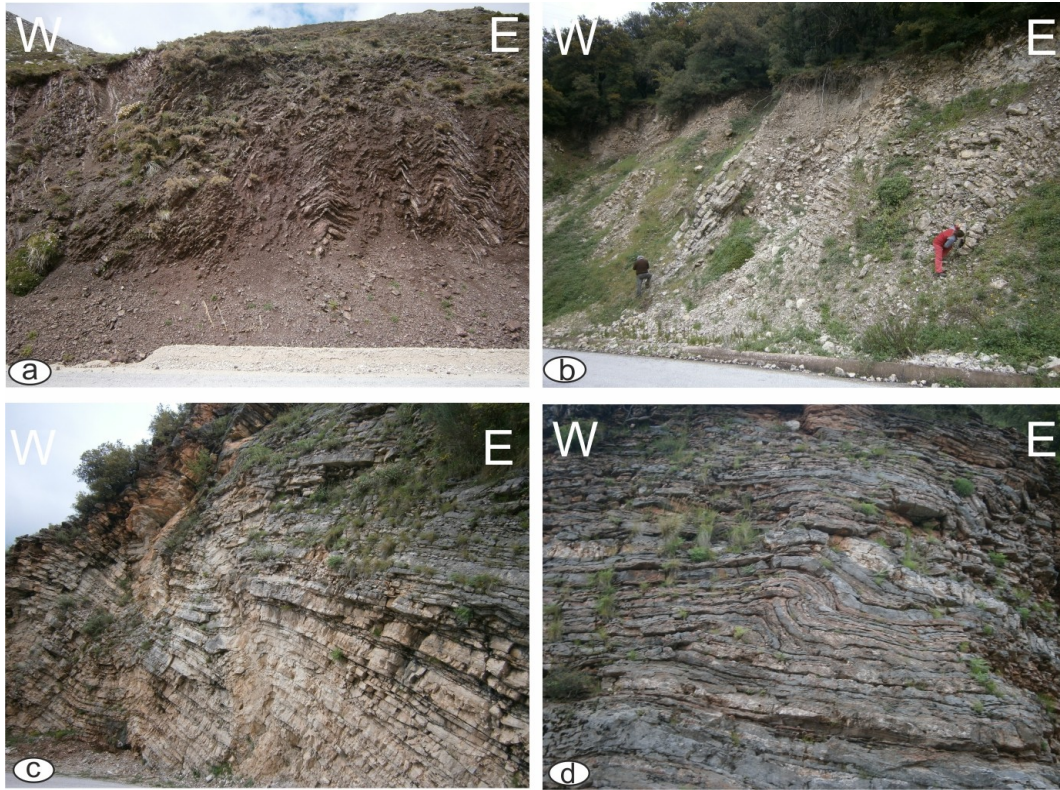
Figure 5.16 Outcrop situation in the western Pindos mountain range ($39^0 28´94´´$N, $21^0 43´35´´$E): **a**) Reddish radiolarites, not dated, but could possibly attributed to the Late Anisian to Early Ladinian. **b**) Grey siliceous limestones. **c**) Late Triassic grey bedded limestones. **d**) Late Triassic reddish-grey limestones with red chert nodule.

Moving further up the section, Late Norian grey siliceous limestones are present, succeeded by resedimented shallow-water debris containing reworked conodonts, as documented by Vitzthum (2018). The section culminates with silicified turbidites and Early Jurassic reddish radiolarites.

Based on the comprehensive description provided so far, it is evident that the entire section corresponds to a complete Hallstatt succession (Sudar et al. 2010, Missoni and Gawlick 2011, Gawlick and Missoni 2015, Gawlick et al. 2017a, 2018, Gawlick and Missoni 2019, and references within).

By establishing this correlation, it is suggested that the dismembered Triassic Hallstatt succession, found within the Avdella mélange as reworked blocks, originated from the Triassic-Early Jurassic western Pindos succession (Kostaki et al. 2023).

5.3 Late Jurassic resedimented carbonates within the Avdella mélange

Resedimented carbonates are also present within the Avdella mélange and were integrated into the mélange as a result of secondary movements that affected it, possibly during the Late Jurassic to Early Cretaceous (Figure 5.17). Field observations were made, and samples were collected from these carbonate rocks for microfacies analysis. The studied outcrops are located in proximity to Ziakas and Perivoli villages, as illustrated in Figure (5.7) at position (3) and (4), respectively.

Figure 5.17 Outcrop situation in the vicinity of Ziakas area with resedimented carbonates within the Avdella mélange ($40^0 02'53''$N, $21^0 25'25''$E).

5.3.1 Ziakas resedimented carbonates

Several samples were collected from resedimented carbonates for microfacies analysis at sampling position (3) as shown in Figure (5.7). These carbonates have a thickness of up to (50) cm and alternate with clayey radiolarites and siliceous claystones (Figures 5.17 and 5.18).

Based on the examination of the thin sections, the collected samples are identified as coarse-grained packstones to grainstones (following Dunham's classification) or packed biomicrite (following Folk's classification) (Plates 1 and 2). The observed bioclasts include crinoids, foraminifera, and possibly a fragment of algae (Plates 1 and 2). Some grains appear to be coated, and the microencruster *Crescentiella morronensis* (Crescenti) is frequent present. Several lithoclasts occur, including ophiolitic material and older sheared components with filaments, which are possibly of Triassic age (Plate 2).

The characteristics of the microfacies suggest a shallow-water environment in close proximity to their depositional setting.
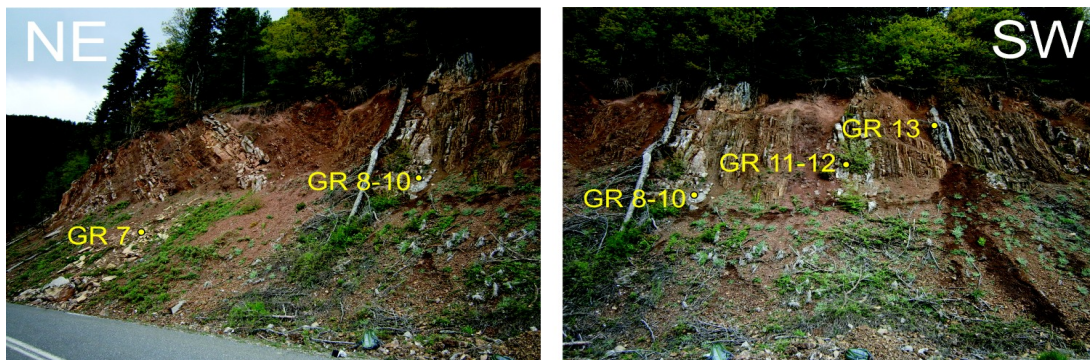
Figure 5.18 Positions of the samples collected from resedimented carbonates for microfacies analysis (Ziakas area; Avdella mélange) (40^{0}02´53´´N, 21^{0}25´25´´E).

Plate 1. Characteristic microfacies from the resedimented carbonates (Ziakas area; Avdella mélange). Samples Gr (4-6) (width of photo: 2 mm): **a**) Coarse-grained grainstone with a possible fragment of a foraminifera (F) and crinoids (C). **b**) Coarse-grained grainstone with the microencruster *Crescentiella morronensis* (Crescenti) (Cm). **c**) Shallow-water debris and fragments of crinoids (C). Sample Gr (7) (width of photo: 1 mm): **d**) Coarse-grained grainstones with algae (A) at the lower part.

Plate 2. Characteristic microfacies from the resedimented carbonates (Ziakas area; Avdella mélange). Sample Gr (8-10) (width of photo: 1 mm): **a**) Coarse-grained grainstone with a Triassic sheared clast with filaments (Fl). Samples Gr (11-12) (width of photo: 2 mm): **b**) Packstone with ophiolitic lithoclasts (OL). Sample Gr (13) (width of photo: 2 mm): **c**, **d**) Packstone with some coated grains and foraminifera (F).

5.3.2 Perivoli resedimented carbonates

Several samples were collected from resedimented carbonates for microfacies analysis at sampling position (4) in the vicinity of Perivoli village, as shown in Figure (5.7). This area is composed of deep-water sediments, which include alternating layers of radiolarites and dark-brownish to red mudstones. These mudstones gradually transition upward into mudstones and sandstones, eventually evolving into sandstone turbidites that contain ophiolite-derived debris (Figures 5.19, 5.20 and 5.21).

Based on the examination of the thin sections, the collected samples are identified as bioclastic packstones to grainstones (following Dunham's classification) or packed biomicrite (following Folk's classification) (Plates 3 - 6).
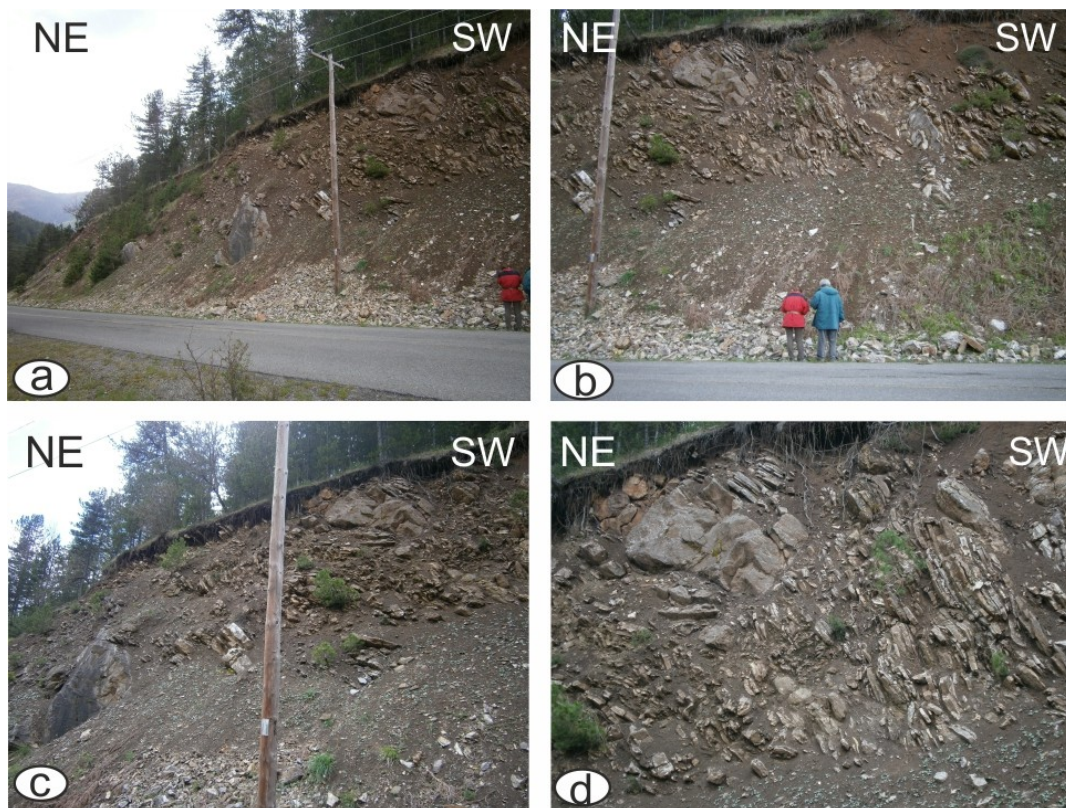
Figure 5.19 Outcrop situation in the vicinity of Perivoli area with resedimented carbonates intergrated within deep-water sediments of the Avdella mélange (39^{0}97´98´´N, 21^{0}12´14´´E).
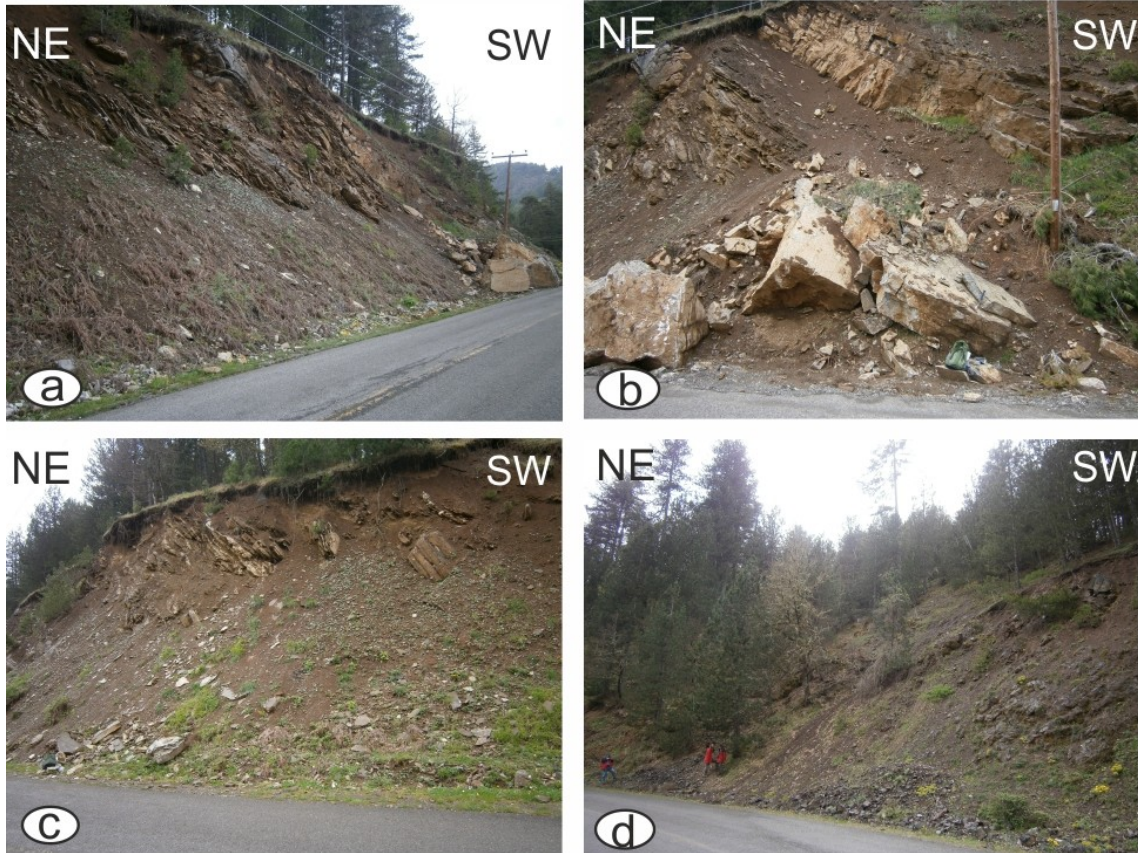
Figure 5.20 Outcrop situation in the vicinity of Perivoli area (Avdella mélange) (39^{0}97′98′′N, 21^{0}12′14′′E): **a**, **b**, and **c**) Resedimented carbonates alternating with sandstone turbidites that contain ophiolite-derived debris. **d**) Pindos ophiolites tectonically positioned above Perivoli section.

The observed bioclasts include reef-building organisms, including sponges and stromatoporoids. Frequent occurrences of encrusting organisms are also noted, along with the presence of the microencruster *Crescentiella morronensis* (Crescenti). Additionally, other bioclasts, including foraminifera, and algae fragments, are identified (Plates 3 - 6). The characteristics of the microfacies and the occurrence of this fossil association strongly suggest a Late Jurassic age.

In specific thin sections, reworked shallow-water components are observed to be mixed with recrystallized radiolaritic lithoclasts, which are likely of Triassic origin (Plates 4 - 6). Additionally, it is noteworthy that the samples collected from the upper

part of the section exhibit a gradual increase in the occurrence of ophiolite-derived lithoclasts (Figure 5.20) (Plates 5 and 6).

Based on these observations, it can be inferred that the depositional setting of this basin was influenced by a shallow-water environment in close proximity. Furthermore, there is evidence to suggest that the basin experienced a subsequent influence from an ophiolite source in the region. Therefore, it is plausible to suggest that the shallow-water carbonate production originally took place on top of the obducted ophiolites during the Late Jurassic and was subsequently affected by erosion processes.
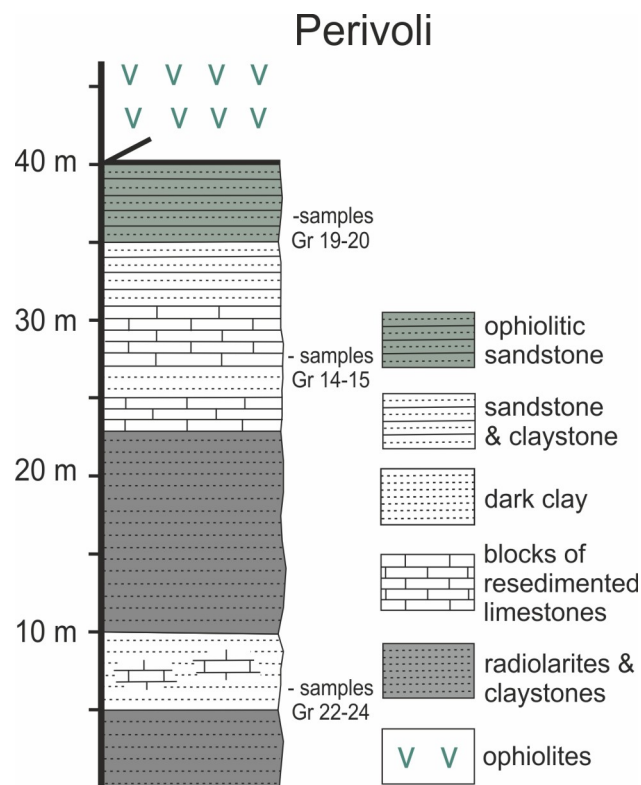
Figure 5.21 Perivoli stratigraphic section (Kostaki et al. 2023). The section is characterized by resedimented carbonates integrated within deep-water sediments of the Avdella mélange. Sampling positions of the resedimented carbonates are marked.
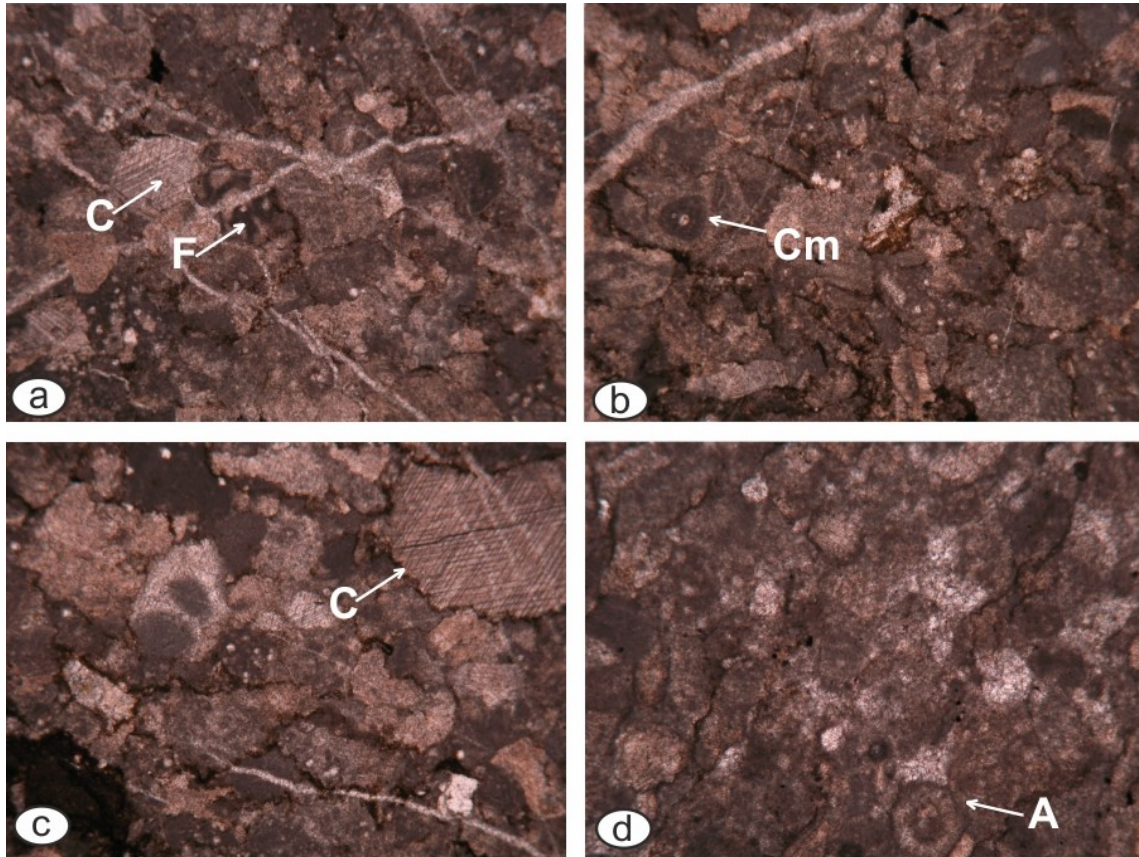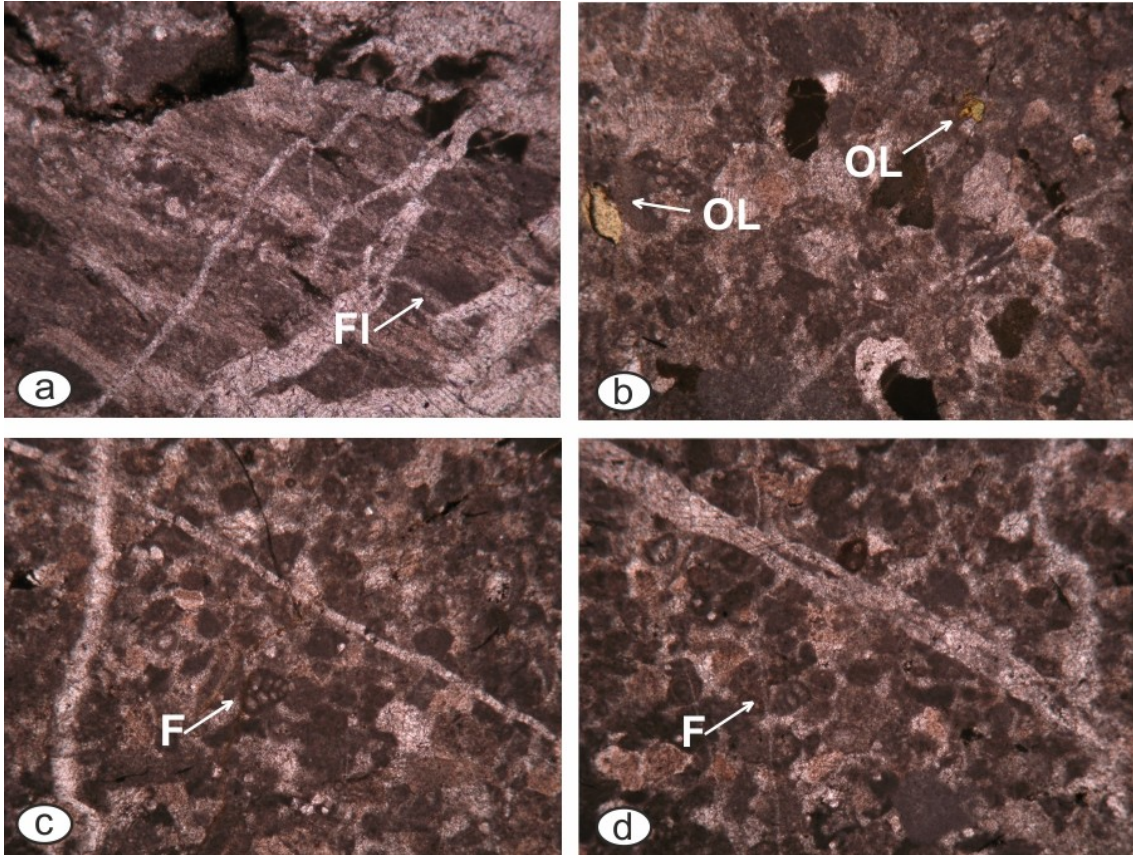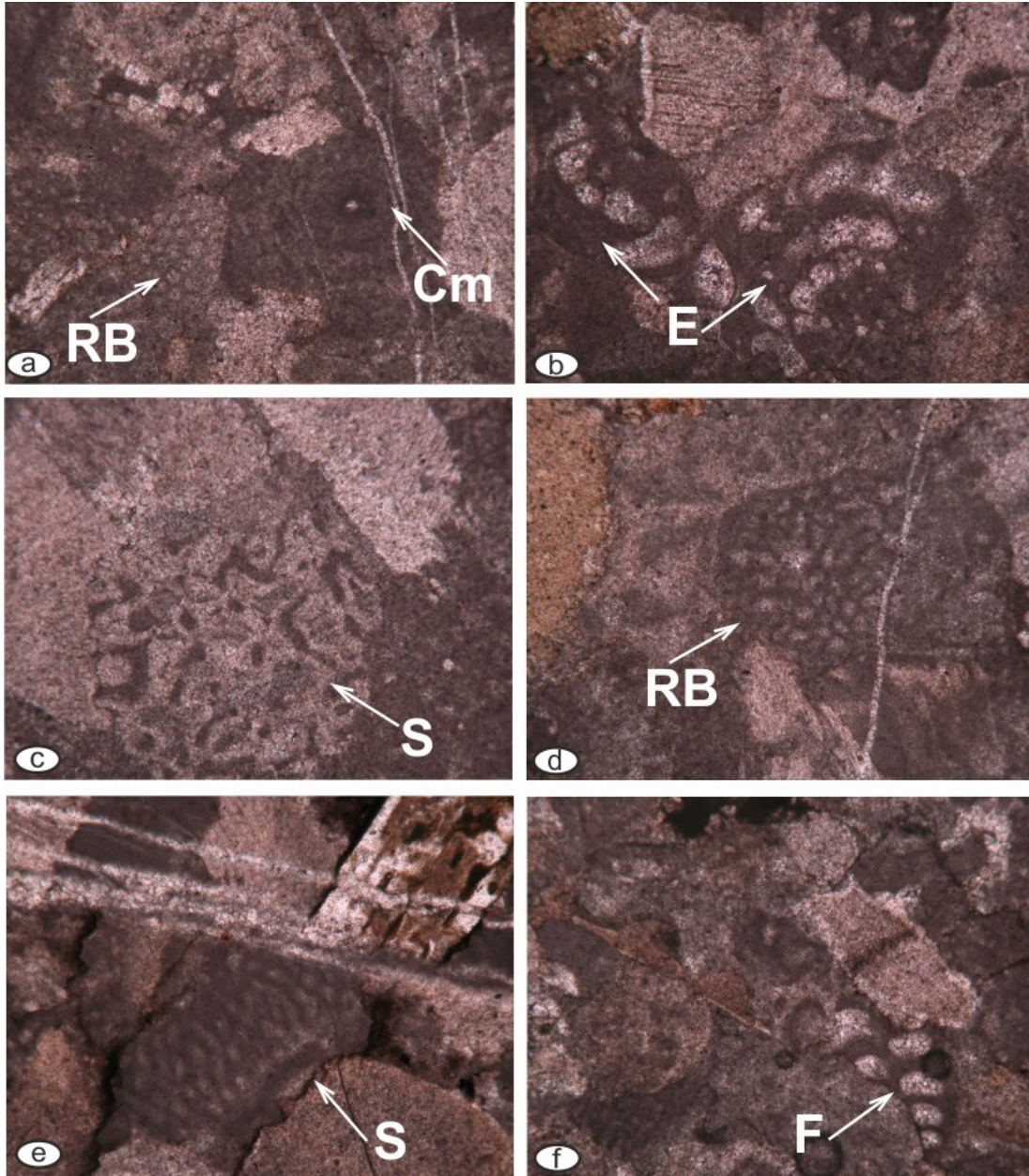
Plate 3. Characteristic microfacies from the resedimented carbonates (Perivoli area; Avdella mélange). Samples Gr (22-24) (width of photo: 1 mm): **a)** Packstone with reef-building organisms (RB) and the microencruster *Crescentiella morronensis* (Crescenti) (Cm). **b)** Packstone composed of different lithoclasts and encrusting organisms (E). **c)** Packstone containing a sponge (S). **d)** Packstone composed of different lithoclasts and a reef-building organism (RB). **e)** Grainstone consisting of different kind of lithoclasts and a reworked fragment of a sponge. **f)** Packstone with a fragment of a foraminifera that exhibits micritic coating (F).
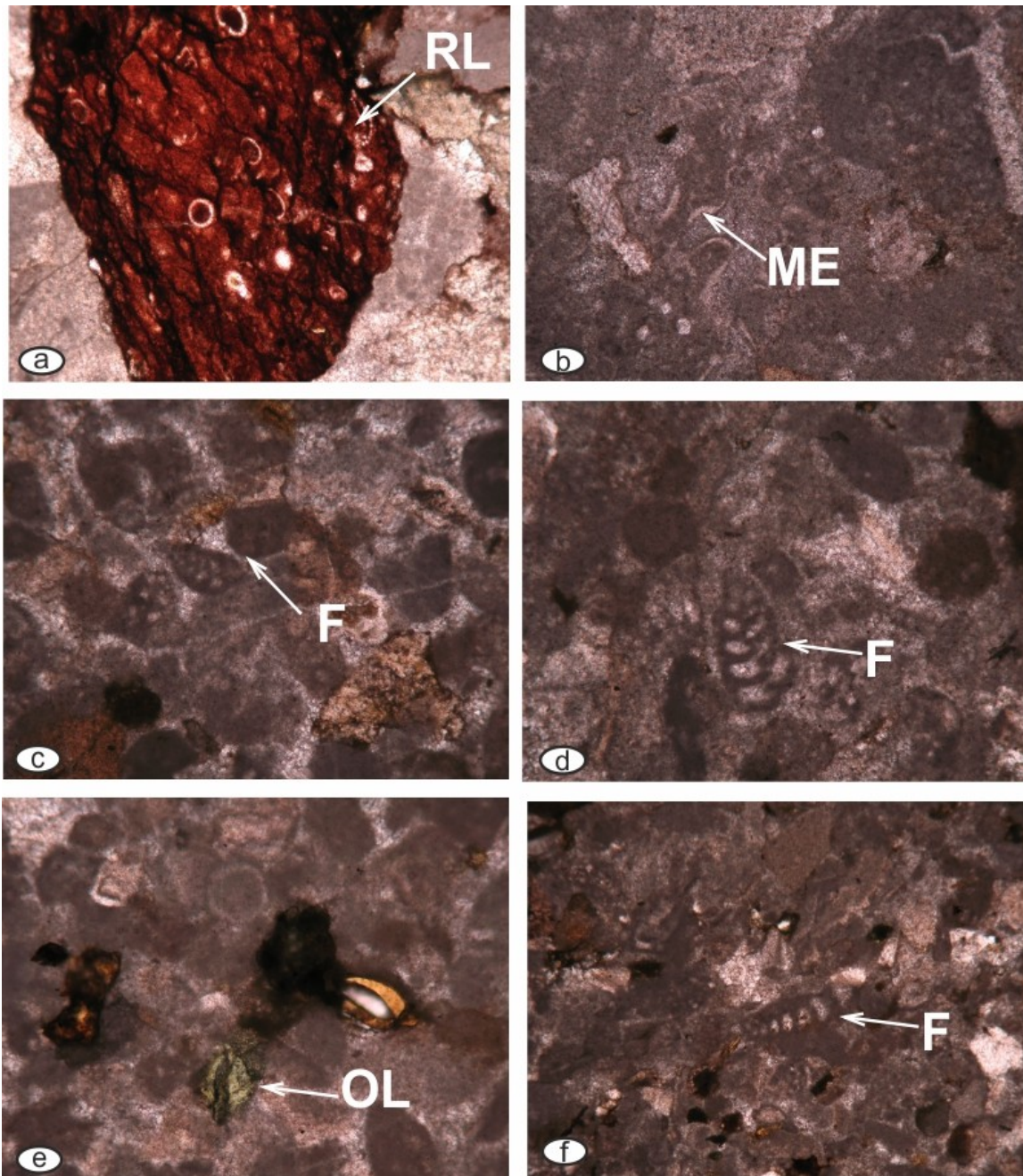
Plate 4. Characteristic microfacies from the resedimented carbonates (Perivoli area; Avdella mélange). Samples Gr (22-24) (width of photo: 1 mm): **a**) Grainstone with an older Triassic lithoclast enclosing recrystallized radiolarians (RL). **b**) Packstone containing grains with micritic encrustations (ME) around them. Samples Gr (14-15): **c**, **d**) Grainstone with different lithoclasts and foraminifera (F) (width of photo: 1 mm). **e**) Packstone containing ophiolitic lithoclasts (OL) (width of photo: 1 mm). **d**) Grainstone consisting of different lithoclasts and foraminifera (F) (width of photo: 2 mm).

99
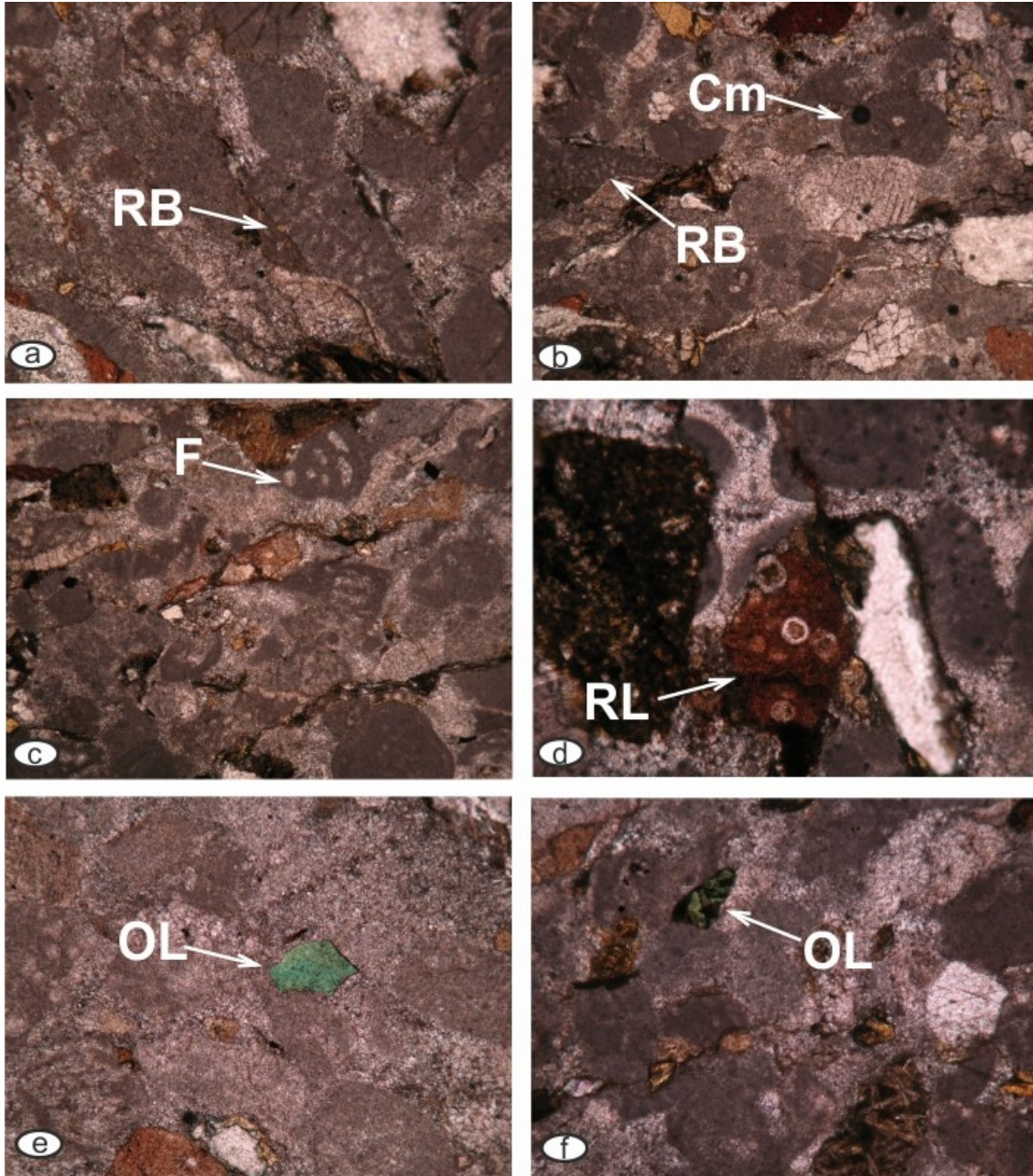
Plate 5. Characteristic microfacies from the resedimented carbonates (Perivoli area; Avdella mélange). Samples Gr (19-21): **a**) Grainstone with a reworded reef-building organism fragment (RB) (width of photo: 1 mm). **b**) Grainstone composed of a reworded reef-building organism fragment (RB), *Crescentiella morronensis* (Crescenti) (Cm) and different kind of lithoclasts (width of photo: 2 mm). **c**) Grainstone composed of different lithoclasts and a coated foraminifera (F) (width of photo: 2 mm). **d**) Grainstone with different lithoclasts, including an older Triassic lithoclast enclosing recrystallized radiolarians (RL) (width of photo: 1 mm). **e**, **f**) Packstone containing ophiolitic lithoclasts (OL) (width of photo: 1 mm).

100
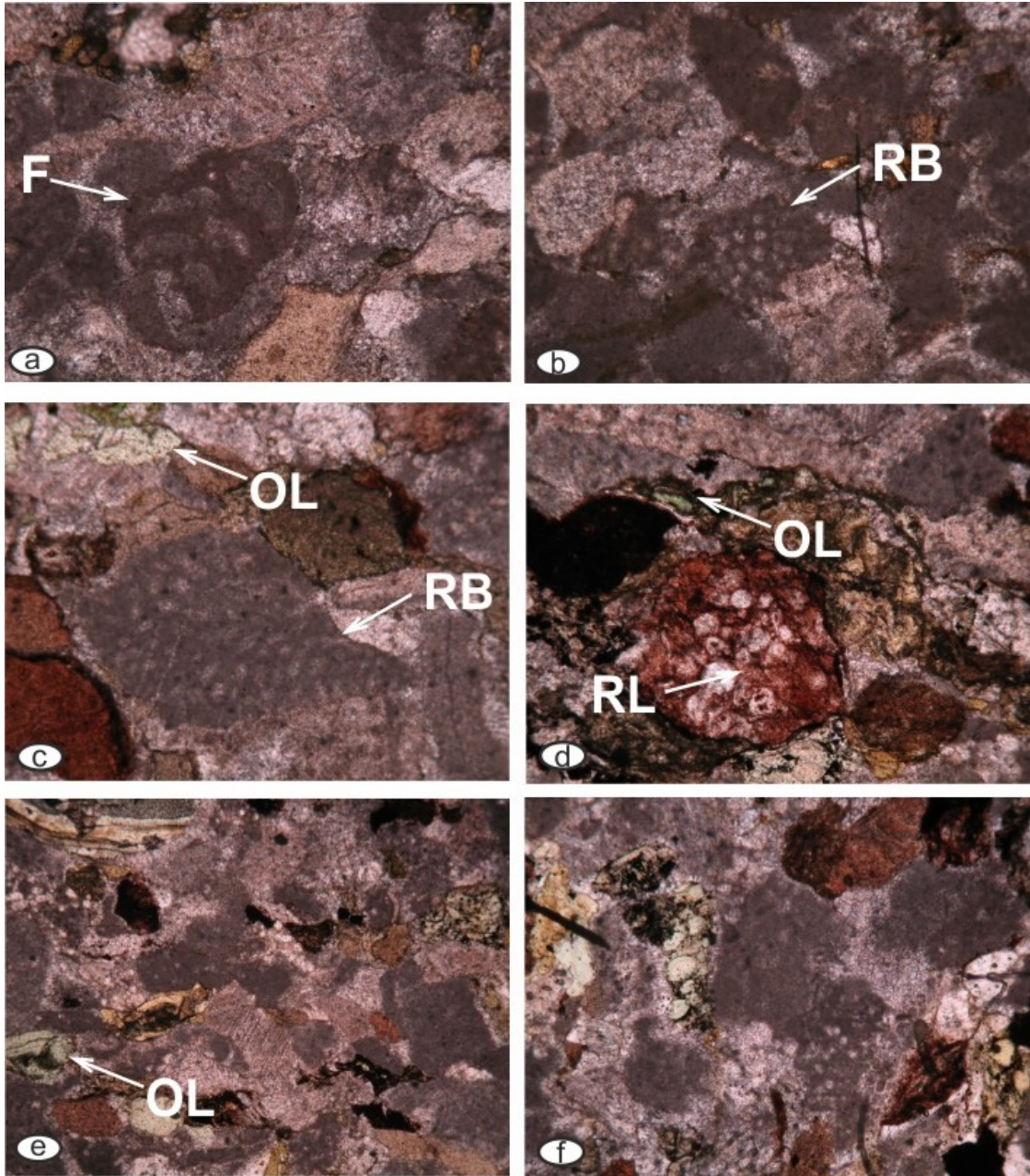
Plate 6. Characteristic microfacies from the resedimented carbonates (Perivoli area; Avdella mélange). Samples Gr (19-21): **a)** Grainstone composed of different lithoclasts and a coated foraminifera (F) (width of photo: 1 mm). **b)** Grainstone containing lithoclasts and reef-building organisms (RB) (width of photo: 1 mm). **c)** Grainstone composed of a reef-building organism (RB) and a mixture of lithoclasts, including ophiolitic lithoclasts (width of photo: 1 mm). **d)** Grainstone including a lithoclast enclosing recrystallized radiolarians (RL) and ophiolitic lithoclasts (width of photo: 1 mm). **e**, **f)** Grainstone composed of a mixture of shallow-water debris and ophiolitic lithoclasts (OL) (width of photo: 2 mm).

5.4 Earliest Cretaceous mass-flow deposits on top of the Vardar-Axios ophiolites

The presence of shallow-water microfacies mixed with ophiolitic-derived debris in the resedimented carbonates found in the Perivoli and Ziakas areas created the necessity to determine their paleogeographic relationship with Late Jurassic microfacies of better preserve carbonate successions associated with the obducted ophiolites. Therefore, a documentation is provided of an Earliest Cretaceous carbonate succession exposed on top of Vardar-Axios ophiolites in the vicinity of Neochorouda village (Figure 5.22). This comparison is essential for identifying potential shared tectono-stratigraphic trends.

This succession is characterized by mass-flow deposits intercalated with some turbiditic layers (Figure 5.23), and it was throughout studied within the framework of Kostaki's master thesis (2013), as well as by other researchers such as Mercier (1968), Kockel and Mollat (1977), Mussalam and Jung (1986), Ricou et al. (1998), and Meinhold et al. (2009). The succession is massive, comprising components of various sizes, including a large number of reefal limestones with impressive fossils, as well as ophiolite-derived debris that can be identified macroscopically (Figure 5.24).

According to Kostaki (2013), sedimentation started on top of the ophiolites with the deposition of a breccia composed of subangular to subrounded components from multiple sources, including ophiolite-derived debris and reworked shallow-water clasts (Figure 5.25).

The collected samples are identified as bioclastic packstones to grainstones (following Dunham's classification) or packed biomicrite (following Folk's classification). In thin sections, remains of reef-building organisms, crinoids, brachiopods, shell fragments, foraminifera, and other lithoclasts are present (Plate 7). The microencruster *Crescentiella morronensis* (Crescenti) is commonly observed, and some grains exhibit coating and encrustation. Additionally, a fragment of the algae *Griphoporella jurassica* (Endo), and the benthic foraminifer *Labyrinthina mirabilis* Weynschenk are encountered. The Kimmeridgian age is determined based on the identification of this fossil assemblage (Schlagintweit et al. 2005, Schlagintweit 2011).
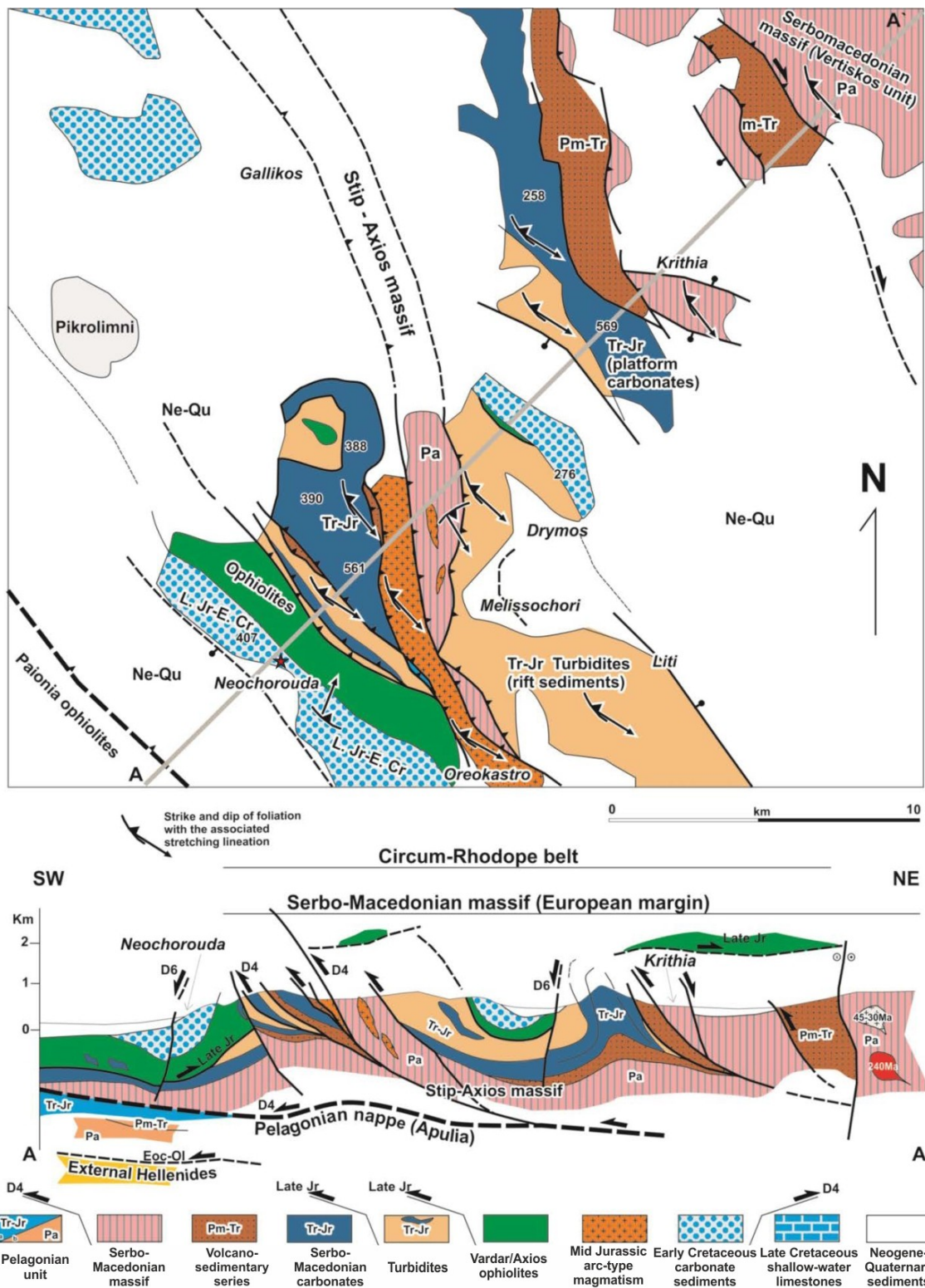
Figure 5. 22 Simplified geological map and cross-sectional representation of the Vardar-Axios ophiolites situated at the Axios Zone (Kilias 2021).

Figure 5.23 Vardar-Axios ophiolites unconformable overlaid by an Early Cretaceous sedimentary succession (Kostaki 2013) ($40^0 44'53''$N, $22^0 52'39''$E).

The succession extends into coarse-grained carbonate mass-flow deposits, incorporating diverse reworked reef components such as boundstones and bafflestones, which are mixed with ophiolite-derived lithoclasts (Plates 7 and 8) (Figures 5.25 and 5.26).

The fossil assemblage is characterized by corals, sponges, benthic foraminifera such as *Pseudocyclammina lituus* (Yokoyama), and a significant present of encrusting microorganisms. The microencruster *Radiomura cautica* Senowbari-Daryan and Schäfer, indicative of (fore-) reefal facies (Senowbari-Daryan and Schäfer 1979, Schlagintweit and Gawlick 2009), is also identified. Additionally, the microencrusters *Labes atramentosa* Eliasova, *Perturbatacrusta leini* Schlagintweit and Gawlick, and *Crescentiella morronensis* (Crescenti) are included. The dasycladales *Griphoporella jurassica* (Endo) and *Neoteutloporella socialis* (Praturlon), along with the calcareous algae T*haumatoporella* sp., are frequently encountered. These taxa are indicative of reefal and peri-reefal facies from the Tithonian age (Plates 7 and 8).
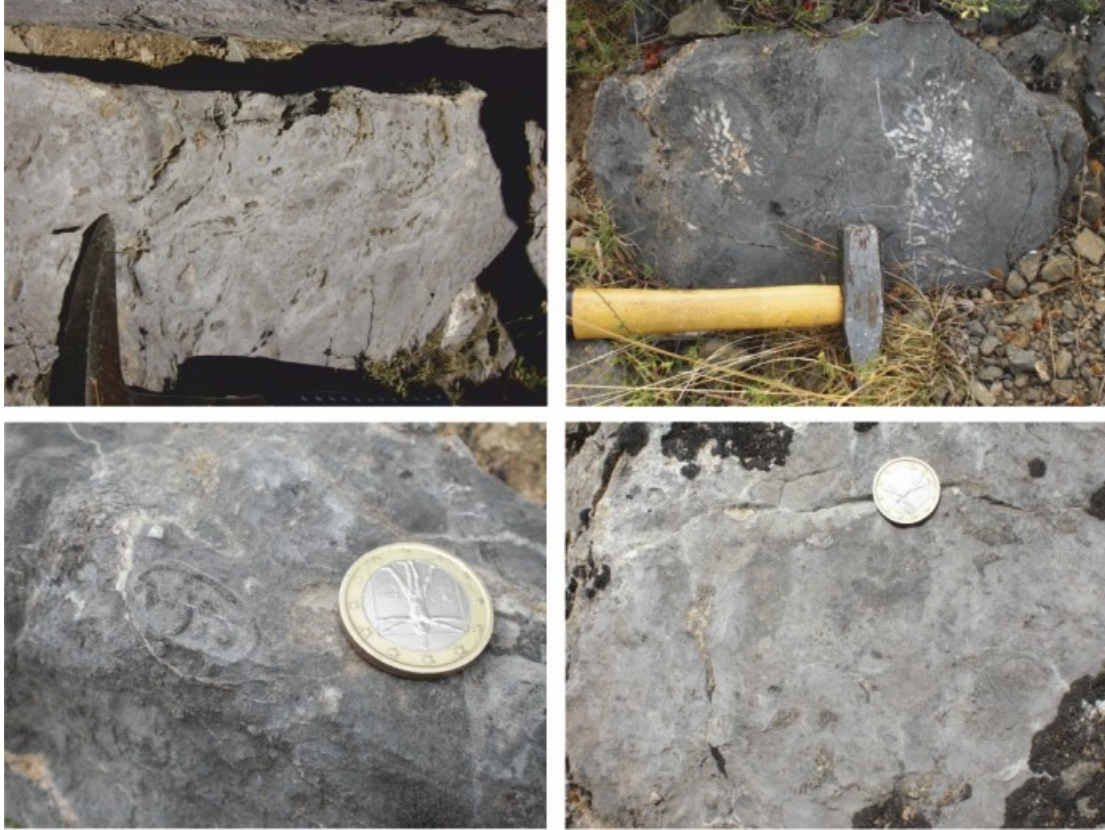
Figure 5.24 Impressive macroscopic appearance of reafal limestones within the mass-flow deposits on top of Vardar-Axios ophiolites (Kostaki 2013) ($40^0 44' 53'' N$, $22^0 52' 39'' E$).

The microfacies and fossil content suggest that the reworked reef components originated from different facies zones of a rimmed shallow-water carbonate platform, with some originating from the central parts of a reef, others from back-reef and fore-reef areas, and several from open and closed lagoon areas (Plates 7 and 8). This Late Jurassic (Kimmeridgian?- Tithonian) shallow-water carbonate platform is inferred to have initially been formed on top of the ophiolite nappe stack (Kostaki 2013, Kostaki et al. 2013, 2014).

Above the mass-flow deposits, there is a transition to a turbiditic sequence with intercalated coarse-grained mass-flows (Figures 5.25 and 5.27). The collected samples are identified as bioclastic grainstone (following Dunham's classification) or poorly washed biosparite (following Folk's classification) (Plate 8). In the thin sections, bioclasts, different kinds of coated grains, and sandstone lithoclasts are present (Plate 8).

e *Crescentiella morronensis*
Suppiluliumaella aff. *methana*
Carpathoporella sp.
Coscinophragma sp.
Selliporella neocomiensis
Andersenolina sp.
Solenoporaceae
Linoporella aff. *capriotica*
Griphoporella cretacea
Furcoporella? vasilijesimici
Radiomura cautica
Griphoporella cretacea
Griphoporella jurassica

c *Dissocladella? bakalovae*
Anchspirocyclina lusitanica
Pseudocyclammina lituus
Labes atramentosa
Mohlerina basiliensis
Crescentiella morronensis
Nautiloculina cf. *oolithica*
Radiomura cautica
Salpingoporella pygmaea
Trinocladus? sp

b *Neoteutloporella socialis*
Crescentiella morronensis
Perturbatacrusta leini
Labes atramentosa
Radiomura cautica
Thaumatoporella sp
Griphoporella jurassica
Pseudocyclammina lituus

a *Labirinthina mirabilis*
Griphoporella jurassica
Crescentiella morronensis

40 m

Legend:
- ~ Phyllites with intercalations of limestone
- Conglomerate
- Turbiditic sequence of sandstone
- Carbonate breccia
- Breccia with gabbroic and carbonate clasts
- Ophiolite complex

Figure 5.25 Stratigraphic section of the Early Cretaceous sedimentary succession on top of Vardar-Axios ophiolites (Kostaki 2013).

The bioclasts include remnants of various reef-building organisms, including corals and sponges (Plate 8). Additionally, foraminifera such as *Pseudocyclammina lituus* (Yokoyama), *Anchispirocyclina lusitanica* (Egger), *Mohlerina basiliensis* (Mohler), and *Nautiloculina* cf. *oolithica* Mohler are present. The Dasycladales algae *Salpingoporella pygmaea* (Gümbel) and *Dissocladella? Bakalovae* Dragastan are also identified. The microencrusters *Radiomura cautica* Senowbari-Daryan and Schäfer, *Labes atramentosa*

106

Eliasova, and *Crescentiella morronensis* (Crescenti) are also encountered. The identification of this fossil association points to a transition into the Early Cretaceous (Plate 8).

This phase, characterized by the inflow of siliciclastic material, was succeeded by the deposition of a massive polymictic breccia with subangular to subrounded components of different dimensions, ranging from centimeters to meters (Figure 5.28). The conglomerate is dominated by older recrystallized carbonates, quartzite, and other siliciclastic rocks that derived from the Triassic to Early Jurassic Pelagonian carbonate platform cover and the underlying crystalline basement. In thin sections, potential Middle Triassic carbonate components containing foraminifera and recrystallized radiolarian can be recognized (Plate 9).

The succession, as described so far, manifests propagated erosion, which at the initial state affected a Late Jurassic shallow-water carbonate platform, sealing the ophiolite emplacement. Subsequently, the erosion extended to the underlying ophiolites, resulting in the deposition of coarse-grained carbonate mass-flows containing material derived from both sources into newly formed basins (reworked reef components incorporated together with ophiolite-derived material). Erosion commenced shortly after the platform sedimentation, occurring during the Late Tithonian to Earliest Cretaceous, as verified by the increasing supply of siliciclastic sediments, which ultimately led to the formation of the turbiditic sequence composed of sandstones (Figure 5. 27).

This process was accompanied by continuous uplift of the accreted Pelagonian region, leading to ongoing erosion of the nappe stack. Subsequently, substantial erosion reached the Triassic-Jurassic Pelagonian carbonate platform cover and the uppermost parts of its crystalline basement, which gave origin to the polymictic conglomerate (Figure 5.28).

Therefore, the Late Jurassic to Early Cretaceous evolution has been defined by profound erosion resulted from crustal unroofing and extension, which ultimately led to exhumation of the crystalline basement and reconfiguration of the ophiolite nappe stack. Consequently, the erosional products of this event were transported and redeposited into newly formed basins.

Figure 5.26 Coarse-grained carbonate mass-flow deposits composed of various reworked reef components on top of Vardar-Axios ophiolites ($40^0 44' 53'' N$, $22^0 52' 39'' E$).

Figure 5.27 Turbiditic sequence with intercalated coarse-grained mass-flow deposits on top of Vardar-Axios ophiolites ($40^0 44' 53'' N$, $22^0 52' 39'' E$).

Figure 5.28 Massive polymictic breccia composed of subangular to subrounded components of different dimensions (Kostaki 2013) (40^{0}44´53´´N, 22^{0}52´39´´E).

In the Early Cretaceous, there was a notable rise in carbonate production in that area, potentially due to basin subsidence east of the uplifted Pelagonian region, which resulted in the formation of shallow-water carbonates (Figure 5.29).

Boundstones containing corals, sponges, and stromatoporoids represent typical microfacies of these carbonates deposited above the polymictic conglomerate (Plate 9). Additionally, dasycladales such as *Linoporella* aff. *capriotica* (Oppenheim), *Furcoporella? vasilijesimici* Radoicic, *Suppiluliumaella* aff. *methana* Dragastan and Richter, *Griphoporella cretacea* (Dragastan), and debris of *Selliporella neocomiensis* (Radoicic) are encountered. The microencruster associations include *Crescentiella morronensis* (Crescenti) and *Radiomura cautica* Senowbari-Daryan and Schäfer. Foraminifera such as *Coscinophragma* sp. and *Andersenolina* sp. are also present. Based on the recovered fauna, the shallow-water carbonates are dated as Berriasian to Valanginian (Plate 9).

A shallow-water carbonate evolution from the Berriasian to Early Valanginian has also been described by Ivanova et al. (2015) and Chatalov et al. (2015) in the eastern Circum-Rhodope Belt.

Figure 5.29 Shallow-water carbonates dated as Berriasian to Early Valanginian (Kostaki 2013) ($40^0 44′53′′$N, $22^0 52′39′′$E).
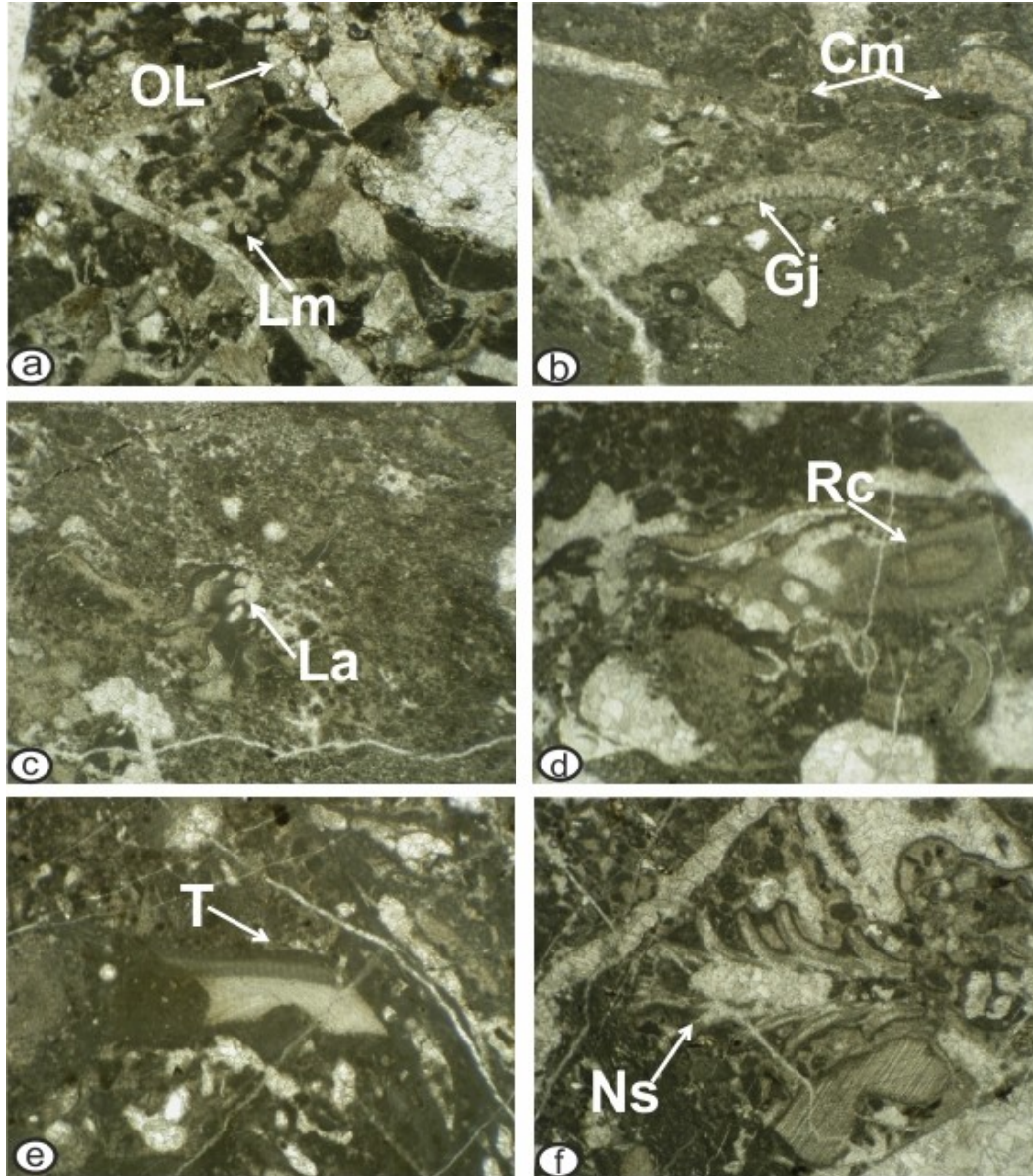
Plate 7. Microfacies of the components in the breccia on top of the ophiolites (width of photo: 1 mm): **a**) Grainstone containing various lithoclasts, including ophiolite-derived lithoclasts (OL) and the benthic foraminifera *Labyrinthina mirabilis* Weynschenk (Lm), some grains are coated and encrusted. **b**) Packstone with lithoclasts, a fragment of the Dasycladales *Griphoporella jurassica* (Endo) (Gj), and the microencruster *Crescentiella morronensis* (Crescenti) (Cm). Microfacies from the coarse-grained carbonate mass-flow deposits consisting of reworked reef components (width of photo: 1 mm): **c**) Boundstone with the microencruster *Labes atramentosa* Eliasova (La); and **d**) *Radiomura cautica* Senowbari-Daryan and Schäfer (Rc). **e**) Boundstone with the calcareous algae *Thaumatoporella* sp. (T); and f) the dasycladale *Neoteutloporella socialis* (Praturlon) (Ns) in longitudinal section. (Adapted from Kostaki 2013).

111
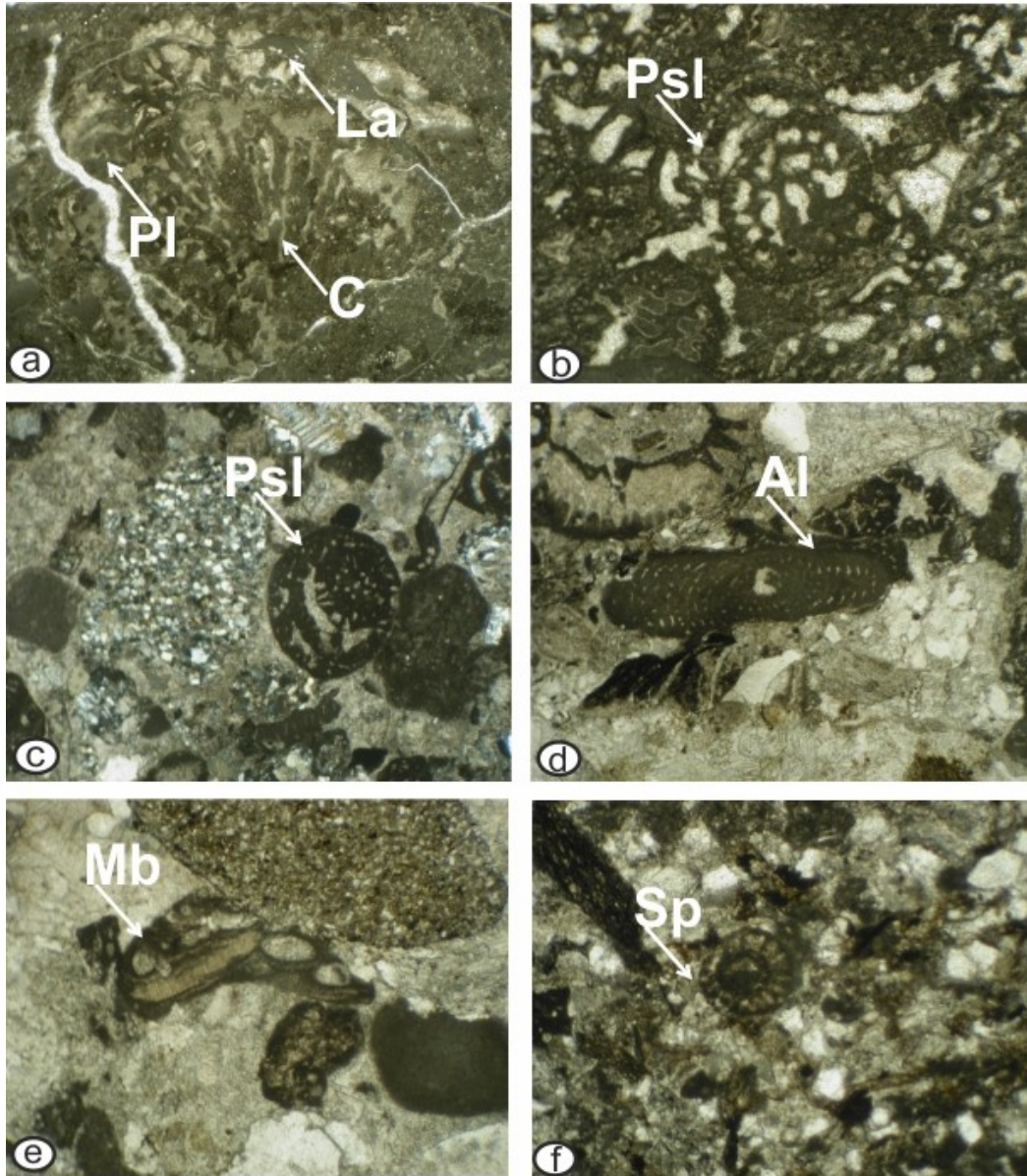
Plate 8. Microfacies from the coarse-grained carbonate mass-flow deposits consisting of reworked reef components (width of photo: 1 mm): **a)** Boundstone composed of a coral (C) that, in the upper part, exhibits the encrustation of *Perturbatacrusta leini* Schlagintweit and Gawlick (Pl) and *Labes atramentosa* Eliasova (La). **b)** Boundstone, including the benthic foraminifer *Pseudocyclammina lituus* (Yokoyama) (Psl). Characteristic microfacies from the turbiditic sequence (width of photo: 1 mm): **c)** Grainstone with the benthic foraminifer *Pseudocyclammina lituus* (Yokoyama) (Psl) and sandstone lithoclasts. **d)** The benthic foraminifera *Anchispirocyclina lusitanica* (Egger) (Al) and quartz lithoclasts. **e)** Grainstone comprised of sandstone lithoclasts, the foraminifer *Mohlerina basiliensis* (Mohler) (Mb); and **f)** *Salpingoporella pygmaea* (Gümbel) (Sp). (Adapted from Kostaki 2013).
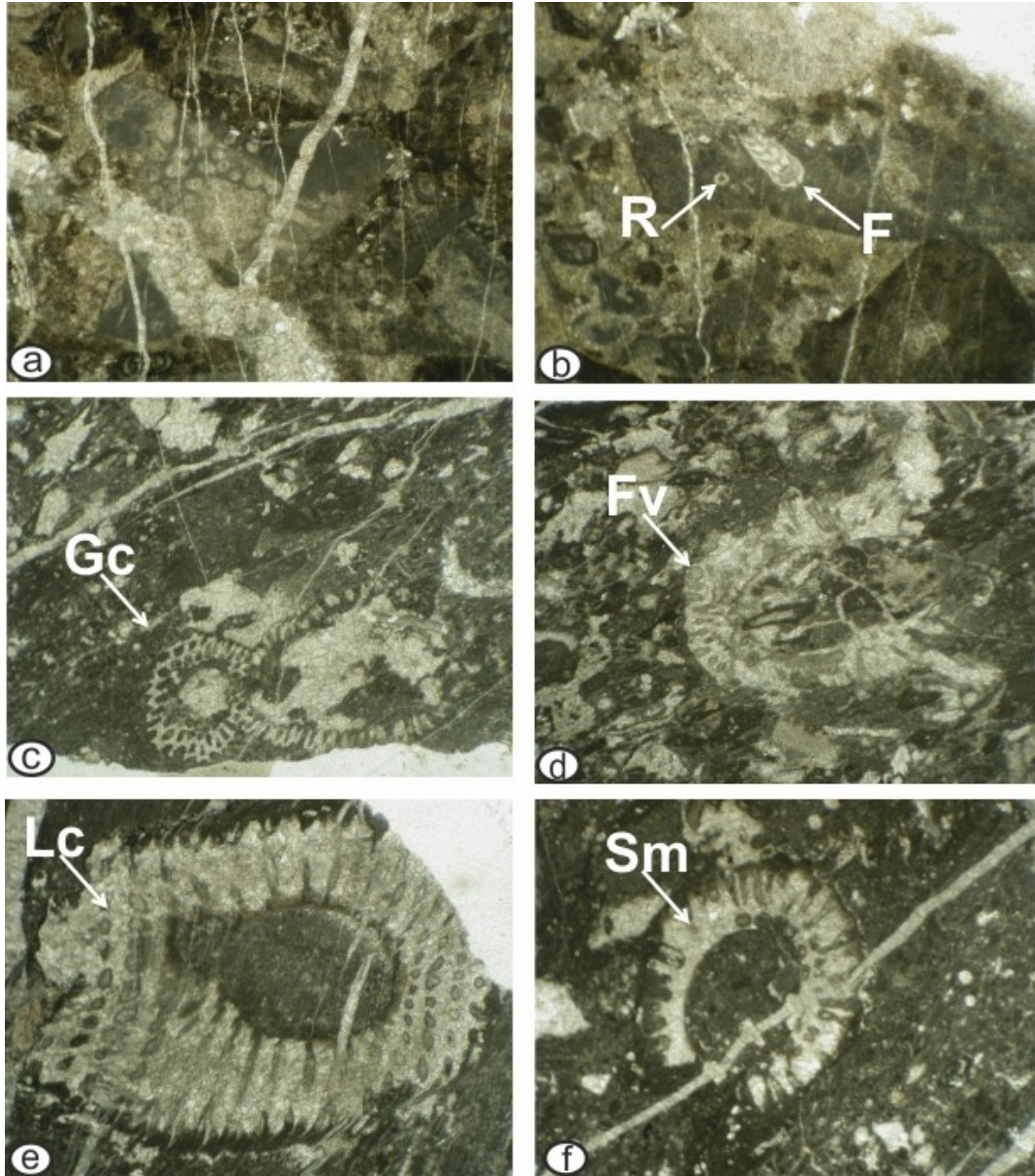
Plate 9. Microfacies of the components within the polymictic conglomerate (width of photo: 1 mm): **a**) Grainstone containing recrystallized shallow-water carbonate components, and **b**) possible Middle Triassic recrystallized carbonate component containing foraminifera (F) and recrystallized radiolarian (R). Microfacies from the Early Cretaceous shallow-water carbonates (width of photo: 1 mm): **c**) Boundstone with the algae *Griphoporella cretacea* (Dragastan) (Gc); **d**) *Furcoporella*? *vasilijesimici* Radoicic (Fv); and **e**) *Linoporella* aff. *Capriotica* (Lc) (Oppenheim). **f**) Boundstone containing the algae *Suppuliumaella* aff. *methana* Dragastan and Richter (Sm). (Adapted from Kostaki 2013).

5.5 Koziakas mélange and basin fill sediments

Microfacies analysis, conodont age dating, and radiolarian age dating were conducted on samples collected from different outcrops of the Koziakas mélange on the eastern slopes of the Koziakas mountain range (Figure 4.1; location 2). This specific location is characterized by the presence of Triassic Hallstatt blocks and slides of various sizes within an argillaceous-radiolaritic matrix of Jurassic origin, representing the lower part of the mélange.

Higher up, basin fill sediments cover this part of the mélange, consisting of thick, multicolored Middle-Late Jurassic radiolarite-rich turbidites intercalated with oolitic limestones (Figure 5.30) (Karfakis 1984, Bortollotti et al. 2004). At even higher stratigraphic levels, the radiolarite-rich turbidites are intercalated with Late Jurassic to Earliest Cretaceous shallow-water carbonate-clastic resediments (Gnon et al. 2018).

Figure 5.30 Panoramic view of the basin fill sediments (radiolarite-rich turbidites intercalated with oolitic limestones) above the Koziakas mélange in the vicinity of Agios Vissarionas village (39^{0}47′53′′N, 21^{0}60′27′′E).

5.5.1 Triassic Hallstatt blocks within Koziakas mélange

Microfacies analysis and conodont age dating methods were employed to analyze several samples collected from different exotic blocks within the Jurassic matrix of the Koziakas mélange (Figure 5.31). These blocks exhibit a range of colors and sizes and were encountered in various outcrops along the local roads connecting the Agios Vissarionas village to the Monastery Dousiko, as indicated in Figure (5.32).

The sample GR (62) was collected from a polymictic breccia found at an outcrop in the lower part of the road leading toward the monastery (Figure 5.31; a). Conodont age dating was conducted based on the identification of the taxa *Gladigondolella*-ME, *Gladigondolella* cf. *malayensis*, *Paragondolella foliata,* and *Paragondolella* cf. *Inclinata*, suggesting a latest Longobardian to earliest Carnian age.
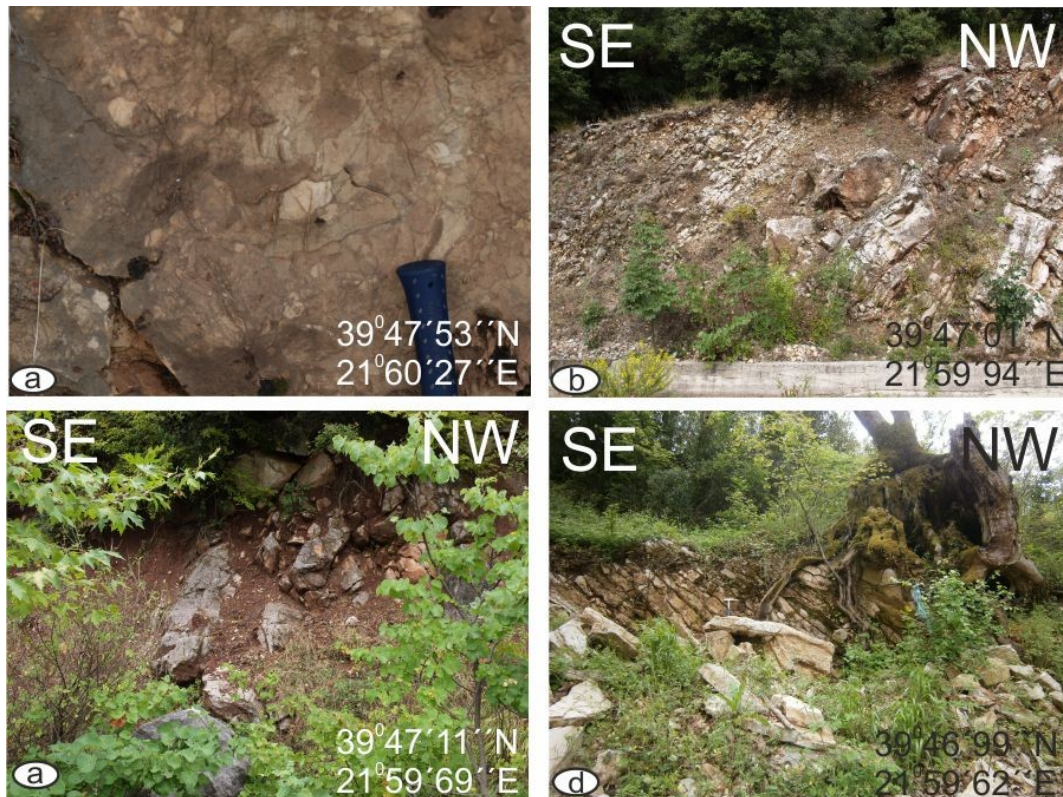
Figure 5.31 Outcrop situation and sampling positions of the exotic open-marine blocks in the argillaceous-radiolaritic matrix of Koziakas mélange: **a)** Polymictic breccia (GR 62). **b)** Filament limestone (GR 69). **c)** Grey micritic limestone with red chert nodules (GR 70). **d)** Medium bedded grey siliceous limestone (Gr 43).
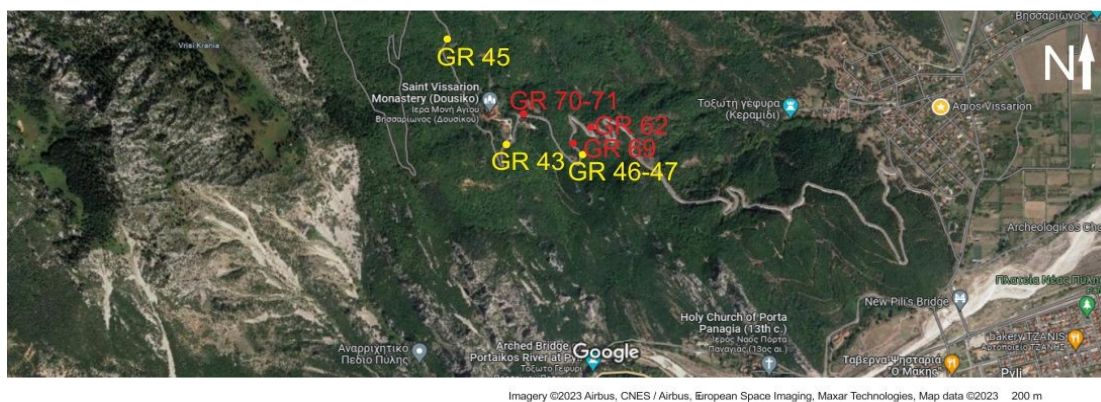
Figure 5.32 Satellite image of the eastern Koziakas mountain range with marked the sampling positions. Yellow dots represent sample positions for microfacies analysis, while red dots indicate position for conodont age dating (Google earth 11/11/2023).

A few meters away, the sample GR (69) was collected from a block of filament limestone situated below radiolarites with turbidites composed of shallow-water debris (Figure 5.31; b). Conodont age dating was conducted based on the identification of the taxa *Gladigondolella*-ME, *Paragondolella foliata*, *Paragondolella* cf. *inclinata*, and *Paragondolella polygnathiformis*, indicating a lowermost Carnian (Cordevolian) age.

The samples GR (70) and GR (71) were collected from an outcrop in the upper part of the road leading toward the monastery. The samples GR (70) was collected from a block of grey micritic limestones containing red chert nodules (Figure 5.31; c). Conodont age dating was conducted based on the identification of the taxa *Epigondolella rigoi* and *Norigondolella hallstattensis*, suggesting an Early Norian age.

The sample GR (71) was collected from a polymictic breccia. Conodont age dating was carried out by identifying the taxon *Paragondolella polygnathiformis* assigning a Carnian age.

The sample Gr (43) was collected from an outcrop near the Monastery Dousiko. This particular sample was collected from a block of medium bedded grey siliceous limestone (Figure 5.31; d). In thin sections, the microfacies are characterized as dark reddish-grey pelagic non-laminated wackestone (following Dunham's classification) or biomicrite (following Folk's classification) containing pelagic microfossils such as radiolarians and thin-shell bivalves (filaments) (Plate 10). Most radiolarians have been

recrystallized into quartz. The biofabric is characterized by loose packing, variation in the sizes of the bioclasts, and medium sorting. These facies indicate open-marine deposition on an outer shelf.

The blocks within the Koziakas mélange, dated as latest Ladinian-earliest Carnian, Carnian, and Early Norian, are inferred to correspond to a dismembered Triassic Hallstatt Limestone succession. These blocks are believed to have originated from the same open-marine shelf as the exotic Hallstatt blocks within the Avdella mélange.

Furthermore, the lowermost Carnian blocks found in the Koziakas mélange are characterized by the influence of shallow-water material, manifesting their development in vicinity of the Wetterstein Carbonate Platform. This suggests that debris deriving from this shallow-water platform was shed in the reef-near outer shelf region, where limestones with bioturbation were originally deposited.
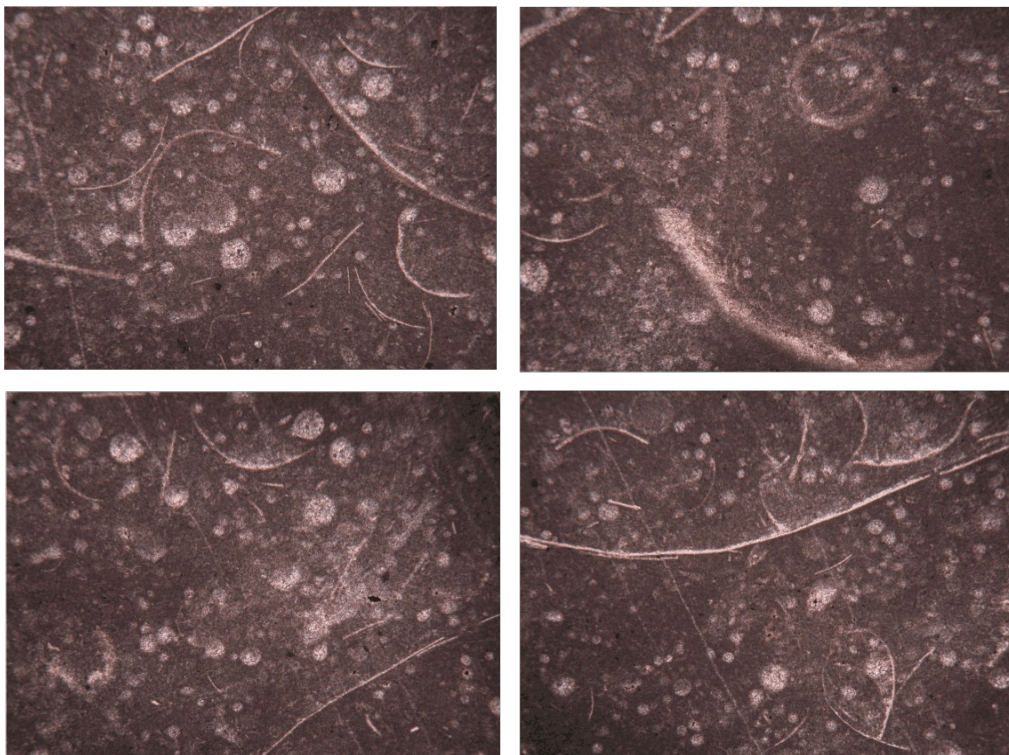
Plate 10. Characteristic microfacies of an open-marine block within Koziakas mélange. Sample Gr (43): Reddish-grey radiolarian-filament wackestone (width of photo: 2 mm).

5.5.2 Late Jurassic to Early Cretaceous basin fill sediments

5.5.2.1 Oolitic limestones

Oolitic limestones are observed intercalated with Middle to Late Jurassic radiolaritic turbidites (Figure 5.33) (Karfakis 1984, Bortollotti et al. 2004). Field observations were made, and samples were collected from the oolitic limestones for microfacies analysis. The studied outcrops are located along the local road connecting Agios Vissarionas village to the forest road above the Monastery Dousiko (Figures 5.32 and 5.33).

Based on the examination of the thin sections, the microfacies of the collected samples are identified as ooidal grainstone (following Dunham's classification) or oomicrite (following Folk's classification), forming a grain-supported fabric in association with bioclasts and aggregated grains (Plates 11 – 14). The fossil assemblage is poor, containing only a few bioclasts, such as some foraminifera, reef-building organisms like calcareous sponge, and bryozoans. Additionally, the foraminifera *Protopeneroplis striata* Weynschenk is encountered within the samples.

Micritic envelopes have devolved around some skeletal and non-skeletal grains, with some foraminifera exhibiting coating, and certain bioclasts presenting an ooid coating. Also, a large quantity of micritized grains occurs.

The grains and ooids display variable sizes. The ooids are well-shaped and characterized by centrifugal growth. In some cases, the ellipsoidal shape of the ooids is controlled by the shape of the core, with some nuclei of the ooids being bioclasts (such as bryozoans, foraminifera, fragments of algae). Moreover, some ooids exhibit additional micritic coating, demonstrating that they have undergone resedimentation.

The age of their deposition cannot be precisely inferred from these samples due to the absence of characteristic fossils. However, the stratigraphic sequence indicates a transition from radiolarite-rich turbidites with intercalated oolitic limestones to turbidites containing shallow-water carbonate-clastic resediments. The latter have been dated as Late Jurassic to Earliest Cretaceous (Ghon et al. 2018), therefore the age of the oolitic limestones can be estimated as Kimmeridgian-Tithonian.

Figure 5.33 Positions of the samples collected from oolitic limestones for microfacies analysis in eastern Koziakas mountain range. **a**, **b**) Oolitic limestones intercalated with Middle-Late Jurassic radiolarite-rich turbidites (Sample Gr 45) ($39^0 46'99''$N, $21^0 59'62''$E). **c**, **d**) Oolitic limestone**s** (Samples Gr 46-47) ($39^0 47'07''$N, $21^0 60'19''$E).
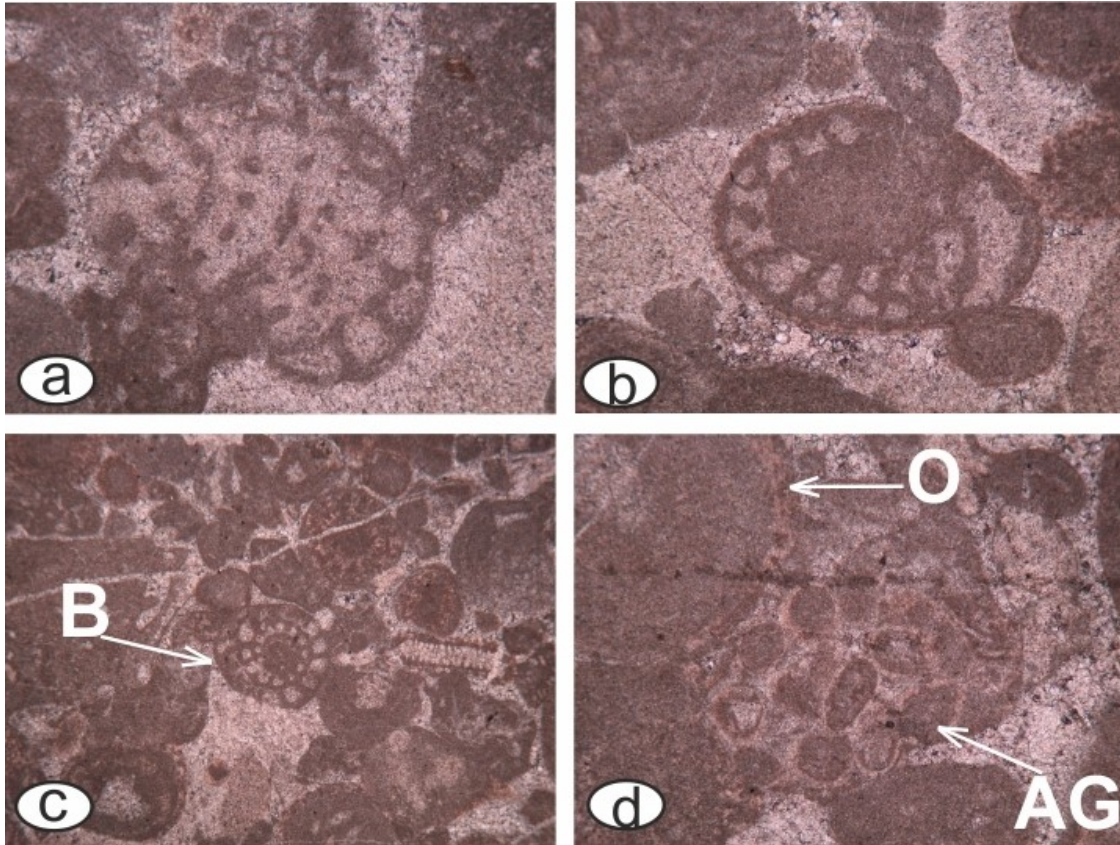
Plate 11. Characteristic microfacies of the oolitic limestone (Sample Gr 45): **a**) Reef-building organism (calcareous sponge) (width of photo: 1 mm). **b**) Ooidal grainstone containing a bioclast that is exhibiting a superficial ooid coating (width of photo: 1 mm). **c**) Grainstone containing a bioclast (B) and some ooids with an elongated shape (width of photo: 2 mm). **d**) Ooidal grainstone, composed of a large ooid (O) and aggregated grains (AG) with cement between the components (width of photo: 1 mm).
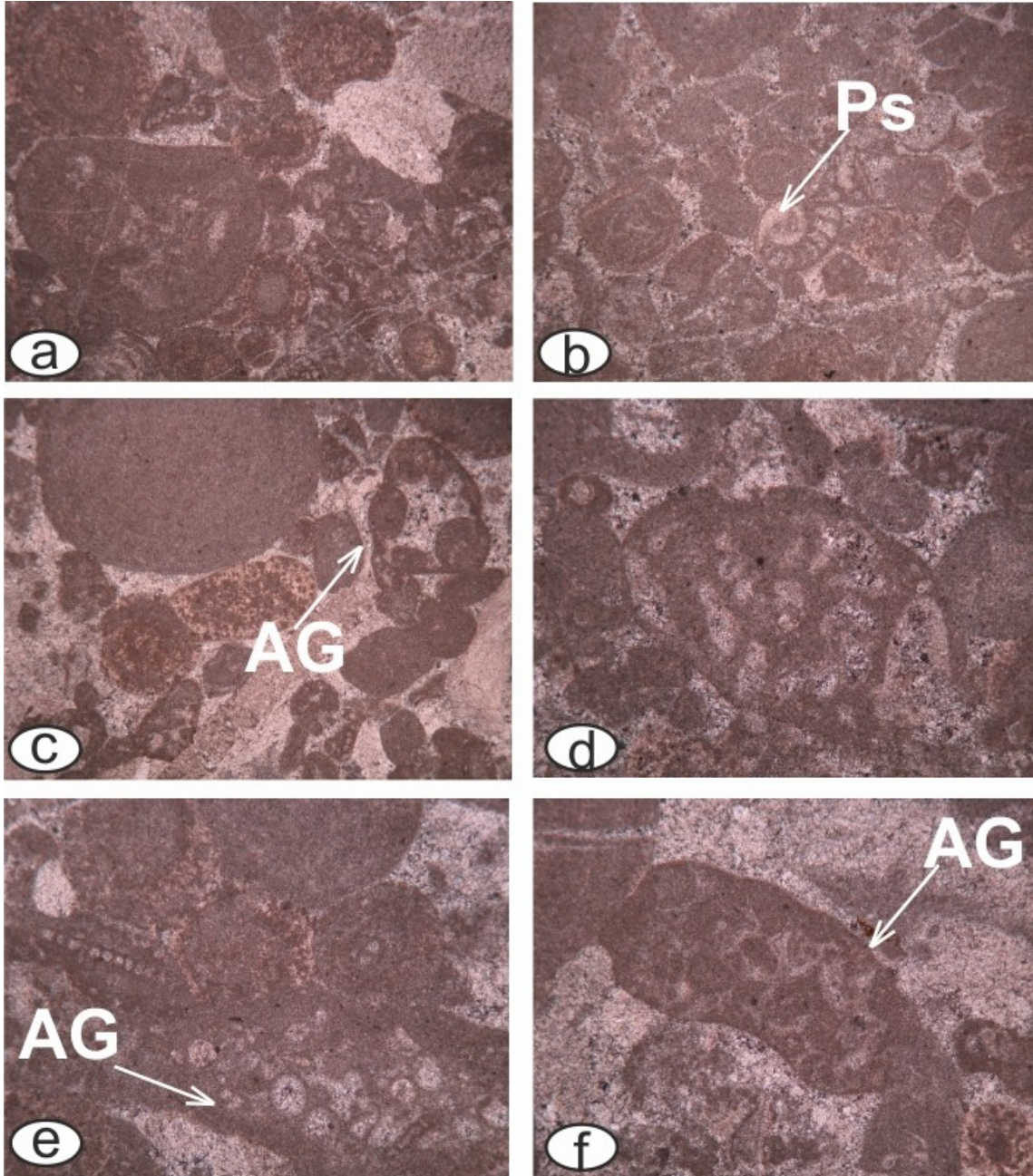
Plate 12. Characteristic microfacies of the oolitic limestone (Sample Gr 45): **a)** Ooidal grainstone consisting of well shaped ooids, characterized by centrifugal growth (width of photo: 2 mm). **b)** Grainstone with micritized rounded grains and *Protopeneroplis striata* Weynschenk (Ps) (width of photo: 2 mm). **c)** Ooidal grainstone composed of aggregated grains (AG) with a typical outline and cement between the components. The grain size is variant, and only a few ooids have an ellipsoidal shape (width of photo: 2 mm). **d)** Micritized skeletal grain (width of photo: 1 mm). **e)** Ooidal grainstone with aggregated grains (AG) (width of photo: 1 mm). **f)** Aggregated grains (AG) mainly containing lumps (width of photo: 1 mm).
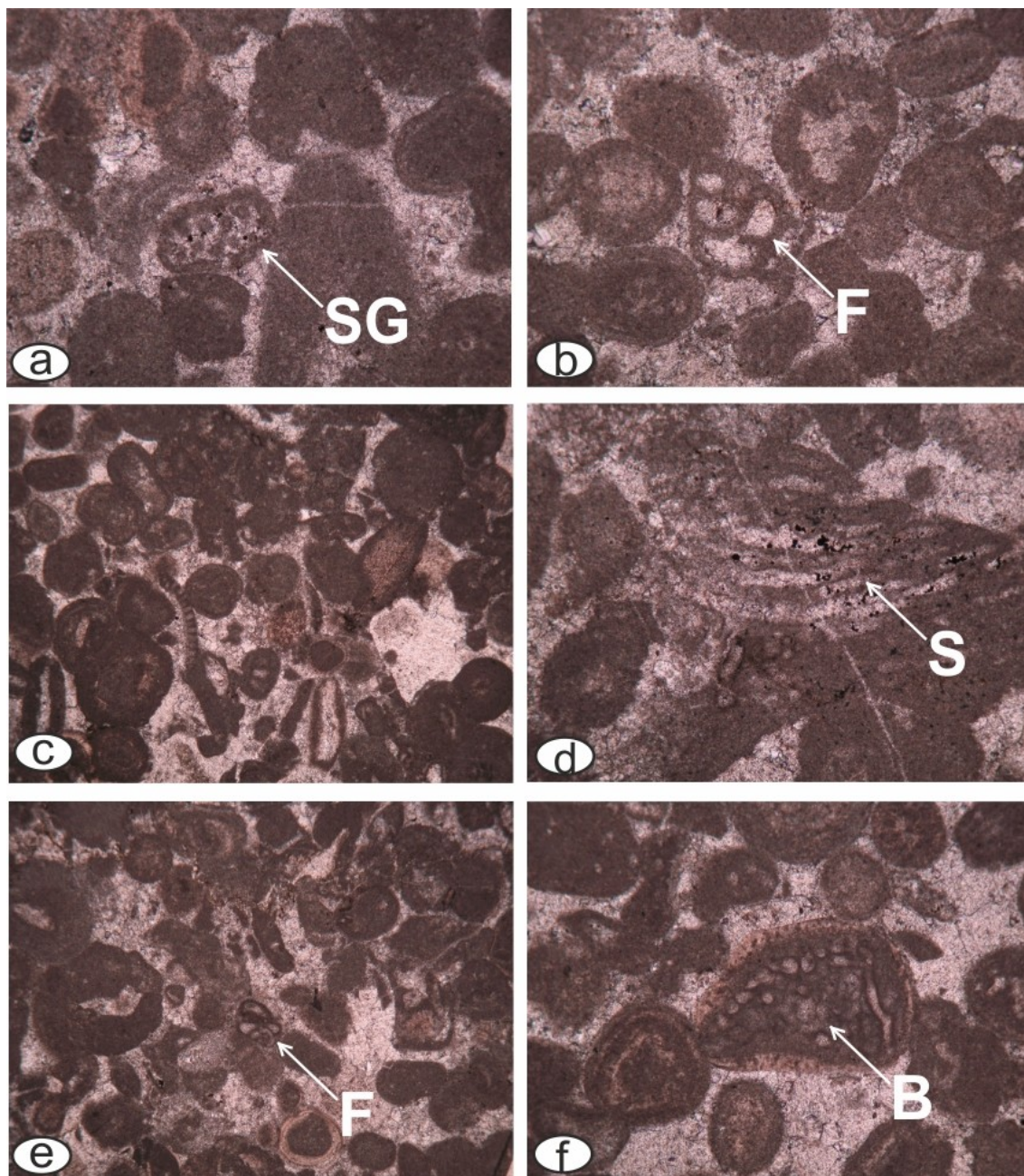
Plate 13. Characteristic microfacies of the oolitic limestone (Sample Gr 46): **a)** Grainstone with micritized grains and a skeletal grain (SG) with ooid coating (width of photo: 1 mm). **b)** Grainstone composed of well shaped ooids and coated foraminifera (F) (width of photo: 1 mm). **c)** Ooidal grainstone with micritised grains and grains with micritic envelopes (width of photo: 2 mm). **d)** Reef-building organism (S) (calcareous sponge) (width of photo: 1 mm). **e)** Grainstone containing ooids, micritized grains and, foraminifera (F) (width of photo: 2 mm). **f)** Ooidal grainstone with some nuclei of ooids being bioclasts (B) (bryozoans) (width of photo: 1 mm).
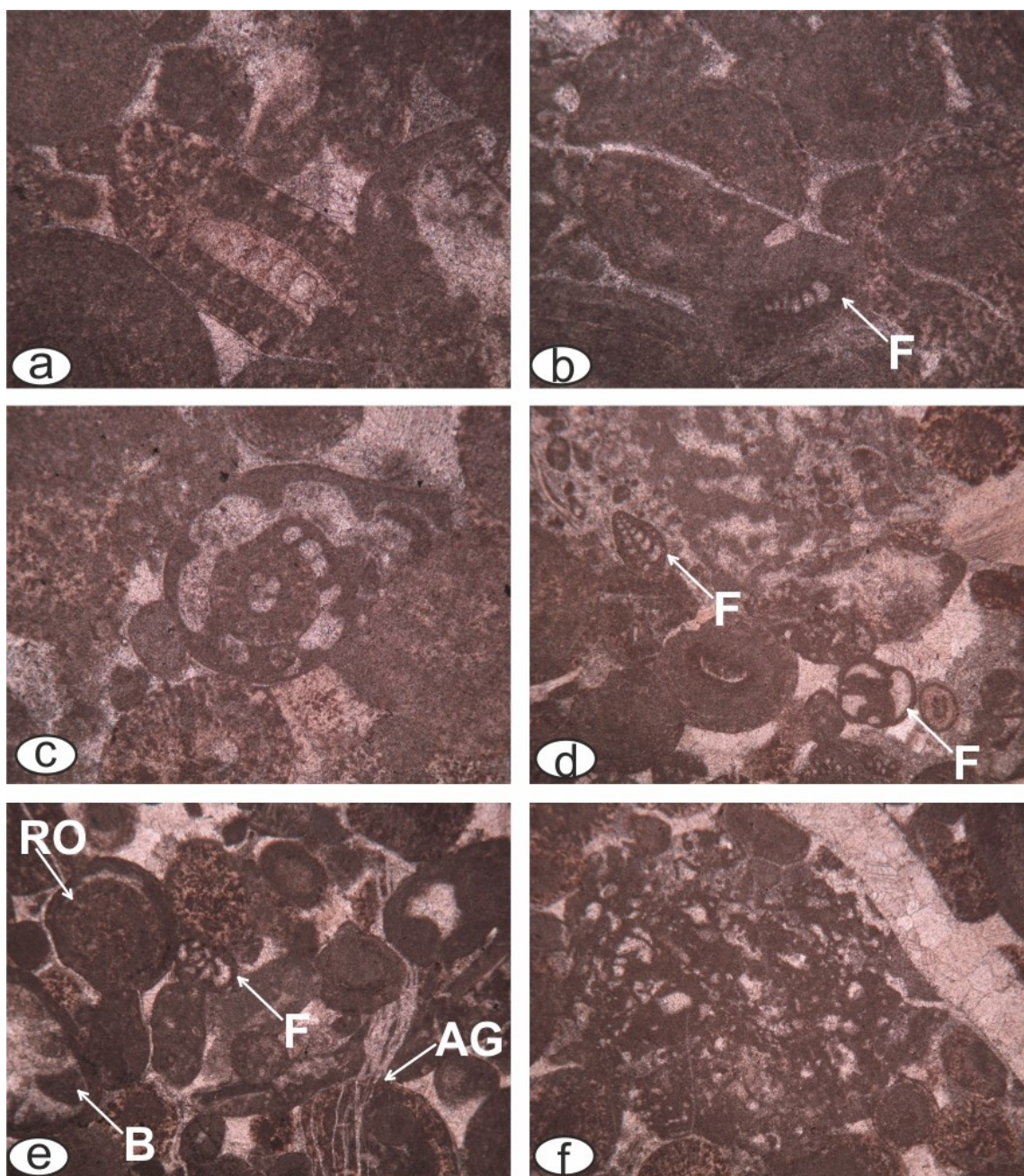
Plate 14. Characteristic microfacies of the oolitic limestone (Sample Gr 47): **a)** Ooid formed around a skeletal grain. (width of photo: 1 mm). **b)** Ooids characterized by centrifugal growth, and a foraminifera (F) exhibits as a nucleus of an ooid (width of photo: 1 mm). **c)** Ooid evolved inside a bioclast (width of photo: 1 mm). **d)** Foraminifera (F) and ooids in a grainstone (width of photo: 2 mm). **e)** Resedimented ooid (RO) shown by the additional micritic coating, also coated foraminifera (F) occur, and a bioclast (B) exhibits as a nucleus of an ooid (bottom left) as well as aggregated grains (AG) (bottom right) (width of photo: 2 mm). **f)** Reef-building organism (sponge) (width of photo: 1 mm).

5.5.2.2 Radiolarite sequence

Radiolarian age dating methods were employed to analyze two samples collected from the radiolarite-rich turbidite sequence. These samples were obtained from higher stratigraphic levels of this sequence, where the turbidites are intercalated with Late Jurassic to Earliest Cretaceous shallow-water carbonate-clastic resediments (Gnon et al. 2018). The studied outcrop is located along the local road connecting Gorgogiri to the Kori villages (Figures 5.34 and 5.35).

The samples exhibit a relative good preservation of the radiolarians. Based on the identification of the radiolarian association as documented in Plate (15), sample Gr (12) can be dated as Oxfordian. Similarly, sample Gr (13), as documented in Plate (16), can be dated as Oxfordian to early Kimmeridgian.

Figure 5.34 Satellite image of the eastern Koziakas mountain range with marked the sampling positions. Yellow dots represent sample positions for microfacies analysis, while blue dots indicate position for radiolarian age dating (Google earth 11/11/2023).

Figure 5.35 Exposures along the local road connecting Gorgogiri village to Kori village, at the eastern Koziakas mountain range (39⁰54′35′′N, 21⁰57′00′′E). **a**) Multicolored Middle-Late Jurassic radiolarite-rich turbidite sequence. **b**) Shallow-water carbonate-clastic resediments (adapted from Ghon 2017).
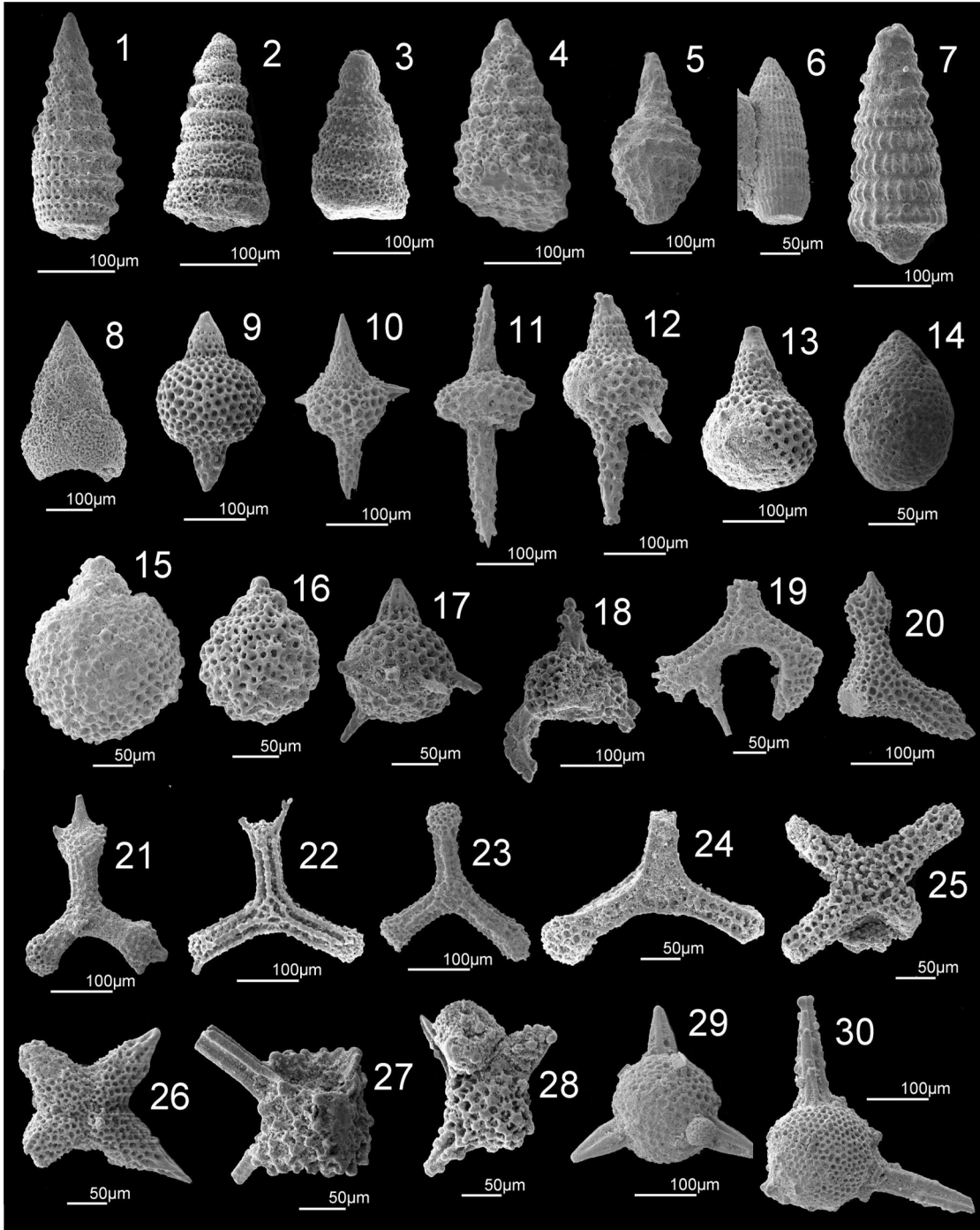
Plate 15. Radiolarian association identified in Sample GR (12), indicating an Oxfordian age: **1**) *Tethysetta mashitaensis* (Mizutani), **2**) *Cinguloturris carpatica* Dumitrica, **3**) *Xitomitra takanoensis* gr. (Aita), **4**) *Xitus* sp., **5**) *Mirifusus chenodes* (Renz), **6**) *Archaeodictyomitra shengi* Yang, **7**) *Transhsuum brevicostatum* gr. (Ožvoldova), **8**) *Spongocapsula perampla* (Rüst), **9**) *Dibolachras chandrika* Kocher, **10**) *Spinosicapsa vannae* (Beccaro), **11**) *Spinosicapsa andreai* (Beccaro), **12**) *Spinosicapsa* sp. cf. *S. spinosa* (Ožvoldova), **13**) *Crococapsa* sp. aff. *S. hexagona* (Hori). In comparison with typical *C. hexagona*, this species has a less abrupt transition from the conical proximal part to the inflated last segment. **14**) *Praewilliriedellum robustum* (Matsuoka), **15**) *Zhamoidellum ventricosum* Dumitrica, **16**) *Arcanicapsa funatoensis* (Aita), **17**) *Fultacapsa* sp. cf. *F. sphaerica* (Ožvoldova), **18**) *Napora lospensis* Pessagno, **19**) *Deviatus diamphidius* s.l. (Foreman), **20**) *Paronaella mulleri* Pessagno, **21**) *Paronaella* sp. aff. *P. broennimanni* Pessagno. The middle spine of the ray tips is considerably longer than the other spines. In typical *P. broennimanni* all spines on the ray tips are equal in length. **22**) *Tritrabs casmaliaensis* (Pessagno), **23**) *Tritrabs* sp. cf. *T. rhododactylus* Baumgartner, **24**) *Angulobracchia* sp. cf. *A. biordinalis* Ožvoldova, **25**) *Higumastra* sp. cf. *H. inflata* Baumgartner, **26**) *Crucella theokaftensis* Baumgartner, **27**) *Emiluvia orea* Baumgartner, **28**) *Emiluvia nana* Baumgartner, **29**) *Triactoma blakei* (Pessagno), **30**) *Triactoma jonesi* (Pessagno).
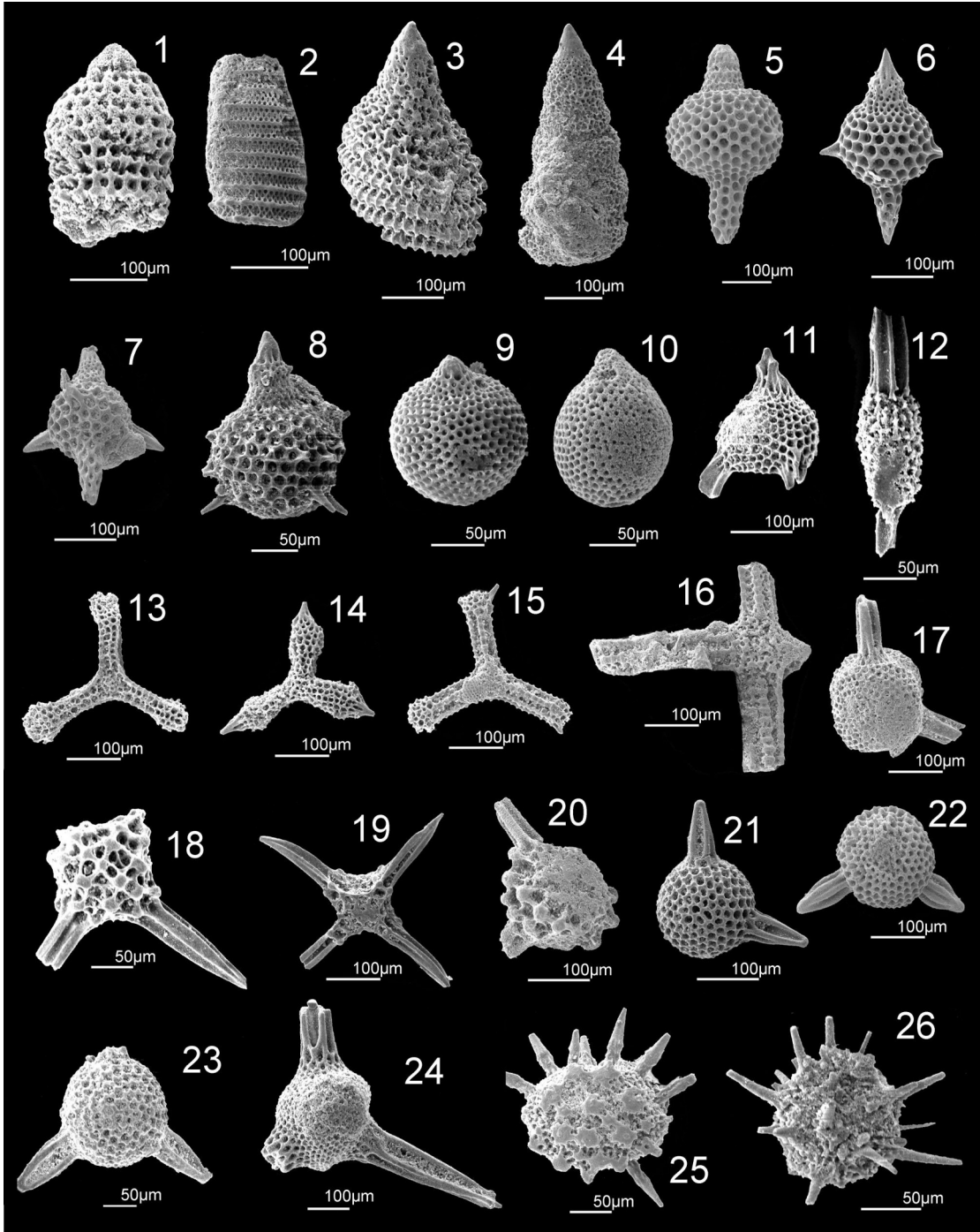
Plate 16. Radiolarian association identified in Sample GR (13), indicating an Oxfordian to early Kimmeridgian age: **1**) *Ristola altissima* (Rüst), **2**) *Ristola* sp., **3**) *Mirifusus dianae* (Karrer), **4**) *Spongocapsula palmerae* Pessagno, **5**) *Dibolachras chandrika* Kocher, **6**) *Spinosicapsa vannae* (Beccaro), **7**) *Spinosicapsa vannae* (Beccaro), **8**) *Arcanicapsa* sp., **9**) *Hemicryptocapsa carpathica* (Dumitrica), **10**) *Praewilliriedellum robustum* (Matsuoka), **11**) *Napora lospensis* Pessagno, **12**) *Archaeospongoprunum elegans* Wu, **13**) *Angulobracchia biordinalis* Ožvoldova, **14**) *Paronaella mulleri* Pessagno, **15**) *Tritrabs casmaliaensis* (Pessagno), **16**) *Tetratrabs* sp., **17**) *Suna echiodes* (Foreman), **18**) *Emiluvia chica* s.l. Foreman, **19**) *Emiluvia salensis* Pessagno, **20**) *Emiluvia orea* Baumgartner, **21**) *Triactoma blakei* (Pessagno), **22**) *Triactoma blakei* (Pessagno), **23**) *Triactoma blakei* (Pessagno), **24**) *Triactoma jonesi* (Pessagno), **25**) *Becus* sp. aff. *B. rotula* Dumitrica, **26**) *Actinomma* ? *matsuokai* Sashida & Uematsu.

5.5.2.3 Carbonate-clastic resediments

The shallow-water carbonate-clastic resediments are observed intercalated at the higher stratigraphic part of the Middle to Late Jurassic radiolarite-rich turbidite sequence (Figure 5.35). Field observations were made, and samples were collected from the carbonate resediments for microfacies analysis. The studied outcrops are located along the local road connecting Gorgogiri to the Kori villages (Figure 5.34).

Based on the examination of the thin sections, the microfacies of the collected samples are identified as bioclastic packstones and grainstones (following Dunham's classification) or packed biomicrite (following Folk's classification), with shallow-water bioclastic being the most frequent components.

In this sections, the bioclasts are bryozoans, foraminifera, crinoids, and debris from reef-building organisms (Plate 17 - 19). The presence of encrusting organism is characteristic, such as the microencruster *Crescentiella morronensis* (Crescenti). Additionally, other bioclasts, such as calcareous algae *Thaumatoporella*, foraminifera *Litualinida*, and *Aptychus* have been identified. These taxa are indicative of reefal facies from the Tithonian age. In specific thin sections, these reworked shallow-water bioclasts are observed to be mixed with older Late Triassic clasts containing the benthic foraminifera *Aulotortus sinuosus* (Ghon 2017, Ghon et al. 2018).

The identification of radiolarian wackestone containing poorly preserved calpionellids, such as *Crassicollaria brevis* or *Calpionella elliptica,* mixed in the resediments suggests that the oldest age of redeposition can be estimated as Berriasian (Ghon 2017, Ghon et al. 2018).

Based on these observations, it can be inferred that the depositional setting of this basin was influenced by redeposition of Late Jurassic shallow-water components blended with Late Triassic carbonate clasts from the Late Jurassic until at least the Berriasian.
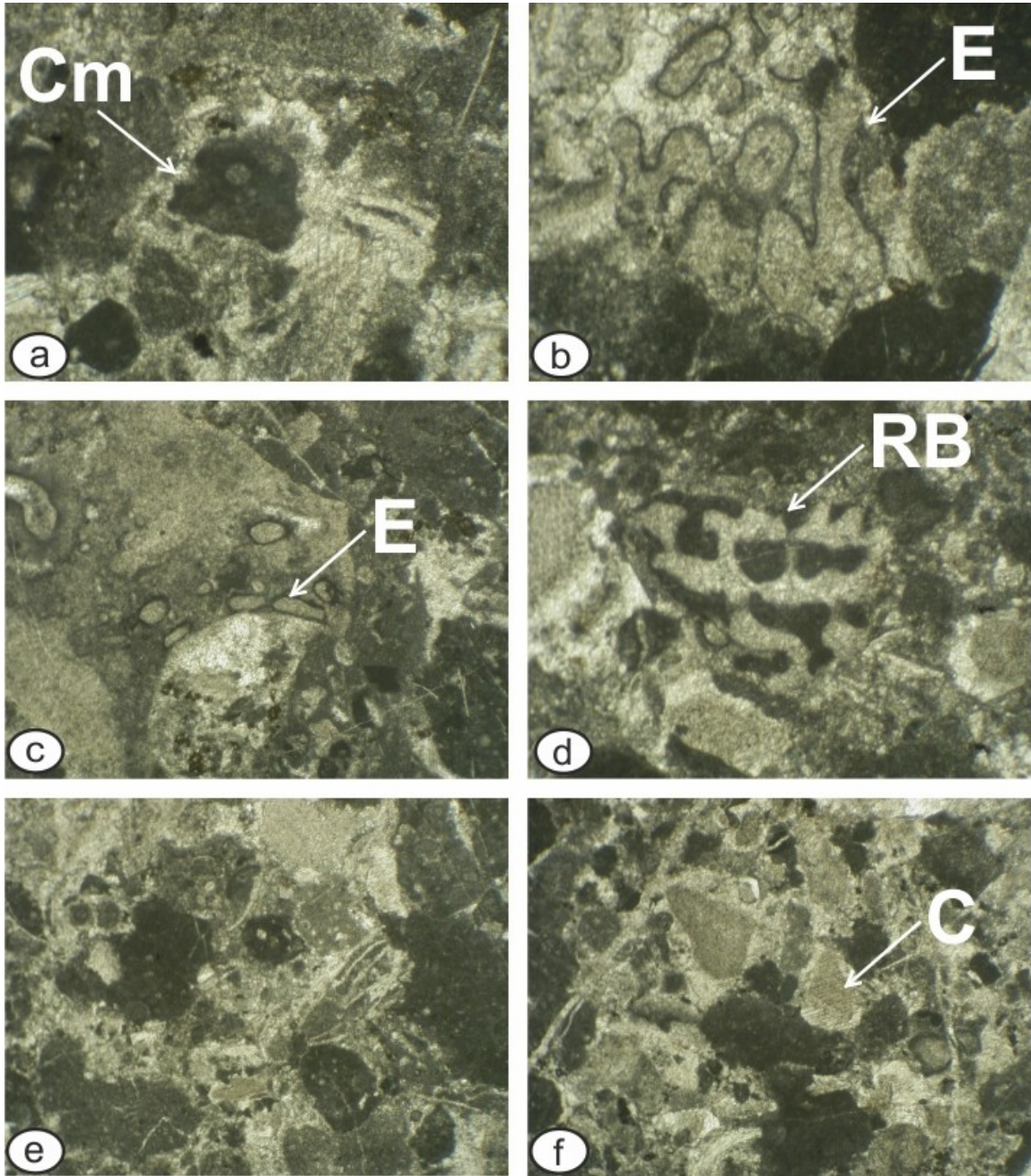
Plate 17. Microfacies from the shallow-water carbonate-clastic resediments: **a**) Grainstone containing the microencruster *Crescentiella morronensis* (Crescenti) (Cm) (width of photo: 1 mm). **b**, **c**) Grainstone with encrusting organisms (E) (width of photo: 1 mm). **d**) Reef-building organism fragment (RB) (width of photo: 1 mm). e, **f**) Grainstone composed of lithoclasts and fragments of crinoids (C) (width of photo: 2 mm). (Adapted from Ghon 2017).
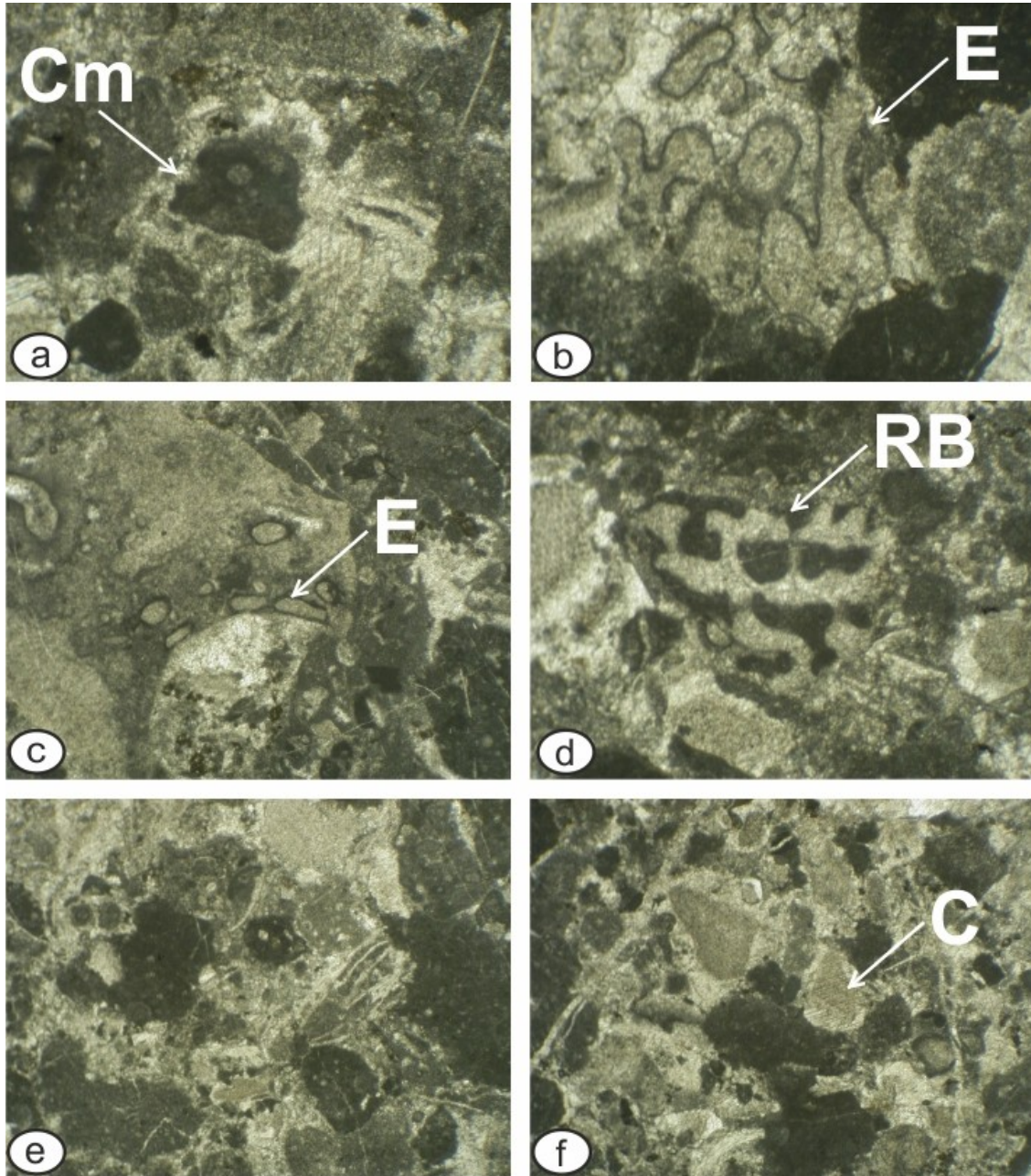
Plate 18. Microfacies from the shallow-water carbonate-clastic resediments: **a**) In the lower part grainstone with a fragment of shell (S) and a foraminifera (F) (width of photo: 2 mm). **b**) Grainstone with the benthic foraminifera *Aulotortus sinuosus* (As) (width of photo: 1 mm). **c**) Crinoid (C) fragment and a clast containing the foraminifera *Litualinida* (L) (width of photo: 2 mm). **d)** Radiolarian wackestone and shallow-water components (SW) (width of photo: 2 mm). **e**) Reef-building organism (RB) (width of photo: 1 mm). **f**) Encrusting organisms (E) and a foraminifera (F) (width of photo: 1 mm). (Adapted from Ghon 2017).
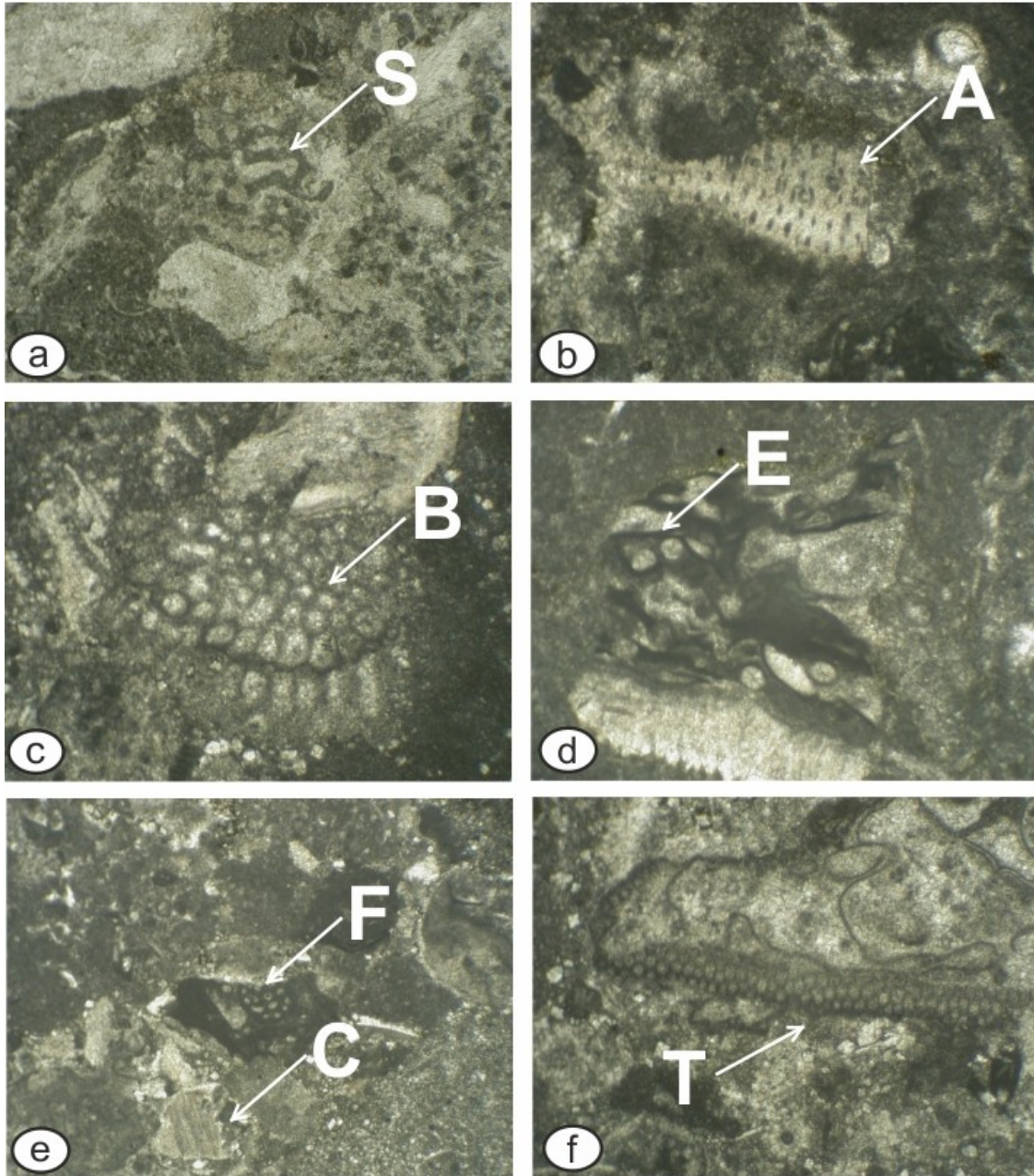
Plate 19. Microfacies from the shallow-water carbonate-clastic resediments: **a)** Grainstone composed of lithoclasts and a sponge (S) fragment (width of photo: 1 mm). **b)** *Aptychus* (A) (width of photo: 1 mm). **c)** Bryozoans (B) (width of photo: 1 mm). **d)** Encrusting organisms (E) (width of photo: 1 mm). **e)** Packstone with fragments of foraminifera (F) and cronoids (C) (width of photo: 2 mm). **f)** *Thaumatoporella* algae (T) (width of photo: 1 mm). (Adapted from Ghon 2017).

5.6 Late Early Cretaceous transgressive sediments - Poros succession

Microfacies analysis was conducted on samples collected from an outcrop exposed along the local road near Poros village, on the eastern side of Aliakmonas river, as illustrated in Figure (5.36) at position (3). This specific location is characterized by the presence of a carbonate sedimentary succession that transgressively overlies the Vourinos ophiolites (Figures 5.37 and 5.38) (Pichon and Lys 1976). It is subsequently overlaid by Late Cretaceous limestones and Upper Eocene to Lower-Middle Miocene deposits of the Mesohellenic Trough.
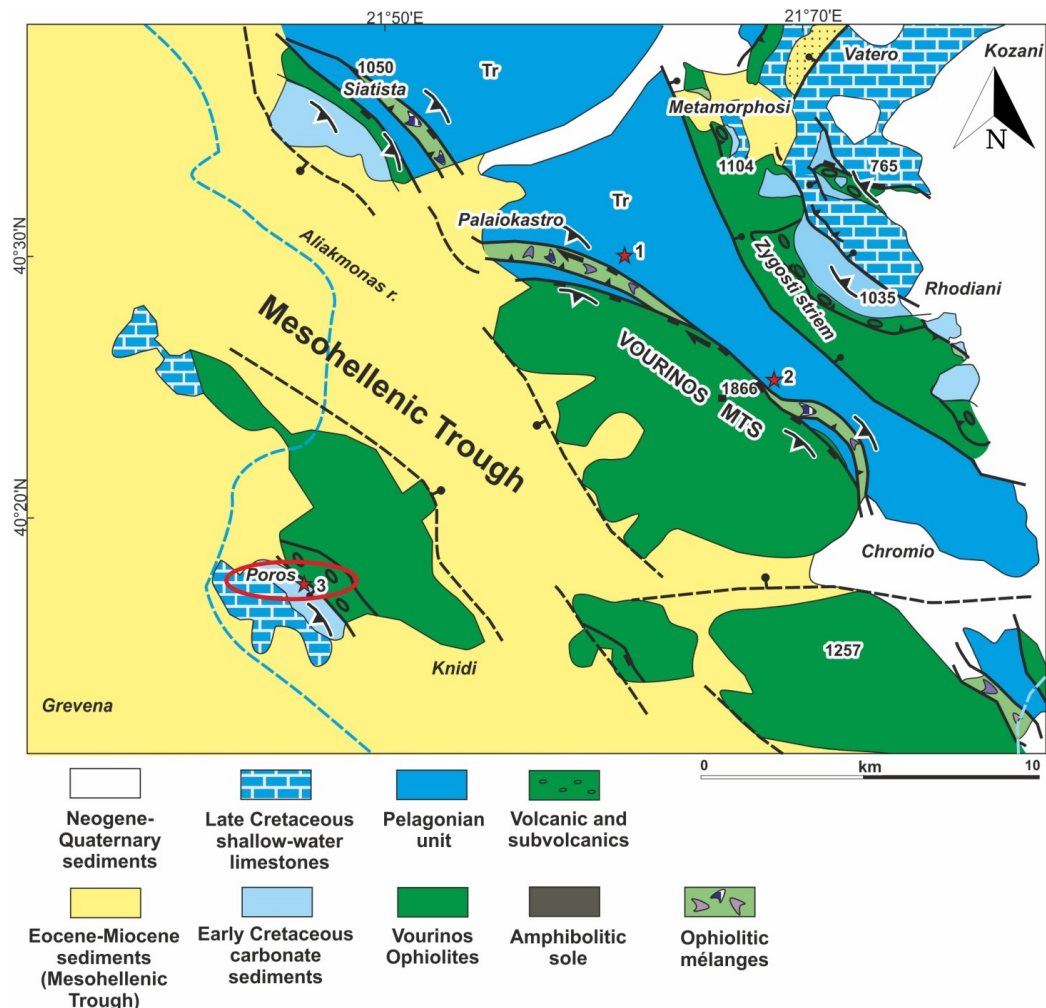
Figure 5.36 Simplified geological map of the Vourinos ophiolites tectonically positioned above the Pelagonian marginal formations and the overlying sedimentary successions (Kostaki et al. 2023, based on Kilias 2021).

Figure 5.37 Late Early Cretaceous transgressive carbonates overlying the Vourinos ophiolites exposed near Poros village ($40^0 11´49´´$N, $21^0 51´12´´$E).

The succession primarily comprises conglomerates, breccias, and reddish-grey carbonate layers exhibiting folding (Figures 5.37, 5.38, and 5.39). The succession starts in the study area with a carbonate conglomerate. Based on the examination of thin sections from samples collected from this part, they are identified as peloidal packstones and grainstones (following Dunham's classification) or pelmicrite and pelsparite (following Folk's classification) (Plate 20). The observed bioclasts include milionid foraminifera, bivalve fragments, stromatoporoids, and echinoderms. Frequent occurrences of Aptychi fragments are also noted, along with the presence of calpionellids (Plate 20). The characteristics of the microfacies and the occurrence of this fossil association suggest a Late Jurassic to earliest Cretaceous age for the original deposition of the components.

In a higher stratigraphic part, reddish-grey carbonate layers are observed. Upon examination of thin sections from sample collected from this part, they are identified as wackestone to packstone (following Dunham's classification) or biomicrite (following Folk's classification). The bioclasts include sponges, foraminifera, and the microencruster *Crescentiella morronensis* (Crescenti) (Plate 21). In specific thin sections, lithoclasts enclosing recrystallized radiolarians are identified (Plate 21).

Figure 5.38 The Vourinos ophiolites and their tectonic contact with the late Early sedimentary succession ($40^0 11´49´´$N, $21^0 51´12´´$E).

Then the succession extends into a polymictic breccia, comprising components of diverse sources (Figure 5.39). Based on the examination of thin sections from samples collected from this part, they are identified as bioclastic packstones (following Dunham's classification) or biomicrite (following Folk's classification) (Plates 22 - 24).

The observed bioclasts include miliolid foraminifera, shell fragments, brachiopods, crinoids, and reef-building organisms (Plates 22 - 24). Frequent occurrences of orbitolinas are also noted, along with the presence *Montseciella? arabica* (Henson) or *Rectodictyoconus giganteus* Schroeder (Plates 22 - 24). The identification of the latter suggests that the age of redeposition can be estimated as Late Barremian-Early Aptian.
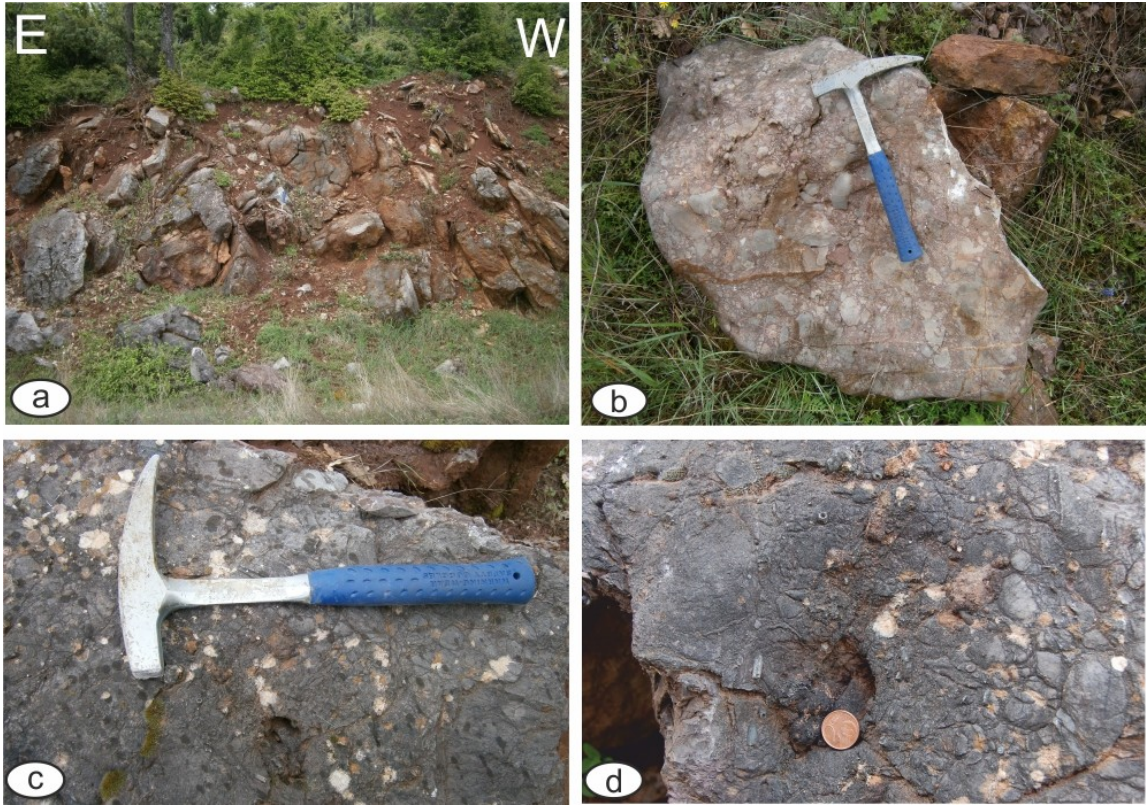
Figure 5.39 Late Early Cretaceous transgressive sediments (Poros succession) ($40^0 11' 49'' N$, $21^0 51' 12'' E$): **a)** Late Early Cretaceous transgressive conglomerates overlying Vourinos ophiolites. **b)** Polymictic breccia composed of components of diverse sources. **c)** Carbonate conglomerate. **d)** Carbonate conglomerate with small belemnites fragments.
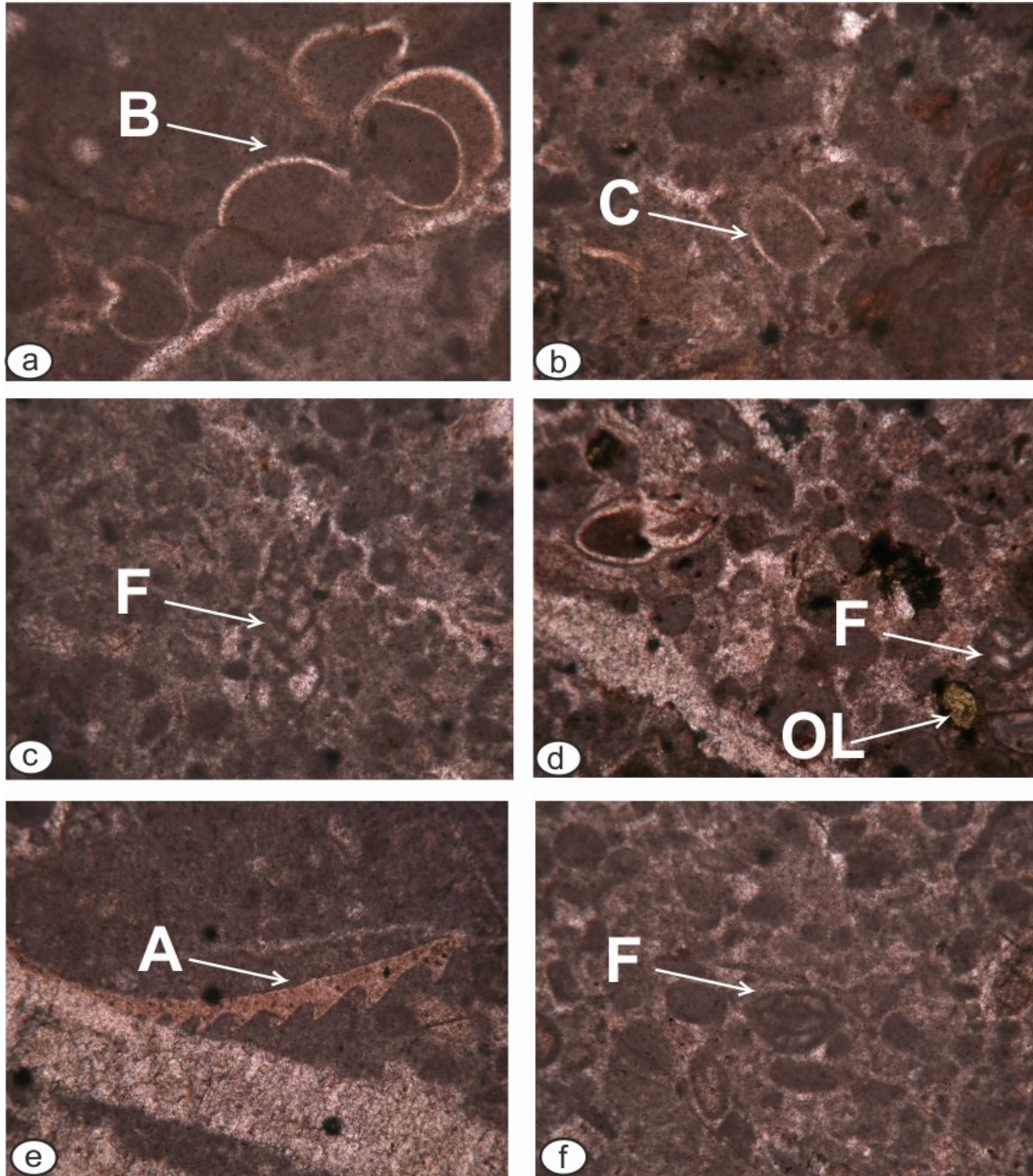
Plate 20. Characteristic microfacies from the redeposited carbonate components of the Poros succession (Samples Gr 26-28) (width of photo: 1 mm): **a**) Wackestone with bivalves (B) fragments. **b**) Possible calpionella (C). **c**) Peloidal packstone containing foraminifera (F). **d**) Grainstone with different coated grains, formaminifera (F), as well as ophiolite-derived lithoclast (OL). **e**) Aptychi fragment (F). **f**) Peloidal packstone containing milionid foraminifera (F) and coated grains.
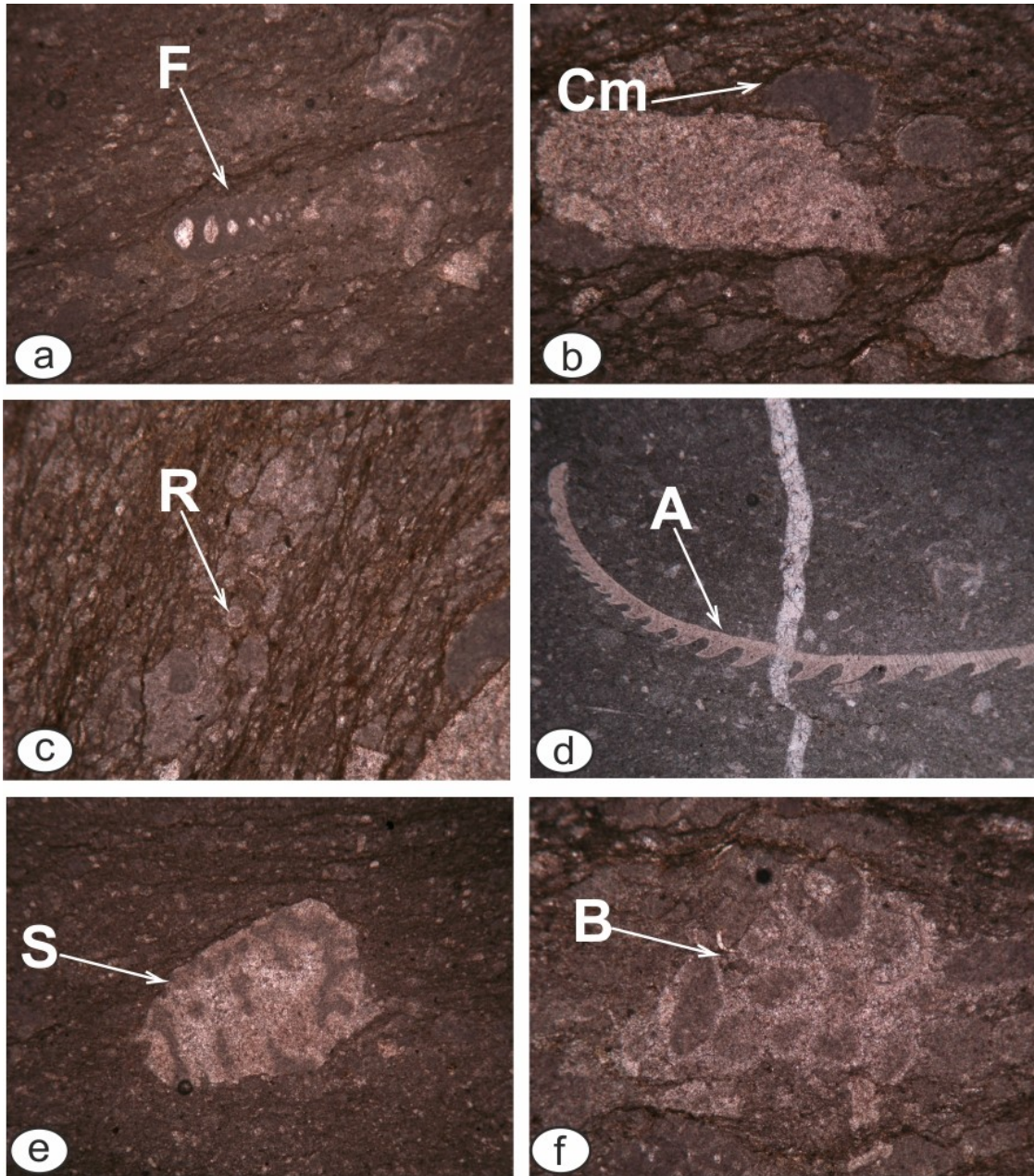
Plate 21. Characteristic microfacies from the reddish-grey carbonate layers of Poros succession (Samples Gr 32-33): **a**) Laminated packstone containing foraminifera (F) (width of photo: 2 mm). **b**) Different lithoclasts and possibly the microencruster *Crescentiella morronensis* (Crescenti) (Cm) (width of photo: 1 mm). **c**) Lithoclasts enclosing recrystallized radiolarians (R) (width of photo: 2 mm). **d**) Aptychi (A) fragment (width of photo: 2 mm). **e**) Fragment of a sponge (S) (width of photo: 2 mm). **f**) Packstone with bryozoans (B) (width of photo: 1 mm).
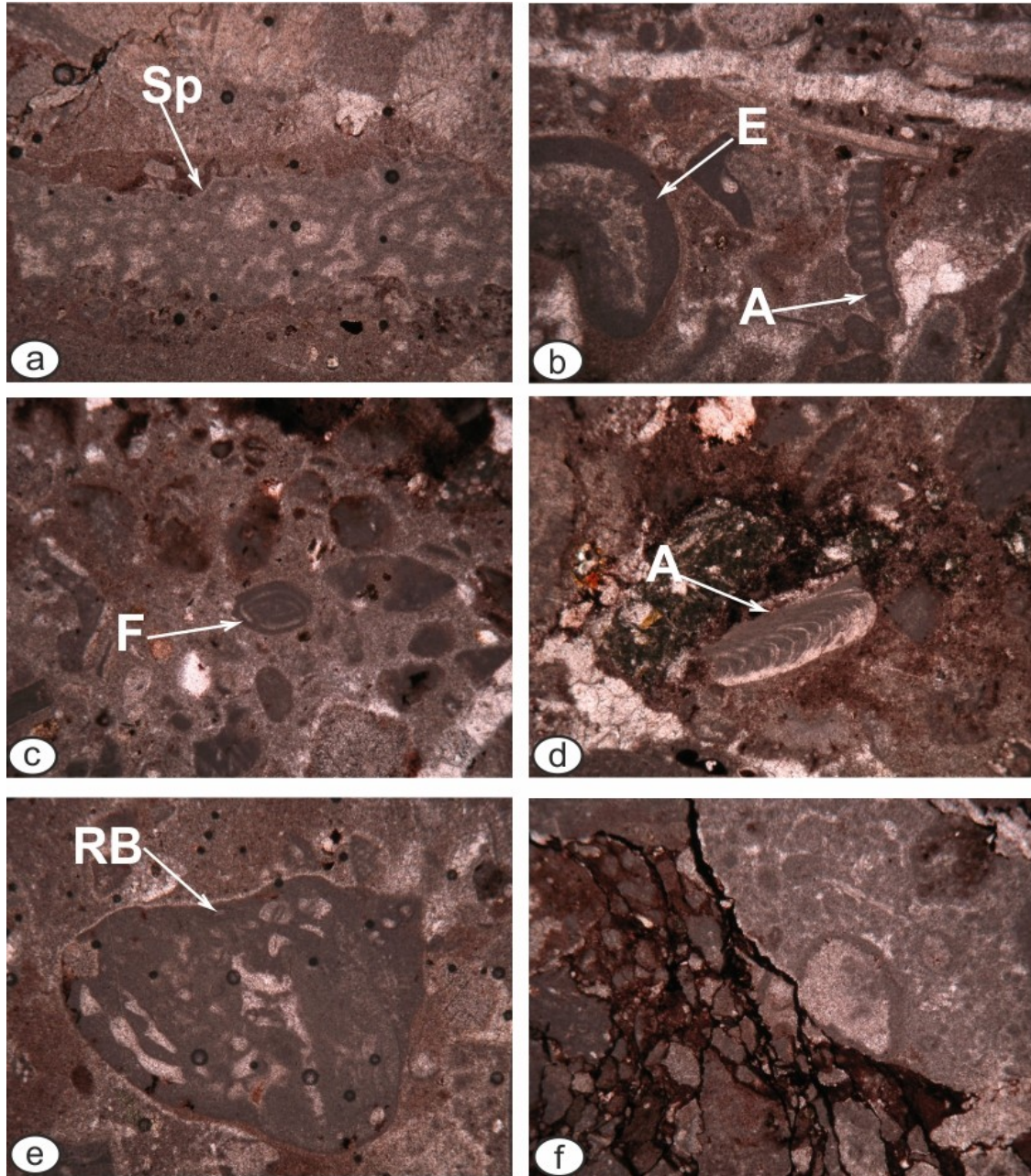
Plate 22. Characteristic microfacies from the polymictic breccia of the Poros succession (Samples Gr 30-31) (width of photo: 2 mm): **a)** Packstone containing a stromatoporoid (Sp). **b)** Packstone with an algae (A) fragment, and other grains with micritic encrustations (E) around them. **c)** Packstone with components of various origins and miliolid foraminifera (F). **d)** Packstone with different kinds of lithoclasts and red algae (A). **e)** Packstone enclosing a reworked reef-building organism (RB). **f)** Grainstone various lithoclasts and a peloidal packstone in the upper part.
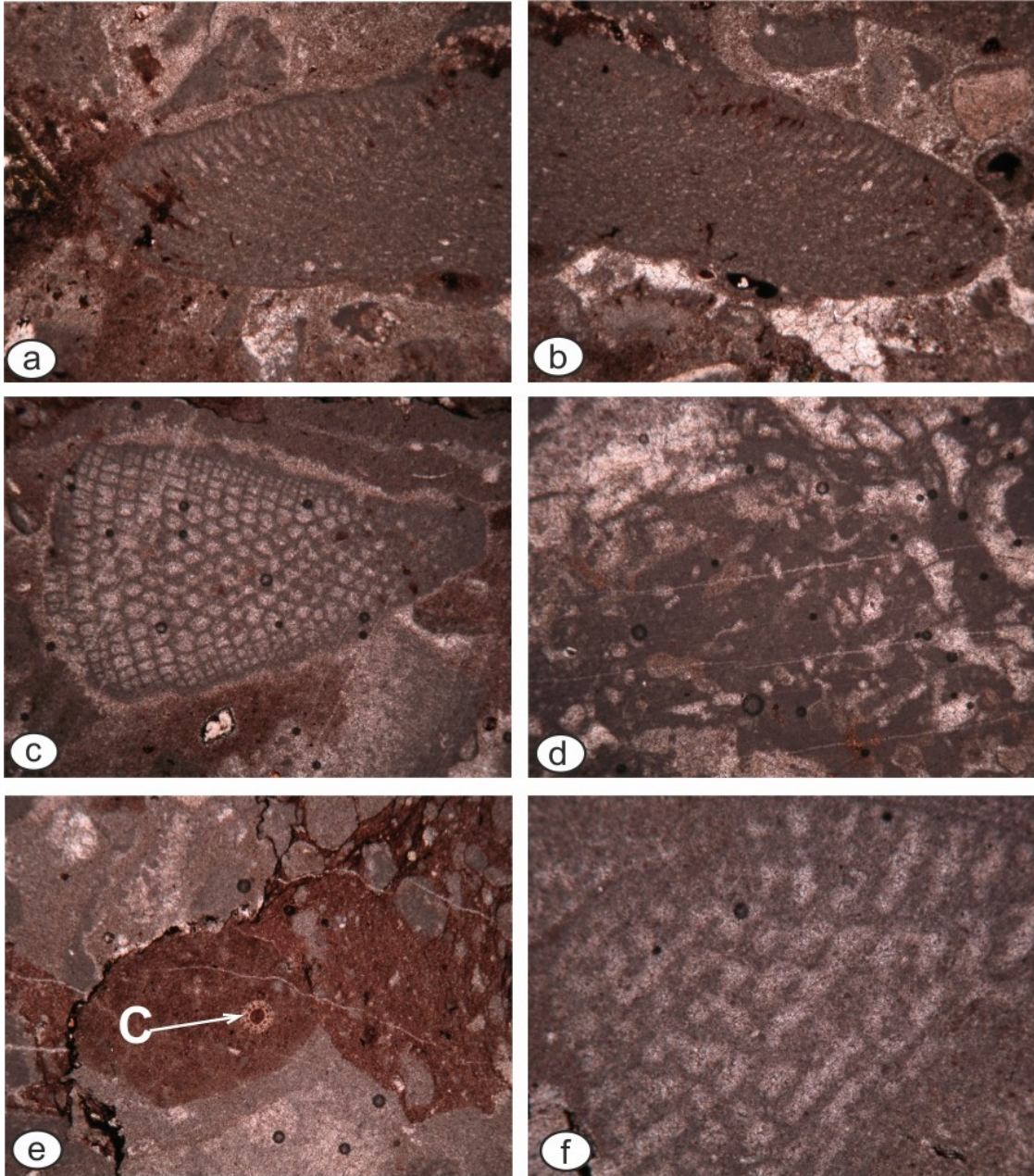
Plate 23. Characteristic microfacies from the polymictic breccia of the Poros succession (Samples Gr 30-31): **a**, **b**) Packstone with *Montseciella? arabica* (Henson) or *Rectodictyoconus giganteus* Schroeder (width of photo: 2 mm). **c**) Orbitolina foraminifera (width of photo: 2 mm). **d**) Reef-building organism (width of photo: 2 mm). **e**) Packstone with different kinds of intraclasts and a crinoid (C) is also included (width of photo: 2 mm). **f**) Stromatoporoid (width of photo: 1 mm).

141
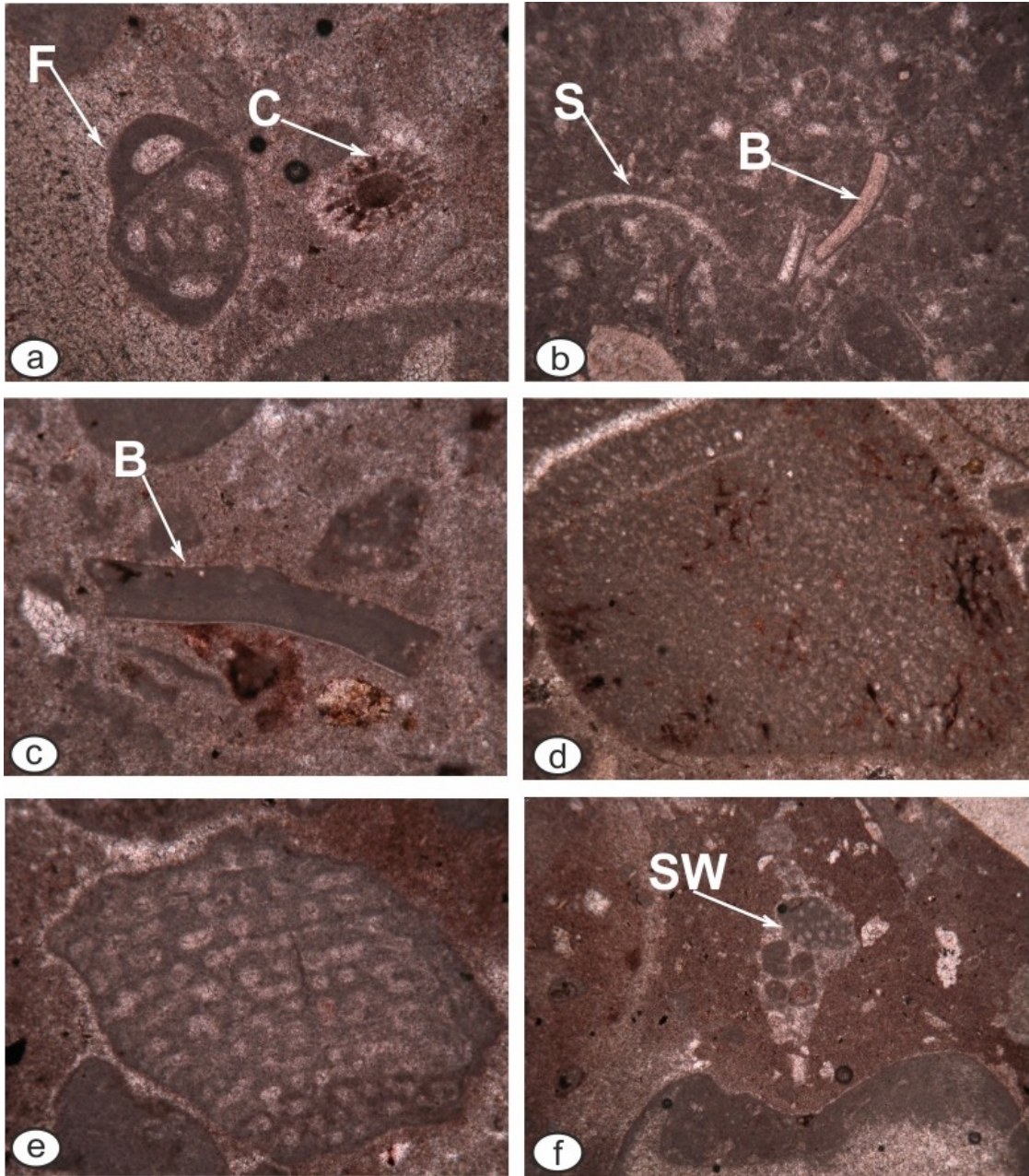
Plate 24. Characteristic microfacies from the polymictic breccia of the Poros succession (Samples Gr 30-31): **a**) Grainstone including a benthic foraminifera (F) and a crinoid (C) (width of photo: 1 mm). **b**) Packstone with micritized sceletical grains (S) and brachiopods (B) with micritic envelopes (width of photo: 2 mm). **c**) Packstone with a fragment of a brachiopod (B) (width of photo: 1 mm). **d**) Micritized shallow-water bioclast (width of photo: 2 mm). **e**) Packstone composed of a reworked shallow-water organism (width of photo: 1 mm). **f**) Packstone with quartz grains and an angular grainstone clast (SW) deriving from older shallow-water carbonate facies (width of photo: 2 mm).

CHAPTER 6. Results - Deformational Events

Since the Middle Jurassic to the present, the studied region has experienced multiple deformational events (Figure 6.1). The structures associated with the oldest event are characterized by NW-SE trending asymmetric tight to sub-isoclinal folds with a predominant sense of movement top-to-the-SW (e.g., Avdella mélange; Figure 5.12). Additionally, ductile to semi-ductile shear zones, exhibiting a prevailing sense of shear top-to-the-SW, are recognized (Figures 6.2 and 6.3). These structures are mainly observable in the ophiolites and their associated mélanges.

This compressional event is inferred to be associated with west-directed ophiolite obduction over the eastern passive Pelagonian margin during the Middle-Late Jurassic, consistent with previous studies such as Gawlick et al. (2008), Kilias et al. (2010), Bortolotti et al. (2012). The Middle-Late Jurassic SW-ward ophiolite obduction predates an Early-Middle Jurassic eastward intra-oceanic subduction and the formation of an amphibolitic sole dated as 171 ±4 Ma (Roddick et al. 1979, Sprey and Roddick 1980, Karamata 2006, Schmid et al. 2020). The amphibolitic sole became intensively imbricated in between the following nappe stack.

Additionally, as a result of the tectonic overpressure throughout the ophiolite emplacement over the Pelagonian marginal formations, high-pressure/low-temperature (HP/LT) metamorphism occurred in the deeper Pelagonian basement rocks (Frisch and Meschede 2007, Kilias et al. 2010, Robertson 2012, Robertson et al. 2012, compare Porkoláb et al. 2020).

AGE	STRESS REGIME & DEFORMATIONS CONDITIONS	KINEMATICS (MAIN DIRECTION OF MOVEMENTS)	STRUCTURES	GEODYNAMIC RESULTS	GEOLOGICAL UNITS AFFECTED
MIDDLE-LATE JURASSIC	COMPRESSION DUCTILE	W-SW	Asymmetric tight to sub-isoclinal folds & semi-ductile shear zones	Intra-oceanic subduction Amphibolitic sole Ensimatic island arc Ophiolite obduction Nappe stacking Foreland basins formation	Ophiolites Triassic-Jurassic carbonates
LATE JURASSIC-EARLY CRETACEOUS	EXTENSION			Basin formation Unroofing Emersion Erosion Crustal exhumation Nappe stack propagation	Ophiolites Pelagonian unit L. Jurassic carbonates
EARLY CRETACEOUS	COMPRESSION (SEMI-) DUCTILE (SEMI-) BRITTLE	SW	Thrust faults Shear zones Tight to sub-isoclinal folds	Imbrication of all units Advance of ophiolites	Ophiolites Pelagonian unit Early Cretaceous carbonates
PALEOCENE EOCENE	COMPRESSION BRITTLE	SW	Thrust faults Open to knick folds	Imbrication of all units Avdella melange thrust over Pal-Eoc sediments	Ophiolites Pelagonian unit Sediments deposited since Early Cretaceous

Figure 6.1 Main deformational events recorded in the studied region (Kostaki et al. 2023).

A different deformational event resulted in the imbrication and folding of all the formations deposited until the late Early Cretaceous (Figure 6.4). The structures associated with this compressional event are dominated by tight to sub-isoclinal folds and shear zones exhibiting a prevailing sense of shear top-to-the-SW (Figure 6.4) (Kilias et al. 2010, Katrivanos et al. 2013, Froitzheim et al. 2014). Additional structural features related to this event are thrust faults. This event is clearly imprinted in the late Early Cretaceous Poros succession overlying Vourinos ophiolites (Figure 6.4; a, b), as well as in the Earliest Cretaceous sedimentary succession overlying Vardar-Axios ophiolites (Figure 6.4; c, b).

Additionally, a Paleocene-Eocene deformational event has been identified, characterized by brittle to semi-brittle structures. This compressional event resulted in further imbrication and folding of all preexisting formations. The structures associated with this event include open to knick folds with a predominant sense of movement top-to-the-SW (Figure 6.5).

Figure 6.2 Ophiolitic mélange exhibiting shear zones with a prevailing sense of shear top-to-the-SW, associated with west-directed Middle-Late Jurassic ophiolite obduction over the eastern passive Pelagonian margin (the sense of shear is indicated by arrows) ($40^0 15'28''$N, $21^0 33'19''$E) (Kostaki et al. 2023).

Figure 6.3 Ophiolites overlying the Triassic Pelagonian marginal formation. The ophiolites are exhibiting shear zones with a prevailing sense of shear top-to-the-SW, associated with west-directed Middle-Late Jurassic ophiolite obduction over the eastern passive Pelagonian margin (the sense of shear is indicated by arrows) ($40^0 26'47''$N, $21^0 55'08''$E) (Kostaki et al. 2023).
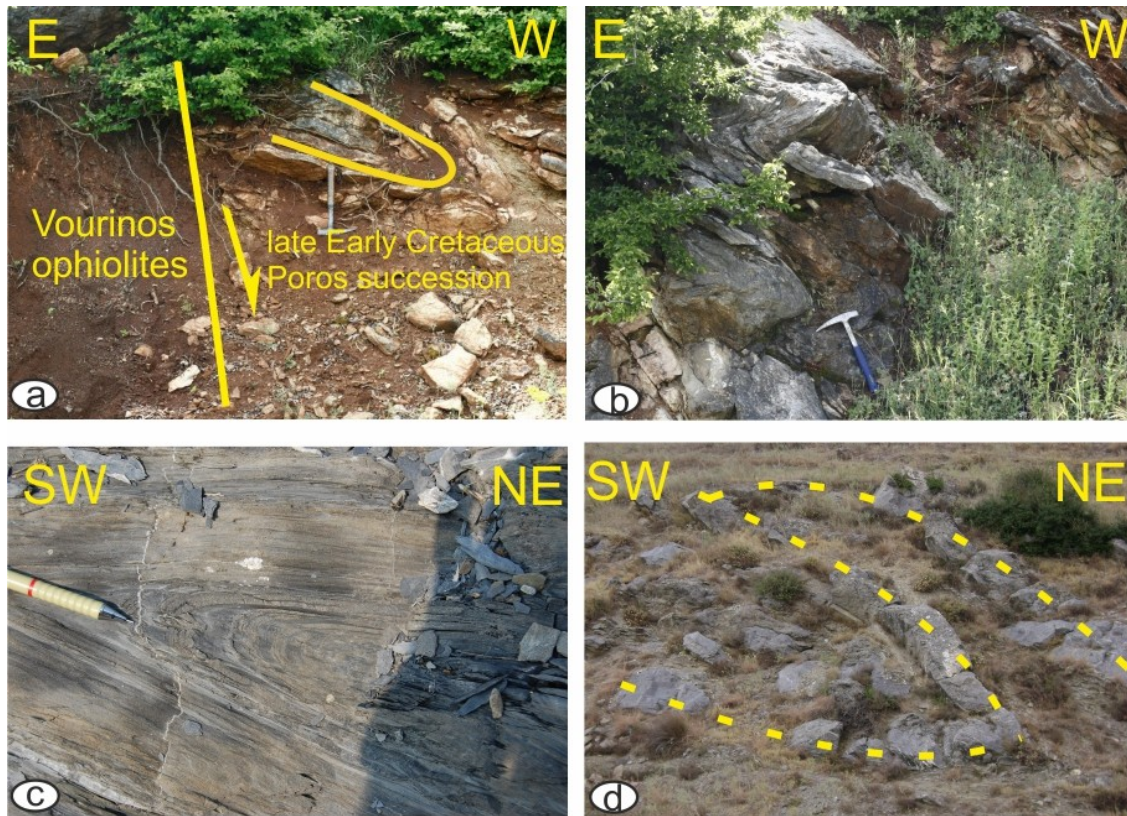
Figure 6.4 a, b) Late Early Cretaceous transgressive carbonates overlying Vourinos ophiolites in the vicinity of Poros village, exhibiting tight to sub-isoclinal folds with a prevailing sense of movement top-to-the-SW ($40^0 07'23''$N, $21^0 31'39''$E) (Kostaki et al. 2023). **c, d**) Earliest Cretaceous carbonates overlying Vardar-Axios ophiolites in the vicinity of Neochorouda village, demonstrating sub-isoclinal folds with a sense of movement top-to-the-SW ($40^0 44'52''$N, $22^0 52'38''$E) (Kostaki 2013).

Additional structural features related to this event are out-of-sequence thrust faults and thrust faults (Figure 6.6). This thrusting caused the westward movement of the Pindos ophiolites and the Avdella mélange as well as all the overlying sedimentary successions over Paleocene-Eocene orogenic sediments (Figures 4.5).

A Eocene-Oligocene to Quaternary deformational event has also affected the region characterized by high angle normal dip-slip and strike-slip faults. In certain instances, this deformation was manifested by transpressional tectonics, as observed in the Mesohellenic Trough (Vamvaka et al. 2006). This event resulted in the dismemberment of all the preexisting structures and formations, and in the formation of pull-apart basins. Subsequently, compression migrated further westward.

Figure 6.5 Late Early Cretaceous transgressive carbonates overlying Vourinos ophiolites in the vicinity of Poros village, exhibiting open folds ($40^0 07´23´´$N, $21^0 31´39´´$E) (Kostaki et al. 2023).
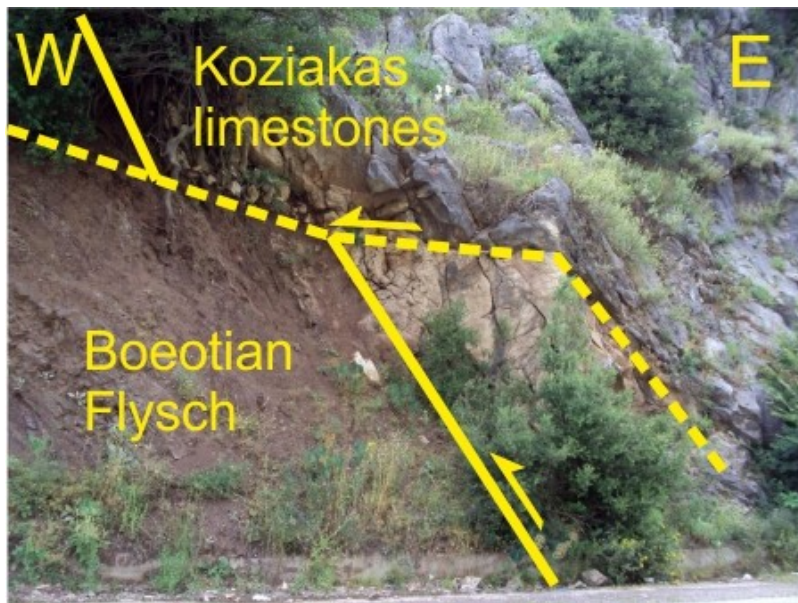
Figure 6.6 Out-of-sequence thrust fault placing Koziakas Jurassic carbonates over the Early Cretaceous Boeotian Flysch ($39^0 46´30´´$N, $21^0 61´64´´$E) (Kostaki et al. 2023).

CHAPTER 7. Discussion

7.1 Importance of the Triassic blocks in the Avdella and Koziakas mélanges

As previously detailed in sub-chapters (5.2), an open-marine shelf reconstruction was derived from the analysis of newly acquired data, including microfacies analysis and conodont age dating of exotic carbonate blocks found in the Avdella and Koziakas mélanges. This reconstruction mirrors the Hallstatt Limestone succession and notably shares similarities with successions in the western Pindos mountain range, situated to the west of the Pelagonian Zone as part of Pindos Zone (Aubouin 1959), referred to as the Hallstatt/Pindos succession.

The original deposition of the Hallstatt Limestones is identified as taking place on the outer shelf from the Middle Triassic until the Early Jurassic. These limestones formed alongside the continental slope Meliata Facies, contributing to the shaping of the eastern Adriatic passive continental margin adjacent to the Neo-Tethys Ocean in the east (Sudar 1986, Krystyn 2008, Sudar et al. 2010, Missoni and Gawlick 2011, Gawlick et al. 2012, Gawlick and Missoni 2015, Gawlick et al. 2017a, 2018).

This interpretation about the Hallstatt Limestone succession is well established, supported by structural analysis and stratigraphic data, with respect to a well-arranged passive continental margin (Schlager 1969, Krystyn 1980, 1983, 2008, Mandl 1984, Lein 1987, Gawlick and Bohm 2000, Frisch and Gawlick 2003, Köver et al. 2009, Sudar

et al. 2010, Missoni and Gawlick 2011, Haas et al. 2011, Gawlick and Missoni 2015, Gawlick et al. 2012, 2017a, 2018).

However, in most instances, the Hallstatt Limestone successions have been shattered and are maintained primarily as components or complete successions within massive blocks and slides found in Middle to Late Jurassic far-traveled mélanges along the Alpine-Carpathian-Dinaridic collisional belt (e.g., Gawlick and Frisch 2003, Frisch and Gawlick 2003, Krystyn 2008, Sudar et al. 2010, Missoni and Gawlick 2011, Gawlick and Missoni 2015, 2019, Gawlick et al. 2016a, 2016b, 2017a, 2018, 2020).

In the situation of the Northern Calcareous Alps, Hallstatt nappes during Middle-Late Jurassic thrusting processes were totally destroyed but resulted in the supply of sediments to new formed deep-water trench-like basins at the forefront of the propagating nappes (Frisch and Gawlick 2003). This can be demonstrated by Hallstatt slides and blocks that range in size from centimeters to a kilometer, incorporated in Middle to Late Jurassic mélanges, characterized by a turbiditic-radiolaritic matrix (Gawlick et al. 2002).

In the Inner Dinarides (Dinaridic Ophiolite Belt), similar Hallstatt mélanges were formed during the Middle Jurassic to early Late Jurassic, composed of kilometer-sized slides and blocks in an argillaceous-radiolaritic matrix (Sudar et al. 2010, Gawlick and Missoni 2015). During the Middle-Late Oxfordian, these mélanges experience overthrusting by an ophiolitic mélange and the ophiolite nappe. Subsequently, in the Late Jurassic to early Cretaceous, they were transported further westward (Gawlick et al. 2017a, 2018, 2020).

Equivalent mélanges are exposed beneath the Mirdita ophiolites in Northern Albania, formed in an identical manner, following the ophiolite obduction processes (Gawlick et al. 2008, 2014, 2016b). In that case, the Hallstatt Limestone succession underwent complete erosion, contributing its materials to deep-water radiolaritic-argillaceous basins formed during the Middle Jurassic that evolved in advance of the progressing nappe stack.

A complete Hallstatt succession has been documented in Hungary by Kovacs (2010) and can also be partially reconstructed from components found in mass transport

deposits within a Middle Jurassic argillaceous-radiolaritic matrix (Köver et al. 2009, Haas et al. 2012, Gawlick and Missoni 2019).

This places the complete Hallstatt/Pindos succession in the western Pindos mountain ranges in an exceptional situation, similar to few other locations, such as successions in the Budva Zone (Missoni et al. 2014). Nevertheless, their current position has led to a misconception regarding their original deposition, which was perceived as parautochthonous. Until recently, two prevailing paleogeographical reconstructions have existed concerning the Pindos Zone and the Middle Triassic to Middle Jurassic rocks it encompasses in the Hellenides.

The first reconstruction, advocating for the presence of Pindos Ocean, suggests that the Pindos Zone is characterized by a continuous sedimentary sequence extending from the Triassic to the Eocene, deposited in proximity to the Pindos Ocean (e.g., Mountrakis 1986, Jones et al. 1991, Robertson et al. 1991, 1996, Robertson and Shallo 2000, Stampfli and Borel 2002, Brown and Robertson 2004, Sharp and Robertson 2006, Rassios and Moores 2006, Karamata 2006, Rassios and Dilek 2009, Robertson 2012).

On the other hand, the second reconstruction is proposing the presence of a deep-water Pindos Basin between Gavrovo and Pelagonian Zones, spanning from the Triassic to Eocene times (Bernoulli and Laubscher 1972, Schmid et al. 2008, 2020, Ferrière et al. 2015, 2016).

Nevertheless, both reconstructions overlook the significance of the occurrence of Hallstatt blocks within the Avdella and Koziakas mélanges, indicating a west to southwestward direction of movement. These mélanges are believed to have originated and advanced ahead of the west-transported ophiolite nappe stack, responding to the gradual closure of the ocean, which was located east of the Pelagonian region (Neo-Tethys Ocean) (Bortolotti et al. 1996, 2012, Ozsvart et al. 2012, Schmid et al. 2008, 2020, Kilias 2021).

In contrast, according to Robertson (2012), the Avdella mélange developed as an accretionary prism (subduction complex) in response to the subduction of the so-called Pindos oceanic floor. Subsequently, during the Late Jurassic, it underwent eastward emplacement, along with the Pindos ophiolites, over the western continental margin of the Pelagonian micro-plate. However, this perspective conflicts with structural analysis,

which predominantly support a main westward obduction direction over the eastern Pelagonian margin, including, besides this work (see chapter 6), e.g., Baumgartner (1985), Most et al. (2001), Kilias et al. (2002, 2010), Gawlick et al. (2008), Schmid et al. (2008, 2020), Bortolotti et al. (2012), Scherreiks et al. (2014), Schenker et al. (2014, 2015), and Kilias (2021).

In addition to the complete Hallstatt/Pindos succession in the western Pindos mountain ranges, various occurrences of Hallstatt Limestone have been documented tectonically aligned between the Pindos and Pelagonian Zone, and they are included in the Sub-Pelagonian Zone (e.g., Mountrakis 1986, Tselepidis 2007, Pomoni and Tselepidis 2013).

Many research groups consider the Sub-Pelagonian Zone as a transitional area between the shallow-water carbonates of Pelagonian Zone and the deep-water sediments and pelagic carbonates, which are believed to have deposited in the direction of the Pindos Ocean or within Pindos Basin (Mountrakis 1986, 2010, Robertson 2012, Robertson et al. 1996, Ferrière 1974, Clift and Robertson 1990, Pomoni and Tselepidis 2013). However, a Pindos Ocean or a Pindos Basin dividing the Hallstatt Limestone into two separate successions would conflict with the sense of their deposition in a common outer shelf setting and does not comply with the broader logic of a well-arranged passive continental margin.

In accordance with the paleogeographic reconstruction of other regions in the Western Tethys realm, the original position of the Hallstatt/Pindos succession during the Middle Triassic until the early Middle Jurassic is considered to be the eastern outer shelf of the Pelagonia margin, which is regarded as forming the passive continental margin of the Adriatic plate facing the Neo-Tethys Ocean (Figures 7.1 and 7.2) (Kostaki et al. 2023).

In the Middle Jurassic, the arrangement of the eastern Pelagonian passive continental margin was disrupted by the initial stages of the closure of the adjacent Neo-Tethys Ocean. This disruption was set in motion by eastward intra-oceanic subduction and subsequent formation of Middle Jurassic metamorphic soles and ophiolitic mélanges (Figure 7.1) (Roddick et al. 1979, Spray and Roddick 1980, Dimo-Lahitte et al. 2001, Karamata 2006, Schmid et al. 2020).

a. Middle Triassic-Early Jurassic configuration
of the Pelagonian passive margin

b. late Early Jurassic intra-oceanic obduction
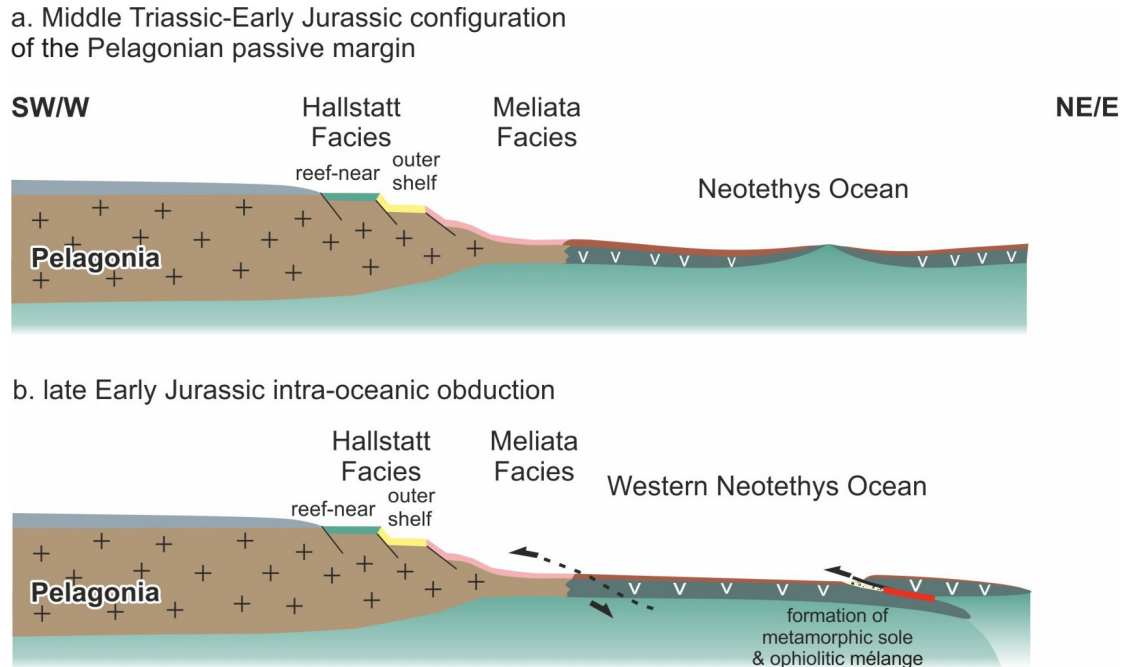
Figure 7.1 Late Triassic to Late Jurassic paleogeographic arrangement of the eastern Pelagonian passive continental margin (Kostaki et al. 2023: based on Gawlick and Missoni 2019): **a**) The central Pelagonian shelf features shallow-water carbonates, with the outer shelf characterized by reef-near Hallstatt Facies and the more deeper outer shelf by the Hallstatt/Pindos succession. **b**) The onset of intra-oceanic subduction settings in the western Neo-Tethys Ocean triggering the westward ophiolite obduction on the eastern Pelagonian margin (as continuation of the Adriatic plate) and leading to the development of metamorphic soles and ophiolitic mélanges.

During intra-oceanic subduction, an ensimatic island-arc formed, and in the back-arc basin, supra-subduction settings evolved, resulting in Jurassic ophiolites (Figure 7.2) (e.g., Zachariades 2007, Dilek et al. 2008, Michail et al. 2016).

The new geodynamic regime in the early Middle Jurassic triggered westward ophiolite obduction in the Bajocian/Bathonian, causing subsidence in the eastern Pelagonian passive continental margin, as reflected by an increased accumulation of radiolarites, primarily in the outer shelf (Figure 7.2) (Baumgartner 1985, Scherreiks et al. 2009).

During the west-directed obduction processes, which led to the disruption of the arrangement and structure of the passive continental margin, the Triassic-Early Jurassic

Hallstatt/Pindos succession, constituting an integral part of the margin, was affected, resulting in the formation of a nappe stack in the lower plate (Figure 7.3). Subsequently, trench-like deep-water basins evolved ahead of the westward advancing nappe stack during Middle to Late Jurassic, receiving blocks and slides, specifically rocks from the former outer shelf (Hallstatt/Pindos succession) and the ophiolites with their radiolarite overlying layer (Figure 7.2). These basins were later integrated into the nappe stack, undergoing shearing, which ultimately resulted in the formation of sedimentary mélanges, as observed in the case of the Avdella mélange. These identical processes also contributed to the formation of the Koziakas mélange.

During the late Middle Jurassic to early Late Jurassic, the nappe stack, which includes the Hallstatt/Pindos succession, underwent bulldozing by the west-directed obducting Neo-Tethys ophiolites (Kostaki et al. 2023). Subsequently, it was transported westward by mass movements onto the foreland, reaching the inner parts of the former continental margin characterized by shallow-water carbonate platform facies.

Taking into account structural observations consistent with other published works (e.g., Baumgartner 1985, Most et al. 2001, Kilias et al. 2002, 2010, Gawlick et al. 2008, Schmid et al. 2008, 2020, Bortolotti et al. 2012, Scherreiks et al. 2014, Schenker et al. 2014, 2015, Kilias 2021), which support the idea that the ophiolites were primarily emplaced through top-to-the-W direction over the eastern passive Pelagonian margin during the Middle-Late Jurassic, the Triassic-Early Jurassic Hallstatt/Pindos succession is interpreted as a Middle Jurassic extensively traveled nappe. Its origins trace back to the eastern Pelagonian margin, constituting the easternmost segment of the Adriatic plate. Consequently, in the early Late Jurassic, in its new position, the Hallstatt/Pindos nappe underwent new sedimentation, resulting in the covering of the Hallstatt/Pindos succession by a subsequent Late Jurassic to Paleogene sequence.

Following this conceptualization, the original Triassic to Middle Jurassic arrangement of the eastern Pelagonian passive continental margin is comprehensive, free from the interruption of a Pindos Ocean or a Pindos Basin, west of the Pelagonian domain. The Triassic shallow-water carbonates define the central Pelagonian shelf domain, while the reef-near Hallstatt Limestones characterize the outer shelf, and the deeper outer shelf is marked by the Hallstatt/Pindos succession (Kostaki et al. 2023)

Figure 7.2 Reconstruction of the Middle to Late Jurassic geotectonic evolution (Kostaki et al. 2023: based on Gawlick and Missoni 2019): **c**) Development of an ensimatic island arc and a supra-subduction setting in the back-arc basin during the intra-oceanic subduction (Michail et al. 2016). Imbrication of the lower plate and nappe stack formation occur due to westward ophiolite obduction in the Bathonian. **d**) Development of trench-like foreland basins ahead of the obducted ophiolites and westward advance of the nappe stack. Onset of Late Jurassic shallow-water platforms on top of the ophiolites, providing erosional products to the under-filled basins. These basins underwent shearing through incorporation into the nappe stack, resulting in the formation of mélanges.

(Figures 7.1 and 7.2). This aligns with research from other authors who support the idea that open-marine limestones and deep-water rocks, along with the ophiolites exposed in Sub-Pelagonian Zone (e.g., Argolis Peninsula and Othrys), constitute far-travel nappes (Vrielynck 1978, Baumgartner 1985, Ferrière et al. 2016). These nappes were also emplaced westward over the Pelagonian margin during the early Late Jurassic,

originating from the Neo-Tethys Ocean situated to the east of the Pelagonian region. Subsequently, they were affected by younger tectonic events, resulting in a complicated arrangement.

7.2 Emplacement of the ophiolites and the subsequent events

The Late Jurassic period is characterized by the initiation of Kimmeridgian-Tithonian shallow-water carbonate sedimentation upon the obducted ophiolites. This indicates that the age of the ophiolite emplacement of over the former Pelagonian passive margin can be estimated as older than the formation of Late Jurassic shallow-water carbonate platforms, therefore as late Middle Jurassic to early late Jurassic (Bathonian to Oxfordian) (Kilias et al. 2010, Kostaki et al. 2013, Missoni and Gawlick 2011, Gawlick et al. 2020).

On the contrary, a different perspective links the emplacement of the ophiolites with the development of the Boeotian Flysch within a foreland basin situated ahead of the obducted ophiolites during the late Late Jurassic to Early Cretaceous (Schmid et al. 2008, 2020, Nirta et al. 2018, 2020). Nonetheless, the development of the Boeotian Flysch can be explained as a subsequent event that took place after the emplacement of the ophiolites. Boeotian Basin could have been developed due to westward sliding of the ophiolite nappe stack after mountain uplift and unroofing of the accreted former Pelagonian margin (Gawlick et al. 2020, Kostaki et al. 2023). Similar circumstances led to the development of time-equivalent basins such as the Firza Basin (Gawlick et al. 2008, Bortolotti et al. 2005), the Bosnian Basin (Mikes et al. 2008), and the Roßfeld Basin (Krische et al. 2014).

The Late Jurassic to Early Cretaceous mountain uplift and unroofing of the Pelagonian Zone is evidenced by the presence of laterites documented across an extended region (Figures 4.9) (Carras et al. 2004, Photiades et al. 2007, Pomoni-Papaioannou and Photiades 2007, Nirta et al. 2018, 2020). This indicates that the Vourinos ophiolites experienced subaerial exposure until the late Early Cretaceous, when a transgressive event occurred. This event led to the establishment of new late

Early Cretaceous carbonate platforms that extensively covered the imbricated Pelagonian Zone (Carras et al. 2004, Photiades et al. 2007, Fazzuoli and Carras 2007, Bortolotti et al. 2004a).

The studied outcrop in the Poros region (sub-chapter 5.6) demonstrates that the lower section of the late Early Cretaceous sedimentary succession features conglomerates and breccias comprised of redeposited components from Late Jurassic-Early Cretaceous shallow-water and deep-water environments. These are followed by reefal limestones and limestones with orbitolinid foraminifera, dated as Late Barremian-Early Aptian.

Thorough examination of newly acquired biostratigraphic data reveals that redeposited components originating from the erosion of the Late Jurassic shallow-water carbonate platform can be identified not only within the late Early Cretaceous transgressive succession but also elsewhere. These components are notably present in redeposited carbonates within the Avdella mélange (Perivoli and Ziakas outcrops) and within carbonate-clastic resediments intercalated within the radiolarite sequence situated above the Koziakas mélange (see also Ghon et al. 2018). Additionally, they are identified within Earliest Cretaceous mass-flow deposits above the Vardar-Axios ophiolites.

Characteristic microfacies originating from a Late Jurassic shallow-water carbonate platform have also been documented on top of the ophiolites in the western regions of the Pelagonian Zone (Gielisch et al. 1993, Galeos et al.1994, Carras and Georgala 1998, Dragastan and Richter 1999, 2003, Scherreiks 2000, Carras et al. 2004, Fazzuoli and Carras 2007, Pomoni-Papaioannou and Photiades 2007).

The microfacies and the fossil content documented in the succession on top of Vardar-Axios ophiolites (sub-chapter 5.4), in particular the Late Jurassic (Kimmeridgian?-Tithonian) reworked reef material, are akin to those described in sub-chapter (4.3.1) from the Zyghosti Platform (Carras et al. 2004, Bortolotti et al. 2004a, Fazzuoli and Carras 2007). The Late Jurassic Zyghosti Platform, exhibiting identical microfacies, is believed to have been formed in a comparable position on top of the Vourinos ophiolites, which are presently located in the western region of the Pelagonian Zone.

Consequently, the identification of Late Jurassic carbonate platform components associated with ophiolites in both eastern and western regions of the Pelagonian Zone defines a consistent paleogeographic provenance area. This correlation suggests the development of an extensive shallow-water platform sealing the ophiolite emplacement, confirming a single west-directed ophiolite nappe stack.

In the Albanides, Schlagintweit et al. (2008) documented analogous Kimmeridgian-Tithonian shallow-water carbonate components within mass-flow deposits. These components are interpreted to have originated from a shallow-water platform, referred to as the Kurbnesh Platform, which formed on top of an ophiolitic mélange from the Mirdita Ophiolite Zone.

Similarly, in the Inner Dinarides, a comparable scenario is observed with Kimmeridgian-Tithonian resedimented shallow-water microfacies. These microfacies are preserved in a former deep-water foreland basin that developed during westward obduction processes (Gawlick et al. 2020). As in the Hellenides, the shallow-water carbonate platform on top of the obducted ophiolites experience erosion following the uplift of the nappe stack.

Last but not least, in the Northern Calcareous Alps, the Late Jurassic shallow-water platform is notably preserved, recognized as the Plassen Carbonate Platform. This platform developed on top of the uplifted Middle to early Late Jurassic nappe stack (Gawlick and Schlagintweit 2006, 2010, Schlagintweit and Gawlick 2007).

This enables the tracing of a Late Jurassic carbonate platform pattern along the suture zone of the Neo-Tethys Ocean during Jurassic times, extending from the Eastern Alps and Western Carpathians in the north, through the eastern Southern Alps, and into the Dinarides and Albanides towards the Hellenides. However, the original paleogeography of this Late Jurassic carbonate platform, which initially formed on top of the ophiolite nappe stack, was disrupted by subsequent polyphase tectonic movements, resulting in a puzzle within the orogens of the eastern Mediterranean region today. In most locations, this puzzle can only be reconstructed from redeposited components found in younger resediments (Schlagintweit and Gawlick 2007, Schlagintweit et al. 2008, Gawlick et al. 2008, 2020, Kukoc et al. 2012, Kostaki et al. 2013, 2014, Gorican et al. 2018, Drvoderic et al. 2023).

The identification of the widespread distribution of eroded components from the Late Jurassic platform and the underlying ophiolites across various depositional settings provides valuable insights into the paleogeographic conditions during the Late Jurassic to Early Cretaceous and the timing of events subsequent to the obduction of the ophiolite nappe stack over the former Pelagonian margin.

Following the westward obduction of the ophiolites, the passive continental margin underwent imbrication, leading to the formation of a nappe stack in the lower plate (Gawlick and Missoni 2019). Subsequently, trench-like deep-water basins developed in advance of the progressing ophiolite nappe stack, receiving blocks from the Hallstatt/Pindos nappe and the ophiolites, forming sedimentary mélanges. This is evidenced by the presence of the dismembered Hallstatt Limestone succession, the ophiolitic blocks, and the Triassic radiolaritic material within the Avdella and Koziakas mélanges (Figure 7.2) (see also Oszvart et al. 2012).

As a consequence of the obduction processes, shallow-water carbonate production took place on top of the obducted ophiolites during the Late Jurassic. Shorty after the establishment of these Late Jurassic (Kimmeridgian-Tithonian) shallow-water platforms, the accreted former Pelagonian margin experience continuous uplift, resulting in ongoing erosion from the latest Tithonian until the Earliest Cretaceous (Gawlick et al. 2020). This erosion primarily affected the Late Jurassic shallow-water carbonates, then extended to the ophiolites and their relevant radiolarite layer, and finally, it reached the Triassic to Early Jurassic Pelagonian carbonate platform cover and its underlying crystalline basement rocks.

This heterogeneous material was successively redeposited, primarily into the trench-like foreland basins that remained under-filled during that time, advancing at the forefront of the west-directed ophiolites. The presence of reworked shallow-water microfacies blended with ophiolite-derived debris and Triassic recrystallized radiolaritic lithoclasts within samples derived from the Perivoli and Ziakas outcrops (Avdella mélange) documents this process (sub-chapter 5.3).

The situation in the Koziakas region differs from that of the Avdella mélange due to the westward sliding of the ophiolite nappe stack, driven by the mountain uplift during the latest Tithonian to Earliest Cretaceous. This movement resulted in the overthrusting

of the ophiolites onto the former foreland basin, forming the Avdella mélange. Meanwhile, in the Koziakas region, the western part of the trench-like foreland basin partially escaped the overthrust of the ophiolite nappe stack. As a result, this basin remained under-filled, allowing sedimentation to continue until the earliest Cretaceous, with the basin fill sediments sustaining slight deformation.

Additional insights into the Late Jurassic to Early Cretaceous paleogeography are offered by the conditions preserved in the eastern Koziakas mountain range. From the Callovian to the Kimmeridgian, after the ophiolite emplacement, a radiolarite sequence was deposited above the underlying sedimentary mélange. The radiolarite-rich turbidites appear to extend up to several meters without any influence from shallow-water material, manifesting a period of tectonic silence during this time span (late Oxfordian to the Kimmeridgian).

The subsequent mountain uplift resulted in further westward transport of the ophiolites and the overlying shallow-water platform, placing them closer to the under-filled foreland basin, which subsequently began to demonstrate a gradual shallow-water influence. Ongoing erosion of the uplifted nappe stack until the Berriasian led to the redeposition of shallow-water material and other erosional products, such as Late Triassic carbonate clasts within the under-filled basin (Ghon et al. 2018). This process resulted in the formation of carbonate-clastic resediments, which are found intercalated within the radiolarite sequence.

Furthermore, in response to the active tectonic environment during the Earliest Cretaceous, there was a reconfiguration of the ophiolite nappe stack and formation of new basins. In these newly formed basins situated above the ophiolites on both sides of the Pelagonian region, the eroded products of the uplifting event were also transported and redeposited as mass-flows, similar to the situation described above the Vardar-Axios ophiolites.

CHAPTER 8. Conclusions

This dissertation thesis aims to contribute a new perspective to the ongoing discussion surrounding the challenging paleogeography of the Hellenic realm. The results obtained from biostratigraphic and microfacies analysis with regard to structural investigations, resulted in an improved comprehension of the Middle Jurassic to Early Cretaceous paleogeography and the timing of related events. The subsequent paleogeographic reconstruction has provided valuable insights into the origin of the ophiolites in the Hellenic realm and the configuration of the overridden former passive continental margin. This comprehension is crucial for the geodynamic interpretation of the entire Hellenides and the determination of the provenance of the ophiolites. A synthesis of the conclusions and implications derived from this study is offered as follows:

◆ In the late Early to early Middle Triassic, shallow-water carbonates were deposited in a restricted setting, followed by the deposition of open-marine limestones. This deepening event marks the final phases of the gradual continental break up of the Neo-Tethys Ocean, accompanied by intense volcanism in the Late Anisian. As a result, the eastern Pelagonian passive margin shaped, facing the Neo-Tethys oceanic domain from the late Middle Triassic until the early Middle Jurassic.

◆ The arrangement of the passive continental margin from the late Middle Triassic until the early Middle Jurassic followed a typical pattern: the central Pelagonian shelf comprised shallow-water carbonates, the outer shelf exhibited open-marine

deposition with influences from shallow-water material, and the deeper outer shelf was characterized by open-marine carbonates. The findings within the Avdella and Koziakas mélanges, leading to a Triassic open-marine shelf reconstruction mirroring the Hallstatt Facies, suggest that the emplacement of the ophiolites occurred westward over the eastern Pelagonian margin. The outer shelf region of this margin exhibited the deposition of Hallstatt Facies throughout the Middle Anisian to Rhaetian, followed in Early Jurassic by hemipelagic sediments.

◆ The Avdella mélange, displaying characteristics identical to the Koziakas mélange, developed during the Middle to early Late Jurassic due to westward ophiolite obduction. In front of the progressing ophiolites, new trench-like deep-water basins formed, where material deriving from the advancing nappe stack, including Hallstatt Limestones and ophiolites, was redeposited. Eventually, these basins underwent shearing as they incorporated into the nappe stack, forming the typical features of mélanges.

◆ The similarities between the resulted from blocks Hallstatt succession and a complete Middle Triassic to Early Jurassic succession in the western Pindos mountain range, situated to the west of the Pelagonian Zone as part of Pindos Zone and referred to as the Hallstatt/Pindos succession, led to further investigation of the western Pindos rocks. This investigation led to the establishment of their paleogeographical relationship, as they notably share identical stratigraphic characteristics. Hence, the Hallstatt/Pindos succession is accordingly considered part of the outer shelf deposited along the eastern Pelagonian margin during the Middle Triassic to Early Jurassic, facing the Neo-Tethys Ocean to the east. Following the west-directed Middle-Late Jurassic obduction processes, the Middle Triassic-Early Jurassic Hallstatt/Pindos succession endured displacement into the foreland.

◆ Throughout the late Middle to early Late Jurassic, the westward ophiolite nappe stack advanced from the outer to the inner Pelagonian shelf domain, leading to subsequent deposition of shallow-water carbonates (Kimmeridgian-Tithonian) covering the obducted ophiolites. Erosion, spanning from the Late Tithonian to

earliest Cretaceous and driven by ongoing uplift of the accreted Pelagonia, affected the newly formed Late Jurassic platforms and the obducted ophiolites. The eroded material from these shallow-water carbonate platforms and the underlying ophiolites underwent redeposition into under-filled trench-like foreland basins (Avdella and Koziakas mélanges). Later, during the latest Tithonian to Earliest Cretaceous, the eroded material were secondarily integrated, resulting in the situation preserved in the Avdella mélange. However, concerning the Koziakas mélange, a portion of the basin remained intact, experiencing only mild shearing, and deposition continued until the Early Cretaceous.

◆ Eroded material originated from the Kimmeridgian-Tithonian shallow-water platform is also present as components in Early Cretaceous mass-flow deposits, exposed on top of the obducted ophiolites on both sides of the Pelagonian Zone. Additionally, these components are identifiable in younger late Early Crataceous transgressive deposits. The analogous formation of Late Jurassic shallow-water platforms over the ophiolite nappe stack, followed by their subsequent total or partial erosion, can be traced in comparable successions throughout the Hellenides, Albanides, Dinarides, Eastern Alps, and Western Carpathians.

◆ The results obtained in the framework of the presented research confirm a single ocean model. Thus, the Pindos ophiolite belt is recognized as a segment of an extensive ophiolite nappe stack originating from the Neo-Tethys Ocean. This ocean was positioned to east of the broader Adria, with the Pelagonian Zone serving as its continuation, without any interruption of an autonomous Pindos Ocean or a Triassic-Jurassic deep-water Pindos Basin.

Extended Abstract

New sedimentological and biostratigraphic research, accompanied by structural analysis, took place on sedimentary successions and mélanges located in northern Greece, both above and below the Jurassic obducted Neo-Tethyan ophiolites. These sedimentary successions and mélanges are associated with Jurassic ophiolite obduction on the Pelagonian margin(s) within the Hellenides. Their study aimed to provide insights regarding the origin of the Neo-Tethyan ophiolites, the timing and direction of their emplacement, the geodynamic evolution of the Neo-Tethys Ocean, and the potential existence of a distinct Pindos Ocean or deep-water Pindos Basin.

Important is the occurrence of redeposited Kimmeridgian-Tithonian shallow-water components, as they reveal the existence of a Late Jurassic carbonate platform formed above the obducted ophiolites. This platform set an upper stratigraphic limit for ophiolite emplacement during the Middle to early Late Jurassic. These redeposited components from this shallow-water platform were identified in various successions: 1) Notably, these components are found in redeposited carbonates within Avdella mélange, as well as in Late Jurassic to Earliest Cretaceous carbonate-clastic resediments situated above Koziakas mélange. 2) They are also present within Earliest Cretaceous mass-flows above Vardar-Axios ophiolites. 3) Additionally, they are evident within a late Early Cretaceous transgressive succession above Vourinos ophiolites.

Consequently, the identification of Late Jurassic carbonate platform components distributed in different depositional settings associated with ophiolites in both eastern and western regions of the Pelagonian Zone defines a consistent paleogeographic

provenance area. This correlation suggests the development of an extensive shallow-water platform sealing the ophiolite emplacement, confirming the presence of a single ophiolite nappe stack.

Moreover, microfacies analysis and conodont age dating of exotic carbonate blocks found in the Middle-Late Jurassic Avdella and Koziakas mélanges resulted in the reconstruction of a Middle-Late Triassic open marine shelf. This reconstruction mirrors the Hallstatt Limestone succession and notably shares similarities with successions in western Pindos mountain range, situated to the west of the Pelagonian Zone as part of Pindos Zone, referred to as the Hallstatt/Pindos succession. The original deposition of the Hallstatt Limestones is identified as occurring on the outer shelf from the Middle Triassic until the Early Jurassic, shaping the eastern Adriatic passive continental margin facing the Neo-Tethys Ocean in the east.

Structural observations, consistent with other published works, support a west-directed ophiolite emplacement over the eastern passive Pelagonian margin during the Middle-Late Jurassic. Consequently, the Hallstatt/Pindos succession is interpreted as a far-traveled Middle-Late Jurassic nappe, originating from the eastern Pelagonian margin, which was bulldozed in front of the west-directed obducting ophiolites onto the Pelagonian foreland. Therefore, it is concluded that the obducted ophiolites originated from the Neo-Tethys Ocean, positioned to east of the broader Adriatic plate, with the Pelagonian Zone serving as its continuation, without the interruption of a distinct Triassic-Jurassic Pindos Ocean or a Triassic-Jurassic deep-water Pindos Basin.

Σύνοψη

Νέες στρωματογραφικές και βιοστρωματογραφικές έρευνες που συνδυάσθηκαν με τεκτονική ανάλυση, πραγματοποιήθηκαν σε ιζηματογενείς σχηματισμούς και μείγματα (mélanges) που βρίσκονται τόσο πάνω όσο κάτω από τους Ιουρασικούς οφιόλιθους της βόρειας Ελλάδας. Κάθε σχηματισμός σχετίζεται με την τοποθέτηση των οφιολίθων επάνω στο Πελαγονικό περιθώριο (ή περιθώρια) στις Ελληνίδες. Ο στόχος της μελέτης τους είναι η κατανόηση ζητημάτων που αφορούν την προέλευση των οφιολίθων, τον χρόνο και την κατεύθυνση της τεκτονικής τοποθέτησής τους επάνω στο Πελαγονικό περιθώριο (ή περιθώρια), την γεωδυναμική εξέλιξη του Ωκεανού της Νεο-Τηθύος και την ενδεχομένη ύπαρξη ενός ανεξάρτητου Ωκεανού της Πίνδου ή της βαθιάς Λεκάνης Πίνδου.

Σημαντική είναι η εύρεση κλαστών ρηχής θάλασσας ηλικίας Κιμμεριδίου-Τιθωνίου, καθώς αποκαλύπτει την εξέλιξη μιας Άνω Ιουρασικής ανθρακικής πλατφόρμας, η οποία αποτέθηκε αρχικά πάνω στους οφιόλιθους κατά τη διάρκεια της πρώιμης - Άνω Ιουρασικής περιόδου, θέτοντας το ανώτατο όριο της οφιολιθικής τοποθέτησης. Τέτοιοι κλάστες, που προέρχονται από τη διάβρωση των πετρωμάτων της ανθρακικής πλατφόρμας, εντοπίστηκαν: 1) Εντός δευτερογενώς επανα-αποτιθέμενων ανθρακικών ιζημάτων στο Αβδέλλα mélange και σε Άνω Ιουρασικά - Κάτω Κρητιδικά ασβεστο-κλαστικά ιζήματα πάνω στο Κόζιακας mélange. 2) Επιπλέον, βρέθηκαν εντός μιας Κάτω Κρητιδικής ιζηματογενούς ακολουθίας που αποτελείται από ροές μαζών πάνω στους οφιόλιθους του Βαρδάρη - Αξιού. 3) Επίσης, μπορούν να αναγνωριστούν σε Κάτω Κρητιδικούς επικλυσιγενείς σχηματισμούς που επικάθονται ασύμφωνα στους

οφιόλιθους του Βούρινου. Συνεπώς, ο εντοπισμός αυτών των κλαστών ρηχής θάλασσας, οι οποίοι κατανέμονται σε διαφορετικά αποθετικά περιβάλλοντα που σχετίζονται με τους οφιόλιθους, τόσο στις δυτικές όσο και στις ανατολικές περιοχές της Πελαγονικής Ζώνης, ορίζει ότι προέρχονται από την ιδία παλαιογεωγραφική πηγή. Αυτή η συσχέτιση υποδηλώνει την ανάπτυξη μιας εκτεταμένης Άνω Ιουρασικής ανθρακικής πλατφόρμας ρηχής θάλασσας πάνω στους επωθημένους οφιόλιθους, σφραγίζοντας αυτό το τεκτονικό γεγονός, επιβεβαιώνοντας την ύπαρξη ενός ενιαίου οφιολιθικού καλύμματος.

Επιπλέον, η μικροφασική ανάλυση και η χρονολόγηση κωνοδόντων των ανθρακικών εξωτικών μπλοκ που βρίσκονται ενσωματωμένα στα Μέσης - Άνω Ιουρασικής ηλικίας mélanges Αβδέλλα και Κόζιακα, οδήγησε στην ανακατασκευή ενός ολοκληρωμένου Μέσο - Άνω Τριαδικού σχηματισμού ηπειρωτικού περιθωρίου ανοιχτής θάλασσας. Αυτή η ανακατασκευή αντικατοπτρίζει την ανθρακική ακολουθία Hallstatt και κυρίως μοιράζεται ομοιότητες με ιζηματογενείς σχηματισμούς στη δυτική οροσειρά της Πίνδου δυτικά της Πελαγονικής που ανήκουν στη Ζώνη της Πίνδου και αναφέρονται ως Hallstatt/Πίνδος στρωματογραφική ακολουθία. Η ακολουθία Hallstatt θεωρείται πως αρχικά αποτέθηκε κατά μήκος του εξωτερικού ηπειρωτικού περιθωρίου κατά τη διάρκεια της Μέσο Τριαδικής έως Κάτω Ιουρασικής περιόδου, διαμορφώνοντας το ανατολικό παθητικό περιθώριο της Αδριατικής, με τον Ωκεανό της Νεο-Τηθύος να τοποθετείται στα ανατολικά της.

Τεκτονικές παρατηρήσεις που πραγματοποιήθηκαν, συμβατές με αυτές άλλων ερευνητών, αναγνωρίζουν μια κύρια προς τα δυτικά κινηματική Άνω Ιουρασικής ηλικίας, συνδεδεμένη με την τοποθέτηση των οφιόλιθων πάνω στην Πελαγονική. Επομένως, προτείνεται ότι η Hallstatt/Πίνδος στρωματογραφική ακολουθία αποτελεί ένα Μέσο – Άνω Ιουρασικό τεκτονικό κάλυμμα το οποίο προήλθε από τα ανατολικά της Πελαγονικής, και το οποίο ωθήθηκε και πτυχώθηκε έντονα προς τα δυτικά στο μέτωπο των επωθημένων οφιολίθων της Νεο-Τηθύος.

Συνεπώς, συμπεραίνεται η ύπαρξη ενός μόνο ωκεανού, αυτού της Νεο-Τηθύος στα ανατολικά της Πελαγονικής, η οποία θεωρείται αναπόσπαστο τμήμα της Αδριατικής πλάκας, χωρίς τη διακοπή της από την ύπαρξη ενός ανεξάρτητου Τριαδικού - Ιουρασικού Ωκεανού της Πίνδου ή μίας Τριαδικής - Ιουρασικής βαθιάς Λεκάνης Πίνδου.

References

Anders, B., Reischmann, T., Poller, U. and Kostopoulos, D., 2005. Age and origin of granitic rocks of the eastern Vardar Zone, Greece: new constraints on the evolution of the Internal Hellenides. *J. Geol. Soc.,* 162(5):857–870.

Angiolini, L., Dragonetti, L., Muttoni, G. and Nicora, A., 1992. Triassic stratigraphy in the Island of Hydra (Greece). *Riuistu Itulianu di Puleontologiue Strutigrafia,* 98: 137-180.

Aubouin, J., 1959. Contribution al' étude géologique de la Grèce septentrional: les confins de l' Epire et de la Thessaly. *Annales Géologiques de Pays Helléniques*, 10: 1–525.

Aubouin, J., 1973. Des tectoniques superposιes et leur signification par rapport aux modeles gιophysiques: l′exemple des Dinarides; paleotectonique, tectonique, tarditectonique, neotectonique. *Bull Soc Gιol France*, S7-XV(5–6):426–460.

Baumgartner, P.O., 1985. Jurassic sedimentary evolution and nappe emplacement in the Argolis Peninsula (Peloponnesus; Greece). *Mémoires de la Société Helvétique des Sciences Naturelles*, 99: 1–111.

Baumgartner, P.O., O'Dogherty, L., Goriˇcan,ˇS., Dumitrica-Jud, R., Dumitrica, P., Pillevuit, A., Urquhart, E., Matsuoka, A., Danelian, T., Bartolini, A.,Carter, E.S., De Wever, P., Kito, N., Marcucci, M. and Steiger, T., 1995. Radiolarian catalogue

and systematics of Middle Jurassic to Early Cretaceous Tethyan genera and species. In: Baumgartner, P.O., O'Dogherty, L., Goriˇcan,ˇS., Urquhart, E., Pillevuit, A., De Wever, P. (Eds.), Middle Jurassic to Lower Cretaceous Radiolaria of Tethys: occurrences, systematics, biochronology. *Mémoires de Géologie* (Lausanne), 23, 37–685.

Bebien, J., Dubois, R. and Gauthier, A., 1986. Example of ensialic ophiolites emplaced in wrench zone: innermost Hellenic ophiolite belt (Greek Macedonia). *Geology*,14: 1016-1019.

Beccalura, L., Ohnenstetter, D., Ohnenstetter, M. and Paupy, A., 1984. Two magmatic series with island arc affinities within the Vourinos ophiolite. *Contrib. Mineral. Petrol.*, 85: 253-271.

Beck, H.H., 1912. Minerals of Lancaster county. Linnean Society. 11pp.

Bender, H., 1962. Tieftriadische Hallstätter Kalke und Tuffe in Nordattika. Marburg: Sitz. Ber. Ges. Zur Beförderung ges. *Naturwiss*, 83-84: 65-79.

Bender, H., 1970. Der Nachweis von Unter-Trias ("Hydasp") auf der Insel Chios. *Annales Géologiques de Pays Helléniques*, 19: 12-464.

Bender, H. and Kockel, F., 1963. Die Conodonten der griechischen Trias. *Annales Géologiques de Pays Helléniques*, 14: 436-445.

Bernoulli, D. and Laubscher, H., 1972. The palinspastic problem of the Hellenides. *Ecl. Geol. Helv.*, 65: 107-118.

Bernoulli, D. and Jenkyns, H.C., 1974. Alpine, Mediterranean and Central Atlantic Mesozoic facies in relation to the Early Evolution of the Tethys. In: *Modern and ancient geosynclinal sedimentation* (Eds Dott, R.H. and Shaver, R.H.). Society of Economic Paleontologists and Minerologists, Special Publications, 19: 129-160.

Blatt, H., 1967. Provenance determinations and recycling of sediments. *J. Sed. Petrol.*, 37: 1031-1044

Bonneau, M., 1984. Correlation of the Hellenides Nappes in the south-east Aegean and their tectonic reconstruction. *Geol. Soc. London*, Spec. Publ. 517-527.

Bortolotti, V., Dal Piaz, G.V. and Passerinia, P., 1969. Ricerche sulle ofioliti delle Catene Alpine. 5 – Nueve osservazioni sul Massiccio del Vourinos (Grecia). *Boll. Soc. Geol. It.*, 88: 35-45.

Bortolotti, V., Kodra, A., Marroni, M., Mustafa, F., Pandolfi, L., Principi, G. and Saccani, E., 1996. Geology and petrology of the ophiolitic sequences in the Mirdita region, northern Albania. *Ofioliti*, 21: 3-20.

Bortolotti, V., Carras, N., Chiari, M., Fazzuoli, M., Photiades, A. and Principi, G., 2004 (a). Sedimentary evolution of the Upper Jurassic Zyghosti platform, Kozani, Northern Greece. Proceedings of International Symposium on Earth System Sciences (ISES) 2004, Istanbul, Turkey, 705-712.

Bortolotti, V., Chiari, M., Marcucci, M., Marroni, M., Pandolfi, L., Principi, G. and Saccani, E., 2004(b). Comparison among the Albanian and Greek ophiolites: In search of constraints for the evolution of the Mesozoic Tethys ocean. *Ofioliti,* 29(1): 19-35.

Bortolotti, V., Marroni, M., Pandolfi, L. and Principi, G., 2005. Mesozoic to Tertiary tectonic history of the Mirdita ophiolites, northern Albania. In: *Evolution of Ophiolites in Convergent and Divergent Plate Boundaries* (eds Y., Dilek, Y., Ogawa, V., Bortolotti and P., Spadea). *The Island Arc,* 14: 471–93.

Bortolotti, V., Chiari, M., Marroni, M., Pandolfi, L., Principi, G. and Saccani, E., 2012. Geodynamic evolution of ophiolites from Albania and Greece (Dinaric-Hellenic – belt): one, two or more oceanic basins? *Inter. Journal of Earth Sciences,* 102: 783-811.

Brown, S.A.M. and Robertson, A.H.F., 2003. Sedimentary geology as a key to understanding the tectonic evolution of the Mesozoic- Early Tertiary Paikon Massif, Vardar suture zone, N Greece. *Sediment. Geol.*, 160: 179-212.

Brown, S.A.M. and Robertson, A.H.F., 2004. Evidence for the Neotethys Ocean rooted in the Vardar zone: evidence from the Voras Mountains, NW Greece. *Tectonophysics,* 381: 143-173.

Brunn, J.H., 1956. Contribution à l' étude géologique du Pinde septentrional et d' une partie de la Macédoine occidnetale. *Annale Géologique de Pays Hellénique,* 7: 1-358.

Burkhard, M., 1988. L'Helvétique de la bordure occidentale du massifde l'Aar (évolution tectonique et métamorphique). *Eclogae Geolhelv*, 81: 63–114.

Camerlenghi, A. and Pini, G.A., 2009. Mud volcanoes, olistostromes and argille scagliose in the Mediterranean redion. Sedimentology. Special issue: From the Mediterranean torward a Global Reinaissance, 56: 319-365.

Capedri, S., Venturelli, G., Bocchi, G., Ostal, J., Garuti, G. and Rossi, A., 1980. The geochemistry and petrogenesis of an ophiolitic sequence from Pindos, Greece. *Contrib. Min. Petr.*, 74: 189-200.

Capedri, S., Lekkas, E., Papanikolaou, D., Skarpelis, N., Venturelli, G. and Gallo, F., 1985. The ophiolite of the Koziakas range- Western Thessaly (Greece). *Neues Jahrbuch Miner. Abh.,* 152: 45-64, Stuttgart.

Carras, N., 1995. La piattaform carbonatica del Parnasso durante il Guirassico Superiore-Cretaceo inferiore. *PhD Thesis Athens* 232 pp.

Carras, N., and Georgala, D., 1998. Upper Jurassic to Lower Cretaceous Carbonate facies of African affinities in a peri-European area: Chalkidiki peninsula, Greece. *Facies,* 38: 153-164.

Carras, N., Fazzuoli, M. and Photiades, A., 2004. Transition from carbonate platform to pelagic depotition (Mid Jurassic- Late Cretaceous), Vourinos Massif, northernGreece. *Riv. Ital. Paleont. Stratigr.,* 110:345-355.

Channell, J.E.T. and Kozur, H., 1997. How many oceans? Meliata, Vardar, and Pindos oceans in the Mesozoic Alpine paleogeography. *Geology,* 25, 183–186.

Chatalov, A., Bonev, N. and Ivanova, D., 2015. Depositional characteristics and constraints on the mid-Valanginian demise of carbonate platform in the intra-Tethys domain, Circum-Rhodope Belt, northern Greece. *Cretaceous Research*, 55: 84-115.

Chiari, M., Bortolotti, V., Marcucci, M., Photiades, A. and Principi, G., 2003. The Middle Jurassic siliceous sedimentary cover at the top of the Vourinos Ophiolite (Greece). *Ofioliti*, 28(2): 95-103.

Chiari, M., Djerić, N., Garfagnoli, F., Hrvatović, H., Krstić, M., Levi, N., Malasoma, A., Marroni, M., Menna, F., Nirta, G., Pandolfi, L., Principi, G., Saccani, E., Stojadinović, U., Trivić, B., 2011. The geology of the Zlatibor-Maljen area (western Serbia): a geotraverse across the ophiolites of the Dinaric-Hellenic collisional belt. *Ofioliti*, 36: 139–166.

Chiari, M., Bortolotti, V., Marcucci, M.C. and Saccani, E., 2012. Radiolarian Biostratigraphy and Geochemistry of the Koziakas Massif Ophiolites (Greece). *Bulletin de la Societe Geologique de France*, 183: 287-306.

Clift, P.D. and Robertson, A.H.F., 1990. Deep-water basins within the Mesozoic carbonate platform of Argolis, Greece. *Journal of the Geological Society London*, 147: 825-836.

Creutzburg, N., Klocker, P., Küss, S. E., 1966. Die erste triadische Ammonoideen-Fauna der Insel Kreta. Ber. Naturf. Ges. Freiburg, 56: 183-207.

Danelian, T. and Robertson A.H.F., 2001. Neotethyaan evolution of eastern Greece (Pagondas Melange, Evia island) inferred from rediolarian biostratigraphy and the geochemistry of associated extrusive rocks. *Geol. Mag.*, 138(3): 345-363.

Dercourt, J., 1970. L'expansion oceanique actuelle et fossile: ses implications geotectoniques. *Bull. Soc. Geol. France*, 12: 261-317.

Dercourt, J., Zonenshain, L.P., Ricou, L.-E., Kazmin, V.G., LePichon, X., Knipper, A.L., Grandjaquet, C., Sbortshhikov, I.M., Geyssant, J., Lepvrier, C., Perchersky, D.H., Boulin, J., Sibuet, J.-C., Savostin, L.A., Sorokhtin, O., Westphal, M., Bazhrnov, M.L., Lauer, J.-P., and Biju-Duval, B., 1986. Geological evolution of the Tethys belt from the Atlantic to the Pamirs since the Lias. *Tectonophysics*, 123: 241–315.

Dewey, J.F., Pitman, W.C., Ryan, W.B.F. and Bonnin, J., 1973. Plate tectonics and the evolution of the Alpine system. *Geol. Soc. Am. Bull.*, 84(3): 137-180.

Dimitriadis, S. and Asvesta, A., 1993. Sedimentation and magmatism related to the Triassic rifting and later events in the Vardar-Axios Zone. *Bull. Geol. Soc. Greece,* 28: 149-168.

Dimitrijevic, M.D., 1974. Sur l'âge du métamorphisme et des plissements dans la masse Sérbo-Macédonienne. *Bull. Assoc. Geol. Carpatho-Balkanique 1963*, 21: 45-48.

Dimitrijević, M.N. and Dimitrijević, M.D. 1991. Triassic carbonate platform of the Drina-Ivanjica element (Dinarides). – Acta Geologica Hungarica, 34(1-2): 15-44.

Dimitrijevic, M.D., 1997. Geology of Yugoslavia. Special publications, Geological Institute, Gemini, Belgrade: 1-187.

Dilek, Y., Furnes, H., and Shallo, M., 2007. Suprasubduction ophiolite formation along the periphery of Mesozoic Gondwana. *Gondwana Research*, 11: 453–475.

Dilek, Y., Shallo, M., and Furnes, H., 2008, Geochemistry of the Jurassic Midita Ophiolite (Albania) and the MORB to SSZ evolution of a marginal basin oceanic crust. *Lithos*, 100: 174–209.

Dimo-Lahitte, A., Monie, P., Vergely, P., 2001. Metamorphic soles from the Albanian ophiolites, petrology, 40Ar/39Ar geochronology, and geodynamic evolution. *Tectonics,* 20: 78–96.

Dragastan, O. and Richter, D.K., 1999. Late Jurassic oolites from the Acrocorinth (NE-Peleponnesus): Calcareous-micro-algae as an exceptional paleoecologic indicator. *Boch Geol Geotech Arb,* 53: 149-172.

Dragastan, O. and Richter, D.K. 2003. Calcareous algae and foraminifers from Neocomian limestones of Methana Peninsula, Asprovouni Mts. (Greece) and from south Dobrogea (Romania). Analele Universitatii Bucuresti Geologie Special Publication 1, 57-128.

Drvoderic, S., Gawlick, H.J., Hisashi, S. and Schlagintweit, F., 2023. Suprasubduction ophiolite (SSZ) components in a Middle to lower Upper Jurassic Hallstatt melange in the Northern Calcareous Alps (Raucherschober/ Schafkogel area), Geosystems and Geoenvironment (2022). DOI: hhttps:/doi.org/12.1016/j.geogeo.2022.100174

Dunham, R.J., 1962. Classification of carbonate rocks according to depositional texture. In: Ham, W.E. (ed.): Classification of carbonate rocks. A symposium. *Amer. Ass. Petrol. Geol. Mem*. 1: 108-171.

Dürr, St., 1975. Über Alter und geotectonische Stellung des Menderes-Kristallins/SW. Marburg: Anatolien und seine äquivalente in der mittleren Ägäis. H. Schr. Univ. Marburg, 106.

Embry, A.F. and Klovan, J.E., 1971. A late Devonian reef tract on northeastern Banks Island. N.W.T. *Bull. Canadian Petroleum Geol.,* 19: 730-781.

Fassoulas, C., Kilias, A. and Mountrakis, D., 1994. Postnappe stacking extension and exhumation of high-pressure/low-temperature rocks in the island of Crete, Greece. *Tectonics*, 13: 127–138.

Fazzuoli, M. and Carras, N., 2007. Development and demise of a carbonate platform by compressional and extensional tectonics: The Zyghosti Platform (Late Jurassic) and the Cretaceous transgression, Kozani, Northern Greece. *IAS Field Trip Guide book Patras* 2007, 173-190.

Ferrière, J., 1974. Étude géologique d`un sectuer des zones Helléniques internes subpelagonienne et pélagonienne (massif de l`Othrys, Grèce continental). Importance et signification de l période orogénique ante-Cretacé superieur. *Bul. de la Soc. Géol. de France*, XVI 543-562.

Ferrière, J., Chanier, F., Baumgartner, P.O., Dumitrica, P., Caridroit, M., Bout-Roumazeilles, V., Graveleau, F., Danelian, T. and Ventalon, S., 2015. The evolution of the Triassic-Jurassic Maliac oceanic lithosphere: insights from the supra-ophiolites series of the Othrys (continental Greece). *Bulletin de la Societe geologique de France*, 186: 399-411.

Ferrière, J., Baumgarthner, P.O. and Chanier, F., 2016. The Maliac Ocean: the origin of the Tethyan Hellenic ophiolites. *International Journal Earth Sciences*, 105: 1941-1963.

Festa, A., Pini, G.A., Dilek, Y and Codegone, G., 2010. Mélanges and mélange-forming processes: a historical overview and new concepts. *International Geology Review*, 52: 1040-1105.

Festa, A., Ogata, K., Pini, G.A., Dilek, Y. and Alonso, J.L., 2016. Origin and significance of the olistostromes in the evolution of the orogenic belts: a global syntheisis. *Gondwana Research*, 39: 180-203.

Festa, A., Pini, G.A., Ogata, K. and Dilek, Y., 2019. Diagnostic features and field-criteria in recognition of tectonic, sedimentary and diapiric melanges in orogenic belts and exhumed subduction-accretion complexes. *Gondwana Research*, Special Issue Melanges. https://doi.org/10.1016/j.gr.2019.01.003

Filippidis, A., Kassoli-Fournaraki, A. and Kantiranis, N., 2000. Chromites in the southern sector of Xerolivado chrome mine of Vourinos, Macedonia, Greece. Conference: 1st Congress of the Economic Geology, Mineralogy and Geochemistry Committee of the Geological Society of Greece (12-13/02/2000).

Flügel, E., 2004. Microfacies of carbonate rocks: Analysis, Interpretation and Application. Springer.

Folk, R. L., 1959. Practical classification of limestone. *Amer. Ass. Petrol. Bull*., 43: 1-38.

Folk, R.L., 1962. Spectral subdivision of limestones types. In: Ham, W.E. (ed.): Classification of carbonate rocks. A symposium. *Amer. Ass. Petrol. Geol. Mem.*, 1: 62-84.

Frisch, W. and Gawlick, H.J., 2003. The nappe structure of the central Nothern Calcareous Alps and its disintegration during Miocene tectonic extrusion-A contribution to understanding the orogenic evolution of the Eastern Alps. *International Journal of Earth Science*, 92: 712-727.

Frisch, W. and Meschede, M., 2007. Plattentektonik: Kontinentverschiebung und Gebirgsbildung. 2., aktualisierte Auflage, WBG, Darmstad, p. 196.

Frisch, W., Blakey, R. and Meschede, M., 2011. Plate Tectonics. DOI 10.1007/978-3-540-76504-2_1, *Springer-Verlag* Berlin Heidelberg.

Galeos, A., Pomoni-Papaioannou, F., Tsaila-Monopolis, S., Turnsek, D. and Ioakim, C., 1994. Upper Jurassic-Lower Cretaceous "Molassic-Type" sedimentation in the western part of Almopia subzone, Loutra Aridhea unit (Northern Greece). - Bulletin of the Geological Society of Greece, Proceedings of the 7 Congress, Thessaloniki, May, 171-184.

Gawlich, H.-J. and Bohm, F., 2000. Sequence and isotope strarigraphy of the Late Triassic distal periplatform limestones from Northern Calcareous Alps

(Kalberstein Quarry, Berchtesgaben Hallstatt Zone). *International Journal of Earth Sciences*, 89: 108-129.

Gawlick, H.-J., Frisch, W., Missoni, S., Suzuki, H., 2002. Middle to Late Jurassic radiolarite basins in the central part of the Northern Calcareous Alps as a key for the reconstruction of their early tectonic history—an overview. *Mem. Soc. Geol. Ital.*, 57:123–132.

Gawlick, H.-J. and Frisch, W., 2003. The Middle to Late Jurassic carbonate clastic radiolaritic flysch sediments in the Northern Calcareous Alps: sedimentology, basin evolution and tectonics - an overview. *Neues Jahrbuch für Geologie und Paläontologie*, Abhandlungen, 230: 163–213.

Gawlick, H.-J. and Schlagintweit, F., 2006. Berriasian drowning of the Plassen carbonate platform at the type-locality and its bearing on the early Eoalpine orogenic dynamics in the Northern Calcareous Alps (Austria). *International Journal of Earth Sciences,* 95: 451-462.

Gawlick, H.-J., Frisch, W., Hoxha, L., Dumitrica, P., Krystyn, L., Lein, R., Missoni, S., and Schlagintweit, F., 2008. Mirdita zone ophiolites and associated sediments in Albania reveal Neotethys Ocean origin. *International Journal of Earth Sciences,* 94: 865-881.

Gawlick, H.-J. and Schlagintweit, F., 2010. The Drowning Sequence of Mount Bürgl in the Salzkammergut Area (Northern Calcareous Alps, Austria): Evidence for a Diachronous Late Jurassic to Early Cretaceous Drowning of the Plassen Carbonate Platform. *Austrian Journal of Earth Sciences*, 103/1: 58-75.

Gawlick, H.-J., Missoni, S., Schlagintweit, F. and Suzuki, H., 2012. Jurassic active continental margin deep-water basin and carbonate platform formation in the north-western Tethyan realm (Austria, Germany). *Journal of Alpine Geology*, 54: 189-291.

Gawlick, H.-J., Lein, R., Missoni, S., Krystyn, L., Frisch, W. and Hoxha, L., 2014. The radiolaritic argillaceous Kcira-Dushi-Komani sub-ophiolitic Hallstatt Mélange in the Mirdita Zone of northern Albania. *Buletini I Shkencave Gjeologjike*, 4: 1–32.

Gawlick, H.-J. and Missoni, S., 2015. Middle Triassic radiolarite pebbles in the Middle Jurassic Hallstatt Mélange of the Eastern Alps: implications for Triassic-Jurassic geodynamic and palaeogeographic reconstructions of the western Tethyan realm. *Facies,* 61, 1–19.

Gawlick, H.-J., Missoni, S., Suzuki, H., Sudan, M., Lein, R. and Jovanovic, D., 2016 (a). Triassic radiolarite and carbonate components from the Jurassic ophiolitic melange (Dinaridic Ophiolite Belt). *Swiss Journal of Geoscience*, 109(3): 473-494.

Gawlick, H-J., Gorican, S., Missoni, S., Dumitrica, P., Lein, R., Frisch, W. and Howha, L., 2016 (b). Middle and Upper Triassic radiolarite components from the Kcira-Dushi-Komani ophiolitic melange and their provenance (Mirdita Zone, Albania). *Revue de micropaleontologie*, 59: 359-380.

Gawlick, H.-J., Missoni, S., Sudar, M.N., Gorican, S., Lein, R., Stanzel, A.I. and Jovanovic, D., 2017 (a). Open-marine Hallstatt Limestones reworked in the Jurassic Zlatar Melange (SW Serbia): a contribution to understanding the orogen evolution of the Inner Dinarides. *Facies*, 63: 29.

Gawlick, H.-J., Sudar, M.N., Missoni, S., Suzuki, H., Lein, R., Jovanovic, D., 2017 (b). Triassic- Jurassic geodynamic evolution of the Dinaridic Ophiolite Belt (Inner Dinarides, SW Serbia). *Journal of Alpine Geology*, 55: 1–167.

Gawlick, H.-J., Missoni, S., Sudar, M.N., Suzuki, H., Meres, S., Lein, R. and Jovanovic, D., 2018. The Jurassic Hallstatt Mélange of the Inner Dinarides (SW Serbia): implications for Triassic-Jurassic geodynamic and palaeogeographic

reconstructions of the Western Tethyan realm. *Neues Jahrbuch Geologie Paläontologie,* Abhandlungen, 288: 1–47.

Gawlick, H.-J. and Missoni, S., 2019. Middle-Late Jurassic sedimentary melange formation related to ophiolite obduction in the Alpine-Carpathian-Dinaridic Mountain Range. *Godwana Res.*, 74: 144-172.

Gawlick, H.-J., Sudar, M., Missoni, S., Aubrecht, R., Schlagintweit, F., Jovanoviv, D. and Mikus, T., 2020. Formation of a Late carbonate platform on top of the obducted Dinaridic ophiolites deduced from analysis of carbonate pepples and ophiolitic detritus in southwestern Serbia. *International Journal of Earth sciences*, 109: 2023-2048.

Ghikas, D., Rassios, A. and Dilek, Y., 2009. Structure and tectonics of subophiolitic melanges in the western Hellenides (Greece): implications for ophiolite emplacement tectonics. *International Geology Review*, 1-31.

Ghon, G., 2017. Microfazielle Untersuchung einer karbonatklastischen Beckenfullung im Hangenden der ophiolitfuhrenden Koziakas Melange in kori, Nordgriechenland. Bachelor Arbeit, Montanuniversiteat Leoben.

Ghon, G., Gawlick, H.-J., Missoni, S., Djeric, N., Kilias, A. and Gorican, S., 2018. Age and microfacies of a carbonate-clastic radiolaritic basin fill above the Koziakas Mélange (Hellenides, Greece). XXI International Congress of CBGA, Salzburg, Austria.

Gielisch, H., Dragastan, O. and Richter, D., 1993. Lagoonal to tidal carbonate sequences of upper Jurassic/Lower Cretaceous age in the Corinthian area: Mélange blocks of the Parnassus Zone. *Bull. Geol. Soc. Greece,* XXVIII/3: 663-676.

Godfriaux, I., 1968. Etude géologique de la région de l' Olympe (Grèce). *Annale Géologique de Pays Hellénique,* 19: 1-271.

Godfriaux, I. and Ricou, L.E., 1991. The Paikon, a tectonic window within the Internal Hellenides, Macedonia, Greece. *Comptes Rendus - Acad. des Sci. Ser.*, II 313: 1479-1484.

Gorican, S., Zibret, L., Kosir, A., et al., 2018. Stratigraphic correlation and structural position of Lower Cretaceous flysch-type deposits in the eastern Southern Alps (NW Slovenia). Internaltional Journal of Earth Sciences, 107(11), DOI: 10.1007/s00531-018-1636-4

Greenly, E., 1919. The geology of Anglesey. Vol I, II: Great Britain Geological. Survey Memoir (980pp).

Haas, J., Kovács, S., Gawlick, H.-J., Gradinaru, E., Karamata, S., Sudar, M., Péró, Cs, Mello, J., Polák, M., Ogorelec, B., Buser, S., 2011. Jurassic evolution of the tectonostratigraphic units of the Circum-Pannonian Region. *Jahrbuch der Geologischen Bundesanstalt*, 151: 281–354.

Haas, J., Pelikan, P., Görög, A., Jozsa, S., Ozsvart, P., 2012. Stratigraphy, facies and geodynamic settings in Jurassic formations in the Bükk Mountains, North Hungary: its relationsns with the other areas of the Neotethyan realm. *Geological Magazine*, 150: 18–49.

Häfner, W.,1924. Geologie des südöstlichen Rätikon (zwischen Klosters und St Antönien). Inaugural-Dissertation Univ. Zürich, 34 S.

Hsü, K.J., 1968. Principles of mélanges and their bearing on the Franciscan-Knoxville Paradox. *Geological Society of America Bulletin*, 79: 1063–1074.

Ivanova, D., Bonev, N. and Chatalov, A., 2015. Biostratigraphy and tectonic significance of the lowermost Cretaceous carbonate rocks of the Circum-Rhodope Belt (Chalkidiki Peninsula and Thrace region, NE Greece). *Cretaceous Research*, 52: 25-63.

Jacobshagen, V., 1986. Geologie von Griechenland. Beitraege zur regionalen Geologie der Erde. Gebrueder Borntraeger Verlag, Berlin, 363 pp.

Jacobshagen, V., Duerr, F., Kockel, K., Kopp, K.O., Kowalczyk, G., Berckhemer, H. and Buttner, D., 1978. Structure and geodynamic evolution of the Aegean region. In: H. Cloos, D. Roeder. and K. Schmidt (eds), Alps, Apennines, Hellenides. E. Schweizerbart` sche Verlagsbuchhandlung, Stuttgart, pp. 537-564.

Jolivet, L., Goffé, B., Monié, P., Truffert-Luxey, C. and Patriat, M., 1994. Miocene detachment in Crete and exhumation P-T-t paths of high-pressure metamorphic rocks. *Tectonics*, 15: 1129–1153.

Jones, G., Robertson, A.H.F. and Cann J.R., 1991. Genesis and emplacement of the supra-subduction zone Pindos Ophiolite, northwestern Greece. In: Peters T.J., Nicolas, A., Coleman, R.G. (eds) Ophiolite genesis and evolution of the oceanic lithosphere. Kluwer Acad. Publ. Dodrecht pp 771-799.

Jones, G. and Robertson, A., 1991. Tectonostratigraphy and evolution of the Mesozoic Pindos ophiolite and related units, northwestern Greece. *J. Geol. Soc. London*, 148: 267-288.

Jones, G., De Wever, P. and Robertson, A.H.F., 1992. Significance of radiolarian age date to the Mesozoic tectonics and sedimentary evolution of the northern Pindos Mountains, Greece. *Geological Magazine,* 129: 358-400.

Jones, G. and Robertson, A., 1994. Rift-Drift-Subduction and emplacement history of the Early Mesozoic Pindos Ocean: Evidence from the Avdella melange, Northern Greece. *Bulletin of the Geological Society of Greece*, Vol. XXX/2, 45-58.

Karamata, S., 2006. The geological development of the Balkan Peninsula related to the approach, collision and compression of Gondwanan and Eurasian units. In: A.H.F. Robertson and D. Mountrakis (eds), *Tectonic Development of the Eastern*

Mediterranean Region. Geological Society of London, Special Publications, 260: 155-178.

Karfakis, J., 1984. Geological Map of Greece, scale 1:50.000, Mouzakion Sheet. Institute of Geology and Mineral Exploration, Athens.

Katrivanos, E., Kilias, A. and Mountrakis, D., 2013. Kinematics of deformation and structural evolution of the Paikon Massif (Cental Macedonia, Greece): a Pelagonian tectonic window? *N. Jb. Geol. Palaon.t Abh.,* 269(2):149–171.

Kauffmann, G., 1976. Perm und Trias im ö̈stlichen Mittelgriechenland und auf einigen Aegeischen Inseln. *Zeitschr. Deutsch Geol. Ges*., 127:387–398

Kauffmann, G., Kockel, F. and Mollat, H., 1976. Notes on the stratigraphic and paleogeographic position of the Svoula Formation in the Innermost Zone of the Hellenides (Northern Greece). *Bull. Soc. geol. France*, (7) XVIII: 255-230.

Kemp, A.E.S. and McCaig, A., 1984. Origins and significance of rocks in an imbricate thrust zone beneath the Pindos ophiolite, northwestern Greece. In: Robertson AHF and Dixon JE(eds) *The Geological Evolution of the Eastern Mediterranean*. Geological Society London, Special publications, 17: 569-580.

Kilias, A. and Mountrakis, D., 1987. Zum tektonschen bau der Zentral-Pelagonischen Zone (Kamvounia Gebirge, N. Griechenland). Zeitschrift der Deutschen Geologischen Gesellschaft, 138, 211-237.

Kilias, A., 1991. Transpressive Tecktonik in den zentralen Helleniden. Aenderung der Translationpfade durch die Transgression Nord-Zentral Griechenland). *Neues Jahrbuch fuer Geologie und Palaeontologie*, Monatshefte, 5: 291-306.

Kilias, A., Fassoulas, C. and Mountrakis, D., 1994. Tertiary extension of continental crust and uplift of Psiloritis metamorphic core complex in the central part of the Hellenic Arc (Crete, Greece). *Geol Rundschau,* 83: 417–430.

Kilias, A., 1995. Emplacement of the blueschists unit in eastern Thessaly and exhumation of Olympos-Ossa carbonate dome as a result of Tertiary extension (central Greece). *Miner. Wealth*, 96: 7-22.

Kilias, A. and Mountrakis, D., 1998. Tertiary extension of the Rhodope massif associated with granite emplacement (Northern Greece). *Acta Vulcanologica*, 10: 331-337.

Kilias, A., Falalakis, G. and Mountrakis, D., 1999. Cretaceous-Tertiary structures and kinematics of the Serbomacedonian metamorphic rocks and their relation to the exhumation of the Hellenic hinterland (Macedonia, Greece). *International Journal of Earth Sciences,* 88: 513-531.

Kilias, A., Tranos, M., Mountrakis, D., Shallo, M., Marto, A. and Turku, I., 2001. Geometry and kinematics of deformation in the Albanian orogenic belt during the Tertiary. *Journal of Geodynamics*, 31: 169-187.

Kilias, A., Tranos, M., Orozco, M., AlonsoChaves, F.M. and Soto, J.I., 2002. Extensional collapse of the Hellenides: A review. *Revista de la Sociedad Geologice de Espana*, 15: 129-139.

Kilias, A., Frisch, W., Avgerinas, A., Dunkl, I., Falalakis, G. and Gawlick, H.-J., 2010. Alpine architecture and kinematics of deformation of the northern Pelagonian nappe pile in the Hellenides. *Austrian Journal of Earth Sciences,* 103/1: 4-28.

Kilias, A., Vamvaka, A., Falalakis, G., Sfeikos, A., Papadimitriou, E., Gkarlaouni, C. and Karakostas, K., 2013. The Mesohellenic trough and the Thrace Basin. Two Tertiary molassic Basins in Hellenides: do they really correlate? *Bulletin of the Geological Society of Greece*, 47: 551-562.

Kilias, A., Vamvaka, A., Falalakis, G., Sfeikos, A. and Papadimitriou, E., et al., 2015. The Mesohellenic Trough and the Paleogene Thrace Basin on the Rhodope Massif, their Structural Evolution and Geotectonic Significance in the Hellenides. J. Geol. Geosci., 4: 198. doi:10.4172/2329-6755.1000198

Kilias, A., Thomaidou, E., Katrivanos, E., Vamvaka, A. and Fassoulas, C., et al., 2016. A geological cross-section through northern Greece from Pindos to Rhodope Mountain Ranges: a field guide across the External and Internal Hellenides. In: (Eds) Kilias, A. and Lozios, S., Geological field trips in the Hellenides. *Journal Virtual Explorer,* 50:1.

Kilias, A., 2021. The Hellenides: A Multiphase Deformed Orogenic Belt, its Structural Architecture, Kinematics and Geotectonic Setting during the Alpine Orogeny: Compression vs Extension the Dynamic Peer for the Orogen Making. A Synthesis. *Journal of Geology and Geoscience,* 5(1): 2021.

Kober, L., 1914. Die Bewegungsrichtung der alpinen Deckengebirge des Mittelmeeres. *Petermann's Geogr Mitt*, 60: 250–256.

Kockel, F., Mollat, H. and Walther, H.W., 1971. Geologie des SerboMazedonischen Massivs und seines mesozoischen Rahmens (Nordgriechenland). *Geol. Jb.*, 89: 529-551.

Kockel, F. and Mollat, H., 1977. Geological map of the Chalkidiki peninsula and adjacent areas (Greece), Scale 1:100000. Bundesanstalt fur Geowissenschaften und Rohstoffe, Hannover.

Koroneos, A., Cristofides, G., Del Moro, A. and Kilias, A., 1993. Rb-Sr geochronology and geochemical aspects of the Eastern Varnountas plutonite (NW Macedonia, Greece). *Neues Jahrbuch fur Mineralogie,* Abhandlungen, 165: 297-315.

Koroneos, A. 2010. Petrogenesis of the Upper Jurassic Monopigadon pluton related to the Vardar-Axios ophiolites (Macedonia, northern Greece) and its geotectonic significance. *Chem Erde,* 70: 221–241

Kostaki, G., Kilias, A., Gawlick, H-J. and Schlagintweit, F., 2013. Kimmeridgian-Tithonian shallow-water platform clasts from mass flows on top of the Vardar/Axios ophiolites. *Bull Geol. Soc. Greece,* XLVII, pp 1–10.

Kostaki, G., 2013. Stratigraphy and geotectonic setting of the ?Kimmeridgian-Tithonian shallow-water pltaform sediments on top of the Axios Ophiolites (Eastern Axios suture zone, Northern Greece). Master Thesis, Aristotle University of Thessaloniki.

Kostaki, G., Kilias, A., Gawlick, H-J. and Schlagintweit, F., 2014. Component analysis in the vardar/axios zone of northern greece reveals an eroded late jurassic carbonate platform comparable to those of the Eastern Alps/Western Carpathian, Dinarides, Albanides and Hellenides. XX CBGA. *Bul Shk Gjeol,* 1: 85–88.

Kostaki, G., Gawlick, H.-J., Missoni, S., Kilias, A. and Katrivanos, E., 2023. New stratigraphic and paleontological data from carbonates related to the Vourinos-Pindos ophiolite emplacement: Implications for the provenance of the ophiolites (Hellenides). Journal of Geological Society of London, DOI: 10.1144/jgs2023-127.

Kovacs, S., 2010. Type section of the Triassic Bodvalenke Limestone Formation (Rudabanya Mts., NE Hungary)—the northwestern-most occurrence of a Neotethyan deep water facies. *Cent Eur Geol*, 53: 121–133.

Köver, S., Haas, J., Ozsvart, P., Görög, A., Götz, A.E., Jozsa, S., 2009. Lithofacies and age data of Jurassic foreslope and basin sediments of Rudabanya Hills (NE Hungary) and their tectonic interpretation. *Geologica Carpathica*, 60: 351–379.

Krische, O., Goričan, Š. And Gawlick, H.J., 2014. Erosion of a Jurassic ophiolitic nappe-stack as indicated by exotic components in the Lower Cretaceous Rossfeld Formation of the central Northern Calcareous Alps (Austria). *Geol Carpath*, 65: 3–24.

Krystyn, L., and Mariolakos, I., 1975. Stratigraphie und Tektonik der Hallstiitter Scholle von Epidauros (Griechenland). Sitz.ber. Math.-Nat.wiss. KI. (1), 184: 181 – 195.

Krystyn, L., 1980. Triassic conodont localities in the Salzkammergut Region (Northern Calcareous Alps), mit Beitragen von B. Plochinger und H. Lobitzer. In:

Schonlaub, H.P. (Ed.). Second European Conodont Symposium – ECOS II, Field trip B. Abhandlungen der Geologischen Bundesanstalt, 35: 61-98.

Krystyn, L., 1983. Das Epidauros-Profil (Griechenland) -ein Beitrag zur Conodonten-Standardzonierung des tethyalen Ladin und Unterkarn. In: Zapf, H., (ed). Neue Beiträge zur Biostratigraphie der Tethys-Trias. *Schriftenr. Erdwiss. Komm. Österr. Akad. Wiss.*, 5: 231-258.

Krystyn, L., 2008. The Hallstatt pelagics- Norian and Rhaetian Fossillagerstaetten of Hallstatt. Berichte der Geologischen Bundesanstalt Wien, 76: 81-98.

Kube, B., Dragastan, O. and Richter, D.K., 1998. A sequence from Late Triassic shallow water carbonates to Jurassic basinal radiolarites: Kap Kastello/Hydra at the western margin of the Pelagonian Platform. *Bulletin of the Geological Society of Greece*, XXXII(2): 31-39.

Kukoč, D., Goričan, Š. and Košir, A., 2012. Lower cretaceous carbonate gravity-flow deposits from Bohinj area (NW Slovenia): evidence of a lost carbonate platformin the Internal Dinarides. Bull Soc Gıol France, 183: 383–392.

Lein, R., 1987. Evolution of the Northern Calcareous Alps during Triassic times. - In: Flugel, H.W. and Faupl, P. (Eds.): Geodynamics of the Eastern Alps: 85-102.

Lewis, D.W., 1984. Practical sedimentology. Hutchinson Ross, Stroudsburg, pp 1-229

Makris, J., 1977. Geophysical investigations of the Hellenides. *Hamburger Geophysikalishe Einzelschriften*, 33.

Manakos, K., 1983. Geological Map of Greece, scale 1:50.000, Map Sheet Mirofilion. Institute of Geology and Mineral Exploration, Athens.

Mandl, G.W., 1984. Zur Trias des Hallstater Faziesraumes – ein Modell am Beispiel Salzkammergut (Nordliche Kalkalpen, Osterreich). Mitteilungen der Gesellschaft der Geologie und Bergbaustudenten in Osterreich, 30/31: 133-176.

Marko, F., Sigdel, A., Bielik, M., Bezák, V., Mojzeš, A., Madarás, J., Papčo, J., Siman, P., Acharya, S. and Fekete, K., 2020. A comparison of Cenozoic Neo-Alpine tectonic evolution of the Western Carpathian and Himalayan orogenic belts (Slovakia – Nepal). *Mineralia Slovaca*, 52: 2 (2020).

Mavridis, A. and Kelepertzis, A., 1993. Geological Map of Greece, scale 1:50.000, Knidhi Sheet. Institute of Geology and Mineral Exploration, Athens.

Meinhold, G., Kostopoulos, D., Reischmann, T., Frei, D. and Bou Dagher-Fadel, M.K., 2009. Geochemistry, provenance and stratigraphic age of metasedimentary rocks from the eastern Vardar suture zone, northern Greece. *Palaeogeography, Palaeoclimatology, Palaeoecology,* 277: 199-225.

Meinhold, G. and Kostopoulos, D., 2012. The Circum-Rhodope, northern Greece: Age, provenance, and tectonic setting. *Tectonophysics*, 595-596: 55-68

Mercier, J., 1968. Etude geologique des zones internes hellenides en Macedoine centrale (Grece). Contribution a l etude du metamorphisme et de l evolution magmatique des zones internes des Hellenides. *Annales geologiques des pays helleniques*, 20: 1-792.

Mercier, J.P., Vergely, P. and Bebien, J., 1975. Les ophiolites helléniques "Obductées" an Jurassique supérieur sontelles les vestiges d' un ocean téthysien ou d' une ocean téthysien ou d'une mer marginale peri-europeenne? Compte Rendue sommaire des Séances de la Socièté Géologique de France, 17: 108-112.

Michail, M., Pipera, K., Koroneos, A., Kilias A. and Ntaflos T., 2016. New perspectives on the origin and emplacement of the Late Jurassic Fanos granite, associated with an intraoceanic subduction within the Neotethyan Axios-Vardar Ocean. *Int J Earth Sci,* 105: 1965–1983.

Mikes, T., Christ, D., Petri, R., Dunkl, I., Frei, D., Baldi-Beke, M., Reitner, J., Wemmer, K., Hrvatović, H., and von Eynatt, H., 2008. Provenance of the Bosnian Flysch. *Swiss J Geosci*, 101(1): 31–54.

Migiros, G. and Tselepidis, V., 1990. der erste Nachweis von Hallstatter Kalken in der Nord- Pindos-Decke (Nordwest-Griechenland). *Neues Jarhbuch fur Pal Mah*, 4: 248-256.

Missoni, S. and Gawlick, H.-J., 2011. Evidence for Jurassic subduction from the Northern Calcareous Alps (Berchtesgaden; Austroalpine, Germany). *International Journal of Earth Sciences,* 100: 1605-1631.

Missoni, S., Gawlick, H.-J., Sudan, M.N., Jovanovic, D. and Lein, R., 2012. Onset and demise of the Wetterstein Carbonate Platform in the melange areas of the Zlatibor Mountain (Sirogojno, SW Serbia). *Facies*, 58: 95-111.

Missoni S, Gawlick HJ, Richoz S, Goricˇan S, Prochaska W, Gratzer R, Lein R, Krystyn L (2014) Carnian-Norian palaeo-seawater and tectonostratigraphy of an open-marine Hallstatt limestone section in the Budva Zone (Montenegro). In: 19th international sedimentological congress, 18–22 Aug 2014, abstract book, p504

Mitzopoulos, M. C., Renz, C., 1938. Fossilführende Trias im griechischen Othrysgebirge. *Eclogae Geologicae Helvetiae*, 31(1): 71-73.

Moores, E.G., 1969. Petrology and structure of the Vourinos Ophiolitic Complex of Northern Greece. *Geol. Soc. Am., Special paper,* 118, 74 pp.

Most, T., Frisch, W., Dunkl, I., Kodosa, B., Boev, B., et al. 2001. Geochonological and structural investigation of the Northern Pelagonian crystalline zone. Constraints from K/Ar and zircon and apatite fission track dating. *Bull Geol Soc Greece,* 34: 91-95.

Mountrakis, D., Sapountzis, E., Kilias, A., Eleftheriadis, G., and Christofides, G., 1983. Paleogeographic conditions in the western Pelagonian margin in Greece during the initial rifting of the continental area. *Can. J. Earth Sci.*, 20: 1673-1681.

Mountrakis, D., 1986. The Pelagonian Zone in Greece: A polyphase deformed fragment of the Cimmerian continent and its role in the geotectonic evolution of the Eastern Mediterranean. *Journal of Geology,* 94: 355-347.

Mountrakis, D., 2010. Geology and Geotectonic evolution if Greece. *University studio press.*

Mussalam, K. and Jung, D., 1986. Geology und Bau des Sithonia-Ophioliths (Chalkidiki, NE Griechenland: Anmerkungen zur Bildung ozeanischer Krusten). *Geologische Rundschau*, 75: 383-409.

Mutti, E., Bernoulli, D., Ricci Lucchi, F. and Tinterri, R., 2009. Turbidites and turbidity currents from Alpine "flysch" to the exploration of continental margins. *Sedimentology,* 56: 267–308.

Neofotistos, P., Mountrakis, D., Tranos, M. and Kilias, A., 2010. Geological structure and deformation of the Koziakas-Itamos Mts. (Central Greece): Implications for the orogenic and late-orogenic processes in the innermost part of the External Hellenides during the Tertiary. *Geotectonic research*, Special issue.

Nirta, G., Bortolotti, V., Chiari, M., Menna, F., Saccani, E., Principi, G. and Vannucchi, P., 2010. Ophiolites from the Grammos-Arrenes area, Northern Greece: Geological, palaeontological and Geochemical data. *Ofioliti*, 35(2): 103-115.

Nirta, G., Moratti, G., Piccardi, L., Montanari, D., Carras, N., Catanzariti, R., Chiari, M. and Marcucci, M., 2018. From obduction to continental collision: new data from Central Greece. *Geological Magazine,* 155: 377–421.

Nirta, G., Aberhan, M., Bortolotti, V., Carras, N., Menna, F. and Fazzuoli, M. 2020. Deciphering the geodynamic evolution of the Dinaric orogen through the study of the 'overstepping' Cretaceous successions. *Geological Magazine*, 157.

Ozsvart, P., Dosztaly, L., Migiros, G., Tselepidis, V. and Kovacs, S., 2012. New radiolarian biostratigraphic age constraints on Middle Triassic basalts and radiolarites from the Inner Hellenides (Northern Pindos and Othrys Mountains, Northern Greece) and their implications for the geodynamic evolution of the early Mesozoic Neotethys. *Int J Earth Sci (Geol Rundsch),* 101: 1487-1501.

Papanikolaou, D., 2009. Timing of tectonic emplacement of the ophiolites and terrane paleogeography in the Hellenides. *Lithos,* 108: 262-280.

Papanikolaou, D., 2013. Tectonostratigraphic models of the Alpine terranes and subduction history of the Hellenides. *Tectonophysics,* 595: 1-24.

Photiades, A., Carras, N., Bortolotti, V., Fazzuali, M. and Principi, G., 2007. The late Early Creataceous Transgression on the laterites in Vourinos and Vermion massifs (Western Macedonia, Greece). *Bulletin of the Geological Society of Greece*, vol. XXXX, 2007, Athens May.

Pomoni-Papaioannou, F. and Photiades, A., 2007. Chlorozoan VS foramol carbonate sedimentary systems in an upper Jurassic-Cretaceous Pelagonian margin: Rhodiani area (West Macedonia, Greece). *Boll. Soc. Geol. It.,* 126(2): 00-00.

Pomonis, P., Tsikouras, B. and Hatzipanagiotou, K., 2002. Origin, evolution and radiometric dating of the sub-ophiolitic metamorphic rocks from the Koziakas ophiolite (W. Thessaly, Greece). *N. Jb. Miner. Abh*., 177: 255-276 Stuttgart.

Pomonis, P., Tsikouras, B. and Hatzipanagiotou, K., 2005. Geological evolution of the Koziakas ophiolitic complex (western Thessaly, Greece). *Ofioliti*, 30(2): 77-89.

Pomonis, P., Tsikouras, B. and Hatzipanagiotou, K., 2007. Petrogenetic evolution of the Koziakas ophiolitic complex (W. Thessaly, Greece). *Mineralogy and Petrology*, 89: 77-111.

Pomoni, F. and Tselepidis, V., 2013. Lithofacies palaeogeography and biostratigraphy of the lowermost horizons of the Middle Triassic Hallstatt Limestones (Argolis Peninsula, Greece). *Journal of Palaeogeography*, 2(3): 252-274.

Porkoláb, K., Willingshofer, E., Sokoutis, D. and Wijbrans, J., 2020. Strain localization during burial and exhumation of the continental upper crust: A case study from the Northern Sporades (Pelagonian thrust sheet, Greece). *Global and Planetary Change*, 194. https://doi.org/10.1016/j.gloplacha.2020.103292

Pichon J.F. and Lys, M., 1976. Sur l'existence d'une série du Jurassique à Crétacé inférieur surmontant les ophiolites, dans les collines de Krapa (massif du Vourinos, Grèce). *C. R. Acad. Sci. Paris*, 282: 523-524.

Rassios, A.H.E. and Moores, E.M., 2006. Heterogenous mantle complex, crustal processes, and obduction kinematics in a unified Pindos-Vourinos ophiolitic slab (nortern Greece). *Tectonic Development of the Eastern Mediterranean Region,* 260: 237-266.

Rassios, A.H.E. and Dilek, Y., 2009. Rotational deformationin the Jurassic Mesohellenic ophiolites, Greece, and its tectonic significance. *Lithos,* 108: 207-223.

Ricou, L.E., Burg, J.P., Godfriaux, L. and Ivanov, Z., 1998. Rhodope and Vardar: the metamorphic and olistostromic paired belts related to the Cretaceous subduction under Europe. *Geodinamica Acta,* 11: 285-309.

Robertson, A.H.F., Clift, P.D., Degnan, P.J. and Jones, G., 1991. Palaeogeographical and palaeotectonic evolution of the eastern Mediterranean Neotethys. *Palaeo*, 87: 289-343.

Robertson, A.H.F., Dixon, J. E., Brown, S., Collins, A., Morris, A., Pickett, E., Sharp, I. and Ustaömer, T., 1996. Alternative tectonic models for the Late Palaeozoic-Early Tertiary development of the Tethys in the Eastern Mediterranean. In: J.E. Dixon and A.H.F. Robertson (eds), The Geological Evolution of the Eastern Mediterranean. *Geological Society of London Special Publications*, 17: 1-74.

Robertson, A.H.F., and Shallo, M., 2000. Mesozoic- Tertiary tectonic evolution of Albania in its regional Eastern Mediterranean context. *Tectonophysics*, 316: 197-214.

Robertson, A.H.F., 2012. Late Paleozoic-Cenozoic tectonic development of Greece and Albania in context of alternative reconstructions of Tethys in the Eastern Mediterranean region. International Geology Review 54: 373-454.

Robertson, A.H.F., Trivic, B., Djeric, N. and Bucur, I.I., 2012. Tectonic development of the Vardar Ocean and its margins: Evidence from the Republic of Macedonia and Greek Macedonia. *Tectonophysics*. Available online at: http://dx.doi.org/10.1016/j.tecto.2012.07.022

Roddick, J., Cameron, W. and Smith, A.G., 1979. Permotriassic and Jurassic Ar/Ar ages from Greek ophiolites and associated rocks. *Nature*, 279: 788-790.

Römermann, H., 1968. Geologie von Hydra (Griechenland). *Geol. and Paleont.*, 2: 163-171.

Saccani, E., Photiades, A. and Padoa, E., 2003. Geochemistry, Petrogenesis and tectono-magmatic significance of the volcanic and sub-volcanic rocks from the Koziakas melange (Western Thessaly, Greece). *Ofioliti*, 28: 43-57.

Saccani, E., Beccaluva, L., Coltorti, M. and Siena, F., 2004. Petrogenesis and tectono-magmatic significance of the Albanide-Hellenide subpelagonian ophiolites. *Ofioliti*, 29(1): 75-93.

191

Saccani, E. and Photiades, A., 2004. Mid-ocean ridge and supra-subduction affinities in the Pindos Massif ophiolites (Greece): implications for magma genesis in a proto-forearc setting. *Lithos*, 73: 229-253.

Saccani, E. and Photiades, A., 2005. Petrogenesis and tectonomagmatic significance of the volcanic and subvolcanic rocks in the Albanide-Hellenide ophiolitic melanges. *The Island Arc*, 14: 494-516.

Saccani, E., Bortolotti, V., Marroni, M., Pandolfi, L., Photiades, A., et al. 2008. The Jurassic association of back arc basin ophiolites and calc-alkaline volcanics in the Guevgueli Complex (Northern Greece): Implication for the evolution of the Vardar Zone. *Ofioliti,* 33: 209–227.

Saccani, E., Dilek, Y., Marroni, M. and Pandolfi, L. 2015. Continental Margin Ophiolites of Neotethys: Remnants of Ancient Ocean–Continent Transition Zone (OCTZ) Lithosphere and Their Geochemistry, Mantle Sources and Melt Evolution Patterns. *Episodes*, 38/4: 230-249. DOI: 10.18814/epigsi/2015/v38i4/82418

Saccani, E., Dilek, Y. and Photiades, A., 2017. Time-progressive mantle-melt evolution and magma production in a Tethyan marginal sea: A case study of the Albanide-Hellenide ophiolites. *Lithosphere*, 9/1 DOI 11.1130/L602.1

Sakellariou, M. B., 1938. Faune triassique près d' Aghia Moni (Nauplie) en Argolide. Prakt. Akad. Athènes, 13: 723.

Savouat, E. and Lalechou, 1972. Geological Map of Greece, scale 1:50.000, Kalabaka Sheet. Institute of Geology and Mineral Exploration, Athens.

Schenker, F.L., Burg, J.P., Kostopoulos, D., Moulas, E., Larionov, A., Von Quadt, A., 2014. From mesoproterozoic magmatism to collisional cretaceous anatexis: Tectonomagmatic history of the Pelagonian Zone, Greece. *Tectonics*, 33: 1552-1576.

Schenker, F.L., Fellin, M.G., Burg, J.P., 2015. Polyphase evolution of Pelagonia (northern Greece) revealed by geological and fissiontrack data. *Solid Earth,* 6: 285–302.

Scherreiks, R., 2000. Platform margin and oceanic sedimentation in a divergent and convergent plate setting (Jurassic, Pelagonian Zone, NE Evvoia, Greece). *International Journal of Earth Sciences,* 89: 90-107.

Scherreiks, R., Bosence, D., BouDagher-Fadel, M., Melendez, G. and Baumgartner, P.O., 2009. Evolution of the Pelagonian carbonate platform complex and the adjacent oceanic realm in response to plate tectonic forcing (Late Triassic and Jurassic), Evvoia, Greece. *Int J Earth Sci.* (Geol Rundsch), 99:1317–1334.

Scherreiks, R., Meléndez, G., BouDagher-Fadel, M., Fermeli, G., Bosence, D., 2014. Stratigraphy and tectonics of a time-transgressive ophiolite obduction onto the eastern margin of the Pelagonian platform from Late Bathonian until Valanginian time, exemplified in northern Evvoia, Greece, *Int. J. Earth Sci.*, 103: 2191-2216.

Scherreiks, R., Meléndez, G., Bouldagher-Fadel, M., Fermeli, G., Bosence, D., 2016. The Callovian unconformity and the ophiolite obduction onto the Pelagonian carbonate platform of the Internal Hellenides. Bulletin of the Geological Society of Greece, vol. L, 2016 Proceedings of the 14th Intern. Congress, Thessaloniki, May 2016.

Schlager, W., 1969. Das Zusammenwirken von Sedimentation und Bruchtektonik in der triadischen Hallstatter Kalken der Ostalpen. *Geologische Rundschau*, 59: 289-308.

Schlager, W. and Schollnberger, W., 1974. Das Prinzip stratigraphischer Wenden in der Schichtfolge der Nordlichen Kalkalpen. Mitteilungen der geologischen Gesellschaft Wien, 66-67: 165-193.

Schlagintweit, F., Gawlick, H.-J. and Lein, R., 2005. Mikropalaeontologie und Biostratigraphie der Plassen-Kaebonatplatform der Typlokalitaet (Ober-Jura bis Unter-Kreide, Salzkammergut, Oesterreich. *Journal of Alpine Geology* (Mitt. Ges. Geol. Bergbaustud. Oesterr.), 47: 11-102.

Schlagintweit, F. and Gawlick, H.-J., 2007. Analysis of the Late to Early Cretaceous algal debris-facies of the Plassen carbonate platform in the Northern Calcareous Alps (Germany, Austria) and in the Kurbnesh area of the Mirdita zone (Albania) – a tool to reconstruct tectonics and paleogeography of eroded platforms. *Facies,* 53: 209-227.

Schlagintweit, F., Gawlick, H.-J., Missoni, S., Hoxha, L., Lein, R. and Frisch, W., 2008. The eroded Late Jurassic Kurbnesh carbonate platform in the Mirdita ophiolite Zone of Albania and its bearing on the Jurassic orogeny of the Neotethys realm. *Swiss Journal of Geosciences,* 101: 125-138.

Schlagintweit, F. and Gawlick, H.-J., 2009. Enigmatic tubes associated with microbial crusts from the Late Jurassic of the Northern Calcareous Alps (Austria): a mutualistic sponge–epibiont consortium? *Lethaia,* 42: 452–461.

Schlagintweit, F., 2011. The dasycladalean algae of the Plassen carbonate platform (Kimmeridgian-Early Berriasian): taxonomic inventory and palaeogeographical implications within the platform-basin-system of the Northern Calcareous Alps (Austria, p.p. Germany). *Geologia Croatica,* 64/3: 185-206.

Schlagintweit, F., Gawlick, H.-J., Lein, R., Missoni, S. and Hoxha, L., 2012. Onset of an Aptian carbonate platform overlying a Middle-Late Jurassic radiolaritic-ophiolithic melange in the Mirdita zone of Albania. *Geologia Croatica*, 65/1: 29-40.

Schmid, S.M., Bernoulli, D., Fugenschuh, B., Matenco, L., Scheffer, S., Schuster, R., Tischler, M. and Ustaszewski, K., 2008. The Alpine-Carpathian-Dinaric orogenic

system: correlation and evolution of tectonic units. *Swiss Journal of Geosciences,* 101: 139-183.

Schmid, S.M., Fugenschuh, B., Kounov, A., Matenco, L., Nievergelt, P., Oberhansli, R., Pleuger, J., Schefer, S., Schuster, R., Tomljenovic, B., Ustaszewski, K. and van Hinsbergen, D.J.J., 2020. Tectonic units of the Alpine collision zone between Eastern Alps and western Turkey. *Gondwana Research*, 78: 308-374.

Şengör, A.M.C., 1984. The Cimmeride orogenic system and the tectonics of Eurasia. *Geological Society of America Special Paper*, 195: 1–82.

Şengör, A.M.C., 1985. Die Alpiden und die Kimmeriden: die verdoppelte Geschichte der Tethys. *Geologische Rundschau*, 74: 181–213.

Şengör, A.M.C., 2003. The repeated rediscovery of mélanges and its implication for the possibility and the role of objective evidence in the scientific enterprise. In: Dilek, Y., Newcomb, S. (Eds.), Ophiolite Concept and the Evolution of Geological Thought. *Geological Society of America Special Paper,* 373: 385–445.

Senowbari-Daryan, B. and Schafer, P., 1979. Neue Kalkschwamme und ein Problematikum (Radiomura cautica n. g., n. sp.) aus Oberrhat-Riffen sudlich von Salzburg (Nordliche Kalkalpen). *Mitt osterr Geol Ges*, 70(1977): 17-42.

Seybold, L., Trepmann, AC. and Janots, E., 2019. A ductile extensional shear zone at the contact area between HP-LT metamorphic units in the Talea Ori, central Crete, Greece: deformation during early stages of exhumation from peak metamorphic conditions. *Int. J. Earth Sciences,* 108: 213-227.

Shallo, M., 1991. Ophiolitic mélange and flyschoidal sediment of the Tithonian–Lower Cretaceous in Albania. *Terra Nova*, 2: 476–483.

Shallo, M., and Dilek, Y., 2003. Development of the ideas on the origin and of Albanian ophiolites, *in* Dilek, Y., and Newcomb, S., eds., Ophiolite concept and the

evolution of geochemical thought: Boulder, Colorado, Geological Society of America, Special Paper, 373: 351–363.

Sharp, I.R. and Roberson, A.H.F., 2006. Tectonicsedimentary evolution of the western margin of the Mesozoic Vardar Ocean: evidence from the Pelagonian and Almopias zones, northern Greece. In: A.H.F. Robertson and D. Mountrakis (eds), Tectonic Development of the Eastern Mediterranean Region. *Geological Society of London,* Special Publications, 260: 373-412.

Silver, E.A. and Beutner, E.C., 1980. Melanges. *Geology,* 8: 32–34.

Skourtsos, M. and Lekkas, E., 2010. Extensional tectonics in Mt Parnon (Peloponnesus, Greece). *Int. J. Earth Sci.* (Geol. Rundsch.)

Smith, A.G., and Spray, J., 1984. A half-ridge transform model of the Hellenic-Dinaric ophiolites, *in* Dixon, J.E., and Robertson, A.H.F., eds., The geological evolution of the Eastern Mediterranean. *Geological Society, London, Special Publications*, 17: 629–644.

Spray, J.G. and Roddick, J.C., 1980. Petrology and 40Ar/39Ar geochronology of some hellenic sub-ophiolite metamorphic rocks. *Contrib. To Mineral. Petrol.*, 72: 43-55.

Spray, J.G., Bebien, J., Rex, D.C. and Roddick, J.C., 1984. Age constraints on the igneous and metamorphic evolution of the Hellenic-Dinaric ophiolites. In: Dixon, J.E., Roberson A.H.F. (eds) The geological evolution of the Eastern Mediterranean. Geol. Soc. London Spec. Publ., 17: 619-627.

Stampfli, G.M., 2000. Tethyan oceans. In: Tectonics and magmatism in Turkey and the Surrounding Area. *Geological Society of London*, Special Publications, 173: 1-23.

Stampfli, G.M. and Borel, G.D., 2002. A plate tectonic model for the Paleozoic and Mesozoic constrained by dynamic plate boundaries and restored synthetic oceanic isochrones. *Earth and Planetary Science Letters*, 169: 17-33.

Stampfli, G.M. and Kozur, H., 2006. Europe from the Variscan to the Alpine cycles. In: Gee, D.G. and Stephenson R.A. (eds) European lithosphere dynamics 32, Geological Society Memoir, London, 57-82.

Sudar, M., 1986. Triassic microfossils and biostratigraphy of the Inner Dinarides between Gucevo and Ljubisnja mts., Yugoslavia. *Geoloski anali Balkanskoga poluostrva*, 50: 151-394 (in Serbo-Croatian, English summary).

Sudar, M.N., Gawlick, H.-J., Lein, R., Missoni, S., Suzuki, H., Jovanovic, D. and Lein, R., 2010. The carbonate-clastic radiolaritic melange of Pavlovica Cuprija: a key to solve the palaeogeography of the Hallstatt Limestone in the Zlater Mountain (SW Serbia). *Journal of Alpine Geology*, 52: 53-57.

Sudar, M.N., Gawlick, H.-J., Lein, R., Missoni, S., Kovacs, S. and Jovanovic, D., 2013. Depositional environment, age and facies of the Middle Triassic Bulog and Rid formation in the Inner Dinarides (Zlatidor Mountain, SW Serbia): evidence for the Anisian break-up of the Neotethys Ocean. *Neues Jahrbuch fur Geologie und Palaontologie Abhandlungen*, 269: 291-320.

Suess, E., 1888. Das Antlitz der Erde. II. F.Tempsky, Prag and Wien and G. Freytag, Leipzig, Prag, Wien, Leipzig, IV, 704 pp.

Suess, E., 1901. Abschieds-Vorlesung. Beitrage zur Paläontologie und Geologie Gesellschaft Österreich-Ungarns und des Orient, 14: 2–8.

Tranos, M., Kilias, A. and Mountrakis, D., 1999. Geometry and kinematics of the Tertiary post-metamorphic Circum Rhodope Belt Thrust System (CRBTS), Northern Greece. *Bull. Geol. Soc. Greece* XXXIII: 5-16.

Tselepidis, V., 2007. Paleontological and stratigraphical study of the ammonoidea from Epidaurus, Greece. Contribution of the knowledge of the palaeogeographic distribution of the "Hallstatt facies" in the Hellenides. Ph.D. Dissertation, Thessaloniki.

Trümpy, R., 2006. Geologie der Iberger Klippen und ihrer Flysch-Unterlage. *Eclogae Geologicae Helvetiae,* 99: 79–121.

Tzamos, E., Kaspiotis, A., Filippidis, A., et al. 2017. Metallogeny of the Chrome Ores of the Xerolivado-Skoumtsa Mine, Vourinos Ophiolite, Greece: Implications on the genesis of IPGE-bearing high-Cr chromitites within a heterogeneously depleted mantle section. *Ore Geology Reviews*, 90: 226-242. DOI:10.1016/j.oregeorev.2017.03.013

Vamvaka, A., Kilias, A., Mountrakis, D. and Papaoikonomou, J., 2006. Geometry and structural evolution of the Mesohellenic Trough (Greece), a new approach. In: Robertson A.H.F. and Mountrakis D. eds., Tectonic Development of the Eastern Mediterranean Region, Geological Society of London, Special Publications, 260: 521-538.

Vamvaka, A., Spiegel, C., Frisch, W., Danišík, M. and Kilias, A., 2010. Fission track data from the Mesohellenic Trough and the Pelagonian zone in NW Greece: Cenozoic tectonics and exhumation of source areas. *Intern. Geol. Review*, 52(2-3): 223-248.

Vergely, P. and Mercier, J., 2000. Données nouvelles sur les chevauchements d'âge post-Crétacé supérieur dans le massif du Païkon (zone de l'Axios-Vardar, Macédoine, Grèce): un nouveau modèle structural, *Comptes Rendus de l'Académie des Sciences de Paris*, 330: 555-561.

Vlahovic, I., Tisljar, J., Velic, I. and Maticec, D., 2005. Evolution of the Adriatic Carbonate Platform: Palaeogeography main events and depositional dynamics. *Palaeogeography, Palaeoclimatology, Palaeoecology*, 220: 333-360.

Vitzthum, M., 2018. Eine spat triassische- fruh unterjurassische offenmarine Abfolge des westlichen Pindos ostlich von Itea, NW Griechenland. Bachelor Arbeit, Montanuniversiteat Leoben.

Vrielynck, B., 1978. Données nouvelles sur les zones internes du Péloponnese. Les massifs a l'est de la plaine d' Argos (Grèce). *Annale Géologique de Pays Hellénique*. 29: 440- 462.

Weidmann, M., Solounias, N., Drake, R.E. and Curtis, G.H., 1984. Neogene stratigraphy of the Eastern basin, Samos island, Greece. *Geobios,* 17: 477-490.

Wendt, J., 1973. Cephalopod accumulations in the Middle Triassic Hallstatt-Limestone of Jugoslavia and Greece. *Neues Jahrbuch für Geologie und Paläontologie, Monatshefte*, 1973: 624-640.

Wilson, J.L., 1975. Carbonate facies in geologic history. Springer.

Zachariadis, P., 2007. Ophiolites of the eastern Vardar Zone, N. Greece. PhD Thesis, University of Mainz, Germany.

Zachariadis, P., Kostopoulos, D., Reischmann, T., Himmerkus, F., Mtukon, D. and Sergeev, S., 2006. U–Pb ion-microprobe zircon dating of subduction-related magmatism from northern Greece: The ages of the Guevgueli, Thessaloniki and Chalkidiki igneous complexes. *Geophysical Research Abstracts*, 8, 05560, 2006

Zimmerman, L.Jr., 1969. The Vourinos complex -an allochthonous alpine ophiolite in northern Greece. Geol. Soc. Am. Abstract with Progr. For 1969, p. 245.

Zimmerman, J., 1972. Emplacement of the Vourinos ophiolites complex, northern Greece. In: Shagam, R. et. al (eds) Studies in earth and space sciences. *Geol. Soc. Am. Mem.*, 132: 225-239.

Zimmerman, J.Jr. and Ross, J.V., 1976. Structural evolution of the Vardar root zone, northern Greece: Discussion and reply. *Bulletin of Geological Society of America,* 90: 126-128.

Zoumpouli, E., Pomoni-Papaioannou, F. and Zelilidis, A., 2010. Studying in the Paxos Zone the carbonate depositional environment changes during upper Cretaceous, in

Sami area of Kefallinia Island. *Greece. Bull. Geol. Soc. Greece*, XLIII 2: 793-801.

Zuffa, G.G., 1980. Hybrid arenites: their composition and classification. J Sed Petr, 50: 21-29

Zuffa, G.G., 1985. Provenance of arenites. D. Reidel Publishing (Dordrecht): 1-408

Online Sources

https://www.britannica.com/place/Tethys-Sea (04/07/2023)

http://www.sepmstrata.org/page.aspx?pageid=89 (26/10/2022).

https://www.beg.utexas.edu/lmod/_IOL-CM01/cm01-step03.htm (26/10/2022).